Journal of Mathematics

Stockwell, Fractional Fourier, and Wavelet Transforms in Linear Canonical Transforms and Clifford Algebra, and Fractional Integral Operators

Lead Guest Editor: Mawardi Bahri
Guest Editors: Ryuichi Ashino and Hendra Gunawan

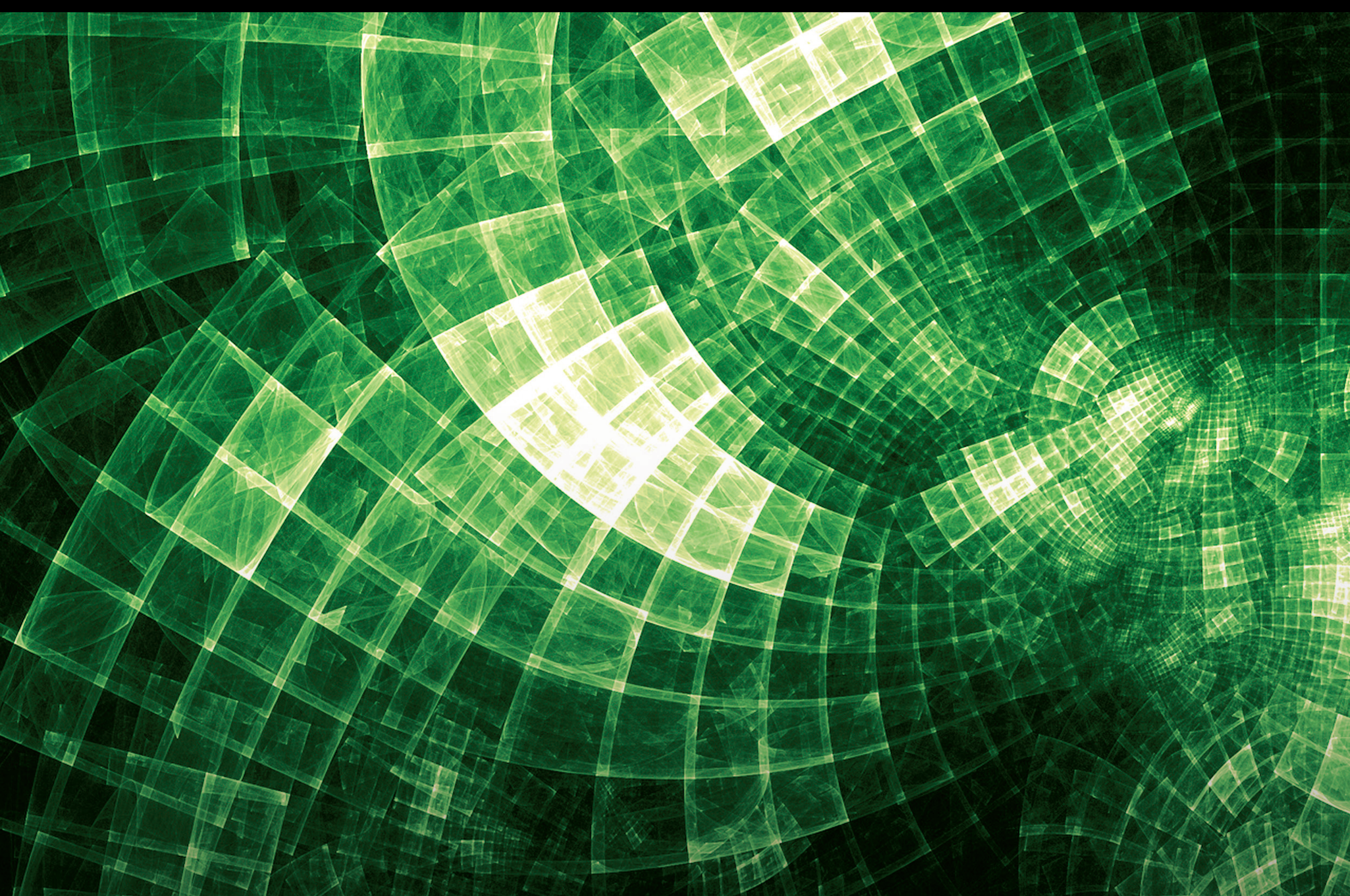

Stockwell, Fractional Fourier, and Wavelet Transforms in Linear Canonical Transforms and Clifford Algebra, and Fractional Integral Operators

Journal of Mathematics

Stockwell, Fractional Fourier, and Wavelet Transforms in Linear Canonical Transforms and Clifford Algebra, and Fractional Integral Operators

Lead Guest Editor: Mawardi Bahri
Guest Editors: Ryuichi Ashino and Hendra Gunawan

Contents

Hindawi
Journal of Mathematics
Volume 2022, Article ID 7848503, 21 pages
https://doi.org/10.1155/2022/7848503

Research Article

Clifford-Valued Shearlet Transforms on $\mathrm{Cl}_{(P,Q)}$-Algebras

Firdous A. Shah[1], **Aajaz A. Teali**[1], and **Mawardi Bahri**[2]

[1]Department of Mathematics, University of Kashmir, South Campus, Anantnag 192101, Jammu and Kashmir, India
[2]Department of Mathematics, Hasanuddin University, Makassar, Indonesia

Correspondence should be addressed to Mawardi Bahri; mawardibahri@gmail.com

Received 28 April 2022; Accepted 21 July 2022; Published 2 September 2022

Academic Editor: Francisco J. Garcia Pacheco

The shearlet transform is a promising and powerful time-frequency tool for analyzing nonstationary signals. In this article, we introduce a novel integral transform coined as the Clifford-valued shearlet transform on $\mathrm{Cl}(p,q)$ algebras which is designed to represent Clifford-valued signals at different scales, locations, and orientations. We investigated the fundamental properties of the Clifford-valued shearlet transform including Parseval's formula, isometry, inversion formula, and characterization of range using the machinery of Clifford Fourier transforms. Moreover, we derived the pointwise convergence and homogeneous approximation properties for the proposed transform. We culminated our investigation by deriving several uncertainty principles such as the Heisenberg–Pauli–Weyl uncertainty inequality, Pitt's inequality, and logarithmic and local-type uncertainty inequalities for the Clifford-valued shearlet transform.

1. Introduction

Wavelet transforms have been proved to be a successful tool for analyzing nontransient signals and have been applied in a number of fields including signal and image processing, differential and integral equations, sampling theory, quantum mechanics, medicine, and so on [1]. However, the efficiency of the wavelet transforms is considerably reduced when applied to higher dimensional signals as they are not able to capture the geometric features like edges and corners at different scales efficiently. The detection of such geometric features in nontransient signals is often highly desirable in numerous practical applications such as medical imaging, remote sensing, crystallography, and several other areas. To circumvent these constraints, a number of novel directional representation systems have been introduced and employed in recent years, such as the wedgelets, ridgelets, ripplets, curvelets, contourlets, surfacelets, brushlets, and shearlets. Among all these geometrical wavelet systems, the shearlet systems have been widely acknowledged and emerged as one of the most effective frameworks for representing multidimensional data because they are nonisotropic nature, and they offer optimally sparse representations [2], allow compactly supported analysing elements [3], are associated with fast decomposition and reconstruction algorithms, and provide a unified treatment of continuum and digital data [4, 5].

Clifford algebras have dethroned both the Grossmann's exterior algebra and Hamilton's quaternion algebra in the sense that they incorporate both the geometrical and algebraic features of Euclidean space into a single structure [6]. As a result, the theory of Clifford algebras has attained an overwhelming response and gained a respectable status in higher-dimensional signal and image processing mainly due to the reason that such algebras encompass all dimensions at once unlike the multidimensional tensorial approach with tensor products of one-dimensional phenomena. This true multidimensional nature allows specific constructions of higher dimensional signal and image processing tools including the Clifford Fourier transforms [7, 8], Clifford Gabor transforms, Clifford wavelet transforms, and other integral transforms in general [9–13].

Motivated and inspired by the contemporary developments in the theory of shearlet transforms abreast the profound applicability of the Clifford algebras, we introduce the notion of Clifford-valued shearlet transforms on $Cl_{(p,q)}$

algebras in the context of multidimensional signal analysis. Unlike the conventional shearlet transform, the proposed transform inherits both the geometric and algebraic properties of shearlet transforms and Clifford algebras. Although a meek analgoue of shearlet transform in the Clifford domain has been proposed in [14], it only deals with the $Cl_{(0,n)}$algebra, where $n = 3\text{mod}4$. Therefore, the centre piece of this study is to construct the Clifford-valued shearlets and the corresponding shearlet transforms in the most general setting $Cl_{(p,q)}$ by employing translations, sharing, scaling, and spinning elements. Besides, we study the basic properties of the Clifford-valued shearlet transforms including Parseval's and inversion formulae and range theorem using the machinery of Clifford Fourier transforms. Moreover, we derive the pointwise convergence and homogeneous approximation properties for the proposed transform. Finally, we formulate some uncertainty inequalities including the classical Heisenberg–Pauli–Weyl inequality, Pitt's inequality, and logarithmic inequality for the Clifford shearlet transforms.

The structure of this article is as follows. Section 2 deals with the preliminaries of Clifford algebras, whereas a comprehensive analysis of the general Clifford-valued shearlet transforms is carried out in Section 3. In Section 4, we study the homogeneous approximation properties for proposed transform. Several uncertainty principles for the proposed transform are also being studied in Section 5. Finally, a conclusion is summarized in Section 6.

2. Basics of Clifford Algebras

In this section, we present a brief overview of the Clifford algebras including the definitions of Clifford Fourier transforms, spin group, and some unitary operators.

The Clifford algebra $Cl_{(p,q)}$ is a noncommutative, associative algebra generated by the orthonormal basis $\{e_1, e_2, \ldots, e_n\}$ of the n-dimensional Euclidean space $\mathbb{R}^n$ governed by the multiplication rule:

$$e_i e_j + e_j e_i = 2\varepsilon_i \delta_{ij}, \quad i, j = 1, 2, \ldots, n, \tag{1}$$

where $n = p + q$, $\varepsilon_i = +1$ for $i = 1, 2, \ldots, p$ and $\varepsilon_i = -1$ for $i = p+1, p+2, \ldots, n$, with δ_{ij} denoting the usual Kronecker's delta function. The noncommutative product and the additional axiom of associativity generates the 2^n- dimensional Clifford geometric algebra $Cl_{(p,q)}$, which can be decomposed as

$$Cl_{(p,q)} = \bigoplus_{k=0}^{n} Cl^k_{(p,q)}, \tag{2}$$

where $Cl^k_{(p,q)}$ denotes the space of k-vectors given by

$$Cl^k_{(p,q)} \coloneqq \text{span}\left\{e_{i_1}, e_{i_2}, \ldots, e_{i_k}; i_1 \le i_2 \le \ldots \le i_k\right\}. \tag{3}$$

Any general element of the Clifford algebra is called a multivector and every multivector $M \in Cl_{(p,q)}$ can be represented in the following form:

$$M = \sum_A M_A e_A = \langle M\rangle_0 + \langle M\rangle_1 + \cdots + \langle M\rangle_n, \quad M_A \in \mathbb{R}, A \subset \{1, 2, \ldots, n\}, \tag{4}$$

where $e_A = e_{i_1} e_{i_2} \ldots e_{i_k}$ and $i_1 \le i_2 \le \ldots \le i_k$. Moreover, $\langle\cdot\rangle_k$ is called as the grade k-part of M, and $\langle\cdot\rangle_0, \langle\cdot\rangle_1, \langle\cdot\rangle_2, \ldots$, respectively, denote the scalar part, vector part, bivector part, and so on. The Clifford conjugate of a multivector $M \in Cl_{(p,q)}$ is given by

$$\overline{M} = \sum_{r=0}^{n} (-1)^{r(r-1)/2} \overline{\langle M\rangle_r}, \tag{5}$$

where the scalar product of multivectors M and $\overline{N}$ is defined as

$$Sc(M\overline{N}) = |MN| = M \star \overline{N} = \sum_A M_A N_A. \tag{6}$$

Moreover, for any pair of multivectors $M, N \in Cl_{(p,q)}$, it can be easily verified that

$$|MN| \le 2^n |M||N|. \tag{7}$$

We now intend to recall the fundamental notion of Clifford Fourier transforms in $L^r(\mathbb{R}^{(p,q)}, Cl_{(p,q)})$, $1 \le r < \infty$ as

$$L^r\left(\mathbb{R}^{(p,q)}, Cl_{(p,q)}\right) = \left\{\mathbf{f}\colon \mathbb{R}^{(p,q)} \longrightarrow Cl_{(p,q)}; \|\mathbf{f}\|_r = \left(\int_{\mathbb{R}^{(p,q)}} |\mathbf{f}(x)|^r d^n x\right)^{1/r} < \infty\right\}. \tag{8}$$

It is imperative to mention that any function $\mathbf{f} \in L^r(\mathbb{R}^{(p,q)}, Cl_{(p,q)})$ can be expressed as a combination of the real-valued functions f_A and the basis elements e_A as

$$\mathbf{f}(x) = \sum_A f_A(x) e_A. \tag{9}$$

Due to the noncommutativity of Clifford-valued functions, several analogues of the Clifford Fourier transforms have been introduced in the literature. However, we shall be interested in following definition due to Bahri et al. [15].

Definition 1. Let $I \in Cl_{(p,q)}$ be a square root of -1. The Clifford Fourier transform of any function $\mathbf{f} \in L^1(\mathbb{R}^{(p,q)}, Cl_{(p,q)})$ is defined by

$$\mathcal{F}_{Cl}[f(x)](\xi) = \frac{1}{(2\pi)^{n/2}} \int_{\mathbb{R}^{(p,q)}} f(x) e^{-I v(\xi,x)} \mathrm{d}^n x, \tag{10}$$

where $nx, \xi \in \mathbb{R}^{(p,q)}$, $\mathrm{d}^n x = \mathrm{d}x_1 \mathrm{d}x_2 \ldots \mathrm{d}x_n$, $v\colon \mathbb{R}^{(p,q)} \times \mathbb{R}^{(p,q)} \longrightarrow \mathbb{R}$, and $v(\xi, x) = \xi_1 x_1 + \xi_2 x_2 + \cdots + \xi_n x_n$.

The inversion and Plancherel formulae associated with the Clifford Fourier transform (10) are given by

$$\mathbf{f}(x) = \frac{1}{(2\pi)^{n/2}} \int_{\mathbb{R}^{(p,q)}} \mathcal{F}_{Cl}[\mathbf{f}(x)](\xi) e^{I v(\xi,x)} \mathrm{d}^n \xi, \tag{11}$$

$$\langle \mathbf{f}, \mathbf{g} \rangle_{L^2(\mathbb{R}^{(p,q)}, Cl_{(p,q)})} = \langle \mathcal{F}_{Cl}[\mathbf{f}], \mathcal{F}_{Cl}[\mathbf{g}] \rangle_{L^2(\mathbb{R}^{(p,q)}, Cl_{(p,q)})},$$

In this case, the inner product of two multivector functions $\mathbf{f}$ and $\mathbf{g}$ is described through

$$\langle \mathbf{f}, \mathbf{g} \rangle_{L^2(\mathbb{R}^{(p,q)}, Cl_{(p,q)})} = \int_{\mathbb{R}^{(p,q)}} \mathbf{f}(x) \overline{\mathbf{g}(x)} \mathrm{d}^n x, \tag{12}$$

and its scalar part is given by

$$\begin{aligned} |\langle \mathbf{f}, \mathbf{g} \rangle|_{L^2(\mathbb{R}^{(p,q)}, Cl_{(p,q)})} &= \int_{\mathbb{R}^{(p,q)}} |\mathbf{f}(x) \mathbf{g}(x)|^2 \mathrm{d}^n x \\ &= \int_{\mathbb{R}^{(p,q)}} Sc(\mathbf{f}(x) \overline{\mathbf{g}(x)}) \mathrm{d}^n x \\ &= Sc\left(\int_{\mathbb{R}^{(p,q)}} f(x) \overline{g(x)} \mathrm{d}^n x \right). \end{aligned} \tag{13}$$

For an efficient representation of Clifford-valued functions, we employ the spin elements obtained from the spin group as defined below.

Definition 2. The spin-group is a double covering of special orthogonal group of $\mathbb{R}^n$ and is defined by

$$\mathrm{Spin}(n) = \left\{ \mathbf{r} \in Cl^+_{(p,q)}; \bar{\mathbf{r}}\mathbf{r} = \mathbf{r}\bar{\mathbf{r}} = 1 \right\}, \tag{14}$$

where $Cl^+_{(p,q)}$ is a subgroup of the invertible elements in the Clifford algebra $Cl_{(p,q)}$.

To facilitate the construction of Clifford-valued shearlets, we define the fundamental unitary operators acting on the space $L^r(\mathbb{R}^{(p,q)})$. For $a > 0$, $s \in \mathbb{R}^{n-1}$ and $b \in \mathbb{R}^n$, and the scaling, shearing, spin-rotation, and translation operators are denoted by D_{A_a}, $\mathcal{D}_{S_s}$, $\mathcal{R}_r$, T_b, respectively, and are defined as

$$\begin{aligned} D_{A_a} \Psi(x) &= \left| \det A_a \right|^{-1/2} \Psi\left(A_a^{-1} x \right), \\ \mathcal{D}_{S_s} \Psi(x) &= \Psi\left(S_s^{-1} x \right), \\ \mathcal{R}_r \Psi(x) &= \mathbf{r} \Psi(\bar{\mathbf{r}} x \mathbf{r}) \bar{\mathbf{r}}, \\ T_b \Psi(x) &= \Psi(x - b), \end{aligned} \tag{15}$$

and the matrices involved in equation (15) are

$$\begin{aligned} A_a &= \begin{pmatrix} a & \mathbf{0}^T_{n-1} \\ \mathbf{0}_{n-1} & \mathrm{sgn}(a) |a|^{1/n} I_{n-1} \end{pmatrix}, \\ S_s &= \begin{pmatrix} 1 & \mathbf{s}^T \\ \mathbf{0}_{n-1} & I_{n-1} \end{pmatrix}, \end{aligned} \tag{16}$$

where $\mathbf{s}^T = (s_1, s_2, \ldots, s_{n-1})$, and $\mathrm{sgn}(\cdot)$ and $\mathbf{0}$ denote the well-known Signum function and the null vector, respectively. Moreover, the composition of the scaling matrix A_a and the shearing matrix S_s is given by

$$S_s A_a = \begin{pmatrix} a & \mathrm{sgn}(a) a^{1/n} s_1 & \mathrm{sgn}(a) a^{1/n} s_2 & \mathrm{sgn}(a) a^{1/n} s_3 & \cdots & \mathrm{sgn}(a) a^{1/n} s_{n-1} \\ 0 & \mathrm{sgn}(a) a^{1/n} & 0 & 0 & \cdots & \cdots \\ \vdots & \vdots & \vdots & \vdots & \vdots & \vdots \\ 0 & 0 & 0 & 0 & 0 & \mathrm{sgn}(a) a^{1/n} \end{pmatrix}. \tag{17}$$

3. The Clifford-Valued Shearlet Transform on $Cl_{(p,q)}$ Algebras

In this section, we shall construct the Clifford-valued shearlets on $Cl_{(p,q)}$ algebras by using the combined action of the scaling, sharing, spin-rotation and translation operators. Besides, we study the fundamental properties of the Clifford-valued shearlet transform including Parseval's formula, inversion formula, and obtain a complete characterization of the range. Prior to that, we shall demonstrate that the novel family of Clifford-valued shearlets is endowed with an affine group structure.

Consider that the set $\mathcal{G} = \mathbb{R}^+ \times \mathrm{Spin}(n) \times \mathbb{R}^{n-1} \times \mathbb{R}^n$ endowed with the binary operation $\odot$ is defined as

$$\begin{aligned} &(a, \mathbf{r}, s, b) \odot (a', \mathbf{r}', s', b') \\ &\quad = \left(aa', \mathbf{r} + \mathbf{r}', s + a^{1-(1/n)} s', b + S_s A_a b' \right), \end{aligned} \tag{18}$$

where $a, a' \in \mathbb{R}^+, s, s' \in \mathbb{R}^{n-1}, b, b' \in \mathbb{R}^n, r, r' \in \mathrm{Spin}(n)$. Clearly, $(1, \mathbf{0}, 0_{n-1}, 0_n,)$ is the neutral element of $\mathcal{G}$, whereas $(a^{-1}, -\mathbf{r}, -a^{1/n-1} s, -A_a^{-1} S_s^{-1} b)$ is the inverse of any arbitrary element $(a, \mathbf{r}, s, b) \in \mathcal{G}$. Moreover, it is easy to verify that

$$((a,\mathbf{r},s,b)\odot(a',\mathbf{r}',s',b'))\odot(a'',\mathbf{r}'',s'',b'') = (a,\mathbf{r},s,b)\odot((a',\mathbf{r}',s',b')\odot(a'',\mathbf{r}'',s'',b'')). \tag{19}$$

Hence, we conclude that $(\mathcal{G},\odot)$ constitutes a group and is formally called as the similitude group of dilations, translations, shearing, and spinning.

Furthermore, we claim that the left Haar measure on $\mathcal{G}$ is given by $\mathrm{d}\eta = \mathrm{d}a\mathrm{d}r\mathrm{d}^{n-1}s\mathrm{d}^n b/a^{n+1}$. In fact, for any function $\mathbf{f}\in L^2(\mathcal{G},Cl_{(p,q)})$, we have

$$\int_{\mathcal{G}}\mathbf{f}[(a,\mathbf{r},s,b)\odot(a',\mathbf{r}',s',b')]\mathrm{d}\eta = \int_{\mathbb{R}^+\times Spin(n)\times\mathbb{R}^n\times\mathbb{R}^n} f\left[\left(aa',\mathbf{r}+\mathbf{r}',s+a^{1-(1/n)}s',b+S_sA_ab'\right)\right]\frac{\mathrm{d}a\mathrm{d}\mathbf{r}\mathrm{d}^{n-1}s\mathrm{d}^n b}{a^{n+1}}. \tag{20}$$

Making use of the substitution $\tilde{a}:=aa'$, $\tilde{\mathbf{r}}:=\mathbf{r}\mathbf{r}'$, $\tilde{s}:=s+(a)^{1-1/n}s'$, $\tilde{b}:=b+S_sA_ab'$, i.e., $\mathrm{d}a=(a')^{-1}\mathrm{d}\tilde{a}$, $\mathrm{d}\mathbf{r}=\mathrm{d}\tilde{\mathbf{r}}$, $\mathrm{d}^{n-1}s=(a)^{-((n-1)^2/n)}\mathrm{d}^{n-1}\tilde{s}$, $\mathrm{d}^n b=(a)^{-2+1/n}\mathrm{d}^n\tilde{b}$, the above expression becomes

$$\begin{aligned}\int_{\mathcal{G}} f[(a,r,s,b)\odot(a',r',s',b')]\mathrm{d}\eta &= \int_{\mathbb{R}^+\times\mathbb{R}^n\times\mathrm{Spin}(n)\times\mathbb{R}^n} f[(\tilde{a},\tilde{r},\tilde{s},\tilde{b})]\frac{(a')^{-1}\mathrm{d}\tilde{a}\mathrm{d}\tilde{r}(a)^{-((n-1)^2/n)}\mathrm{d}^{n-1}\tilde{s}(a)^{-2+1/n}\mathrm{d}^n\tilde{b}}{(\tilde{a}/a')^{n+1}}\\ &= \int_{\mathbb{R}^+\times\mathbb{R}^n\times\mathrm{Spin}(n)\times\mathbb{R}^n} f[(\tilde{a},\tilde{r},\tilde{s},\tilde{b})]\frac{\mathrm{d}\tilde{a}\mathrm{d}\tilde{r}\mathrm{d}^{n-1}\tilde{s}\mathrm{d}^n\tilde{b}}{(\tilde{a})^{n+1}},\end{aligned} \tag{21}$$

which validates the claim that $\mathrm{d}\eta=\mathrm{d}a\mathrm{d}\mathbf{r}\mathrm{d}^{n-1}s\mathrm{d}^n b/a^{n+1}$ is indeed the left Haar measure on $\mathcal{G}$.

Next, we shall construct a novel class of shearlet systems on $Cl_{(p,q)}$ algebras by the combined action of the scaling D_{A_a}, sharing $\mathcal{D}_{S_s}$, spin-rotation $\mathcal{R}_{\mathbf{r}}$, and translation T_b operators on any analyzing function $\Psi\in L^2(\mathbb{R}^{(p,q)},Cl_{(p,q)})$.

For any $a\in\mathbb{R}^+, s\in\mathbb{R}^{n-1}, b\in\mathbb{R}^n$, and $\mathbf{r}\in\mathrm{Spin}(n)$, consider the family of analyzing functions:

$$\Psi^r_{a,s,b}(x)=\left\{D_{A_a}\mathcal{D}_{S_s}\mathcal{R}_rT_b\Psi(x)=a^{(1/2n)-1}\mathbf{r}\Psi\left(A_a^{-1}S_s^{-1}\overline{\mathbf{r}}(x-b)\mathbf{r}\right)\overline{\mathbf{r}}\right\}, \tag{22}$$

which is called as the family of Clifford-valued shearlets on the geometric algebra-$C\ell_{(p,q)}$. The system of functions (22) satisfies the following properties:

(i) The system (22) is a dense subspace of $L^2(\mathbb{R}^n,Cl_{(p,q)})$

(ii) The following norm equality holds good:

$$\left\|\Psi^r_{a,s,b}\right\|_{L^2\left(\mathbb{R}^n,Cl_{(p,q)}\right)}=\|\Psi\|_{L^2\left(\mathbb{R}^n,Cl_{(p,q)}\right)}. \tag{23}$$

(iii) The Clifford Fourier transform of the family of functions $\Psi^{\mathbf{r}}_{a,s,b}(x)$ reads

$$\mathcal{F}_{Cl}\left[\Psi^{\mathbf{r}}_{a,s,b}\right](\xi)=a^{1-(1/2n)}\mathcal{F}_{Cl}[r\Psi(\cdot)\overline{\mathbf{r}}](\mathbf{r}S_sA_a\xi\overline{\mathbf{r}})e^{-Iv(\xi,b)}. \tag{24}$$

Next, we shall present the notion of an admissible Clifford-valued shearlet on the space of Clifford-valued functions $L^2(\mathbb{R}^n,Cl_{(p,q)})$.

Definition 3 (Admissibility). A nontrivial function $\Psi\in L^2(\mathbb{R}^n,Cl_{(p,q)})$ is called an admissible Clifford-valued shearlet if

$$C_\Psi=\int_{\mathbb{R}^+\times\mathbb{R}^{n-1}\times\mathrm{Spin}(n)}\overline{\{\mathcal{F}_{Cl}[\mathbf{r}\Psi(\cdot)\overline{\mathbf{r}}](\mathbf{r}S_sA_a\xi\overline{\mathbf{r}})\}}\{\mathcal{F}_{Cl}[\mathbf{r}\Psi(\cdot)\overline{\mathbf{r}}](\mathbf{r}S_sA_a\xi\overline{\mathbf{r}})\}\frac{\mathrm{d}a\mathrm{d}^{n-1}s\mathrm{d}\mathbf{r}}{a^{(n^2-n+1/n)}}, \tag{25}$$

which is an invertible multivector and finite, i.e., $\xi\in\mathbb{R}^{(p,q)}$.

Remark 1. It is worth noticing that $\mathcal{F}_{Cl}[\mathbf{r}\Psi(\cdot)\overline{\mathbf{r}}](0)=0$, for $\xi=0$; that is, $\Psi(x)=\sum_A\Psi_A(x)e_A$. and

$$\int_{\mathbb{R}^{(p,q)}}\Psi_A(x)e_Ae^{-Iv(0,x)}\mathrm{d}^nx=0, \tag{26}$$

which in turn implies that for every component Ψ_A of the Clifford-valued shearlet Ψ is zero; that is,

$$\int_{\mathbb{R}^{(p,q)}}\Psi_A(x)\mathrm{d}^nx=0. \tag{27}$$

Based on the novel family of Clifford-valued shearlets defined in equation (22), we have the following main definition of the continuous Clifford-valued shearlet transform.

Definition 4. The continuous Clifford-valued shearlet transform of any multivector signal $\mathbf{f} \in L^2(\mathbb{R}^n, Cl_{(p,q)})$ with respect to an analysing Clifford-valued shearlet $\Psi \in L^2(\mathbb{R}^{(p,q)}, Cl_{(p,q)})$ is defined by

$$\begin{aligned}\mathscr{C}\mathscr{S}_\Psi \mathbf{f}(a,r,s,b) &= \langle f, \Psi^r_{a,s,b}\rangle_{L^2\left(\mathbb{R}^{(p,q)},Cl_{(p,q)}\right)} \\ &= \int_{\mathbb{R}^{(p,q)}} \mathbf{f}(x)\overline{\Psi^r_{a,s,b}(x)}\mathrm{d}^n x.\end{aligned} \tag{28}$$

where $\Psi^{\mathbf{r}}_{a,s,b}(x)$ is given by equation (22).

The corresponding spectral representation of the Clifford-valued shearlet transform is

$$\begin{aligned}\mathscr{C}\mathscr{S}_\Psi \mathbf{f}(a,\mathbf{r},s,b) = a^{1-(1/2n)}\int_{\mathbb{R}^n} \mathscr{F}_{Cl}[\mathbf{f}](\xi) \\ \cdot e^{Iv(\xi,b)}\overline{\mathscr{F}_{Cl}[\mathbf{r}\Psi(\cdot)\overline{\mathbf{r}}](\mathbf{r}S_s A_a \xi\overline{\mathbf{r}})}\mathrm{d}^n\xi.\end{aligned} \tag{29}$$

We now present an example for the lucid illustration of the proposed Clifford-valued shearlet transform (28).

Example 1. Consider the Clifford-valued Hermite wavelets [16]as

$$\begin{aligned}\psi_n(x) &= (-1)^n \partial_x^n\left[\exp\left(-\frac{|x|^2}{2}\right)\right], \\ \partial_x^n &= \left(\frac{\partial^n}{\partial x_1} + \frac{\partial^n}{\partial x_2} + \cdots + \frac{\partial^n}{\partial x_n}\right).\end{aligned} \tag{30}$$

Therefore, the corresponding Clifford-valued shearlets of $\psi_n(x)$ are obtained as

$$\Psi^{\mathbf{r}}_{a,s,b}(x) = \left|\det A_a\right|^{-1/2}\mathbf{r}\left(A_a^{-1}S_s^{-1}(x-b)^n\right)\exp\left(-\frac{\left|A_a^{-1}S_s^{-1}(x-b)\right|^2}{2}\right)\overline{\mathbf{r}}, \tag{31}$$

and the Clifford-valued shearlet transform (28) of any function $\mathbf{f} \in L^2(\mathbb{R}^n, Cl_n)$, with respect to the analyzing shearlets (31) can be computed as

$$\begin{aligned}\mathscr{C}\mathscr{S}_\Psi \mathbf{f}(a,\mathbf{r},s,b) = \left|\det A_a\right|^{-1/2}\int_{\mathbb{R}^n} \mathbf{f}(x)\mathbf{r}\left(A_a^{-1}S_s^{-1}(x-b)^n\right) \\ \times \exp\left(-\frac{\left|A_a^{-1}S_s^{-1}(x-b)\right|^2}{2}\right)\overline{\mathbf{r}}\mathrm{d}^n x.\end{aligned} \tag{32}$$

For simplicity, we shall compute the two-dimensional Clifford-valued shearlet transform for the given function $\mathbf{f}$ with respect to the shearlets:

$$\begin{aligned}\Psi^{\mathbf{r}}_{a,s,b}(x_1,x_2) = \left|\det A_a\right|^{-1/2}\left(A_a^{-1}S_s^{-1}\left[(x_1-b_1)^2, (x_2-b_2)^2\right]\right) \\ \times \exp\left(-\frac{\left|A_a^{-1}S_s^{-1}(x_1-b_1, x_2-b_2)\right|^2}{2}\right),\end{aligned} \tag{33}$$

where $A_a = \begin{bmatrix} a & 0 \\ 0 & a^{1/2}\end{bmatrix}, S_s = \begin{bmatrix} 1 & s \\ 0 & 1\end{bmatrix}$. After simplifying, we obtain

$$\begin{aligned}\Psi^{\mathbf{r}}_{a,s,b}(x_1,x_2) = \sqrt{a}\left((x_1-b_1)^2 - \left(s-a^{3/2}\right)(x_2-b_2)^2\right) \\ \times \exp\left(-\frac{(x_1-b_1)^2 + \left(s-a^{-(1/2)}\right)(x_2-b_2)^2}{2a^2}\right).\end{aligned} \tag{34}$$

The two-dimensional analyzing shearlets $\psi^{\mathbf{r}}_{a,s,b}(x_1,x_2)$ given by equation (34) at different values of $a, s, \mathbf{r}$, and b are plotted in Figure 1. The parameters a and s determine the scaling anisotropy and the decaying rate of shearlets providing more accurate location and orientation. In comparison with wavelets, shearlets not only inherits advantages of wavelets $(s = 0)$ but also provide detailed information of position, normal and curvature of discontinuities.

The Clifford-valued shearlet transform of $\mathbf{f}(x_1,x_2) = \exp\{-(x_1^2 + x_2^2)/2\}$ is computed as

$$\mathscr{C}\mathscr{S}_\psi \mathbf{f}(a,\mathbf{r},s,b) = \sqrt{a}\int_{\mathbb{R}^2}\left((x_1-b_1)^2 - \left(s-a^{3/2}\right)(x_2-b_2)^2\right) \times \exp\left(-\frac{(x_1-b_1)^2 + \left(s-a^{-1/2}\right)(x_2-b_2)^2 + a^2\left(x_1^2+x_2^2\right)}{2a^2}\right)\mathrm{d}x_1\mathrm{d}x_2. \tag{35}$$

For different values of $a, s, \mathbf{r}$, and b, the corresponding Clifford-valued shearlet transforms of $\mathbf{f}(x_1,x_2)$ with respect the analysing shearlets (34) are depicted in Figure 2 after computing the integrals (35) in *Mathematica* software. From the simulation, we infer that the Clifford-valued shearlet transform enables a precise characterization of location, orientation, and curvature of discontinuities in two dimensional signals.

In the following theorem, we assemble some of the basic properties of the Clifford-valued shearlet transform (28).

Theorem 1. $\Psi^{\mathbf{r}}_{a,s,b}(x_1,x_2)$*for* $\mathbf{f},\mathbf{g} \in L^2(\mathbb{R}^{(p,q)}, Cl_{(p,q)})$, *and admissible Clifford-valued shearlets* Ψ *and* Φ. *The continuous Clifford-valued shearlet transform (28) satisfies the following properties:*

(i) *Linearity*: $\mathscr{C}\mathscr{S}_\Psi(\alpha\mathbf{f} + \beta\mathbf{g})(a,\mathbf{r},s,b) = \alpha\mathscr{C}\mathscr{S}_\Psi\mathbf{f}(a, \mathbf{r}, s, b) + \beta\mathscr{C}\mathscr{S}_\Psi\mathbf{g}(a,\mathbf{r},s,b), \alpha,\beta \in \mathbf{Cl}_{(\mathbf{p},\mathbf{q})}$

(ii) *Anti* − *linearity*: $\mathscr{C}\mathscr{S}_{\alpha\Psi+\beta\Phi}\mathbf{f}(a,\mathbf{r},s,b) = \mathscr{C}\mathscr{S}_\Psi\mathbf{f}(a,\mathbf{r}, s,b)\overline{\alpha} + \mathscr{C}\mathscr{S}_\Phi\mathbf{f}(a,\mathbf{r},s,b)\overline{\beta}$

(iii) *Translation covariance*: $\mathscr{C}\mathscr{S}_\Psi(T_k\mathbf{f})(a,\mathbf{r},s,b) = \mathscr{C}\mathscr{S}_\Psi\mathbf{f}(a,\mathbf{r},s,b-k)$

(iv) *Dilation covariance*: $\mathscr{C}\mathscr{S}_\Psi(\mathscr{D}_{(1/\gamma)}\mathbf{f}(x))(a,\mathbf{r},s,b) = (\mathscr{C}\mathscr{S}_{\mathscr{D}_\gamma\Psi}\mathbf{f}(x))(a,\mathbf{r},s,(b/\gamma)), \gamma \in \mathbb{R}$

(v) *Parity*: $\mathscr{C}\mathscr{S}_\Psi(P\mathbf{f}(x))(a,\mathbf{r},s,b) = (-1)^n\mathscr{C}\mathscr{S}_{P\Psi}(\mathbf{f}(x))(a,\mathbf{r},s,-b), P\mathbf{f}(x) = \mathbf{f}(-x)$

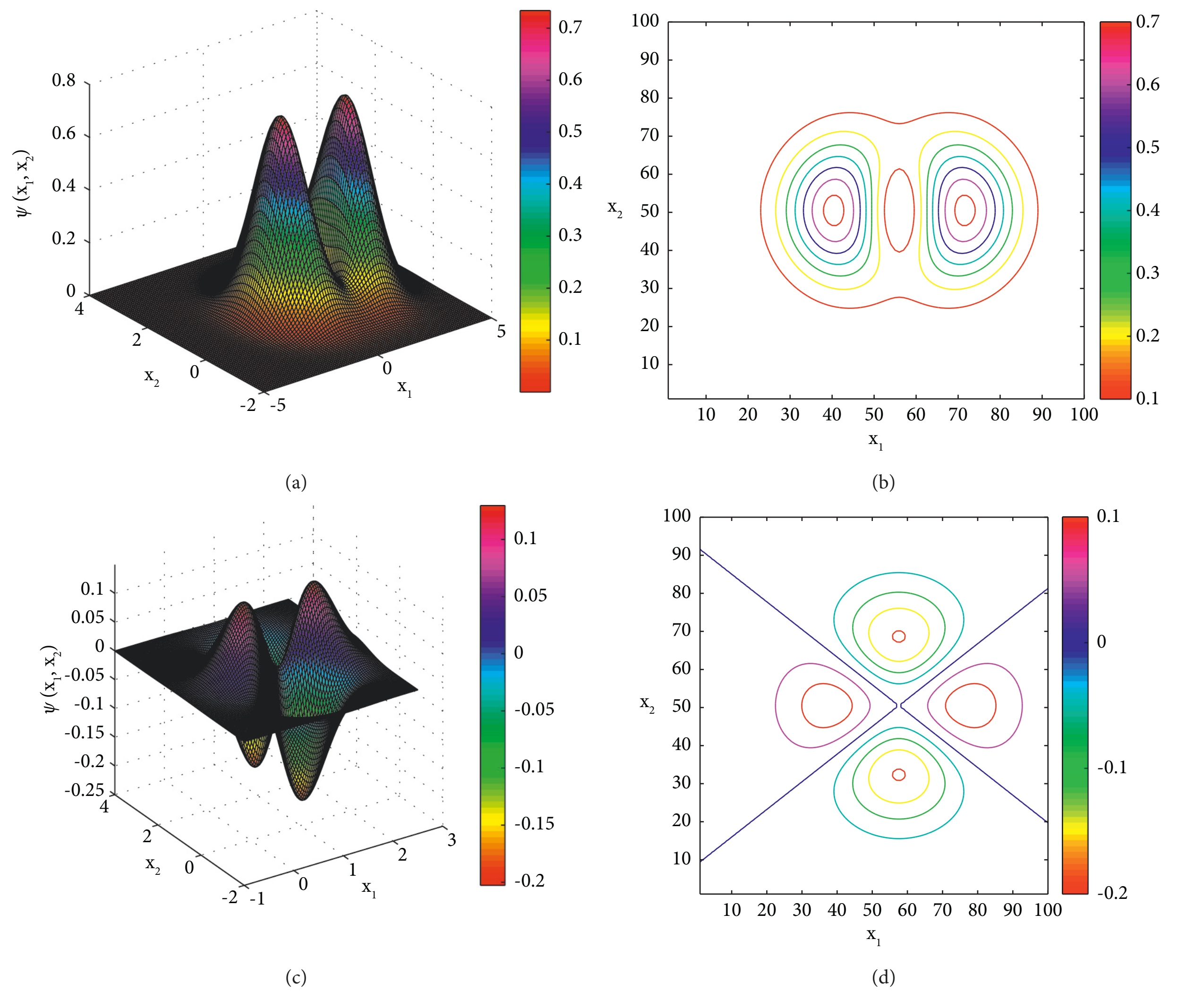

FIGURE 1: Two-dimensional analyzing shearlets $\psi^{\mathbf{r}}_{a,s,b}(x_1, x_2)$ given by equation (34) at different values of $a, \mathbf{r}, b$, and s. (a) 2D-shearlets at $a = 1$, $b = 1$, and $s = 0$. (b) Contour plot of 2D-shearlets at $a = 1$, $b = 1$, and $s = 0$. (c) 2D-shearlets at $a = 1/2$, $b = 1$ and $s = 1$. (d) Contour plot of 2D-shearlets at $a = 1/2$, $b = 1$ and $s = 1$.

(vi) *Translation in* Ψ: $\mathcal{CS}_{T_k\Psi}(\mathbf{f}(x))(a, \mathbf{r}, s, b) = \mathcal{CS}_{\Psi}(\mathbf{f}(x))(a, \mathbf{r}, s, b + k)$

Proof. For the sake of brevity, we omit the proof.

In our next theorem, we show that the Clifford-valued shearlet transform sets up an isometry from $L^2(\mathbb{R}^{(p,q)}, Cl_{(p,q)})$ to $L^2(\mathbb{R}^+ \times \mathbb{R}^{n-1} \times \mathbb{R}^n \times \mathrm{Spin}(n), Cl_{(p,q)})$. □

Theorem 2. *(Plancherel theorem). Let* $\mathcal{CS}_{\Psi}\mathbf{f}(a, \mathbf{r}, s, b)$ *and* $\mathcal{CS}_{\Psi}\mathbf{g}(a, \mathbf{r}, s, b)$ *be the Clifford-valued shearlet transforms of the multivector signals* $\mathbf{f}$ *and* $\mathbf{g}$*, respectively. Then, we have*

$$\int_{\mathbb{R}^+\times\mathbb{R}^{n-1}\times\mathbb{R}^n\times\mathrm{Spin}(n)} Sc\left(\mathcal{CS}_{\Psi}\mathbf{f}(a, \mathbf{r}, s, b)\overline{\mathcal{CS}_{\Psi}\mathbf{g}(a, \mathbf{r}, s, b)}\right)\frac{\mathrm{d}a\mathrm{d}^{n-1}s\mathrm{d}^n b\mathrm{d}\mathbf{r}}{a^{n+1}}$$
$$= (2\pi)^n \int_{\mathbb{R}^{(p,q)}} Sc\left(\mathbf{f}(x)C_{\Psi}\overline{\mathbf{g}(x)}\right)\mathrm{d}^n x = (2\pi)^n \left|\langle \mathbf{f}C_{\Psi}, \mathbf{g}\rangle\right|_{L^2\left(\mathbb{R}^{(p,q)}, Cl_{(p,q)}\right)}, \tag{36}$$

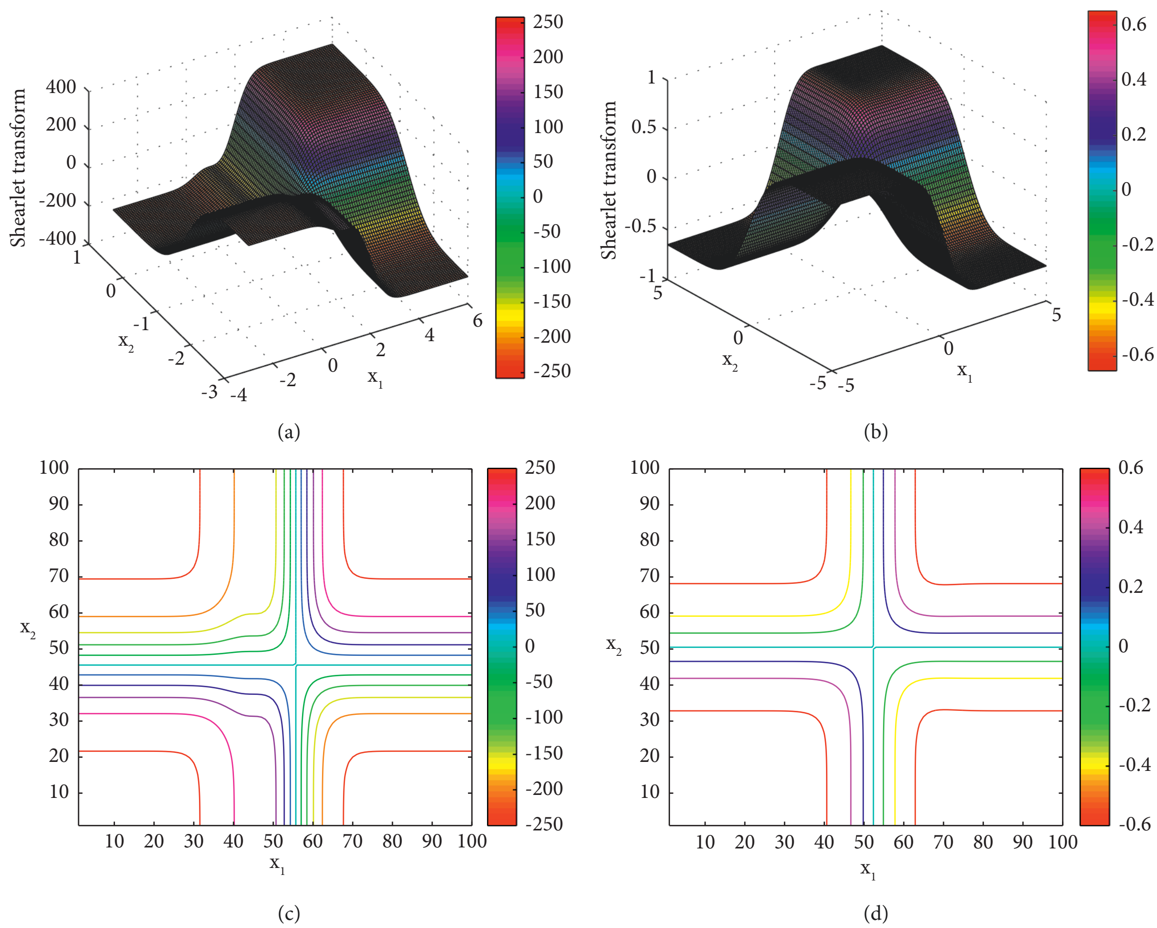

FIGURE 2: Two-dimensional Clifford-valued shearlet transforms of $\mathbf{f}(x_1, x_2) = \exp\{-(x_1^2 + x_2^2)/2\}$ with respect to analyzing function $\Psi^{\mathbf{r}}_{a,s,b}(x_1, x_2)$ given by equation (35). (a) Clifford-valued ST of f at $a = 1/2$, $b = 1$, and $s = 1/2$. (b) Clifford-valued ST of f at $a = b = 1$, and $s = 1$. (c) Contour plot of Clifford-valued ST of f at $a = 1/2$, $b = 1$, and $s = 1/2$. (d) Contour plot of Clifford-valued ST of f at $a = b = 1$, and $s = 1$.

where C_Ψ is given by equation (25).

Proof. .Invoking the spectral representation (29) of Clifford shearlet transforms, we obtain

$$\begin{aligned}
&\int_{\mathbb{R}^+\times\mathbb{R}^{n-1}\times\mathbb{R}^n\times\mathrm{Spin}(n)} Sc\Big(\mathscr{CS}_\Psi \mathbf{f}(a,\mathbf{r},s,b)\overline{\mathscr{CS}_\Psi \mathbf{g}(a,\mathbf{r},s,b)}\Big)\frac{\mathrm{d}a\mathrm{d}^{n-1}s\mathrm{d}^n b\mathrm{d}\mathbf{r}}{a^{n+1}}\\
&= \int_{\mathbb{R}^+\times\mathbb{R}^{n-1}\times\mathbb{R}^n\times\mathrm{Spin}(n)} a^{2-(1/n)} Sc\Big(\int_{\mathbb{R}^n}\mathscr{F}_{Cl}[\mathbf{f}](\xi)e^{Iv(\xi,b)}\overline{\mathscr{F}_{Cl}[\mathbf{r}\Psi(\cdot)\overline{\mathbf{r}}]\left(\mathbf{r}S_sA_a\xi\overline{\mathbf{r}}\right)}\mathrm{d}^n\xi\\
&\times\int_{\mathbb{R}^n}\overline{\mathscr{F}_{Cl}[\mathbf{g}](\xi')e^{Iv(\xi',b)}\overline{\mathscr{F}_{Cl}[\mathbf{r}\Psi(\cdot)\overline{\mathbf{r}}]\left(\mathbf{r}S_sA_a\xi'\overline{\mathbf{r}}\right)}}\mathrm{d}^n\xi'\Big)\frac{\mathrm{d}a\mathrm{d}^{n-1}s\mathrm{d}^n b\mathrm{d}\mathbf{r}}{a^{n+1}},\\
&= \int_{\mathbb{R}^+\times\mathbb{R}^{n-1}\times\mathbb{R}^n\times\mathrm{Spin}(n)} a^{2-(1/n)}\int_{\mathbb{R}^n}\int_{\mathbb{R}^n} Sc\Big(\mathscr{F}_{Cl}[\mathbf{f}](\xi)e^{Iv(\xi,b)}\overline{\mathscr{F}_{Cl}[\mathbf{r}\Psi(\cdot)\overline{\mathbf{r}}]\left(\mathbf{r}S_sA_a\xi\overline{\mathbf{r}}\right)}\\
&\times\mathscr{F}_{Cl}[\mathbf{r}\Psi(\cdot)\overline{\mathbf{r}}]\left(\mathbf{r}S_sA_a\xi'\overline{\mathbf{r}}\right)e^{-Iv(\xi',b)}\overline{\mathscr{F}_{Cl}[\mathbf{g}](\xi')}\Big)\mathrm{d}^n\xi\mathrm{d}^n\xi'\frac{\mathrm{d}a\mathrm{d}^{n-1}s\mathrm{d}^n b\mathrm{d}\mathbf{r}}{a^{n+1}}.
\end{aligned}\tag{37}$$

Then, equation (37) can be rewritten as

$$\int_{\mathbb{R}^+\times\mathbb{R}^{n-1}\times\mathbb{R}^n\times\mathrm{Spin}(n)} Sc\left(\mathscr{C}\mathscr{S}_\Psi \mathbf{f}(a,\mathbf{r},s,b)\overline{\mathscr{C}\mathscr{S}_\Psi \mathbf{g}(a,\mathbf{r},s,b)}\right)\frac{\mathrm{d}a\mathrm{d}^{n-1}s\mathrm{d}^n b\mathrm{d}\mathbf{r}}{a^{n+1}}$$

$$= \int_{\mathbb{R}^+\times\mathbb{R}^{n-1}\times\mathbb{R}^n\times\mathrm{Spin}(n)}\int_{\mathbb{R}^n}\int_{\mathbb{R}^n} Sc\Big(\mathscr{F}_{Cl}[\mathbf{f}](\xi)e^{Iv(\xi,b)}e^{-Iv(\xi',b)}$$

$$\times\overline{\{\mathscr{F}_{Cl}[\mathbf{r}\Psi(\cdot)\overline{\mathbf{r}}](\mathbf{r}S_s A_a\xi\overline{\mathbf{r}})\}}\{\mathscr{F}_{Cl}[\mathbf{r}\Psi(\cdot)\overline{\mathbf{r}}](\mathbf{r}S_s A_a\xi'\overline{\mathbf{r}})\}\overline{\mathscr{F}_{Cl}[\mathbf{g}](\xi')}\Big)\mathrm{d}^n\xi\mathrm{d}^n\xi'\frac{\mathrm{d}a\mathrm{d}\mathbf{r}\mathrm{d}^{n-1}s\mathrm{d}^n b}{a^{(n^2-n+1/n)}}\Bigg)$$

$$= (2\pi)^n\int_{\mathbb{R}^n}\int_{\mathbb{R}^n} Sc\left(\mathscr{F}_{Cl}[\mathbf{f}](\xi)\frac{1}{(2\pi)^n}\int_{\mathbb{R}^n} e^{Iv(\xi-\xi',b)}\mathrm{d}^n b\right)$$

$$\times\int_{\mathbb{R}^+\times\mathrm{Spin}(n)\times\mathbb{R}^{n-1}}\overline{\{\mathscr{F}_{Cl}[\mathbf{r}\Psi(\cdot)\overline{\mathbf{r}}](\mathbf{r}S_s A_a\xi\overline{\mathbf{r}})\}}\{\mathscr{F}_{Cl}[\mathbf{r}\Psi(\cdot)\overline{\mathbf{r}}](\mathbf{r}S_s A_a\xi'\overline{\mathbf{r}})\}\frac{\mathrm{d}a\mathrm{d}\mathbf{r}\mathrm{d}^{n-1}s}{a^{(n^2-n+1/n)}}\times\overline{\mathscr{F}_{Cl}[\mathbf{g}](\xi')}\Big)\mathrm{d}^n\xi\mathrm{d}^n\xi'$$

$$= (2\pi)^n\Big[\int_{\mathbb{R}^n}\int_{\mathbb{R}^n} Sc\big(\mathscr{F}_{Cl}[\mathbf{f}](\xi)\delta(\xi-\xi')$$

$$\times\int_{\mathbb{R}^+\times\mathrm{Spin}(n)\times\mathbb{R}^{n-1}}\overline{\{\mathscr{F}_{Cl}[\mathbf{r}\Psi(\cdot)\overline{\mathbf{r}}](\mathbf{r}S_s A_a\xi\overline{\mathbf{r}})\}}\{\mathscr{F}_{Cl}[\mathbf{r}\Psi(\cdot)\overline{\mathbf{r}}](\mathbf{r}S_s A_a\xi'\overline{\mathbf{r}})\}\frac{\mathrm{d}a\mathrm{d}\mathbf{r}\mathrm{d}^{n-1}s}{a^{(n^2-n+1/n)}}\times\overline{\mathscr{F}_{Cl}[\mathbf{g}](\xi')}\Big)\mathrm{d}^n\xi\mathrm{d}^n\xi'$$

$$= (2\pi)^n\int_{\mathbb{R}^n} Sc\left(\mathscr{F}_{Cl}[\mathbf{f}](\xi)\times\int_{\mathbb{R}^+\times\mathrm{Spin}(n)\times\mathbb{R}^{n-1}}\overline{\{\mathscr{F}_{Cl}[\mathbf{r}\Psi(\cdot)\overline{\mathbf{r}}](\mathbf{r}S_s A_a\xi\overline{\mathbf{r}})\}}\{\mathscr{F}_{Cl}[\mathbf{r}\Psi(\cdot)\overline{\mathbf{r}}](\mathbf{r}S_s A_a\xi\overline{\mathbf{r}})\}\frac{\mathrm{d}a\mathrm{d}\mathbf{r}\mathrm{d}^{n-1}s}{a^{(n^2-n+1/n)}}\times\overline{\mathscr{F}_{Cl}[\mathbf{g}](\xi)}\right)\mathrm{d}^n\xi$$

$$= (2\pi)^n\int_{\mathbb{R}^n} Sc\left(\mathscr{F}_{Cl}[\mathbf{f}](\xi)C_\Psi\overline{\mathscr{F}_{Cl}[\mathbf{g}](\xi)}\right)\mathrm{d}^n\xi$$

$$= (2\pi)^n\int_{\mathbb{R}^{(p,q)}} Sc\left(\mathbf{f}(x)C_\Psi\overline{\mathbf{g}(x)}\right)\mathrm{d}^n x. \tag{38}$$

This completes the proof of Theorem 2. □

Corollary 1. *For* $\mathbf{f}=\mathbf{g}$, *we have the following identity:*

$$\int_{\mathbb{R}^+\times\mathbb{R}^{n-1}\times\mathbb{R}^n\times\mathrm{Spin}(n)}\left|\mathscr{C}\mathscr{S}_\Psi\mathbf{f}(a,\mathbf{r},s,b)\right|^2\frac{\mathrm{d}a\mathrm{d}^{n-1}s\mathrm{d}^n b\mathrm{d}\mathbf{r}}{a^{n+1}} = (2\pi)^n\int_{\mathbb{R}^{(p,q)}} Sc\left(\mathbf{f}(x)C_\Psi\overline{\mathbf{f}(x)}\right)\mathrm{d}^n x. \tag{39}$$

By taking $\Psi\in L^2(\mathbb{R}^{(p,q)},Cl_{(p,q)})$ with $C_\Psi=1$, the Clifford-valued shearlet transform $\mathscr{C}\mathscr{S}_\Psi\mathbf{f}(a,\mathbf{r},s,b)$ becomes an isometry from $L^2(\mathbb{R}^{(p,q)},Cl_{(p,q)})$ to $L^2(\mathbb{R}^+\times\mathbb{R}^{n-1}\times\mathbb{R}^n\times\mathrm{Spin}(n),Cl_{(p,q)})$.

The next theorem guarantees the reconstruction of the input Clifford-valued signal from the corresponding Clifford-valued shearlet transform.

Theorem 3 (Inversion formula). *Any Clifford-valued signal* $\mathbf{f}\in L^2(\mathbb{R}^{(p,q)},Cl_{(p,q)})$ *can be reconstructed from the Clifford-valued shearlet transform* $\mathscr{C}\mathscr{S}_\Psi\mathbf{f}(a,\mathbf{r},s,b)$ *via the formula:*

$$\mathbf{f}(x) = \frac{1}{(2\pi)^n}\int_{\mathbb{R}^+\times\mathbb{R}^{n-1}\times\mathbb{R}^n\times\mathrm{Spin}(n)}\mathscr{C}\mathscr{S}_\Psi\mathbf{f}(a,\mathbf{r},s,b)\Psi^{\mathbf{r}}_{a,s,b}(x)C_\Psi^{-1}\frac{\mathrm{d}a\mathrm{d}^{n-1}s\mathrm{d}^n b\mathrm{d}\mathbf{r}}{a^{n+1}}. \tag{40}$$

Proof. Implication of Plancherel theorem of Clifford-valued shearlet transform (36) for every $g \in L^2(\mathbb{R}^{(p,q)}, Cl_{(p,q)})$ yields that

$$
\begin{aligned}
(2\pi)^n \left|\langle \mathbf{f}C_\Psi, \mathbf{g}\rangle\right|_{L^2\left(\mathbb{R}^{(p,q)},Cl_{(p,q)}\right)} &= \left|\langle \mathcal{CS}_\Psi \mathbf{f}, \mathcal{CS}_\Psi \mathbf{g}\rangle\right|_{L^2\left(\mathcal{G},Cl_{(p,q)}\right)} \\
&= \int_{\mathbb{R}^+\times\mathbb{R}^{n-1}\times\mathbb{R}^n\times\mathrm{Spin}(n)} Sc\left(\mathcal{CS}_\Psi \mathbf{f}(a,\mathbf{r},s,b)\overline{\mathcal{CS}_\Psi \mathbf{g}(a,\mathbf{r},s,b)}\right)\frac{\mathrm{d}a\mathrm{d}^{n-1}s\mathrm{d}^n b\mathrm{d}\mathbf{r}}{a^{n+1}} \\
&= \int_{\mathbb{R}^+\times\mathbb{R}^{n-1}\times\mathbb{R}^n\times\mathrm{Spin}(n)} Sc\left(\mathcal{CS}_\Psi \mathbf{f}(a,\mathbf{r},s,b)\int_{\mathbb{R}^{(p,q)}} \overline{\mathbf{g}(x)\overline{\Psi^{\mathbf{r}}_{a,s,b}(x)}}\right)\mathrm{d}^n x\frac{\mathrm{d}a\mathrm{d}^{n-1}s\mathrm{d}^n b\mathrm{d}\mathbf{r}}{a^{n+1}} \\
&= \int_{\mathbb{R}^+\times\mathbb{R}^{n-1}\times\mathbb{R}^n\times\mathrm{Spin}(n)} \int_{\mathbb{R}^{(p,q)}} Sc\left(\mathcal{CS}_\Psi \mathbf{f}(a,\mathbf{r},s,b)\Psi^{\mathbf{r}}_{a,s,b}(x)\overline{\mathbf{g}(x)}\right)\mathrm{d}^n x\frac{\mathrm{d}a\mathrm{d}^{n-1}s\mathrm{d}^n b\mathrm{d}\mathbf{r}}{a^{n+1}} \\
&= \int_{\mathbb{R}^{(p,q)}}\int_{\mathbb{R}^+\times\mathbb{R}^{n-1}\times\mathbb{R}^n\times\mathrm{Spin}(n)} Sc\left(\mathcal{CS}_\Psi \mathbf{f}(a,\mathbf{r},s,b)\Psi^{\mathbf{r}}_{a,s,b}(x)\right)\frac{\mathrm{d}a\mathrm{d}^{n-1}s\mathrm{d}^n b\mathrm{d}\mathbf{r}}{a^{n+1}}\overline{\mathbf{g}(x)}\mathrm{d}^n x \\
&= \left|\left\langle \int_{\mathbb{R}^+\times\mathbb{R}^{n-1}\times\mathbb{R}^n\times\mathrm{Spin}(n)} \mathcal{CS}_\Psi \mathbf{f}(a,\mathbf{r},s,b)\Psi^{\mathbf{r}}_{a,s,b}(x)\frac{\mathrm{d}a\mathrm{d}^{n-1}s\mathrm{d}^n b\mathrm{d}\mathbf{r}}{a^{n+1}}, \mathbf{g}\right\rangle\right|_{L^2\left(\mathbb{R}^{(p,q)},Cl_{(p,q)}\right)},
\end{aligned}
\tag{41}
$$

where we used the Fubini–Tonelli theorem in getting the second last step. Since $\mathbf{g} \in L^2(\mathbb{R}^{(p,q)}, Cl_{(p,q)})$ is arbitrary, we have

$$
(2\pi)^n \mathbf{f}(x)C_\Psi = \int_{\mathbb{R}^+\times\mathbb{R}^{n-1}\times\mathbb{R}^n\times\mathrm{Spin}(n)} \mathcal{CS}_\Psi \mathbf{f}(a,\mathbf{r},s,b)\Psi^{\mathbf{r}}_{a,s,b}(x)\frac{\mathrm{d}a\mathrm{d}^{n-1}s\mathrm{d}^n b\mathrm{d}\mathbf{r}}{a^{n+1}}, \tag{42}
$$

or equivalently

$$
\mathbf{f}(x) = \frac{1}{(2\pi)^n}\int_{\mathbb{R}^+\times\mathbb{R}^{n-1}\times\mathbb{R}^n\times\mathrm{Spin}(n)} \mathcal{CS}_\Psi \mathbf{f}(a,\mathbf{r},s,b)\Psi^{\mathbf{r}}_{a,s,b}(x)C_\Psi^{-1}\frac{\mathrm{d}a\mathrm{d}^{n-1}s\mathrm{d}^n b\mathrm{d}\mathbf{r}}{a^{n+1}}. \tag{43}
$$

This completes the proof of Theorem 3.

The next theorem presents a characterization of the range of the Clifford-valued shearlet transform $\mathcal{CSH}_\Psi$. The result follows as a consequence of the reconstruction formula (40) and the well known Fubini theorem. □

Theorem 4 (Characterization of range of $\mathcal{CS}_\Psi$). *If $\mathbf{h} = \mathcal{CS}_\Psi \mathbf{f} \in L^2(\mathcal{G}, Cl_{(p,q)})$, let Ψ be an admissible Clifford-valued shearlet. Then, $\mathbf{h}$ is a Clifford-valued shearlet transform of a function $\mathbf{f} \in L^2(\mathcal{G}, Cl_{(p,q)})$ if and only if it satisfies the reproducing property:*

$$
\mathbf{h}(a',\mathbf{r}',s',b') = \frac{1}{(2\pi)^n}\int_{\mathcal{G}} \mathbf{h}(a,\mathbf{r},s,b)\langle \Psi^{\mathbf{r}}_{a,s,b}C_\Psi^{-1}, \Psi^{\mathbf{r}'}_{a',s',b'}\rangle_{L^2\left(\mathbb{R}^{(p,q)},Cl_{(p,q)}\right)}\frac{\mathrm{d}a\mathrm{d}^{n-1}s\mathrm{d}^n b\mathrm{d}\mathbf{r}}{a^{n+1}}. \tag{44}
$$

Proof. Let $\mathbf{h}$ belongs to the range of the Clifford-valued shearlet transform $\mathcal{CS}_\Psi$. Then, there exist a Clifford-valued function $\mathbf{f} \in L^2(\mathbb{R}^{(p,q)}, Cl_{(p,q)})$ such that $\mathcal{CS}_\Psi \mathbf{f} = \mathbf{h}$. In order to show that $\mathbf{h}$ satisfies equation (44), we proceed as

$$\begin{aligned}
\mathbf{h}(a',\mathbf{r}',s',b') &= \mathscr{C}\mathscr{S}_\Psi\mathbf{f}(a',\mathbf{r}',s',b')\\
&= \int_{\mathbb{R}^{(p,q)}} \mathbf{f}(x)\overline{\Psi^{\mathbf{r}'}_{a',s',b'}}\,\mathrm{d}^n x\\
&= \int_{\mathbb{R}^{(p,q)}} \left[\frac{1}{(2\pi)^n}\int_{\mathscr{G}} \mathscr{C}\mathscr{S}_\Psi\mathbf{f}(a,\mathbf{r},s,b)\Psi^{\mathbf{r}}_{a,s,b}(x)C_\Psi^{-1}\frac{\mathrm{d}a\mathrm{d}^{n-1}s\mathrm{d}^n b\mathrm{d}\mathbf{r}}{a^{n+1}}\right]\overline{\Psi^{\mathbf{r}'}_{a',s',b'}}\,\mathrm{d}^n x\\
&= \frac{1}{(2\pi)^n}\int_{\mathscr{G}} \mathscr{C}\mathscr{S}_\Psi\mathbf{f}(a,\mathbf{r},s,b)\left[\int_{\mathbb{R}^{(p,q)}} \Psi^{\mathbf{r}}_{a,s,b}(x)C_\Psi^{-1}\overline{\Psi^{\mathbf{r}'}_{a',s',b'}}\,\mathrm{d}^n x\right]\frac{\mathrm{d}a\mathrm{d}^{n-1}s\mathrm{d}^n b\mathrm{d}\mathbf{r}}{a^{n+1}}\\
&= \frac{1}{(2\pi)^n}\int_{\mathscr{G}} \mathscr{C}\mathscr{S}_\Psi\mathbf{f}(a,\mathbf{r},s,b)\langle\Psi^{\mathbf{r}}_{a,s,b}C_\Psi^{-1},\Psi^{\mathbf{r}'}_{a',s',b'}\rangle_{L^2(\mathbb{R}^{(p,q)},Cl_{(p,q)})}\frac{\mathrm{d}a\mathrm{d}^{n-1}s\mathrm{d}^n b\mathrm{d}\mathbf{r}}{a^{n+1}}\\
&= \frac{1}{(2\pi)^n}\int_{\mathscr{G}} \mathbf{h}(a,\mathbf{r},s,b)\langle\Psi^{\mathbf{r}}_{a,s,b}C_\Psi^{-1},\Psi^{\mathbf{r}'}_{a',s',b'}\rangle_{L^2(\mathbb{R}^{(p,q)},Cl_{(p,q)})}\frac{\mathrm{d}a\mathrm{d}^{n-1}s\mathrm{d}^n b\mathrm{d}\mathbf{r}}{a^{n+1}}.
\end{aligned} \tag{45}$$

Conversely, suppose that an arbitrary function $\mathbf{h}\in L^2(\mathscr{G},Cl_{(p,q)})$ satisfies equation (44). Then, we show that there exists $\mathbf{f}\in L^2(\mathbb{R}^{(p,q)},Cl_{(p,q)})$, such that $\mathscr{C}\mathscr{S}_\Psi\mathbf{f}=\mathbf{h}$. Assume that

$$\mathbf{f}(x) = \frac{1}{(2\pi)^n}\int_{\mathscr{G}} \mathbf{h}(a,\mathbf{r},s,b)\Psi^{\mathbf{r}}_{a,s,b}(x)C_\Psi^{-1}\frac{\mathrm{d}a\mathrm{d}^{n-1}s\mathrm{d}^n b\mathrm{d}\mathbf{r}}{a^{n+1}}. \tag{46}$$

Then, it can be easily verified that

$$\|\mathbf{f}\|^2_{L^2(\mathbb{R}^{(p,q)},Cl_{(p,q)})} = \frac{1}{(2\pi)^{2n}}\left|C_\Psi^{-1}\right|^2\|\Psi^{\mathbf{r}}_{a,s,b}\|^2_{L^2(\mathbb{R}^{(p,q)},Cl_{(p,q)})}\|\mathbf{h}(a,\mathbf{r},s,b)\|^2_{L^2(\mathscr{G},Cl_{(p,q)})}, \tag{47}$$

which implies that $\mathbf{f}\in L^2(\mathbb{R}^{(p,q)},Cl_{(p,q)})$. Moreover, as a consequence of the well-known Fubini theorem and inversion Theorem (40), we have

$$\begin{aligned}
\mathscr{C}\mathscr{S}_\Psi\mathbf{f}(a',\mathbf{r}',s',b') &= \int_{\mathbb{R}^{(p,q)}} \mathbf{f}(x)\overline{\Psi^{\mathbf{r}'}_{a',s',b'}(x)}\,\mathrm{d}^n x\\
&= \int_{\mathbb{R}^{(p,q)}} \left[\frac{1}{(2\pi)^n}\int_{\mathscr{G}} \mathscr{C}\mathscr{S}_\Psi\mathbf{f}(a,\mathbf{r},s,b)\Psi^{\mathbf{r}}_{a,s,b}C_\Psi^{-1}\frac{\mathrm{d}a\mathrm{d}^{n-1}s\mathrm{d}^n b\mathrm{d}\mathbf{r}}{a^{n+1}}\right]\overline{\Psi^{\mathbf{r}'}_{a',s',b'}(x)}\,\mathrm{d}^n x\\
&= \frac{1}{(2\pi)^n}\int_{\mathscr{G}} \mathscr{C}\mathscr{S}_\Psi\mathbf{f}(a,\mathbf{r},s,b)\int_{\mathbb{R}^{(p,q)}} \Psi^{\mathbf{r}}_{a,s,b}C_\Psi^{-1}\overline{\Psi^{\mathbf{r}'}_{a',s',b'}(x)}\,\mathrm{d}^n x\frac{\mathrm{d}a\mathrm{d}^{n-1}s\mathrm{d}^n b\mathrm{d}\mathbf{r}}{a^{n+1}}\\
&= \frac{1}{(2\pi)^n}\int_{\mathscr{G}} \mathbf{h}(a,\mathbf{r},s,b)\langle\Psi^{\mathbf{r}}_{a,s,b}C_\Psi^{-1},\Psi^{\mathbf{r}'}_{a',s',b'}\rangle_{L^2(\mathbb{R}^{(p,q)},Cl_{(p,q)})}\frac{\mathrm{d}a\mathrm{d}^{n-1}s\mathrm{d}^n b\mathrm{d}\mathbf{r}}{a^{n+1}}\\
&= \mathbf{h}(a',\mathbf{r}',s',b').
\end{aligned} \tag{48}$$

This evidently completes the proof of theorem. □

Corollary 2. *For an admissible Clifford shearlet $\Psi\in L^2(\mathbb{R}^{(p,q)},Cl_{(p,q)})$, the range of the Clifford shearlet transform 28) is a reproducing kernel in $L^2(\mathbb{R}^{(p,q)},Cl_{(p,q)})$ with kernel that can be given by*

$$K_\Psi(a,\mathbf{r},s,b,a',\mathbf{r}',s',b') = \frac{1}{(2\pi)^n}\langle\Psi^{\mathbf{r}}_{a,s,b}C_\Psi^{-1},\Psi^{\mathbf{r}'}_{a',s',b'}\rangle_{L^2(\mathbb{R}^{(p,q)},Cl_{(p,q)})}. \tag{49}$$

4. HAP Property for the Clifford-Valued Shearlet Transforms

Homogeneous approximation property (HAP) means that the approximation rate in a reconstruction of signal is essentially invariant under time-scale shifts. The HAP is being extensively used for studying frame density [17]. In this section, we investigate the homogeneous approximation property for the proposed Clifford-valued shearlet transforms. Initially, we shall present some results related to the pointwise convergence of the reconstruction formula (40).

Theorem 5. *Let* $\mathscr{C}\mathscr{S}_\Psi \mathbf{f}(a,\mathbf{r},s,b)$ *be the Clifford-valued shearlet transform of any* $\mathbf{f}\in L^2(\mathbb{R}^{(p,q)},Cl_{(p,q)})$ *such that*

$$\mathbf{f}_{M,N}(x)=\frac{1}{(2\pi)^n}\int_M^N\int_{\mathbb{R}^n\times\mathbb{R}^{n-1}\times \mathrm{Spin}(n)}\mathscr{C}\mathscr{S}_\Psi \mathbf{f}(a,\mathbf{r},s,b)\Psi^{\mathbf{r}}_{a,s,b}(x)C_\Psi^{-1}\frac{\mathrm{d}\mathbf{r}\mathrm{d}^{n-1}s\mathrm{d}^n b\mathrm{d}a}{a^{n+1}},\quad N>M>0, \tag{50}$$

where $\Psi\in L^2(\mathbb{R}^{(p,q)},Cl_{(p,q)})$ *is an admissible Clifford-valued shearlet with* $C_\Psi\neq 0$*, real valued. Then, we have*

$$\mathscr{F}_{Cl}\left[\mathbf{f}_{M,N}\right](\xi)=\mathscr{F}_{Cl}[\mathbf{f}](\xi)\int_M^N\int_{\mathbb{R}^{n-1}\times \mathrm{Spin}(n)}\left|\mathscr{F}_{Cl}[\mathbf{r}\Psi(\cdot)\overline{\mathbf{r}}]\left(\mathbf{r}S_sA_a\xi'\overline{\mathbf{r}}\right)\right|^2C_\Psi^{-1}\frac{\mathrm{d}\mathbf{r}\mathrm{d}^{n-1}s\mathrm{d}a}{a^{\left(n^2-n+1/n\right)}}. \tag{51}$$

Proof. For $M,N\in\mathbb{R}^+$, we define

$$\mathbf{f}_{M,N}(x)=\frac{1}{(2\pi)^n}\int_M^N\int_{\mathbb{R}^n\times\mathbb{R}^{n-1}\times \mathrm{Spin}(n)}\mathscr{C}\mathscr{S}_\Psi \mathbf{f}(a,\mathbf{r},s,b)\Psi^{\mathbf{r}}_{a,s,b}(x)C_\Psi^{-1}\frac{\mathrm{d}\mathbf{r}\mathrm{d}^{n-1}s\mathrm{d}^n b\mathrm{d}a}{a^{n+1}}. \tag{52}$$

Then, the application of Schwartz's inequality implies that

$$\begin{aligned}
&\int_M^N\int_{\mathbb{R}^n\times\mathbb{R}^{n-1}\times \mathrm{Spin}(n)}\left|\mathscr{C}\mathscr{S}_\Psi \mathbf{f}(a,\mathbf{r},s,b)\Psi^{\mathbf{r}}_{a,s,b}(x)\right|C_\Psi^{-1}\frac{\mathrm{d}\mathbf{r}\mathrm{d}^{n-1}s\mathrm{d}^n b\mathrm{d}a}{a^{n+1}}\leq\int_M^N\left\{\int_{\mathbb{R}^n\times\mathbb{R}^{n-1}\times \mathrm{Spin}(n)}\left|\mathscr{C}\mathscr{S}_\Psi \mathbf{f}(a,\mathbf{r},s,b)\right|^2\mathrm{d}\mathbf{r}\mathrm{d}^{n-1}s\mathrm{d}^n b\right\}^{1/2}\\
&\quad\times\left\{\int_{\mathbb{R}^n\times\mathbb{R}^{n-1}\times \mathrm{Spin}(n)}\left|\Psi^{\mathbf{r}}_{a,s,b}(x)\right|^2\mathrm{d}\mathbf{r}\mathrm{d}^{n-1}s\mathrm{d}^n b\right\}^{1/2}C_\Psi^{-1}\frac{\mathrm{d}a}{a^{n+1}}\\
&\quad=\int_M^N\left\{\int_{\mathbb{R}^n\times\mathbb{R}^{n-1}\times \mathrm{Spin}(n)}\left|\mathscr{C}\mathscr{S}_\Psi \mathbf{f}(a,\mathbf{r},s,b)\right|^2\mathrm{d}\mathbf{r}\mathrm{d}^{n-1}s\mathrm{d}^n b\right\}^{1/2}\\
&\quad\times\left\|\Psi^{\mathbf{r}}_{a,s,b}(x)\right\|_{L^2\left(R^n\times R^{n-1}\times \mathrm{Spin}(n)\right)}C_\Psi^{-1}\frac{\mathrm{d}a}{a^{n+1}}\\
&\quad\leq\left\{\int_M^N\int_{\mathbb{R}^n\times\mathbb{R}^{n-1}\times \mathrm{Spin}(n)}\left|\mathscr{C}\mathscr{S}_\Psi \mathbf{f}(a,\mathbf{r},s,b)\right|^2\mathrm{d}\mathbf{r}\mathrm{d}^{n-1}s\mathrm{d}^n b\frac{\mathrm{d}a}{a^{n+1}}\right\}^{1/2}\\
&\quad\times\|\Psi\|_{L^2\left(R^n\times R^{n-1}\times \mathrm{Spin}(n)\right)}C_\Psi^{-1}\left\{\int_M^N\frac{\mathrm{d}a}{a^{n+1}}\right\}^{1/2}\leq\left\{(2\pi)^n\left|\langle \mathbf{f}C_\Psi,\mathbf{f}\rangle\right|_{L^2\left(\mathbb{R}^{(p,q)},Cl_{(p,q)}\right)}\right\}^{1/2}\\
&\quad\|\Psi\|_{L^2\left(R^n\times R^{n-1}\times \mathrm{Spin}(n)\right)}C_\Psi^{-1}\frac{1}{\sqrt{n}}\left[M^{-n}-N^{-n}\right]^{1/2}<\infty.
\end{aligned} \tag{53}$$

This shows that $\mathbf{f}_{M,N}$ is well defined on $\mathbb{R}^2$.

Next, we show that $\mathbf{f}_{M,N}$ is uniformly continuous on $\mathbb{R}^n$. For any $x, x' \in \mathbb{R}^n$, we have

$$\begin{aligned}
\left|\mathbf{f}_{M,N}(x) - \mathbf{f}_{M,N}(x')\right| &= \left|\frac{1}{(2\pi)^n}\int_M^N \int_{\mathbb{R}^n\times\mathbb{R}^{n-1}\times\mathrm{Spin}(n)} \mathscr{C}\mathscr{S}_\Psi \mathbf{f}(a,\mathbf{r},s,b)\left[\Psi^{\mathbf{r}}_{a,s,b}(x) - \Psi^{\mathbf{r}}_{a,s,b}(x')\right] C_\Psi^{-1}\frac{\mathrm{d}\mathbf{r}\mathrm{d}^{n-1}s\mathrm{d}^n b\mathrm{d}a}{a^{n+1}}\right| \\
&\le \left\{\frac{1}{(2\pi)^n}\int_M^N \int_{\mathbb{R}^n\times\mathbb{R}^{n-1}\times\mathrm{Spin}(n)} \left|\mathscr{C}\mathscr{S}_\Psi \mathbf{f}(a,\mathbf{r},s,b)\right|^2 \frac{\mathrm{d}\mathbf{r}\mathrm{d}^{n-1}s\mathrm{d}^n b\mathrm{d}a}{a^{n+1}}\right\}^{1/2} \\
&\quad \times \left\{\frac{1}{(2\pi)^n}\int_M^N \int_{\mathbb{R}^n\times\mathbb{R}^{n-1}\times\mathrm{Spin}(n)} \left|\Psi^{\mathbf{r}}_{a,s,b}(x) - \Psi^{\mathbf{r}}_{a,s,b}(x')\right|^2 \frac{\mathrm{d}\mathbf{r}\mathrm{d}^{n-1}s\mathrm{d}^n b\mathrm{d}a}{a^{n+1}}\right\}^{1/2} \left|C_\Psi^{-1}\right| \\
&\le \frac{1}{(2\pi)^{n/2}}\left\{\left|\langle \mathbf{f}C_\Psi, \mathbf{f}\rangle\right|_{L^2(\mathbb{R}^{(p,q)}, Cl_{(p,q)})}\right\}^{1/2} \times \left\{\int_M^N \int_{\mathbb{R}^n\times\mathbb{R}^{n-1}\times\mathrm{Spin}(n)} \left|\Psi^{\mathbf{r}}_{a,s,b}(x) - \Psi^{\mathbf{r}}_{a,s,b}(x')\right|^2 \frac{\mathrm{d}\mathbf{r}\mathrm{d}^{n-1}s\mathrm{d}^n b\mathrm{d}a}{a^{n+1}}\right\}^{1/2} \left|C_\Psi^{-1}\right|.
\end{aligned} \tag{54}$$

From equation (54), we observe that $|\mathbf{f}_{M,N}(\mathbf{x}) - \mathbf{f}_{M,N}(\mathbf{x}')| \longrightarrow 0$ as $\|x - x'\| \longrightarrow 0$. Thus, we conclude that $\mathbf{f}_{M,N}$ is uniformly continuous on $\mathbb{R}^{(p,q)}$.

Moreover, for any $\mathbf{g} \in L^1 \cap L^2(\mathbb{R}^{(p,q)}, Cl_{(p,q)})$, we have

$$\begin{aligned}
\left|\langle \mathbf{f}_{M,N}, \mathbf{g}\rangle\right|_{L^2(\mathbb{R}^n, Cl_{(p,q)})} &= \int_{\mathbb{R}^n} Sc\left(\mathbf{f}_{M,N}(x)\overline{\mathbf{g}(x)}\right)\mathrm{d}^n x \\
&= Sc\left(\int_{\mathbb{R}^n}\left\{\frac{1}{(2\pi)^n}\int_M^N \int_{\mathbb{R}^n\times\mathbb{R}^{n-1}\times\mathrm{Spin}(n)} \mathscr{C}\mathscr{S}_\Psi \mathbf{f}(a,\mathbf{r},s,b)\Psi^{\mathbf{r}}_{a,s,b}(x) C_\Psi^{-1}\frac{\mathrm{d}\mathbf{r}\mathrm{d}^{n-1}s\mathrm{d}^n b\mathrm{d}a}{a^{n+1}}\right\}\overline{\mathbf{g}(x)}\right)\mathrm{d}^n x \\
&= \frac{1}{(2\pi)^n}\int_M^N \int_{\mathbb{R}^n\times\mathbb{R}^{n-1}\times\mathrm{Spin}(n)} Sc\left(\mathscr{C}\mathscr{S}_\Psi \mathbf{f}(a,\mathbf{r},s,b)\left\{\int_{\mathbb{R}^n}\Psi^{\mathbf{r}}_{a,s,b}(x)\overline{\mathbf{g}(x)}\mathrm{d}^n x\right\}C_\Psi^{-1}\right)\frac{\mathrm{d}\mathbf{r}\mathrm{d}^{n-1}s\mathrm{d}^n b\mathrm{d}a}{a^{n+1}} \\
&= \frac{1}{(2\pi)^n}\int_M^N \int_{\mathbb{R}^n\times\mathbb{R}^{n-1}\times\mathrm{Spin}(n)} Sc\left(\mathscr{C}\mathscr{S}_\Psi \mathbf{f}(a,\mathbf{r},s,b)\overline{\mathscr{C}\mathscr{S}_\Psi \mathbf{g}(a,\mathbf{r},s,b)}\mathrm{d}^n x C_\Psi^{-1}\right)\frac{\mathrm{d}\mathbf{r}\mathrm{d}^{n-1}s\mathrm{d}^n b\mathrm{d}a}{a^{n+1}} \\
&= \frac{1}{(2\pi)^n} Sc\left(\int_M^N \int_{\mathbb{R}^n\times\mathbb{R}^{n-1}\times\mathrm{Spin}(n)}\left\{a^{1-(1/2n)}\int_{\mathbb{R}^n}\mathscr{F}_{Cl}[\mathbf{f}](\xi)e^{Iv(\xi,b)}\overline{\mathscr{F}_{Cl}[\mathbf{r}\Psi(\cdot)\overline{\mathbf{r}}](\mathbf{r}S_sA_a\xi\overline{\mathbf{r}})}\mathrm{d}^n\xi\right\}\right. \\
&\quad \left.\times \overline{\left\{a^{1-(1/2n)}\int_{\mathbb{R}^n}\mathscr{F}_{Cl}[\mathbf{g}](\xi')e^{Iv(\xi,b)}\overline{\mathscr{F}_{Cl}[\mathbf{r}\Psi(\cdot)\overline{\mathbf{r}}](\mathbf{r}S_sA_a\xi'\overline{\mathbf{r}})}\mathrm{d}^n\xi'\right\}} C_\Psi^{-1}\frac{\mathrm{d}\mathbf{r}\mathrm{d}^{n-1}s\mathrm{d}^n b\mathrm{d}a}{a^{n+1}}\right) \\
&= \frac{1}{(2\pi)^n} Sc\left(\int_M^N \int_{\mathbb{R}^n\times\mathbb{R}^{n-1}\times\mathrm{Spin}(n)}\int_{\mathbb{R}^n}\mathscr{F}_{Cl}[\mathbf{f}](\xi)e^{Iv(\xi,b)}\overline{\mathscr{F}_{Cl}[\mathbf{r}\Psi(\cdot)\overline{\mathbf{r}}](\mathbf{r}S_sA_a\xi\overline{\mathbf{r}})}\mathrm{d}^n\xi\right. \\
&\quad \left.\times \int_{\mathbb{R}^n}\mathscr{F}_{Cl}[\mathbf{r}\Psi(\cdot)\overline{\mathbf{r}}](\mathbf{r}S_sA_a\xi'\overline{\mathbf{r}})e^{-Iv(\xi',b)}\overline{\mathscr{F}_{Cl}[\mathbf{g}](\xi')}\mathrm{d}^n\xi' C_\Psi^{-1}\frac{\mathrm{d}\mathbf{r}\mathrm{d}^{n-1}s\mathrm{d}^n b\mathrm{d}a}{a^{(n^2-n+1/n)}}\right) \\
&= \frac{1}{(2\pi)^n} Sc\left(\int_M^N \int_{\mathbb{R}^n\times\mathbb{R}^{n-1}\times\mathrm{Spin}(n)}\int_{\mathbb{R}^n}\int_{\mathbb{R}^n}\mathscr{F}_{Cl}[\mathbf{f}](\xi)e^{Iv(\xi,b)}e^{-Iv(\xi',b)}\overline{\mathscr{F}_{Cl}[\mathbf{r}\Psi(\cdot)\overline{\mathbf{r}}](\mathbf{r}S_sA_a\xi\overline{\mathbf{r}})}\mathrm{d}^n\xi\right. \\
&\quad \left.\times \mathscr{F}_{Cl}[\mathbf{r}\Psi(\cdot)\overline{\mathbf{r}}](\mathbf{r}S_sA_a\xi'\overline{\mathbf{r}})\overline{\mathscr{F}_{Cl}[\mathbf{g}](\xi')}\mathrm{d}^n\xi' C_\Psi^{-1}\frac{\mathrm{d}\mathbf{r}\mathrm{d}^{n-1}s\mathrm{d}^n b\mathrm{d}a}{a^{(n^2-n+1/n)}}\right)
\end{aligned}$$

$$
\begin{aligned}
&= Sc\Bigg(\int_M^N \int_{\mathbb{R}^n\times\mathbb{R}^{n-1}\times \mathrm{Spin}(n)} \int_{\mathbb{R}^n} \mathscr{F}_{Cl}[\mathbf{f}](\xi)\frac{1}{(2\pi)^n}\int_{\mathbb{R}^n} e^{I\upsilon(\xi-\xi',b)}\mathrm{d}^n b\overline{\mathscr{F}_{Cl}[\mathbf{r}\Psi(\cdot)\overline{\mathbf{r}}](\mathbf{r}S_sA_a\xi\overline{\mathbf{r}})}\mathrm{d}^n\xi \\
&\quad\times\mathscr{F}_{Cl}[\mathbf{r}\Psi(\cdot)\overline{\mathbf{r}}](\mathbf{r}S_sA_a\xi\overline{\mathbf{r}})\overline{\mathscr{F}_{Cl}[\mathbf{g}](\xi')}\mathrm{d}^n\xi' C_\Psi^{-1}\frac{\mathrm{d}\mathbf{r}\mathrm{d}^{n-1}s\mathrm{d}^n b\mathrm{d}a}{a^{(n^2-n+1/n)}}\Bigg) \\
&= Sc\Bigg(\int_M^N \int_{\mathbb{R}^n\times\mathbb{R}^{n-1}\times \mathrm{Spin}(n)} \int_{\mathbb{R}^n} \mathscr{F}_{Cl}[\mathbf{f}](\xi)\delta(\xi-\xi')\overline{\mathscr{F}_{Cl}[\mathbf{r}\Psi(\cdot)\overline{\mathbf{r}}](\mathbf{r}S_sA_a\xi\overline{\mathbf{r}})} \\
&\quad\times\mathscr{F}_{Cl}[\mathbf{r}\Psi(\cdot)\overline{\mathbf{r}}](\mathbf{r}S_sA_a\xi'\overline{\mathbf{r}})\overline{\mathscr{F}_{Cl}[\mathbf{g}](\xi')}\mathrm{d}^n\xi' C_\Psi^{-1}\Bigg)\frac{\mathrm{d}\mathbf{r}\mathrm{d}^{n-1}s\mathrm{d}a}{a^{(n^2-n+1/n)}} \\
&= Sc\Bigg(\int_M^N \int_{\mathbb{R}^n\times\mathbb{R}^{n-1}\times \mathrm{Spin}(n)} \int_{\mathbb{R}^n} \mathscr{F}_{Cl}[\mathbf{f}](\xi)\overline{\mathscr{F}_{Cl}[\mathbf{r}\Psi(\cdot)\overline{\mathbf{r}}](\mathbf{r}S_sA_a\xi\overline{\mathbf{r}})} \\
&\quad\overline{\times\mathscr{F}_{Cl}[\mathbf{g}](\xi)\overline{\mathscr{F}_{Cl}[\mathbf{r}\Psi(\cdot)\overline{\mathbf{r}}](\mathbf{r}S_sA_a\xi\overline{\mathbf{r}})}}\mathrm{d}^n\xi C_\Psi^{-1}\frac{\mathrm{d}\mathbf{r}\mathrm{d}^{n-1}s\mathrm{d}a}{a^{(n^2-n+1/n)}}\Bigg) \\
&= \int_M^N \int_{\mathbb{R}^{n-1}\times \mathrm{Spin}(n)} \int_{\mathbb{R}^n} Sc\Big(\mathscr{F}_{Cl}[\mathbf{f}](\xi)\big|\mathscr{F}_{Cl}[\mathbf{r}\Psi(\cdot)\overline{\mathbf{r}}](\mathbf{r}S_sA_a\xi\overline{\mathbf{r}})\big|^2\overline{\mathscr{F}_{Cl}[\mathbf{g}](\xi)}\mathrm{d}^n\xi C_\Psi^{-1}\Big)\frac{\mathrm{d}\mathbf{r}\mathrm{d}^{n-1}s\mathrm{d}a}{a^{(n^2-n+1/n)}} \\
&= \int_{\mathbb{R}^n} Sc\Bigg(\bigg\{\mathscr{F}_{Cl}[\mathbf{f}](\xi)\int_M^N \int_{\mathbb{R}^{n-1}\times \mathrm{Spin}(n)} \big|\mathscr{F}_{Cl}[\mathbf{r}\Psi(\cdot)\overline{\mathbf{r}}](\mathbf{r}S_sA_a\xi\overline{\mathbf{r}})\big|^2 C_\Psi^{-1}\frac{\mathrm{d}\mathbf{r}\mathrm{d}^{n-1}s\mathrm{d}a}{a^{(n^2-n+1/n)}}\bigg\}\overline{\mathscr{F}_{Cl}[\mathbf{g}](\xi)}\Bigg)\mathrm{d}^n\xi.
\end{aligned}
\tag{55}
$$

Invoking scalar part for the Clifford Fourier transform, we can deduce that

$$
\mathscr{F}\left[\mathbf{f}_{M,N}\right](\xi) = \mathscr{F}_{Cl}[\mathbf{f}](\xi)\int_M^N \int_{\mathbb{R}^{n-1}\times \mathrm{Spin}(n)} \big|\mathscr{F}_{Cl}[\mathbf{r}\Psi(\cdot)\overline{\mathbf{r}}](\mathbf{r}S_sA_a\xi\overline{\mathbf{r}})\big|^2 C_\Psi^{-1}\frac{\mathrm{d}\mathbf{r}\mathrm{d}^{n-1}s\mathrm{d}a}{a^{(n^2-n+1/n)}}. \tag{56}
$$

This completes the proof of Theorem 5. □

Theorem 6. *Let $\Psi \in L^2(\mathbb{R}^{(p,q)}, Cl_{(p,q)})$ be an admissible Clifford-valued shearlet. Then, for any $\mathbf{f} \in L^1 \cap L^2(\mathbb{R}^{(p,q)}, Cl_{(p,q)})$, we have*

$$
\begin{aligned}
&\lim_{M\longrightarrow 0}, N \longrightarrow \infty\left\|\mathbf{f}-\mathbf{f}_{M,N}\right\|_\infty = 0, \\
&\lim_{M\longrightarrow 0}, N \longrightarrow \infty\left\|\mathbf{f}-\mathbf{f}_{M,N}\right\|_2 = 0.
\end{aligned}
\tag{57}
$$

Proof. Using Parseval's formula for the Clifford Fourier transforms together with an application of Theorem 5, we have

$$
\begin{aligned}
\left\|\mathbf{f}-\mathbf{f}_{M,N}\right\|_{L^\infty(\mathbb{R}^n, Cl_{(p,q)})} &\le \left\|\mathbf{f}-\mathbf{f}_{M,N}\right\|_{L^1(\mathbb{R}^n, Cl_{(p,q)})} \\
&= \left\|\mathscr{F}_{Cl}[\mathbf{f}](\xi)-\mathscr{F}_{Cl}\left[\mathbf{f}_{M,N}\right](\xi)\right\|_{L^1(\mathbb{R}^n, Cl_{(p,q)})} \\
&= \|\mathscr{F}_{Cl}[\mathbf{f}](\xi)-\bigg\{\mathscr{F}_{Cl}[\mathbf{f}](\xi)\int_M^N\int_{\mathbb{R}^{n-1}}\times\mathrm{Spin}(n)\times\big|\mathscr{F}_{Cl}[\mathbf{r}\Psi(\cdot)\overline{\mathbf{r}}](\mathbf{r}S_sA_a\xi\overline{\mathbf{r}})\big|^2\frac{\mathrm{d}\mathbf{r}\mathrm{d}^{n-1}s\mathrm{d}a}{a^{(n^2-n+1/n)}}C_\Psi^{-1}\bigg\}\|_{L^1(\mathbb{R}^n, Cl_{(p,q)})} \\
&= \|\mathscr{F}_{Cl}[\mathbf{f}](\xi)\bigg\{1-\int_M^N\int_{\mathbb{R}^{n-1}}\times\mathrm{Spin}(n)\times\big|\mathscr{F}_{Cl}[\mathbf{r}\Psi(\cdot)\overline{\mathbf{r}}](\mathbf{r}S_sA_a\xi\overline{\mathbf{r}})\big|^2\frac{\mathrm{d}\mathbf{r}\mathrm{d}^{n-1}s\mathrm{d}a}{a^{(n^2-n+1/n)}}C_\Psi^{-1}\bigg\}\|_{L^1(\mathbb{R}^n, Cl_{(p,q)})} \\
&= \int_{\mathbb{R}^n}\big|\mathscr{F}_{Cl}[\mathbf{f}](\xi)\big|\|1-\int_M^N\int_{\mathbb{R}^{n-1}}\times\mathrm{Spin}(n)\times\big|\mathscr{F}_{Cl}[\mathbf{r}\Psi(\cdot)\overline{\mathbf{r}}](\mathbf{r}S_sA_a\xi\overline{\mathbf{r}})\big|^2\frac{\mathrm{d}\mathbf{r}\mathrm{d}^{n-1}s\mathrm{d}a}{a^{(n^2-n+1/n)}}C_\Psi^{-1}|\mathrm{d}^n\xi.
\end{aligned}
\tag{58}
$$

Since Ψ is given to be admissible, it follows that

$$\begin{aligned}&\int_M^N\int_{\mathbb{R}^{n-1}\times\mathrm{Spin}(n)}\left|\mathscr{F}_{Cl}[\mathbf{r}\Psi(\cdot)\overline{\mathbf{r}}](\mathbf{r}S_sA_a\xi\overline{\mathbf{r}})\right|^2\frac{\mathrm{d}\mathbf{r}\mathrm{d}^{n-1}s\mathrm{d}a}{a^{(n^2-n+1/n)}}\\&\leq\int_{\mathbb{R}^+}\int_{\mathbb{R}^{n-1}\times\mathrm{Spin}(n)}\left|\mathscr{F}_{Cl}[\mathbf{r}\Psi(\cdot)\overline{\mathbf{r}}](\mathbf{r}S_sA_a\xi\overline{\mathbf{r}})\right|^2\frac{\mathrm{d}\mathbf{r}\mathrm{d}^{n-1}s\mathrm{d}a}{a^{(n^2-n+1/n)}}=C_\Psi<\infty.\end{aligned}\tag{59}$$

Therefore, we have

$$\lim_{M\longrightarrow 0}, N\longrightarrow\infty\left|1-\int_M^N\int_{\mathbb{R}^{n-1}\times\mathrm{Spin}(n)}\mathscr{F}_{Cl}[\mathbf{r}\Psi(\cdot)\overline{\mathbf{r}}](\mathbf{r}S_sA_a\xi\overline{\mathbf{r}})|^2\frac{\mathrm{d}\mathbf{r}\mathrm{d}^{n-1}s\mathrm{d}a}{a^{(n^2-n+1/n)}}C_\Psi^{-1}\right|=0.\tag{60}$$

Using dominated convergence theorem in equation (58), we conclude that

$$\lim_{M\longrightarrow 0}, N\longrightarrow\infty\|\mathbf{f}-\mathbf{f}_{M,N}\|_{L^\infty(\mathbb{R}^n,Cl_{(p,q)})}=0.\tag{61}$$

Proceeding in a manner similar to the above case, we can show that

$$\lim_{M\longrightarrow 0}, N\longrightarrow\infty\|\mathbf{f}-\mathbf{f}_{M,N}\|_{L^2(\mathbb{R}^n,Cl_{(p,q)})}=0.\tag{62}$$

This completes the proof of Theorem 6.

In the sequel, we study the homogeneous approximation property for the proposed Clifford-valued shearlet transforms. Prior to that, we introduce some notations as given below:

For every $(a',\mathbf{r}',s',b')\in L^2(\mathbb{R}^+\times\mathrm{Spin}(n)\times\mathbb{R}^{n-1}\times\mathbb{R}^n,Cl_{(p,q)})$ and $M>N,P>0$, we denote

$$\begin{aligned}Q_{M,N;P}&=([-N,-M]\cup[N,M])\times\mathrm{Spin}(n)\times[-P,P]^{n-1}\times[-P,P]^n,\\(a',s',b',\mathbf{r}')Q_{M,N;P}&=\{(a',s',b',\mathbf{r}')(a,s,b,\mathbf{r})\\&=\left(a'a,s'+a'^{1-(1/n)}s+s',b'+S_{s'}A_{a'}b,\mathbf{r}'\mathbf{r}\right)\Big\},\end{aligned}\tag{63}$$

where $a\in[-N,-M]\cup[N,M],\mathbf{r}\in\mathrm{Spin}(n),s\in[-P,P]^{n-1}$ and $b\in[-P,P]^n$. □

Theorem 7. *Let $\Psi\in L^2(\mathbb{R}^{(p,q)},Cl_{(p,q)})$be an admissible Clifford-valued shearlet with $C_\Psi\neq 0$, real valued. Then, for any $\mathbf{f}\in L^2(\mathbb{R}^{(p,q)},Cl_{(p,q)})$ and $\varepsilon>0$, there exist some constants $N>M>0,P>0$, such that for any $(a',\mathbf{r}',s',b')\in L^2(\mathbb{R}^+\times Spin(n)\times\mathbb{R}^{n-1}\times\mathbb{R}^n,Cl_{(p,q)})$, with any $0<M'\leq M,N\leq N'$ and $P'\geq P$, we have*

$$\left\|\mathbf{f}_{a',s',b'}^{\mathbf{r}'}-\int_{(a,s,b,\mathbf{r})\in\mathscr{Q}}\langle\mathbf{f}_{a',s',b'}^{\mathbf{r}'},\Psi_{a,s,b}^{\mathbf{r}}\rangle C_\Psi^{-1}\Psi_{a,s,b}^{\mathbf{r}}\frac{\mathrm{d}a\mathrm{d}^{n-1}s\mathrm{d}^nb\mathrm{d}\mathbf{r}}{a^{n+1}}\right\|_{L^2(\mathbb{R}^{(p,q)},Cl_{(p,q)})}^2<\varepsilon,\tag{64}$$

where $(a',s',b',\mathbf{r}')Q_{M',N';P'}=\mathscr{Q}'$.

Proof. For an arbitrary $\mathbf{g}\in L^2(\mathbb{R}^{(p,q)},Cl_{(p,q)})$, we have

$$
\begin{aligned}
&\left\| \mathbf{f}_{a'}, s', b'^{\mathbf{r}} - \int_{(a,s,b,\mathbf{r})\in \mathcal{Q}} \langle \mathbf{f}_{a'}, s', b'^{\mathbf{r}}, \Psi^{\mathbf{r}}_{a,s,b}\rangle C_{\Psi}^{-1}\Psi^{\mathbf{r}}_{a,s,b}\frac{\mathrm{d}a\mathrm{d}^{n-1}s\mathrm{d}^{n}b\mathrm{d}\mathbf{r}}{a^{n+1}}\right\|^{2}_{L^{2}\mathbb{R}^{(p,q)},Cl_{(p,q)}} \\
&= \sup_{\|\mathbf{g}\|=1}\left|\langle \mathbf{f}_{a'}, s', b'^{\mathbf{r}} - \int_{(a,s,b,\mathbf{r})\in \mathcal{Q}'} \langle \mathbf{f}_{a'}, s', b'^{\mathbf{r}}, \Psi^{\mathbf{r}}_{a,s,b}\rangle C_{\Psi}^{-1}\Psi^{\mathbf{r}}_{a,s,b}\frac{\mathrm{d}a\mathrm{d}^{n-1}s\mathrm{d}^{n}b\mathrm{d}\mathbf{r}}{a^{n+1}}, \mathbf{g}\rangle\right|^{2} \\
&= \sup_{\|\mathbf{g}\|=1}\left|\langle \mathbf{f}_{a'}, s', b'^{\mathbf{r}}, \mathbf{g}\rangle \left\langle \int_{(a,s,b,\mathbf{r})\in \mathcal{Q}'} \langle \mathbf{f}_{a'}, s', b'^{\mathbf{r}}, \Psi^{\mathbf{r}}_{a,s,b}\rangle C_{\Psi}^{-1}\Psi^{\mathbf{r}}_{a,s,b}\frac{\mathrm{d}a\mathrm{d}^{n-1}s\mathrm{d}^{n}b\mathrm{d}\mathbf{r}}{a^{n+1}}, \mathbf{g}\right\rangle\right|^{2} \\
&= \sup_{\|\mathbf{g}\|=1}\left|\langle \mathbf{f}_{a'}, s', b'^{\mathbf{r}}, \mathbf{g}\rangle - \int_{(a,s,b,\mathbf{r})\in \mathcal{Q}'} \langle \mathbf{f}_{a'}, s', b'^{\mathbf{r}}, \Psi^{\mathbf{r}}_{a,s,b}\rangle C_{\Psi}^{-1}\Psi^{\mathbf{r}}_{a,s,b}\frac{\mathrm{d}a\mathrm{d}^{n-1}s\mathrm{d}^{n}b\mathrm{d}\mathbf{r}}{a^{n+1}}\right|^{2} \\
&= \sup_{\|\mathbf{g}\|=1}\left|\int_{(a,s,b,\mathbf{r})\notin \mathcal{Q}'} \langle \mathbf{f}_{a'}, s', b'^{\mathbf{r}}, \Psi^{\mathbf{r}}_{a,s,b}\rangle C_{\Psi}^{-1}\Psi^{\mathbf{r}}_{a,s,b}\frac{\mathrm{d}a\mathrm{d}^{n-1}s\mathrm{d}^{n}b\mathrm{d}\mathbf{r}}{a^{n+1}}\right|^{2} \\
&\leq \sup_{\|\mathbf{g}\|=1}\int_{(a,s,b,\mathbf{r})\notin \mathcal{Q}'} \langle \mathbf{f}_{a'}, s', b'^{\mathbf{r}}, \Psi^{\mathbf{r}}_{a,s,b}\rangle \left|C_{\Psi}^{-1}\right|^{2}\frac{\mathrm{d}a\mathrm{d}^{n-1}s\mathrm{d}^{n}b\mathrm{d}\mathbf{r}}{a^{n+1}} \times \int_{(a,s,b,\mathbf{r})\notin \mathcal{Q}'} \left|\langle \Psi^{\mathbf{r}}_{a,s,b}, \mathbf{g}\rangle^{2}\right|\frac{\mathrm{d}a\mathrm{d}^{n-1}s\mathrm{d}^{n}b\mathrm{d}\mathbf{r}}{a^{n+1}} \\
&= \int_{(a,s,b,\mathbf{r})\notin \mathcal{Q}'} \left|\langle \mathbf{f}_{a'}, s', b'^{\mathbf{r}}, \Psi^{\mathbf{r}}_{a,s,b}\rangle\right|^{2} \left|C_{\Psi}^{-1}\right|^{2}\frac{\mathrm{d}a\mathrm{d}^{n-1}s\mathrm{d}^{n}b\mathrm{d}\mathbf{r}}{a^{n+1}} \times \sup_{\|\mathbf{g}\|=1}\int_{(a,s,b,\mathbf{r})\notin \mathcal{Q}'} \left|\langle \mathbf{g}, \Psi^{\mathbf{r}}_{a,s,b}\rangle^{2}\right|\frac{\mathrm{d}a\mathrm{d}^{n-1}s\mathrm{d}^{n}b\mathrm{d}\mathbf{r}}{a^{n+1}} \\
&= \int_{(a,s,b,\mathbf{r})\notin \mathcal{Q}'} \left|\langle \mathbf{f}_{a'}, s', b'^{\mathbf{r}}, \Psi^{\mathbf{r}}_{a,s,b}\rangle\right|^{2} \left|C_{\Psi}^{-1}\right|^{2}\frac{\mathrm{d}a\mathrm{d}^{n-1}s\mathrm{d}^{n}b\mathrm{d}\mathbf{r}}{a^{n+1}} \times \sup_{\|\mathbf{g}\|=1}\int_{(a,s,b,\mathbf{r})\notin \mathcal{Q}'} \left|\mathscr{C}\mathscr{S}_{\Psi}\mathbf{g}(a,s,b,\mathbf{r})\right|^{2}\frac{\mathrm{d}a\mathrm{d}^{n-1}s\mathrm{d}^{n}b\mathrm{d}\mathbf{r}}{a^{n+1}} \\
&= \int_{(a,s,b,\mathbf{r})\notin \mathcal{Q}'} \left|\langle \mathbf{f}_{a'}, s', b'^{\mathbf{r}}, \Psi^{\mathbf{r}}_{a,s,b}\rangle\right|^{2} \left|C_{\Psi}^{-1}\right|^{2}\frac{\mathrm{d}a\mathrm{d}^{n-1}s\mathrm{d}^{n}b\mathrm{d}\mathbf{r}}{a^{n+1}} \times C_{\Psi} \\
&= \int_{(a,s,b,\mathbf{r})\notin \mathcal{Q}_{M',N';P'}} \left|\langle \mathbf{f}, \Psi^{\mathbf{r}}_{a,s,b}\rangle\right|^{2}\frac{\mathrm{d}a\mathrm{d}^{n-1}s\mathrm{d}^{n}b\mathrm{d}\mathbf{r}}{a^{n+1}}\left|C_{\Psi}^{-1}\right|^{2} \times C_{\Psi}.
\end{aligned}
\tag{65}
$$

By choosing N and P large enough and M arbitrary small, we can make R. H. S as small as we need. This completes the proof of Theorem 7. □

5. Uncertainty Principles for the Clifford-Valued Shearlet Transforms

In this section, we shall establish several uncertainty inequalities including Heisenberg–Pauli–Weyl uncertainty inequality, Pitt's inequality, and logarithmic and local uncertainty inequality for the Clifford-valued shearlet transform as defined by equation (28). Prior to establishing the uncertainty principle for the Clifford-valued shearlet transform, we have the following lemma which shall be employed for deriving certain uncertainty inequalities and whose proof follows directly from the Parseval's and inversion formulae of the Clifford Fourier transforms.

Lemma 1. *Let* $\Psi \in L^2(\mathbb{R}^{(p,q)}, Cl_{(p,q)})$ *be an admissible Clifford-valued shearlet. Then, for any* $\mathbf{f} \in L^2(\mathbb{R}^{(p,q)}, Cl_{(p,q)})$*, we have*

$$
\mathscr{F}_{Cl}\left[\mathscr{C}\mathscr{S}_{\Psi}\mathbf{f}(a,\mathbf{r},s,b)\right](\xi) = (2\pi)^{(n/2)}a^{1-(1/2n)}\mathscr{F}_{Cl}[\mathbf{f}](\xi)\overline{\mathscr{F}_{Cl}\left[\mathbf{r}\Psi(\cdot)\overline{\mathbf{r}}\right]\left(\mathbf{r}S_{s}A_{a}\xi\overline{\mathbf{r}}\right)}. \tag{66}
$$

Theorem 8 (Heisenberg–Weyl inequality). *Let* $\mathscr{C}\mathscr{S}_{\Psi}\mathbf{f}(a,\mathbf{r},s,b)$ *be the Clifford-valued shearlet transform of any Clifford-valued function* $\mathbf{f} \in L^2(\mathbb{R}^{(p,q)}, Cl_{(p,q)})$*. Then, the following inequality follows*

$$\left\|b\mathscr{C}\mathscr{S}_{\Psi}\mathbf{f}(a,\mathbf{r},s,b)\right\|_{L^2\left(\mathscr{G},Cl_{(p,q)}\right)}\left\|\xi\mathscr{F}_{Cl}[\mathbf{f}](\xi)C_{\Psi}\right\|_{L^2\left(\mathbb{R}^{(p,q)},Cl_{(p,q)}\right)}\geq\frac{1}{2}\left|\langle\mathbf{f}(x)C_{\Psi},\mathbf{f}(x)\rangle\right|_{L^2\left(\mathscr{G},Cl_{(p,q)}\right)}. \tag{67}$$

Proof. For any Clifford-valued function $\mathbf{f}\in L^2(\mathbb{R}^{(p,q)}, Cl_{(p,q)})$, the Heisenberg–Paul–Weyl inequality for the Clifford Fourier transforms [8, 18] is given by

$$\left\{\int_{\mathbb{R}^n}|b|^2|\mathbf{f}(b)|^2\mathrm{d}^n b\right\}^{1/2}\left\{\int_{\mathbb{R}^n}|\xi|^2\left|\mathscr{F}_{Cl}[\mathbf{f}](\xi)\right|\mathrm{d}^n\xi\right\}^{1/2}\geq\frac{1}{2(2\pi)^{n/2}}\int_{\mathbb{R}^n}|\mathbf{f}(b)|^2\mathrm{d}^n b. \tag{68}$$

Considering $\mathscr{C}\mathscr{S}_{\Psi}\mathbf{f}(a,\mathbf{r},s,b)$ as a function of b and replacing $\mathbf{f}$ by $\mathscr{C}\mathscr{S}_{\Psi}\mathbf{f}(a,\mathbf{r},s,b)$ in (68), we get

$$\left\{\int_{\mathbb{R}^n}|b|^2\left|\mathscr{C}\mathscr{S}_{\Psi}\mathbf{f}(a,\mathbf{r},s,b)\right|^2\mathrm{d}^n b\right\}^{1/2}\left\{\int_{\mathbb{R}^n}|\xi|^2\left|\mathscr{F}_{Cl}\left[\mathscr{C}\mathscr{S}_{\Psi}\mathbf{f}(a,\mathbf{r},s,b)\right](\xi)\right|^2\mathrm{d}^n\xi\right\}^{1/2}\geq\frac{1}{2(2\pi)^{(n/2)}}\int_{\mathbb{R}^n}\left|\mathscr{C}\mathscr{S}_{\Psi}\mathbf{f}(a,\mathbf{r},s,b)\right|^2\mathrm{d}^n b. \tag{69}$$

We now integrate the above inequality with respect to measure $(\mathrm{d}\mathbf{r}\mathrm{d}^{n-1}s\mathrm{d}a/a^{n+1})$, and using Schwartz inequality, to obtain

$$\begin{aligned}&\left\{\int_{\mathbb{R}^+\times\mathbb{R}^{n-1}\times\mathrm{Spin}(n)}\int_{\mathbb{R}^n}|b|^2\left|\mathscr{C}\mathscr{S}_{\Psi}\mathbf{f}(a,\mathbf{r},s,b)\right|^2\mathrm{d}^n b\frac{\mathrm{d}\mathbf{r}\mathrm{d}^{n-1}s\mathrm{d}a}{a^{n+1}}\right\}^{1/2}\times\left\{\int_{\mathbb{R}^+\times\mathbb{R}^{n-1}\times\mathrm{Spin}(n)}\int_{\mathbb{R}^n}|\xi|^2\left|\mathscr{F}_c\left[\mathscr{C}\mathscr{S}_{\Psi}\mathbf{f}(a,\mathbf{r},s,b)\right](\xi)\right|^2\mathrm{d}^n\xi\frac{\mathrm{d}\mathbf{r}\mathrm{d}^{n-1}s\mathrm{d}a}{a^{n+1}}\right\}^{1/2}\\&\geq\frac{1}{2(2\pi)^{(n/2)}}\int_{\mathbb{R}^+\times\mathbb{R}^{n-1}\times\mathrm{Spin}(n)}\int_{\mathbb{R}^n}\left|\mathscr{C}\mathscr{S}_{\Psi}\mathbf{f}(a,\mathbf{r},s,b)\right|^2\frac{\mathrm{d}\mathbf{r}\mathrm{d}^{n-1}s\mathrm{d}a}{a^{n+1}}\mathrm{d}^n b.\end{aligned} \tag{70}$$

Using Lemma 1 together with Fubini theorem, we obtain

$$\begin{aligned}&\left\{\int_{\mathbb{R}^n\times\mathbb{R}^+\times\mathbb{R}^{n-1}\times\mathrm{Spin}(n)}|b|^2\left|\mathscr{C}\mathscr{S}_{\Psi}\mathbf{f}(a,\mathbf{r},s,b)\right|^2\mathrm{d}^n b\frac{\mathrm{d}\mathbf{r}\mathrm{d}^{n-1}s\mathrm{d}a}{a^{n+1}}\right\}^{(1/2)}\\&\times\left\{\int_{\mathbb{R}^+\times\mathbb{R}^{n-1}\times\mathrm{Spin}(n)}\int_{\mathbb{R}^n}|\xi|^2\left|(2\pi)^{(n/2)}a^{1-(1/2n)}\mathscr{F}_{Cl}[\mathbf{f}](\xi)\overline{\mathscr{F}_{Cl}[\mathbf{r}\Psi(\cdot)\overline{\mathbf{r}}]\left(\mathbf{r}S_sA_a\xi\overline{\mathbf{r}}\right)}\right|^2\mathrm{d}^n\xi\frac{\mathrm{d}\mathbf{r}\mathrm{d}^{n-1}s\mathrm{d}a}{a^{n+1}}\right\}^{(1/2)}\\&\geq\frac{1}{2(2\pi)^{(n/2)}}\int_{\mathbb{R}^n\times\mathbb{R}^+\times\mathbb{R}^{n-1}\times\mathrm{Spin}(n)}\left|\mathscr{C}\mathscr{S}_{\Psi}\mathbf{f}(a,\mathbf{r},s,b)\right|^2\frac{\mathrm{d}\mathbf{r}\mathrm{d}^{n-1}s\mathrm{d}a}{a^{n+1}}\mathrm{d}^n b.\end{aligned} \tag{71}$$

Equivalently, we have

$$\begin{aligned}&\left\{\int_{\mathscr{G}}|b|^2\left|\mathscr{C}\mathscr{S}_{\Psi}\mathbf{f}(a,\mathbf{r},s,b)\right|^2\mathrm{d}\eta\right\}^{1/2}\times\left\{\int_{\mathbb{R}^n}|\xi|^2\left|\mathscr{F}_{Cl}[\mathbf{f}](\xi)\right|^2\int_{\mathbb{R}^+\times\mathbb{R}^{n-1}\times\mathrm{Spin}(n)}\left|\overline{\mathscr{F}_{Cl}[\mathbf{r}\Psi(\cdot)\overline{\mathbf{r}}]\left(\mathbf{r}S_sA_a\xi\overline{\mathbf{r}}\right)}\right|^2\mathrm{d}^n\xi\frac{\mathrm{d}\mathbf{r}\mathrm{d}^{n-1}s\mathrm{d}a}{a^{(n^2-n+1/n)}}\mathrm{d}^n\xi\right\}^{1/2}\\&\geq\frac{1}{2(2\pi)^n}\int_{\mathscr{G}}\left|\mathscr{C}\mathscr{S}_{\Psi}\mathbf{f}(a,\mathbf{r},s,b)\right|^2\mathrm{d}\eta.\end{aligned} \tag{72}$$

Using the definition of C_Ψ in L. H. S and Corollary 1 in R. H. S, we obtain the desired result as follows

$$\left\|b\mathscr{C}\mathscr{S}_\Psi \mathbf{f}(a,\mathbf{r},s,b)\right\|_{L^2\left(\mathscr{G},Cl_{(p,q)}\right)}\left\|\xi\mathscr{F}_{Cl}[\mathbf{f}](\xi)C_\Psi\right\|_{L^2\left(\mathbb{R}^{(p,q)},Cl_{(p,q)}\right)} \geq \frac{1}{2}\left|\langle \mathbf{f}(x)C_\Psi, \mathbf{f}(x)\rangle\right|_{L^2\left(\mathscr{G},Cl_{(p,q)}\right)}. \tag{73}$$

This completes the proof of Theorem 8. □

Remark 2. For real-valued C_Ψ, Theorem 5 boils down to

$$\left\|b\mathscr{C}\mathscr{S}_\Psi \mathbf{f}(a,\mathbf{r},s,b)\right\|_{L^2\left(\mathscr{G},Cl_{(p,q)}\right)}\left\|\xi\mathscr{F}_{Cl}[\mathbf{f}](\xi)\right\|_{L^2\left(\mathbb{R}^{(p,q)},Cl_{(p,q)}\right)} \geq \frac{\sqrt{C_\Psi}}{2}\left\|\mathbf{f}(x)\right\|^2_{L^2\left(\mathscr{G},Cl_{(p,q)}\right)}. \tag{74}$$

The classical Pitt's inequality expresses a fundamental relationship between a sufficiently smooth function $\mathbf{f}$ and the corresponding Clifford Fourier transform [19]. We derive the Pitt's type inequality for the proposed Clifford-valued shearlet transform (28). The Schwartz space on $C\ell_{(p,q)}$ algebras is given by

$$\mathbb{S}\left(\mathbb{R}^{(p,q)},Cl_{(p,q)}\right) = \left\{\mathbf{f}\in C^\infty\left(\mathbb{R}^{(p,q)},Cl_{(p,q)}\right):\ \sup_{t\in\mathbb{R}^{(p,q)}}\left|t^\alpha\partial_t^\beta \mathbf{f}(t)\right| < \infty\right\}, \tag{75}$$

where $C^\infty(\mathbb{R}^{(p,q)},Cl_{(p,q)})$ is the class of smooth functions, and α,β denote multiindices, and ∂_t denotes the usual partial differential operator.

Theorem 9 (Pitt's inequality for $\mathscr{C}\mathscr{S}_\Psi$). *For any $\mathbf{f}\in\mathbb{S}(\mathbb{R}^{(p,q)},Cl_{(p,q)})$, the Pitt's inequality for the Clifford-valued shearlet transform (28) is given by*

$$\int_{\mathbb{R}^n}|\xi|^{-\lambda}\left|\mathscr{F}_{Cl}[\mathbf{f}](\xi)\right|^2 d^n\xi \leq \frac{C_\lambda}{(2\pi)^2}\int_{\mathscr{G}}|b|^\lambda\left|\mathscr{C}\mathscr{S}_\Psi \mathbf{f}(a,\mathbf{r},s,b)\right|^2 C_\Psi^{-1}d\eta, \tag{76}$$

where C_Ψ is the admissibility condition of Clifford-valued shearlet, and C_λ is given by

$$C_\lambda = \pi^\lambda\left[\frac{\Gamma'(n-\lambda/4)}{\Gamma(n+\lambda/4)}\right]^2,\quad 0\leq\lambda<n, \tag{77}$$

where $\Gamma(\cdot)$ denotes the well-known Euler's gamma function.

Proof. Considering $\mathscr{C}\mathscr{S}_\Psi \mathbf{f}(a,\mathbf{r},s,b)$ as a function of the translation variable b, the Pitt's inequality in the Clifford Fourier domain implies 13:

$$\int_{\mathbb{R}^n}|\xi|^{-\lambda}\left|\mathscr{F}_{C\ell}\left[\mathscr{C}\mathscr{S}_\Psi \mathbf{f}(a,\mathbf{r},s,b)\right](\xi)\right|^2 d^n\xi \leq \frac{C_\lambda}{(2\pi)^n}\int_{\mathbb{R}^n}|b|^\lambda\left|\mathscr{C}\mathscr{S}_\Psi \mathbf{f}(a,\mathbf{r},s,b)\right|^2 d^n b, \tag{78}$$

which upon integration with respect to the measure $(d\mathbf{r}d^{n-1}sda/a^{n+1})$ yields

$$\begin{aligned}&\int_{\mathbb{R}^+\times\mathbb{R}^{n-1}\times\mathrm{Spin}(n)}\int_{\mathbb{R}^n}|\xi|^{-\lambda}\left|\mathscr{F}_{Cl}\left[\mathscr{C}\mathscr{S}_\psi \mathbf{f}(a,\mathbf{r},s,b)\right](\xi)\right|^2 d^n\xi\frac{d\mathbf{r}d^{n-1}sda}{a^{n+1}}\\&\leq\frac{C_\lambda}{(2\pi)^n}\int_{\mathbb{R}^+\times\mathbb{R}^{n-1}\times\mathrm{Spin}(n)}\int_{\mathbb{R}^n}|b|^\lambda\left|\mathscr{C}\mathscr{S}_\Psi \mathbf{f}(a,\mathbf{r},s,b)\right|^2 d^n b\frac{d\mathbf{r}d^{n-1}sda}{a^{n+1}}.\end{aligned} \tag{79}$$

Invoking Lemma 1, we can express the inequality (79) in the following manner:

$$\begin{aligned}&\int_{\mathbb{R}^+\times\mathbb{R}^{n-1}\times\mathrm{Spin}(n)}\int_{\mathbb{R}^n}|\xi|^{-\lambda}\left|(2\pi)^{(n/2)}a^{1-(1/2n)}\mathcal{F}_{Cl}[\mathbf{f}](\xi)\overline{\mathcal{F}_{Cl}[\mathbf{r}\Psi(\cdot)\overline{\mathbf{r}}](\mathbf{r}S_sA_a\xi\overline{\mathbf{r}})}\right|^2\mathrm{d}^n\xi\frac{\mathrm{d}\mathbf{r}\mathrm{d}^{n-1}s\mathrm{d}a}{a^{n+1}}\\&\leq\frac{C_\lambda}{(2\pi)^n}\int_{\mathbb{R}^+\times\mathbb{R}^{n-1}\times\mathrm{Spin}(n)}\int_{\mathbb{R}^n}|b|^\lambda\left|\mathcal{CS}_\Psi\mathbf{f}(a,\mathbf{r},s,b)\right|^2\mathrm{d}^nb\frac{\mathrm{d}\mathbf{r}\mathrm{d}^{n-1}s\mathrm{d}a}{a^{n+1}}.\end{aligned}\tag{80}$$

Equivalently, we have

$$\begin{aligned}&\int_{\mathbb{R}^n}|\xi|^{-\lambda}\left|\mathcal{F}_{Cl}[\mathbf{f}](\xi)\right|^2\int_{\mathbb{R}^+\times\mathbb{R}^{n-1}\times\mathrm{Spin}(n)}\left|\mathcal{F}_{Cl}[\mathbf{r}\Psi(\cdot)\overline{\mathbf{r}}](\mathbf{r}S_sA_a\xi\overline{\mathbf{r}})\right|^2\frac{\mathrm{d}\mathbf{r}\mathrm{d}^{n-1}s\mathrm{d}a}{a^{(n^2-n+1/n)}}\mathrm{d}^n\xi\\&\leq\frac{C_\lambda}{(2\pi)^{2n}}\int_{\mathbb{R}^+\times\mathbb{R}^{n-1}\times\mathrm{Spin}(n)}\int_{\mathbb{R}^n}|b|^\lambda\left|\mathcal{CS}_\Psi\mathbf{f}(a,\mathbf{r},s,b)\right|^2\mathrm{d}^nb\frac{\mathrm{d}\mathbf{r}\mathrm{d}^{n-1}s\mathrm{d}a}{a^{n+1}}.\end{aligned}\tag{81}$$

Since Ψ is an admissible Clifford shearlet, inequality (81) boils down to

$$\int_{\mathbb{R}^n}|\xi|^{-\lambda}\left|\mathcal{F}_{Cl}[\mathbf{f}](\xi)\right|^2C_\Psi\mathrm{d}^n\xi\leq\frac{C_\lambda}{(2\pi)^{2n}}\int_{\mathcal{G}}|b|^\lambda\left|\mathcal{CS}_\Psi\mathbf{f}(a,\mathbf{r},s,b)\right|^2\mathrm{d}\eta.\tag{82}$$

which is the desired Pitt's inequality for the Clifford-valued shearlet transform. □

Remark 3. For $\lambda=0$, equality which holds in equation (76) is equivalent to equation (39).

Next, we shall formulate the logarithmic uncertainty principle for the Clifford-valued shearlet transform $\mathcal{CS}_\Psi\mathbf{f}(a,\mathbf{r},s,b)$ given by equation (28).

Theorem 10 (Logarithmic uncertainty principle). *For any $\mathbf{f}\in\mathbb{S}(\mathbb{R}^{(p,q)},Cl_{(p,q)})$, the Clifford-valued shearlet transform $\mathcal{CS}_\Psi\mathbf{f}(a,\mathbf{r},s,b)$ satisfies the following logarithmic estimate of the uncertainty inequality:*

$$\frac{1}{(2\pi)^n}\int_{\mathcal{G}}\left|\mathcal{CS}_\Psi\mathbf{f}(a,\mathbf{r},s,b)\right|^2\ln|b|\mathrm{d}\eta+(2\pi)^n\int_{\mathbb{R}^n}\left|\mathcal{F}_{Cl}[\mathbf{f}](\xi)\right|^2C_\Psi\ln|\xi|\mathrm{d}^n\xi\geq\left(\frac{\Gamma'(n/4)}{\Gamma(n/4)}-\ln\pi\right)\left|\langle\mathbf{f}C_\Psi,\mathbf{f}\rangle\right|_{L^2(\mathcal{G},Cl_{(p,q)})},\tag{83}$$

provided the left hand side of this inequality is defined.

Proof. For the Clifford-valued function $\mathbf{f}\in\mathbb{S}(\mathbb{R}^{(p,q)},Cl_{(p,q)})$, the logarithmic uncertainty inequality in the Clifford Fourier domain yields [18]

$$\int_{\mathbb{R}^n}|\mathbf{f}(b)|^2\ln|b|\mathrm{d}^nb+(2\pi)^n\int_{\mathbb{R}^n}\left|\mathcal{F}_{Cl}[\mathbf{f}](\xi)\right|^2\ln|\xi|\mathrm{d}^n\xi\geq\left(\frac{\Gamma'(n/4)}{\Gamma(n/4)}-\ln\pi\right)\int_{\mathbb{R}^n}|\mathbf{f}(b)|^2\mathrm{d}^nb.\tag{84}$$

Upon replacing $\mathbf{f}(b)$ by $\mathcal{CS}_\Psi\mathbf{f}(a,\mathbf{r},s,b)$ in the above inequality, we obtain

$$\int_{\mathbb{R}^n} \left|\mathscr{C}\mathscr{S}_\Psi \mathbf{f}(a,\mathbf{r},s,b)\right|^2 \ln|b| \mathrm{d}^n b + (2\pi)^n \int_{\mathbb{R}^n} \left|\mathscr{F}_{Cl}\left[\mathscr{C}\mathscr{S}_\Psi \mathbf{f}(a,\mathbf{r},s,b)\right](\xi)\right|^2 \ln|\xi| \mathrm{d}^n \xi \geq \left(\frac{\Gamma'(n/4)}{\Gamma(n/4)} - \ln\pi\right)\int_{\mathbb{R}^n} \left|\mathscr{C}\mathscr{S}_\Psi \mathbf{f}(a,\mathbf{r},s,b)\right|^2 \mathrm{d}^n b. \tag{85}$$

Integrating equation (85) with respect to measure $(\mathrm{d}\mathbf{r}\mathrm{d}^{n-1}s\mathrm{d}a/a^{n+1})$ and then invoking the Fubini theorem, we obtain

$$\int_{\mathscr{G}} \left|\mathscr{C}\mathscr{S}_\Psi \mathbf{f}(a,\mathbf{r},s,b)\right|^2 \ln|b| \mathrm{d}^n b \frac{\mathrm{d}\mathbf{r}\mathrm{d}^{n-1}s\mathrm{d}a}{a^{n+1}} + (2\pi)^n \int_{\mathscr{G}} \left|\mathscr{F}_{Cl}\left[\mathscr{C}\mathscr{S}_\Psi \mathbf{f}(a,\mathbf{r},s,b)\right](\xi)\right|^2 \ln|\xi| \mathrm{d}^n \xi \frac{\mathrm{d}\mathbf{r}\mathrm{d}^{n-1}s\mathrm{d}a}{a^{n+1}} \geq \left(\frac{\Gamma'(n/4)}{\Gamma(n/4)} - \ln\pi\right)\int_{\mathscr{G}} \left|\mathscr{C}\mathscr{S}_\Psi \mathbf{f}(a,\mathbf{r},s,b)\right|^2 \mathrm{d}^n b \frac{\mathrm{d}\mathbf{r}\mathrm{d}^{n-1}s\mathrm{d}a}{a^{n+1}}. \tag{86}$$

Using Lemma 1, the inequality (86) can be further simplified as

$$\int_{\mathscr{G}} \left|\mathscr{C}\mathscr{S}_\Psi \mathbf{f}(a,\mathbf{r},s,b)\right|^2 \ln|b| \mathrm{d}^n b \frac{\mathrm{d}\mathbf{r}\mathrm{d}^{n-1}s\mathrm{d}a}{a^{n+1}} + (2\pi)^n \int_{\mathscr{G}} \left|(2\pi)^{(n/2)} a^{1-(1/2n)} \mathscr{F}_{Cl}[\mathbf{f}](\xi)\overline{\mathscr{F}_{Cl}\left[\mathbf{r}\Psi(\cdot)\overline{\mathbf{r}}\right]\left(\mathbf{r}S_s A_a \xi \overline{\mathbf{r}}\right)}\right|^2 \ln|\xi| \mathrm{d}^n \xi \frac{\mathrm{d}\mathbf{r}\mathrm{d}^{n-1}s\mathrm{d}a}{a^{n+1}} \times \ln|\xi| \mathrm{d}^n \xi \frac{\mathrm{d}\mathbf{r}\mathrm{d}^{n-1}s\mathrm{d}a}{a^{n+1}} \geq \left(\frac{\Gamma'(n/4)}{\Gamma(n/4)} - \ln\pi\right)\int_{\mathscr{G}} \left|\mathscr{C}\mathscr{S}_\Psi \mathbf{f}(a,\mathbf{r},s,b)\right|^2 \mathrm{d}^n b \frac{\mathrm{d}\mathbf{r}\mathrm{d}^{n-1}s\mathrm{d}a}{a^{n+1}}. \tag{87}$$

Alternatively, the above inequality can be rewritten as

$$\int_{\mathscr{G}} \left|\mathscr{C}\mathscr{S}_\Psi \mathbf{f}(a,\mathbf{r},s,b)\right|^2 \ln|b| \mathrm{d}\eta + (2\pi)^{2n} \int_{\mathbb{R}^n} \left|\mathscr{F}_{Cl}[\mathbf{f}](\xi)\right|^2 \times \int_{\mathbb{R}^+\times\mathbb{R}^{n-1}\times\mathrm{Spin}(n)} \left|\mathscr{F}_{Cl}\left[\mathbf{r}\Psi(\cdot)\overline{\mathbf{r}}\right]\left(\mathbf{r}S_s A_a \xi \overline{\mathbf{r}}\right)\right|^2 \frac{\mathrm{d}\mathbf{r}\mathrm{d}^{n-1}s\mathrm{d}a}{a^{(n^2-n+1/n)}} \ln|\xi| \mathrm{d}^n \xi \geq \left(\frac{\Gamma'(n/4)}{\Gamma(n/4)} - \ln\pi\right)\int_{\mathscr{G}} \left|\mathscr{C}\mathscr{S}_\Psi \mathbf{f}(a,\mathbf{r},s,b)\right|^2 \mathrm{d}\eta. \tag{88}$$

Noting that Ψ is admissible and using Corollary 1, we obtain the desired result as

$$\frac{1}{(2\pi)^n}\int_{\mathscr{G}} \left|\mathscr{C}\mathscr{S}_\Psi \mathbf{f}(a,\mathbf{r},s,b)\right|^2 \ln|b| \mathrm{d}\eta + (2\pi)^n \int_{\mathbb{R}^n} \left|\mathscr{F}_{Cl}[\mathbf{f}](\xi)\right|^2 C_\Psi \ln|\xi| \mathrm{d}^n \xi \geq \left(\frac{\Gamma'(n/4)}{\Gamma(n/4)} - \ln\pi\right)\left|\langle \mathbf{f}C_\Psi, \mathbf{f}\rangle\right|_{L^2\left(\mathscr{G}, Cl_{(p,q)}\right)}. \tag{89}$$

This completes the proof of Theorem 10.

In the following, we establish a local-type uncertainty principle for the Clifford-valued sharelet transform $\mathscr{C}\mathscr{S}_\Psi \mathbf{f}$ defined by equation (28). More precisely, we shall demonstrate that the portion of $\mathscr{C}\mathscr{S}_\Psi$ lying outside some given set $\mathscr{M}$ of finite Lebesgue measure cannot be arbitrarily small. □

Theorem 11 (Concentration of $\mathscr{C}\mathscr{S}_\Psi$ in small sets). *Let $\Psi \in L^2(\mathbb{R}^{(p,q)}, Cl_{(p,q)})$ be an admissible Clifford-valued shearlet satisfying $0 < (|a|^{(1/2n)-1}\|\Psi\|^2\mu(\mathscr{M})/C_\Psi) < 1$. Then, for any measurable subset $\mathscr{M}$ of $\mathscr{G} = \mathbb{R}^+ \times \mathbb{R}^{n-1} \times \mathbb{R}^n \times Spin(n)$ and $\mathbf{f} \in L^2(\mathbb{R}^{(p,q)}, Cl_{(p,q)})$, we have*

$$\left\|\mathscr{C}\mathscr{S}_\Psi \mathbf{f}(a,\mathbf{r},s,b)\right\|_{L^2\left(E^c,Cl_{(p,q)}\right)} \geq \sqrt{C_\Psi}\left(1-\frac{|a|^{(1/2n)-1}\mu(\mathscr{M})\|\Psi\|^2_{L^2\left(\mathbb{R}^{(p,q)},Cl_{(p,q)}\right)}}{C_\Psi}\right)^{1/2}\|f\|_{L^2\left(\mathbb{R}^{(p,q)},Cl_{(p,q)}\right)}, \tag{90}$$

where $\mu(\mathscr{M})$ denotes the measure of $\mathscr{M}$.

Proof. Using the definition of Clifford-valued shearlet transforms, we have

$$\begin{aligned}\left|\mathscr{C}\mathscr{S}_\Psi \mathbf{f}(a,\mathbf{r},s,b)\right|_{L^2\left(\mathbb{R}^{(p,q)},Cl_{(p,q)}\right)} &= \left|a^{(1/2n)-1}\int_{\mathbb{R}^{(p,q)}}\mathbf{f}(x)\overline{\mathbf{r}}\overline{\Psi\left(A_a^{-1}S_s^{-1}\overline{\mathbf{r}}(x-b)\mathbf{r}\right)}\mathbf{r}\mathrm{d}^n x\right|_{L^2\mathbb{R}^{(p,q)},Cl_{(p,q)}}\\ &\leq |a|^{(1/2n)-1}\int_{\mathbb{R}^{(p,q)}}|\mathbf{f}(x)|\left|\overline{\mathbf{r}}\overline{\Psi\left(A_a^{-1}S_s^{-1}\overline{\mathbf{r}}(x-b)\mathbf{r}\right)}\mathbf{r}\right|\mathrm{d}^n x.\end{aligned} \tag{91}$$

By virtue of Holders inequality, we have

$$\left\|\mathscr{C}\mathscr{S}_\Psi \mathbf{f}(a,\mathbf{r},s,b)\right\|_{L^2\left(\mathbb{R}^{(p,q)},Cl_{(p,q)}\right)} \leq |a|^{((1/2n)-1)}\|f\|_{L^2\left(\mathbb{R}^{(p,q)},Cl_{(p,q)}\right)}\|\Psi\|_{L^2\left(\mathbb{R}^{(p,q)},Cl_{(p,q)}\right)}. \tag{92}$$

On the other hand, we can write

$$\begin{aligned}\left\|\mathscr{C}\mathscr{S}_\Psi \mathbf{f}(a,\mathbf{r},s,b)\right\|^2_{L^2\left(\mathscr{G},Cl_{(p,q)}\right)\}} &= \int\iiint_{\mathscr{G}}\left|\mathscr{C}\mathscr{S}_\Psi \mathbf{f}(a,\mathbf{r},s,b)\right|^2_{L^2\left(\mathbb{R}^{(p,q)},Cl_{(p,q)}\right)}\mathrm{d}\eta\\ &= \int\iiint_{\mathscr{M}}\left|\mathscr{C}\mathscr{S}_\Psi \mathbf{f}(a,\mathbf{r},s,b)\right|^2_{L^2\left(\mathbb{R}^{(p,q)},Cl_{(p,q)}\right)}\mathrm{d}\eta+\int\iiint_{\mathscr{M}^c}\left|\mathscr{C}\mathscr{S}_\Psi \mathbf{f}(a,\mathbf{r},s,b)\right|^2_{L^2\left(\mathbb{R}^{(p,q)},Cl_{(p,q)}\right)}\mathrm{d}\eta\\ &\leq |a|^{(1/2n)-1}\mu(\mathscr{M})\|f\|^2_{L^2\left(\mathbb{R}^{(p,q)},Cl_{(p,q)}\right)}\|\Psi\|^2_{L^2\left(\mathbb{R}^{(p,q)},Cl_{(p,q)}\right)}+\left\|\mathscr{C}\mathscr{S}_\Psi \mathbf{f}(a,\mathbf{r},s,b)\right\|^2_{L^2\left(E^c,Cl_{(p,q)}\right)}.\end{aligned} \tag{93}$$

Application of Corollary 1 for the real-valued C_Ψ implies that

$$C_\Psi\|f\|^2_{L^2\left(\mathbb{R}^{(p,q)},Cl_{(p,q)}\right)} \leq |a|^{(1/2n)-1}\mu(\mathscr{M})\|f\|^2_{L^2\left(\mathbb{R}^{(p,q)},Cl_{(p,q)}\right)}\|\Psi\|^2_{L^2\left(\mathbb{R}^{(p,q)},Cl_{(p,q)}\right)}+\left\|\mathscr{C}\mathscr{S}_\Psi \mathbf{f}(a,\mathbf{r},s,b)\right\|^2_{L^2\left(E^c,Cl_{(p,q)}\right)}, \tag{94}$$

or

$$\begin{aligned}\left\|\mathscr{C}\mathscr{S}_\Psi \mathbf{f}(a,\mathbf{r},s,b)\right\|_{L^2\left(E^c,Cl_{(p,q)}\right)} &\geq \left(C_\Psi-|a|^{(1/2n)-1}\mu(\mathscr{M})\|\Psi\|^2_{L^2\left(\mathbb{R}^{(p,q)},Cl_{(p,q)}\right)}\right)^{1/2}\|f\|_{L^2\left(\mathbb{R}^{(p,q)},Cl_{(p,q)}\right)}\\ &= \sqrt{C_\Psi}\left(1-\frac{|a|^{(1/2n)-1}\mu(\mathscr{M})\|\Psi\|^2_{L^2\left(\mathbb{R}^{(p,q)},Cl_{(p,q)}\right)}}{C_\Psi}\right)^{1/2}\|f\|_{L^2\left(\mathbb{R}^{(p,q)},Cl_{(p,q)}\right)}.\end{aligned} \tag{95}$$

This completes the proof of Theorem 11. □

6. Conclusion

In the present study, we formulated the notion of continuous Clifford-valued shearlet transform on the generalized geometric algebra $Cl_{p,\,q}$. The proposed transform has the advantage of efficiently handling Clifford-valued signals at various scales, positions and orientations while upholding the affine structure. Besides, studying the fundamental aspects of the Clifford-valued shearlet transform, the homogeneous approximation property is also investigated in detail. Nevertheless, some prominent uncertainty inequalities, such as the Hesienberg–Puali–Weyl logarithmic and local uncertainty principles are obtained at the end.

Data Availability

No data were generated.

Conflicts of Interest

The authors declare that they have no conflicts of interest.

Acknowledgments

The first author was supported by SERB (DST), Government of India under Grant No. EMR/2016/007951. Mawardi Bahri was funded by Grant from Ministry of Education, Culture, Research, and Technology, Indonesia under the WCR scheme.

References

[1] L. Debnath and F. A. Shah, *Lectuer Notes on Wavelet Transforms*, Birkhäuser, Boston, MA, USA, 2017.

[2] D. Labate, W. Q. Li, G. Kutyniok, and G. Weiss, “Sparse multidimensional representation using shearlets,” *SPIE Proceedings*, vol. 5914, pp. 254–262, 2005.

[3] W. Q. Lim, “The discrete shearlet transform: a new directional transform and compactly supported shearlet frames,” *IEEE Transactions on Image Processing*, vol. 19, no. 5, pp. 1166–1180, 2010.

[4] S. Dahlke, G. Steidl, and G. Teschke, “The continuous shearlet transform in arbitrary space dimensions,” *Journal of Fourier Analysis and Applications*, vol. 16, no. 3, pp. 340–364, 2010.

[5] K. Guo and D. Labate, “Characterization and analysis of edges using the continuous shearlet transform,” *SIAM Journal on Imaging Sciences*, vol. 2, no. 3, pp. 959–986, 2009.

[6] E. Hitzer, T. Nitta, and Y. Kuroe, “Applications of clifford’s geometric algebra,” *Advances in Applied Clifford Algebras*, vol. 23, no. 2, pp. 377–404, 2013.

[7] F. Brackx, N. De Schepper, and F. Sommen, “The Clifford fourier transform,” *Journal of Fourier Analysis and Applications*, vol. 11, no. 6, pp. 669–681, 2005.

[8] E. M. S. Hitzer and B. Mawardi, “Clifford fourier transform on multivector fields and uncertainty principles for dimensions $n = 2$ (mod 4) and $n = 3$ (mod 4),” *Advances in Applied Clifford Algebras*, vol. 18, no. 3-4, pp. 715–736, 2008.

[9] F. Brackx, E. Hitzer, and S. Sangwine, “Quaternion and clifford fourier transforms and wavelets,” *Trends in Mathematics*, vol. 27, 2013.

[10] J. Ebling and G. Scheuermann, “Clifford fourier transform on vector fields,” *IEEE Transactions on Visualization and Computer Graphics*, vol. 11, no. 4, pp. 469–479, 2005.

[11] F. A. Shah, A. A. Teali, and M. Bahri, “Clifford-valued stockwell transform and the associated uncertainty principles,” *Advances in Applied Clifford Algebras*, vol. 32, no. 2, 2022.

[12] F. A. Shah and A. A. Teali, “Clifford-valued wave-packet transform with applications to benchmark signals,” *Bulletin of the Malaysian Mathematical Sciences Society*, 2022.

[13] F. A. Shah and A. A. Teali, “Clifford-valued linear canonical transform: convolution and uncertainty principles,” *Optik*, vol. 265, Article ID 169436, 2022.

[14] J. Sharma and S. K. Singh, “Clifford valued shearlet transform,” *Advances in Applied Clifford Algebras*, vol. 30, no. 3, 2020.

[15] M. Bahri, M. I. Azis, N. Aris, and C. Lande, “Some properties associated with Clifford-Fourier transform,” *Journal of Physics: Conference Series*, vol. 1341, no. 6, Article ID 062003, 2019.

[16] F. Brackx and F. Sommen, “Clifford-hermite wavelets in euclidean space,” *Journal of Fourier Analysis and Applications*, vol. 6, no. 3, pp. 299–310, 2000.

[17] B. Liu and W. Sun, “Homogeneous approximation property for multivariate continuous wavelet transforms,” *Numerical Functional Analysis and Optimization*, vol. 30, no. 7-8, pp. 784–798, 2009.

[18] P. Lian, “Sharp inequalities for geometric fourier transform and associated ambiguity function,” *Journal of Mathematical Analysis and Applications*, vol. 484, no. 2, Article ID 123730, 2020.

[19] W. Beckner, “Pitt’s inequality and the uncertainty principle,” *Proceedings of the American Mathematical Society*, vol. 123, no. 6, pp. 1897–1905, 1995.

Hindawi
Journal of Mathematics
Volume 2022, Article ID 9999070, 20 pages
https://doi.org/10.1155/2022/9999070

Research Article

A Highly Accurate Technique to Obtain Exact Solutions to Time-Fractional Quantum Mechanics Problems with Zero and Nonzero Trapping Potential

Muhammad Imran Liaqat,[1] **Adnan Khan**,[1] **Md. Ashraful Alam**,[2] **and M. K. Pandit**[2]

[1]*National College of Business Administration and Economics, Lahore, Pakistan*
[2]*Department of Mathematics, Jahangirnagar University, Savar, Dhaka, Bangladesh*

Correspondence should be addressed to Md. Ashraful Alam; ashraf_math20@juniv.edu

Received 5 March 2022; Revised 20 March 2022; Accepted 20 April 2022; Published 31 May 2022

Academic Editor: Mawardi Bahri

In this study, the highly accurate analytical Aboodh transform decomposition method (ATDM) in the sense of Caputo fractional derivative is used to determine the approximate and exact solutions of both linear and nonlinear time-fractional Schrodinger differential equations (SDEs) with zero and nonzero trapping potential that describe the nonrelativistic quantum mechanical activity. The Adomian decomposition method (ADM) and the Aboodh transform of Caputo's fractional derivative are combined in this method. The recurrence and absolute error of the four problems are analyzed to evaluate the efficiency and consistency of the presented method. In addition, numerical results are also compared with other methods such as the fractional reduced differential transform method (FRDTM), the homotopy analysis method (HAM), and the homotopy perturbation method (HPM). The results obtained by the proposed method show excellent agreement with these methods, which indicates its effectiveness and reliability. This technique has the benefit of not requiring any minor or major physical parameter assumptions in the problem. As a result, it may be used to solve both weakly and strongly nonlinear problems, overcoming some of the inherent constraints of classic perturbation approaches. To solve nonlinear fractional-order differential equations, just a few computations are necessary. As a consequence, it outperforms homotopy analysis and homotopy perturbation approaches significantly. The procedure is quick, precise, and easy to implement. Convergence analysis of the series solution is also offered.

1. Introduction

The shortcoming of classical mechanics to explain several physical processes, including those on microscopic scales, such as the photoelectric effect, black body radiation, and atomic stability, led to the development of modern quantum mechanics. It is explained by the fact that all physical quantities of a bound system are confined to discrete value quantization. Quantum mechanics may successfully describe various modern physics processes in atomic and nuclear physics, as well as other fields of modern physics, where the Schrödinger equation can be used to describe the behavior of electrons in atomic physics and nucleons in nuclear physics [1]. This equation was developed by Austrian physicist Erwin Schrodinger in late 1925 and published in 1926.

Fractional partial differential equations (PDEs), which are an extension of integer-order PDEs, have subsequently received much interest. They can be used to extract memory and hereditary qualities from a variety of materials and processes. Fractional PDEs such as the Boussinesq equation, Korteweg-de Vries equation, Schrodinger equation, Burger's equation, and others are frequently used to describe varied nonlinear wave processes in mechanics, physics, biology, chemistry, and other areas [2]. The time-fractional SDE is the fundamental physics equation for characterizing nonrelativistic quantum mechanical activity. Electromagnetic waves, quantitative finance, quantum development of complex systems, and dielectric polarization have all been pulled into the time-fractional SDE in recent years [3, 4].

We examined the exact and numerical approaches to comprehend the physical mechanism of such a natural phenomenon. As a result, we are looking for a mathematical solution to PDEs that is both precise and numerical. Many papers have focused on constructing solutions to PDEs through well-known methods. Lie symmetry analysis [5], inverse scattering approach [6], spectral collocation method [7], Hirota method [8], Backlund transformation method [9], Modified Kudryashov method [10], Laplace transform coupled with Adomian decomposition method [11], Elzaki residual power series method [12], adaptation on power series method with conformable operator [13], Legendre wavelet method [14] and modified conformable Shehu transform decomposition method [15] are some of the most effective and efficient methods.

Differential equations (DEs), partial integrodifferential equations (PIDs), and delayed differential equations (DDEs) are all solved by employing integral transforms, which are among the most valuable techniques in mathematics. The conversion of DEs and integral equations into terms of a simple algebraic equation is enabled by the appropriate selection of integral transforms. The origins of integral transforms can be traced back to P. S. Laplace's work in the 1780s and Joseph Fourier's work in 1822. In the beginning, ordinary and PDEs were solved using the Laplace transform and the Fourier transform which are two well-known transforms. These modifications were then applied to fractional-order DEs in the domain of fractional calculus [16–19]. In recent years, researchers have proposed lots of new different transformations to solve a variety of mathematical problems. Fractional-order DEs are solved using the Laplace transform [20], fractional complex transform [21], travelling wave transform [22], Elzaki transform [23], Sumudu transforms [24], and ZZ transforms [25], among others. These transformations are paired with additional analytical, numerical, or homotopy-based techniques to handle fractional-order DEs.

The general state of quantum mechanics equations, which are commonly described as fractional-order SDEs, will be solved in this study using an appealing and effective analytical technique, the Aboodh transform decomposition method (ATDM). The Aboodh transform was established in 2013 by Khalid Aboodh to facilitate solving ordinary DEs and PDEs in the time domain [26]. The Aboodh transform is generated using the traditional Fourier integral. The Elzaki transform and the Laplace transform are intimately related to this integral transform. The A-T, which has been used by several researchers for fractional-order DEs [27–31], has recently caught the interest of many mathematicians.

We analyze then on linear time fractional-order SDE with zero trapping potential in its more general version, which is represented by the complex-valued function $\xi(\varpi,\tau)$ of the form [32].

$$iD_\tau^\nu \xi(\varpi,\tau) + D_{\varpi\varpi}\xi(\varpi,\tau) + \eta|\xi(\varpi,\tau)|^{2\lambda}\xi(\varpi,\tau) = 0, \tag{1}$$

where $\eta \in R$, $0<\nu\le 1$, $i=\sqrt{-1}$, D_τ^ν indicates Caputo fractional derivative of order ν, $\xi(\varpi,\tau)$ is the unknown complex-valued function to be determined, $\varpi \in R$, $\tau \ge 0$, and $|\xi(\varpi,\tau)|$ represent the modulus of $\xi(\varpi,\tau)$; with the following initial and boundary conditions given by $\xi(\varpi,0)=\Upsilon(\varpi)$, $\xi(0,\tau)=A(\varpi)$, and $\xi_\varpi(0,\tau)=B(\varpi)$.

The time-fractional nonlinear SDE with nonzero trapping potential has the following form [33]:

$$\begin{gathered} iD_\tau^\nu \xi(\varpi,\tau) = -\frac{1}{2}\mathfrak{J}_\varpi \xi(\varpi,\tau) + \Theta(\varpi)\xi(\varpi,\tau) + H_d Q(\xi(\varpi,\tau)), \\ \tau \ge 0,\ 0<\nu\le 1,\ \varpi \in R, \end{gathered} \tag{2}$$

with the initial condition:

$$\xi(\varpi,0)=\Upsilon(\varpi), \tag{3}$$

where $\varpi \in R$, $\Theta_d(\varpi)$ is the trapping potential and H_d is a real constant $\mathfrak{J}_\varpi$ is a linear operator, $Q(\xi(\varpi,\tau))$ is a nonlinear function, and D_τ^ν is the Caputo fractional differential operator.

The physical model (2) and its generalized forms arise in various areas of physics, including nonlinear optics, plasma physics, superconductivity, and quantum mechanics [34].

The time-fractional SDE has been investigated through various methods, such as the homotopy perturbation method [35], exponential rational function method [36], residual power series method [37], modified transformation method [38], two-dimensional differential transform method [39], extended simple equation method [40], trigonometric B-spline method [41], fractional reduced differential transform method [42], and homotopy analysis method [43]. All these methods have their own specific limits and deficiencies. These methods require enormous computational work and high running times. In this study, we used the simple and efficient technique known as the ATDM to solve the SDE of the fractional derivative in the sense of Caputo. The recommended method is simple to use and can be applied to both linear and nonlinear problems. It also has the ability to reduce the complexity of the computational effort. The set of rules of ATDM depends on converting the SDE into Aboodh transform space and, after converting the SDE into an algebraic equation, applying inverse A-T and then introducing a series of solutions to the obtained algebraic equation, at the final step, obtaining the target result through the iteration process.

The structure of the paper is as follows: we will employ various fundamental definitions and results from fractional calculus theory in the next section. The primary idea of the ATDM is investigated in Section 3 in order to establish fractional SDE solutions. Section 4 demonstrates the method's potential, capability, and simplicity by obtaining approximate and exact solutions to four SDE problems. The proposed method is illustrated numerically and graphically in Section 5, and the numerical results are evaluated in Section 5. The conclusion is covered in Section 6.

Table 1: The absolute error in ATDM and FRDTM for Example 1 at $\nu = 1$.

τ	Real part [ATDM] Abs. error	Img. part [ATDM] Abs. error	Real part [FRDTM] Abs. error	Img. part [FRTDM] Abs. error
0.2	0	$2.775557561562891 \times 10^{-17}$	0	$2.775557561562891 \times 10^{-17}$
0.4	$3.508304757815494 \times 10^{-14}$	$6.661338147750939 \times 10^{-16}$	$3.508304757815494 \times 10^{-14}$	$6.66133814775093 \times 10^{-16}$
0.6	$4.540257059204578 \times 10^{-12}$	$1.743050148661495 \times 10^{-14}$	$4.540257059204578 \times 10^{-12}$	$1.743050148661495 \times 10^{-14}$
0.8	$1.43222100845719 \times 10^{-10}$	$1.645683589401869 \times 10^{-12}$	$1.43222100845719 \times 10^{-10}$	$1.645683589401869 \times 10^{-12}$
1.0	$2.081645966711676 \times 10^{-9}$	$5.585931717178028 \times 10^{-11}$	$2.081645966711676 \times 10^{-9}$	$5.585931717178028 \times 10^{-11}$

2. Basic Concepts and Representations in Fractional Calculus Theory

Fractional calculus is a modified version of classical calculus. Fractional calculus can explain a wide range of complex phenomena, including memory and heredity. This subject has drawn many researchers because of its worldwide aspect and numerous applications in several domains of science, such as physics, signal processing, modeling, control theory, economics, and chemistry [44, 45]. In this section, we covered some definitions and basic features of fractional calculus theory, as well as the fundamentals of the Aboodh transformation, which will be used later in this paper.

Definition 1 (see [43]). The Aboodh transform (A-T) for function $\xi(\tau)$ of exponential order over the set of functions is defined as

$$R = \left\{\xi(\tau) | \exists M,\, u_1,\, u_2 > 0,\, |\xi(\tau)| < Me^{-\hbar\tau}\right\}, \tag{4}$$

where M is a finite number and u_1, u_2 may be finite or infinite. A-T is denoted by the operator $A\,[.]$ and defined as

$$A[\xi(\tau)] = Q(\hbar) = \frac{1}{\hbar}\int_0^\infty \xi(\tau)e^{-\tau\hbar}\mathrm{d}\tau,\ \tau \geq 0,\ u_1 \leq \hbar \leq u_2. \tag{5}$$

Definition 2 (see [46]). The Inverse A-T of function $\xi(\tau)$ is denoted by $A^{-1}[Q(\hbar)]$ and defined as

$$A^{-1}[Q(\hbar)] = \xi(\tau) = \frac{1}{2\pi i}\int_{w-i\infty}^{w+i\infty} \hbar e^{\hbar\tau}Q(\hbar)\mathrm{d}\hbar. \tag{6}$$

A-T of several functions can be seen in Table 1 [27–29]. A-T for some elementary functions is given as

$$\begin{aligned} &\xi(\tau)Q(\hbar) = A[\xi(\tau)] \\ &1\frac{1}{\hbar} \\ &\tau\frac{1}{\hbar^2} \\ &\tau^\alpha\frac{\alpha!}{\hbar^{\alpha+2}},\ \alpha = 1, 2, \ldots \\ &\tau^\nu\frac{\Gamma(\nu+1)}{\hbar^{\nu+2}}. \end{aligned} \tag{7}$$

Definition 3 (see [47]). The Caputo fractional derivative of order $\nu > 0$ is defined by

$$D_\tau^\nu\xi(\tau) = \begin{cases} \dfrac{\mathrm{d}^\alpha}{\mathrm{d}\tau^\alpha}\xi(\tau),\ \alpha = \nu \in N, \\ \dfrac{1}{\Gamma(\alpha-\nu)}\displaystyle\int_0^\tau (\tau-\rho)^{\alpha-\nu-1}\xi^{(\alpha)}(\rho)d\rho,\ \alpha - 1 < \nu < \alpha. \end{cases} \tag{8}$$

We have a few properties of Caputo's fractional derivative.

$$\begin{aligned} &D_\tau^{\nu_1}D_\tau^{\nu_2}\xi(\tau) = D_\tau^{\nu_1+\nu_2}\xi(\tau), \\ &D_\tau^\nu C = 0,\ C \in R, \\ &D_\tau^\nu(\tau-\eta)^\beta = \frac{\Gamma(\beta+1)}{\Gamma(\beta+1-\nu)}(\tau-\eta)^{\beta-\nu}, \\ &\alpha - 1 < \nu \leq \alpha,\ \beta > \alpha - 1,\ \alpha \in N,\ \beta \in R, \\ &D_\tau^\nu(C_1\xi_1(\tau) + C_2\xi_2(\tau)) = C_1D_\tau^\nu\xi_1(\tau) + C_2D_\tau^\nu\xi_2(\tau),\ C_1,\ C_2 \in R. \end{aligned} \tag{9}$$

i. $D_\tau^\nu(J_\tau^\nu\xi(\tau)) = \xi(\tau)$, J_τ^ν is the R-L integral of $\xi(\tau)$ order ν.

Lemma 1 (see [27–31]). *If $\xi_1(\tau)$ and $\xi_2(\tau)$ are piecewise continuous on $[0, \infty)$ and are of exponential order $A[\xi_1(\tau)] = Q_1(\hbar)$, $A[\xi_2(\tau)] = Q_2(\hbar)$, and C_1, C_2 are constants, then the properties mentioned below are valid:*

$$\begin{aligned} &A[C_1\xi_1(\tau) + C_2\xi_2(\tau)] = C_1Q_1(\hbar) + C_2Q_2(\hbar), \\ &A^{-1}[C_1Q_1(\hbar) + C_2Q_2(\hbar)] = C_1\xi_1(\tau) + C_2\xi_2(\tau), \\ &A[D_\tau^\nu\xi(\tau)] = \hbar^\nu Q(\hbar) - \sum_{\kappa=0}^{\alpha-1}\frac{\xi^{(\kappa)}(0)}{\hbar^{\kappa-\nu+2}}, \\ &\alpha - 1 < \nu \leq \alpha,\ \alpha \in N. \end{aligned} \tag{10}$$

3. Analysis of the Aboodh Transform Decomposition Method

In this section, we derive the main algorithms of the ATDM separately for the time-fractional Schrodinger differential equation with zero and nonzero trapping potential. The convergence analysis of the expansion solution is also presented.

To present the ATDM on the general SDE with zero trapping potential given in equation (1), we first rewrite equation (1) as

$$D_\tau^\nu \xi(\varpi,\tau) = iD_{\varpi\varpi}\xi(\varpi,\tau) + i\eta|\xi(\varpi,\tau)|^{2ƛ}\xi(\varpi,\tau). \tag{11}$$

Now, applying the A-T to equation (11), we have

$$A\left[D_\tau^\nu \xi(\varpi,\tau)\right] = A\left[iD_{\varpi\varpi}\xi(\varpi,\tau) + i\eta|\xi(\varpi,\tau)|^{2ƛ}\xi(\varpi,\tau)\right]. \tag{12}$$

Using the differentiation property of the A-T and the initial condition of equation (12), we get

$$ħ^\nu A[\xi(\varpi,\tau)] - \frac{\xi(\varpi,0)}{ħ^{2-\nu}} = A\left[iD_{\varpi\varpi}\xi(\varpi,\tau)\right] + A\left[i\eta|\xi(\varpi,\tau)|^{2ƛ}\xi(\varpi,\tau)\right]. \tag{13}$$

$$A[\xi(\varpi,\tau)] = \frac{\xi(\varpi,0)}{ħ^{2-\nu}} + \frac{1}{ħ^\nu}A\left[iD_{\varpi\varpi}\xi(\varpi,\tau)\right] + \frac{1}{ħ^\nu}A\left[i\eta|\xi(\varpi,\tau)|^{2ƛ}\xi(\varpi,\tau)\right]. \tag{14}$$

Taking the inverse A-T on equation (14), we get as

$$\xi(\varpi,\tau) = A^{-1}\left\{\frac{\xi(\varpi,0)}{ħ^2}\right\} + A^{-1}\left\{\frac{1}{ħ^\nu}A\left[iD_{\varpi\varpi}\xi(\varpi,\tau)\right]\right\} + A^{-1}\left\{\frac{1}{ħ^\nu}A\left[i\eta|\xi(\varpi,\tau)|^{2ƛ}\xi(\varpi,\tau)\right]\right\}. \tag{15}$$

So, according to the ATDM, we can acquire the solution $\xi(\varpi,\tau)$ to equation (15) as follows:

$$\xi(\varpi,\tau) = \sum_{\alpha=0}^{\infty}\xi_\alpha(\varpi,\tau). \tag{16}$$

The nonlinear operator is decomposed as

$$\aleph(\xi(\varpi,\tau)) = \sum_{\alpha=0}^{\infty}W_\alpha(\xi_0, \xi_1, \xi_2, \ldots), \tag{17}$$

where

$$W_\alpha = \frac{1}{\alpha!}\frac{d^\alpha}{dƛ^\alpha}\left[\aleph\left(\sum_{\kappa=0}^{\alpha}ƛ^\kappa\xi_\kappa(\varpi,\tau)\right)\right]_{ƛ=0}. \tag{18}$$

The few terms of the decomposed nonlinear terms which are calculated from equation (18) are given as

$$\begin{aligned}
W_0 &= \xi_0^2(\varpi,\tau)\overline{\xi(\varpi,\tau)},\\
W_1 &= \xi_0^2(\varpi,\tau)\overline{\xi_1(\varpi,\tau)} + 2\xi_0(\varpi,\tau)\xi_1(\varpi,\tau)\overline{\xi_0(\varpi,\tau)},\\
W_2 &= \xi_1^2(\varpi,\tau)\overline{\xi_0(\varpi,\tau)} + 2\xi_0(\varpi,\tau)\xi_2(\varpi,\tau)\overline{\xi_0(\varpi,\tau)}\\
&\quad + 2\xi_0(\varpi,\tau)\xi_1(\varpi,\tau)\overline{\xi_1(\varpi,\tau)} + \xi_0^2(\varpi,\tau)\overline{\xi_0(\varpi,\tau)}.
\end{aligned} \tag{19}$$

Now, by replacing equations (18) and (16) with equation (15), we attain as follows:

$$\sum_{\alpha=0}^{\infty}\xi_\alpha(\varpi,\tau) = A^{-1}\left\{\frac{\xi(\varpi,0)}{ħ^2}\right\} + A^{-1}\left\{\frac{1}{ħ^\nu}A\left[iD_{\varpi\varpi}\sum_{\alpha=0}^{\infty}\xi_\alpha(\varpi,\tau)\right]\right\} + A^{-1}\left\{\frac{1}{ħ^\nu}A\left[i\eta\sum_{\alpha=0}^{\infty}W_\alpha\right]\right\}. \tag{20}$$

Equating the like terms on both sides of equation (20) yields the general solution of equation (11), which is recursively expressed as

$$\begin{aligned}
\xi_0(\varpi,\tau) &= A^{-1}\left\{\frac{\xi(\varpi,0)}{ħ^2}\right\},\\
\xi_1(\varpi,\tau) &= A^{-1}\left\{\frac{1}{ħ^\nu}A\left[iD_{\varpi\varpi}\sum_{\alpha=0}^{\infty}\xi_0(\varpi,\tau)\right]\right\} + A^{-1}\left\{\frac{1}{ħ^\nu}A\left[\eta iW_0\right]\right\},\\
\xi_2(\varpi,\tau) &= A^{-1}\left\{\frac{1}{ħ^\nu}A\left[iD_{\varpi\varpi}\sum_{\alpha=0}^{\infty}\xi_1(\varpi,\tau)\right]\right\} + A^{-1}\left\{\frac{1}{ħ^\nu}A\left[\eta iW_1\right]\right\},\\
\xi_3(\varpi,\tau) &= A^{-1}\left\{\frac{1}{ħ^\nu}A\left[iD_{\varpi\varpi}\sum_{\alpha=0}^{\infty}\xi_2(\varpi,\tau)\right]\right\} + A^{-1}\left\{\frac{1}{ħ^\nu}A\left[\eta iW_2\right]\right\},\\
\xi_4(\varpi,\tau) &= A^{-1}\left\{\frac{1}{ħ^\nu}A\left[iD_{\varpi\varpi}\sum_{\alpha=0}^{\infty}\xi_3(\varpi,\tau)\right]\right\} + A^{-1}\left\{\frac{1}{ħ^\nu}A\left[\eta iW_3\right]\right\},\\
\xi_{\alpha+1}(\varpi,\tau) &= A^{-1}\left\{\frac{1}{ħ^\nu}A\left[iD_{\varpi\varpi}\sum_{\alpha=0}^{\infty}\xi_\alpha(\varpi,\tau)\right]\right\} + A^{-1}\left\{\frac{1}{ħ^\nu}A\left[i\eta\sum_{\alpha=0}^{\infty}W_\alpha\right]\right\}.
\end{aligned} \tag{21}$$

where $\alpha = 0, 1, 2, \ldots$

Now, to present the ATDM on the general SDE with nonzero trapping potential given in equation (2), we first rewrite equation (2) as

$$D_\tau^\nu \xi(\varpi,\tau) = -i\left(-\frac{1}{2}\mathfrak{I}_\varpi\xi(\varpi,\tau) + \Theta_d(\varpi)\xi(\varpi,\tau) + H_d Q(\xi(\varpi,\tau))\right). \tag{22}$$

Now, applying the A-T to equation (22), we have:

$$A\left[D_\tau^\nu \xi(\varpi,\tau)\right] = -iA\Big(-\frac{1}{2}\mathfrak{J}_\varpi \xi(\varpi,\tau) + \Theta_d(\varpi)\xi(\varpi,\tau) + H_d Q(\xi(\varpi,\tau))\Big). \tag{23}$$

Using the differentiation property of the A-T and the initial condition on equation (23), we get

$$\hbar^\nu A[\xi(\varpi,\tau)] - \frac{\xi(\varpi,0)}{\hbar^{2-\nu}} = -iA\Big(-\frac{1}{2}\mathfrak{J}_\varpi \xi(\varpi,\tau) + \Theta_d(\varpi)\xi(\varpi,\tau) + H_d Q(\xi(\varpi,\tau))\Big). \tag{24}$$

$$A[\xi(\varpi,\tau)] = \frac{\xi(\varpi,0)}{\hbar^2} - \frac{1}{\hbar^\nu} iA\Big(-\frac{1}{2}\mathfrak{J}_\varpi \xi(\varpi,\tau) + \Theta_d(\varpi)\xi(\varpi,\tau) + H_d Q(\xi(\varpi,\tau))\Big). \tag{25}$$

Taking the inverse A-T on equation (25), we get as

$$\xi(\varpi,\tau) = A^{-1}\left\{\frac{\xi(\varpi,0)}{\hbar^2}\right\} - A^{-1}\left\{\frac{1}{\hbar^\nu} iA\Big(-\frac{1}{2}\mathfrak{J}_\varpi \xi(\varpi,\tau) + \Theta_d(\varpi)\xi(\varpi,\tau) + H_d Q(\xi(\varpi,\tau))\Big)\right\}. \tag{26}$$

So, according to the ATDM, we can acquire the solution $\xi(\varpi,\tau)$ to equation (26) as follows:

$$\xi(\varpi,\tau) = \sum_{\alpha=0}^{\infty} \xi_\alpha(\varpi,\tau). \tag{27}$$

$$Q(\xi(\varpi,\tau)) = \sum_{\alpha=0}^{\infty} W_\alpha. \tag{28}$$

$$W_\alpha = \frac{1}{\alpha!}\frac{d^\alpha}{d\lambda^\alpha}\left[\aleph\left(\sum_{\kappa=0}^{\alpha} \lambda^\kappa \xi_\kappa(\varpi,\tau)\right)\right]_{\lambda=0}. \tag{29}$$

The few terms of the decomposed nonlinear terms which are calculated from equation (29) are given as

$$\begin{aligned}
W_0 &= \xi_0^2(\varpi,\tau)\overline{\xi(\varpi,\tau)},\\
W_1 &= \xi_0^2(\varpi,\tau)\overline{\xi_1(\varpi,\tau)} + 2\xi_0(\varpi,\tau)\xi_1(\varpi,\tau)\overline{\xi_0(\varpi,\tau)},\\
W_2 &= \xi_1^2(\varpi,\tau)\overline{\xi_0(\varpi,\tau)} + 2\xi_0(\varpi,\tau)\xi_2(\varpi,\tau)\overline{\xi_0(\varpi,\tau)}\\
&\quad + 2\xi_0(\varpi,\tau)\xi_1(\varpi,\tau)\overline{\xi_1(\varpi,\tau)} + \xi_0^2(\varpi,\tau)\overline{\xi_0(\varpi,\tau)}.
\end{aligned} \tag{30}$$

Now, by replacing equations (27) and (29) with equation (26), we attain as follows:

$$\sum_{\alpha=0}^{\infty} \xi_\alpha(\varpi,\tau) = A^{-1}\left\{\frac{\xi(\varpi,0)}{\hbar^2}\right\} - A^{-1}\left\{\frac{1}{\hbar^\nu} iA\left(-\frac{1}{2}\mathfrak{J}_\varpi \sum_{\alpha=0}^{\infty}\xi_\alpha(\varpi,\tau) + \Theta_d(\varpi)\sum_{\alpha=0}^{\infty}\xi_\alpha(\varpi,\tau) + H_d\sum_{\alpha=0}^{\infty} W_\alpha\right)\right\}. \tag{31}$$

Equating the like terms on both sides of equation (20), we finally obtain the general solution of equation (22) given recursively as

$$\begin{aligned}
\xi_0(\varpi,\tau) &= \xi(\varpi,0),\\
\xi_1(\varpi,\tau) &= -A^{-1}\left\{\frac{1}{\hbar^\nu} iA\Big(-\frac{1}{2}\mathfrak{J}_\varpi \xi_0(\varpi,\tau) + \Theta_d(\varpi)\xi_0(\varpi,\tau) + H_d W_0\Big)\right\},\\
\xi_2(\varpi,\tau) &= -A^{-1}\left\{\frac{1}{\hbar^\nu} iA\Big(-\frac{1}{2}\mathfrak{J}_\varpi \xi_1(\varpi,\tau) + \Theta_d(\varpi)\xi_1(\varpi,\tau) + H_d W_1\Big)\right\},\\
\xi_3(\varpi,\tau) &= -A^{-1}\left\{\frac{1}{\hbar^\nu} iA\Big(-\frac{1}{2}\mathfrak{J}_\varpi \xi_2(\varpi,\tau) + \Theta_d(\varpi)\xi_2(\varpi,\tau) + H_d W_2\Big)\right\},\\
\xi_{\alpha+1}(\varpi,\tau) &= -A^{-1}\left\{\frac{1}{\hbar^\nu} iA\Big(-\frac{1}{2}\mathfrak{J}_\varpi \xi_\alpha(\varpi,\tau) + \Theta_d(\varpi)\xi_\alpha(\varpi,\tau) + H_d W_\alpha\Big)\right\},\\
\xi(\varpi,\tau) &= \xi_0(\varpi,\tau) + \xi_1(\varpi,\tau) + \xi_2(\varpi,\tau) + \cdots,
\end{aligned} \tag{32}$$

where $\alpha = 0, 1, 2, \ldots$

The following theorem describes the criteria for the expansion solution to converge.

Theorem 1. *Let M be a Banach space with an appropriate norm . and a series of partial sums $\sum_{\alpha=0}^{\infty} \xi_\alpha(\varpi,\tau)$ defined over it. Assume that the initial guess $w_0 = \xi_0(\varpi,\tau)$ remains inside the ball $B_r(\xi)$ of the solution $\xi(\varpi,\tau)$. Then, the series solution $\sum_{\alpha=0}^{\infty} \xi_\alpha(\varpi,\tau)$ converges if $\exists \sigma > 0$ such that $\xi_{\alpha+1}(\varpi,\tau) \le \sigma \xi_\alpha(\varpi,\tau)$.*

Proof. The following is the description of a sequence of partial sums:

$$\begin{aligned}
\Theta_0 &= \xi_0(\varpi,\tau),\\
\Theta_1 &= \xi_0(\varpi,\tau) + \xi_1(\varpi,\tau),\\
\Theta_2 &= \xi_0(\varpi,\tau) + \xi_1(\varpi,\tau) + \xi_2(\varpi,\tau),\\
\Theta_3 &= \xi_0(\varpi,\tau) + \xi_1(\varpi,\tau) + \xi_2(\varpi,\tau) + \xi_3(\varpi,\tau),\\
&\vdots \quad \vdots \quad \vdots\\
\Theta_\alpha &= \xi_0(\varpi,\tau) + \xi_1(\varpi,\tau) + \xi_2(\varpi,\tau)\\
&\quad + \xi_3(\varpi,\tau) + \cdots + \xi_\alpha(\varpi,\tau).
\end{aligned} \tag{33}$$

Then, we would have to demonstrate that $\{\Theta_\alpha\}_{\alpha=0}^{\infty}$ is a Cauchy sequence in M. To demonstrate this, consider the relationship that

$$\begin{aligned}
\Theta_{\alpha+1} - \Theta_\alpha &= \xi_{\alpha+1}(\varpi,\tau) \le \sigma\xi_\alpha(\varpi,\tau) \le \sigma^2\xi_{\alpha-1}(\varpi,\tau)\\
&\le \sigma^3\xi_{\alpha-2}(\varpi,\tau) \le \cdots \sigma^{\alpha+1}\xi_0(\varpi,\tau),
\end{aligned} \tag{34}$$

where $\alpha = 0, 1, 2, 3, \ldots$

For every $\ell, \alpha \in \mathrm{N}, \alpha \ge \ell$, we have

$$\begin{aligned}
\Theta_\alpha - \Theta_\ell &= (\Theta_\alpha - \Theta_{\alpha-1}) + (\Theta_{\alpha-1} - \Theta_{\alpha-2})\\
&\quad + (\Theta_{\alpha-2} - \Theta_{\alpha-3}) + (\Theta_{\alpha-3} - \Theta_{\alpha-4}) + \sigma^4\\
&\xi_{\alpha-3}(\varpi,\tau) \le \cdots + (\Theta_{\ell+1} - \Theta_\ell).
\end{aligned} \tag{35}$$

We get the following from the triangle inequality:

$$\begin{aligned}
&(\Theta_\alpha - \Theta_{\alpha-1}) + (\Theta_{\alpha-1} - \Theta_{\alpha-2}) + (\Theta_{\alpha-2} - \Theta_{\alpha-3})\\
&\quad + (\Theta_{\alpha-3} - \Theta_{\alpha-4}) + \cdots + (\Theta_{\ell+1} - \Theta_\ell)\\
&\le (\Theta_\alpha - \Theta_{\alpha-1}) + (\Theta_{\alpha-1} - \Theta_{\alpha-2}) + (\Theta_{\alpha-2} - \Theta_{\alpha-3})\\
&\quad + (\Theta_{\alpha-3} - \Theta_{\alpha-4}) + \cdots + (\Theta_{\ell+1} - \Theta_\ell),\\
&(\Theta_\alpha - \Theta_{\alpha-1}) + (\Theta_{\alpha-1} - \Theta_{\alpha-2})\\
&\quad + (\Theta_{\alpha-2} - \Theta_{\alpha-3}) + (\Theta_{\alpha-3} - \Theta_{\alpha-4}) + \cdots +\\
&(\Theta_{\ell+1} - \Theta_\ell) \le \sigma^\alpha\xi_0(\varpi,\tau) + \sigma^{\alpha-1}\xi_0(\varpi,\tau) + \sigma^{\alpha-2}\xi_0(\varpi,\tau) + \cdots\\
&\quad + \sigma^\ell\xi_0(\varpi,\tau) = \left(\frac{1-\sigma^{\alpha-\ell}}{1-\sigma}\right)\sigma^{\ell+1}\xi_0(\varpi,\tau).
\end{aligned} \tag{36}$$

As a result, we have the following inequality:

$$\Theta_\alpha - \Theta_\ell \le \left(\frac{1-\sigma^{\alpha-\ell}}{1-\sigma}\right)\sigma^{\alpha+1}\xi_0(\varpi,\tau). \tag{37}$$

Demonstrating that the sequence is bounded and we can attain for $0 < \sigma < 1$, that,

$$\lim_{\ell,\alpha\longrightarrow\infty} \Theta_\alpha - \Theta_\ell = 0. \tag{38}$$

As a consequence, the sequence of partial sums of the ATDM is Cauchy and so convergent. □

4. Approximate and Exact Solutions to SDEs with Zero and Nonzero Trapping Potential

In this part, we determined the exact solution to linear and nonlinear time-fractional SDEs with zero and nonzero potential by using the ATDM.

Example 1. We consider the following linear SDE with zero trapping potential:

$$\begin{aligned}
&iD_\tau^\nu\xi(\varpi,\tau) + D_{\varpi\varpi}\xi(\varpi,\tau) = 0,\\
&\qquad 0 < \nu \le 1,\ \tau \ge 0, \varpi \in R,
\end{aligned} \tag{39}$$

with the initial condition:

$$\xi(\varpi,0) = be^{ia\varpi}. \tag{40}$$

By using the A-T on both sides of equation (39), we get as follows:

$$A\left[iD_\tau^\nu\xi(\varpi,\tau) + D_{\varpi\varpi}\xi(\varpi,\tau)\right] = 0. \tag{41}$$

Using the third part of Lemma 1, equation (41) is transformed as follows:

$$A[\xi(\varpi,\tau)] = \frac{\xi(\varpi,0)}{\hbar^2} - \frac{1}{\hbar^\nu}D_{\varpi\varpi}A[\xi\varpi,\tau]. \tag{42}$$

By using the inverse A-T, equation (42) becomes as

$$\xi(\varpi,\tau) = A^{-1}\left\{\frac{\xi(\varpi,0)}{\hbar^2}\right\} - A^{-1}\left\{\frac{1}{\hbar^\nu}D_{\varpi\varpi}A[\xi(\varpi,\tau)]\right\}. \tag{43}$$

By using the procedure of ATDM, as explained in Section 3, the expansion solution of equation (39) can be represented by the expansion form as follows:

$$\xi(\varpi,\tau) = \sum_{\alpha=0}^{\infty}\xi_\alpha(\varpi,\tau). \tag{44}$$

We get as by substituting equation (44) into equation (43).

$$\sum_{\alpha=0}^{\infty}\xi_\alpha(\varpi,\tau) = A^{-1}\left\{\frac{\xi(\varpi,0)}{\hbar^2}\right\} - A^{-1}\left\{\frac{1}{\hbar^\nu}D_{\varpi\varpi}A\left[\sum_{\alpha=0}^{\infty}\xi_\alpha(\varpi,\tau)\right]\right\}. \tag{45}$$

Using the approach outlined in Section 3, we can get the following from equation (45):

$$\xi_0(\varpi,\tau) = be^{ia\varpi}, \tag{46}$$

$$\xi_{\alpha+1}(\varpi,\tau) = -A^{-1}\left\{\frac{1}{\phi^{\nu}}D_{\varpi\varpi}Q\left[\xi_{\alpha}(\varpi,\tau)\right]\right\}, \quad \alpha = 0, 1, 2, \ldots. \tag{47}$$

By repeating the iteration process in equation (47), we obtain the following results:

$$\begin{aligned}
\xi_1(\varpi,\tau) &= -\frac{i\tau^{\nu}a^2be^{ia\varpi}}{\Gamma(\nu+1)},\\
\xi_2(\varpi,\tau) &= -\frac{\tau^{2\nu}a^4be^{ia\varpi}}{\Gamma(2\nu+1)},\\
\xi_3(\varpi,\tau) &= \frac{i\tau^{3\nu}a^6be^{ia\varpi}}{\Gamma(3\nu+1)},\\
\xi_4(\varpi,\tau) &= \frac{\tau^{4\nu}a^8be^{ia\varpi}}{\Gamma(4\nu+1)},\\
\xi_5(\varpi,\tau) &= -\frac{i\tau^{5\nu}a^{10}be^{ia\varpi}}{\Gamma(5\nu+1)}.
\end{aligned} \tag{48}$$

As a result, we can find the series solution as

$$\begin{aligned}
\xi(\varpi,\tau) = be^{ia\varpi} &- \frac{i\tau^{\nu}a^2be^{ia\varpi}}{\Gamma(\nu+1)} - \frac{\tau^{2\nu}a^4be^{ia\varpi}}{\Gamma(2\nu+1)} + \frac{i\tau^{3\nu}a^6be^{ia\varpi}}{\Gamma(3\nu+1)}\\
&+ \frac{\tau^{4\nu}a^8be^{ia\varpi}}{\Gamma(4\nu+1)} - \frac{i\tau^{5\nu}a^{10}be^{ia\varpi}}{\Gamma(5\nu+1)} + \cdots.
\end{aligned} \tag{49}$$

When we use $\nu = 1$ in equation (49), we get the following precise solution to equation (39).

$$\xi(\varpi,\tau) = be^{ia(\varpi - a\tau)}. \tag{50}$$

Example 2. Consider the following one-dimensional nonlinear SDE with zero trapping potential:

$$\begin{aligned}
iD_{\tau}^{\nu}\xi(\varpi,\tau) + D_{\varpi\varpi}\xi(\varpi,\tau) + 2|\xi(\varpi,\tau)|^2\xi(\varpi,\tau) = 0,\\
0 < \nu \le 1,\ \tau \ge 0, \varpi \in R,
\end{aligned} \tag{51}$$

with the initial condition:

$$\xi(\varpi,0) = e^{i\varpi}. \tag{52}$$

By using A-T on both sides of equation (52), we get as

$$A[\xi(\varpi,\tau)] = \frac{\xi(\varpi,0)}{\hbar^{2-\nu}} + \frac{1}{\hbar^{\nu}}A\left[iD_{\varpi\varpi}\xi(\varpi,\tau)\right] + \frac{1}{\hbar^{\nu}}A\left[2i|\xi(\varpi,\tau)|^2\xi(\varpi,\tau)\right]. \tag{53}$$

By following the process stated in Section 3, we achieve the following result:

$$\begin{aligned}
\xi(\varpi,\tau) = A^{-1}\left\{\frac{e^{i\varpi}}{\hbar^2}\right\} + A^{-1}\left\{\frac{1}{\hbar^{\nu}}A\left[iD_{\varpi\varpi}\xi(\varpi,\tau)\right]\right\}\\
+ A^{-1}\left\{\frac{1}{\hbar^{\nu}}A\left[2i|\xi(\varpi,\tau)|^2\xi(\varpi,\tau)\right]\right\}.
\end{aligned} \tag{54}$$

$$\begin{aligned}
\xi(\varpi,\tau) &= \sum_{\alpha=0}^{\infty}\xi_{\alpha}(\varpi,\tau),\\
|\xi(\varpi,\tau)|^2\xi(\varpi,\tau) &= \aleph(\xi(\varpi,\tau)),\\
\aleph(\xi(\varpi,\tau)) &= \sum_{\alpha=0}^{\infty}Q_{\alpha}(\xi_0,\xi_1,\xi_2,\ldots),\\
W_0 &= \xi_0^2(\varpi,\tau)\overline{\xi(\varpi,\tau)},\\
W_1 &= \xi_0^2(\varpi,\tau)\overline{\xi_1(\varpi,\tau)}\\
&\quad + 2\xi_0(\varpi,\tau)\xi_1(\varpi,\tau)\overline{\xi_0(\varpi,\tau)},\\
W_2 &= \xi_1^2(\varpi,\tau)\overline{\xi_0(\varpi,\tau)}\\
&\quad + 2\xi_0(\varpi,\tau)\xi_2(\varpi,\tau)\overline{\xi_0(\varpi,\tau)}\\
&\quad + 2\xi_0(\varpi,\tau)\xi_1(\varpi,\tau)\overline{\xi_1(\varpi,\tau)}\\
&\quad + \xi_0^2(\varpi,\tau)\overline{\xi_0(\varpi,\tau)}.
\end{aligned} \tag{55}$$

By using equation (55) in equation (54), we obtain as follows:

$$\begin{aligned}
\sum_{\alpha=0}^{\infty}\xi_{\alpha}(\varpi,\tau) = A^{-1}\left\{\frac{e^{i\varpi}}{\hbar^2}\right\} + A^{-1}\left\{\frac{1}{\hbar^{\nu}}A\left[iD_{\varpi\varpi}\sum_{\alpha=0}^{\infty}\xi_{\alpha}(\varpi,\tau)\right]\right\}\\
+ A^{-1}\left\{\frac{1}{\hbar^{\nu}}A\left[2i\sum_{\alpha=0}^{\infty}Q_{\alpha}\right]\right\}.
\end{aligned} \tag{56}$$

By following the process stated in Section 3, we achieve the following result:

$$\begin{aligned}
\xi_0(\varpi,\tau) &= e^{i\varpi},\\
\xi_1(\varpi,\tau) &= \frac{e^{i\varpi}(i\tau^{\nu})^1}{\Gamma(\nu+1)},\\
\xi_2(\varpi,\tau) &= \frac{e^{i\varpi}(i\tau^{\nu})^2}{\Gamma(2\nu+1)},\\
\xi_3(\varpi,\tau) &= \frac{e^{i\varpi}(i\tau^{\nu})^3}{\Gamma(3\nu+1)},\\
\xi_4(\varpi,\tau) &= \frac{e^{i\varpi}(i\tau^{\nu})^4}{\Gamma(4\nu+1)},\\
\xi_5(\varpi,\tau) &= \frac{e^{i\varpi}(i\tau^{\nu})^5}{\Gamma(5\nu+1)}.
\end{aligned} \tag{57}$$

As a result, we get the following solution in series form for equation (51).

$$\xi(\varpi,\tau)=e^{i\varpi}+\frac{e^{i\varpi}(i\tau^{\nu})^{1}}{\Gamma(\nu+1)}+\frac{e^{i\varpi}(i\tau^{\nu})^{2}}{\Gamma(2\nu+1)}+\frac{e^{i\varpi}(i\tau^{\nu})^{3}}{\Gamma(3\nu+1)}+\frac{e^{i\varpi}(9i\tau^{\nu})^{4}}{\Gamma(4\nu+1)}+\frac{e^{i\varpi}(i\tau^{\nu})^{5}}{\Gamma(5\nu+1)}+\cdots. \tag{58}$$

When we use $\nu=1$ in equation (58), we get the following precise solution to equation (51).

$$\xi(\varpi,\tau)=e^{i(\varpi+\tau)}. \tag{59}$$

Example 3. Consider the following one-dimensional nonlinear SDE with trapping potential:

$$D_{\tau}^{\nu}\xi(\varpi,\tau)=-i\left(-\frac{1}{2}D_{\varpi}\xi(\varpi,\tau)+\cos^{2}\varpi\xi(\varpi,\tau)+|\xi(\varpi,\tau)|^{2}\xi(\varpi,\tau)\right),\quad 0<\nu\leq 1,\ \tau\geq 0,\varpi\in R. \tag{60}$$

with the initial condition:

$$\xi(\varpi,0)=\sin\varpi. \tag{61}$$

By using the A-T on both sides of equation (69), we obtain as follows:

$$A[D_{\tau}^{\nu}\xi(\varpi,\tau)]=A\left[-i\left(-\frac{1}{2}D_{\varpi}\xi(\varpi,\tau)+\cos^{2}\varpi\xi(\varpi,\tau)+|\xi(\varpi,\tau)|^{2}\xi(\varpi,\tau)\right)\right]. \tag{62}$$

Using the third part of Lemma 1, equation (62) is transformed as follows:

$$A[\xi(\varpi,\tau)]=\frac{\xi(\varpi,0)}{\hbar^{2}}+\frac{1}{\hbar^{\nu}}A\left[-i\left(-\frac{1}{2}D_{\varpi}\xi(\varpi,\tau)+\cos^{2}\varpi\xi(\varpi,\tau)+|\xi(\varpi,\tau)|^{2}\xi(\varpi,\tau)\right)\right]. \tag{63}$$

On both sides of equation (63), consider the inverse of the A-T.

$$\xi(\varpi,\tau)=A^{-1}\left\{\frac{\xi(\varpi,0)}{\hbar^{2}}\right\}+A^{-1}\left\{\frac{1}{\hbar^{\nu}}A\left[-i\left(-\frac{1}{2}D_{\varpi}\xi(\varpi,\tau)+\cos^{2}\varpi\xi(\varpi,\tau)+|\xi(\varpi,\tau)|^{2}\xi(\varpi,\tau)\right)\right]\right\}. \tag{64}$$

By following the process stated in Section 3, we achieve the following result:

$$\xi(\varpi,\tau)=\sum_{\alpha=0}^{\infty}\xi_{\alpha}(\varpi,\tau),\quad Q(\xi(\varpi,\tau))=|\xi(\varpi,\tau)|^{2}\xi(\varpi,\tau)=\sum_{\alpha=0}^{\infty}W_{\alpha}. \tag{65}$$

Using equation (65) in equation (64), we get as follows:

$$\sum_{\alpha=0}^{\infty}\xi_{\alpha}(\varpi,\tau)=A^{-1}\left\{\frac{\xi(\varpi,0)}{\hbar^{2}}\right\}+A^{-1}\left\{\frac{1}{\hbar^{\nu}}A\left[-i\left(-\frac{1}{2}D_{\varpi}\sum_{\alpha=0}^{\infty}\xi_{\alpha}(\varpi,\tau)+\cos^{2}\varpi\sum_{\alpha=0}^{\infty}\xi_{\alpha}(\varpi,\tau)+\sum_{\alpha=0}^{\infty}W_{\alpha}\right)\right]\right\}. \tag{66}$$

By equating the like terms on both sides of equation (66), we get as follows:

$$\xi_{0}(\varpi,\tau)=A^{-1}\left\{\frac{\xi(\varpi,0)}{\hbar^{2}}\right\},\quad \xi_{\alpha+1}(\varpi,\tau)=A^{-1}\left\{\frac{1}{\hbar^{\nu}}A\left[-i\left(-\frac{1}{2}D_{\varpi}\xi_{\alpha}(\varpi,\tau)+\cos^{2}\varpi\xi_{\alpha}(\varpi,\tau)+W_{\alpha}\right)\right]\right\}. \tag{67}$$

The following results are obtained from equation (67) using the iteration procedure stated in Section 3.

$$\begin{aligned}
\xi_{0}(\varpi,\tau)&=\sin\varpi,\\
\xi_{1}(\varpi,\tau)&=-\frac{3i\tau^{\nu}}{2\Gamma(\nu+1)}\sin\varpi,\\
\xi_{2}(\varpi,\tau)&=-\frac{9\tau^{2\nu}}{4\Gamma(2\nu+1)}\sin\varpi,\\
\xi_{3}(\varpi,\tau)&=\frac{27i\tau^{3\nu}}{8\Gamma(3\nu+1)}\sin\varpi,\\
\xi_{4}(\varpi,\tau)&=\frac{81\tau^{4\nu}}{16\Gamma(4\nu+1)}\sin\varpi,\\
\xi_{5}(\varpi,\tau)&=-\frac{243i\tau^{5\nu}}{32\Gamma(5\nu+1)}\sin\varpi.
\end{aligned} \tag{68}$$

As a result, we get the following solution in series form for equation (60).

$$\xi(\varpi,\tau)=\sin\varpi-\frac{3i\tau^{\nu}}{2\Gamma(\nu+1)}\sin\varpi-\frac{9\tau^{2\nu}}{4\Gamma(2\nu+1)}\sin\varpi+\frac{27i\tau^{3\nu}}{8\Gamma(3\nu+1)}\sin\varpi+\frac{81\tau^{4\nu}}{16\Gamma(4\nu+1)}\sin\varpi-\frac{243i\tau^{5\nu}}{32\Gamma(5\nu+1)}\sin\varpi+\cdots. \tag{69}$$

When we use $\nu = 1$ in equation (69), we get the following precise solution to equation (60).

$$\xi(\varpi, \tau) = \sin \varpi e^{-(3i/2)\tau}. \tag{70}$$

Example 4. Consider the nonlinear three-dimensional SDE with trapping potential:

$$D_\tau^\nu \xi(\varpi, \beta, \mu, \tau) = -i\left(-\frac{1}{2}\left(\frac{\partial^2}{\partial \varpi^2} + \frac{\partial^2}{\partial \beta^2} + \frac{\partial^2}{\partial \mu^2}\right)\xi(\varpi, \beta, \mu, \tau) + K(\varpi, \beta, \mu)\xi(\varpi, \beta, \mu, \tau) + |\xi(\varpi, \beta, \mu, \tau)|^2 \xi(\varpi, \beta, \mu, \tau)\right), \tag{71}$$

where $0 < \nu \leq 1,\ \tau \geq 0, \varpi, \beta, \mu \in R \times R \times R$, and $K(\varpi, \beta, \mu) = 1 - \sin^2\varpi \sin^2\beta \sin^2\mu$, with the initial condition:

$$\xi(\varpi, \beta, \mu, 0) = \sin \varpi \sin \beta \sin \mu. \tag{72}$$

Using the A-T on equation (71), we get:

$$A\left[D_\tau^\nu \xi(\varpi, \beta, \mu, \tau)\right] = A\left[-i\left(-\frac{1}{2}\left(\frac{\partial^2}{\partial \varpi^2} + \frac{\partial^2}{\partial \beta^2} + \frac{\partial^2}{\partial \mu^2}\right)\xi(\varpi, \tau) + K(\varpi, \beta, \mu)\xi(\varpi, \beta, \mu, \tau) + |\xi(\varpi, \beta, \mu, \tau)|^2 \xi(\varpi, \beta, \mu, \tau)\right)\right]. \tag{73}$$

Using the third part of Lemma 1, equation (73) is transformed as follows:

$$A[\xi(\varpi, \beta, \mu, \tau)] = \frac{\xi(\varpi, \beta, \mu, 0)}{\hbar^2} + \frac{1}{\hbar^\nu} A\left[-i\left(-\frac{1}{2}\left(\frac{\partial^2}{\partial \varpi^2} + \frac{\partial^2}{\partial \beta^2} + \frac{\partial^2}{\partial \mu^2}\right)\xi(\varpi, \beta, \mu, \tau) + K(\varpi, \beta, \mu)\xi(\varpi, \beta, \mu, \tau) + |\xi(\varpi, \beta, \mu, \tau)|^2 \xi(\varpi, \beta, \mu, \tau)\right)\right]. \tag{74}$$

On both sides of equation (74), consider the inverse of the A-T.

$$\begin{aligned}\xi(\varpi, \beta, \mu, \tau) &= A^{-1}\left\{\frac{\xi(\varpi, \beta, \mu, 0)}{\hbar^2}\right\} \\ &\quad + A^{-1}\left\{\frac{1}{\hbar^\nu} A\left[-i\left(-\left(\frac{\partial^2}{\partial \varpi^2} + \frac{\partial^2}{\partial \beta^2} + \frac{\partial^2}{\partial \mu^2}\right)\frac{1}{2}\xi(\varpi, \beta, \mu, \tau) + K(\varpi, \beta, \mu)\xi(\varpi, \beta, \mu, \tau) + |\xi(\varpi, \beta, \mu, \tau)|^2 \xi(\varpi, \beta, \mu, \tau)\right)\right]\right\}.\end{aligned} \tag{75}$$

By following the process stated in Section 3, we achieve the following result:

$$\begin{aligned}\xi(\varpi, \beta, \mu, \tau) &= \sum_{\alpha=0}^{\infty} \xi_\alpha(\varpi, \beta, \mu, \tau), \\ Q(\xi(\varpi, \beta, \mu, \tau)) &= |\xi(\varpi, \beta, \mu, \tau)|^2 \xi(\varpi, \beta, \mu, \tau) = \sum_{\alpha=0}^{\infty} W_\alpha.\end{aligned} \tag{76}$$

Using equation (76) in equation (75), we get as follows:

$$\begin{aligned}\sum_{\alpha=0}^{\infty} \xi_\alpha(\varpi, \beta, \mu, \tau) &= A^{-1}\left\{\frac{\xi(\varpi, \beta, \mu, 0)}{\hbar^2}\right\} \\ &\quad + A^{-1}\left\{\frac{1}{\hbar^\nu} A\left[-i\left(-\frac{1}{2}\left(\frac{\partial^2}{\partial \varpi^2} + \frac{\partial^2}{\partial \beta^2} + \frac{\partial^2}{\partial \mu^2}\right)\sum_{\alpha=0}^{\infty} \xi_\alpha(\varpi, \beta, \mu, \tau) + K(\varpi, \beta, \mu)\sum_{\alpha=0}^{\infty} \xi_\alpha(\varpi, \beta, \mu, \tau) + \sum_{\alpha=0}^{\infty} W_\alpha\right)\right]\right\}.\end{aligned} \tag{77}$$

By equating the like terms on both sides of equation (77), we get as follows:

$$\xi_0(\varpi,\beta,\mu,\tau) = A^{-1}\left\{\frac{\xi(\varpi,\beta,\mu,0)}{\hbar^2}\right\},$$
$$\xi_{\alpha+1}(\varpi,\beta,\mu,\tau) = A^{-1}\left\{\frac{1}{\hbar^\nu}A\left[-i\left(-\frac{1}{2}\left(\frac{\partial^2}{\partial\varpi^2}+\frac{\partial^2}{\partial\beta^2}+\frac{\partial^2}{\partial\mu^2}\right)\xi_\alpha(\varpi,\beta,\mu,\tau)+K(\varpi,\beta,\mu)\xi_\alpha(\varpi,\beta,\mu,\tau)+W_\alpha\right)\right]\right\}. \tag{78}$$

The following results are obtained from equation (78) using the iteration procedure stated in Section 3.

$$\begin{aligned}
\xi_0(\varpi,\beta,\mu,\tau) &= \sin\varpi\sin\beta\sin\mu,\\
\xi_1(\varpi,\beta,\mu,\tau) &= -\frac{5i\tau^\nu}{2\Gamma(\nu+1)}\sin\varpi\sin\beta\sin\mu,\\
\xi_2(\varpi,\beta,\mu,\tau) &= \frac{25i^2\tau^{2\nu}}{4\Gamma(2\nu+1)}\sin\varpi\sin\beta\sin\mu,\\
\xi_3(\varpi,\beta,\mu,\tau) &= -\frac{125i^3\tau^{3\nu}}{8\Gamma(3\nu+1)}\sin\varpi\sin\beta\sin\mu,\\
\xi_4(\varpi,\beta,\mu,\tau) &= \frac{625i^4\tau^{4\nu}}{16\Gamma(4\nu+1)}\sin\varpi\sin\beta\sin\mu,\\
\xi_5(\varpi,\beta,\mu,\tau) &= -\frac{3125i^5\tau^{5\nu}}{32\Gamma(5\nu+1)}\sin\varpi\sin\beta\sin\mu.
\end{aligned} \tag{79}$$

As a result, we get the following solution in series form for equation (78).

$$\begin{aligned}
\xi(\varpi,\beta,\mu,\tau) = {}& \sin\varpi\sin\beta\sin\mu - \frac{5i\tau^\nu}{2\Gamma(\nu+1)}\sin\varpi\sin\beta\sin\mu\\
&+\frac{25i^2\tau^{2\nu}}{4\Gamma(2\nu+1)}\sin\varpi\sin\beta\sin\mu\\
&-\frac{125i^3\tau^{3\nu}}{8\Gamma(3\nu+1)}\sin\varpi\sin\beta\sin\mu\\
&+\frac{625i^4\tau^{4\nu}}{16\Gamma(4\nu+1)}\sin\varpi\sin\beta\sin\mu\\
&-\frac{3125i^5\tau^{5\nu}}{32\Gamma(5\nu+1)}\sin\varpi\sin\beta\sin\mu+\cdots.
\end{aligned} \tag{80}$$

When we use $\nu = 1$ in equation (80), we get the following precise solution to equation (78).

$$\xi(\varpi,\beta,\mu,\tau) = \sin\varpi\sin\beta\sin\mu e^{-(i5/2)\tau}. \tag{81}$$

5. Numerical Simulation and Discussion

In this section, we discuss and evaluate the graphic and numerical results of the approximate and exact solutions to the models discussed in Examples 1–4. Figures 1–8 represent the 2D graphs of the 5th approximate solution obtained by ATDM at $\nu = 0.6, 0.7, 0.8, 0.9, 1.0$ and the exact solution. These figures show that the approximate solutions obtained by the ATDM approach the exact solutions. The approximate result corresponds with the precise result at $\nu = 1$, and this proves the effectiveness and precision of the suggested method. Figures 9–16 demonstrate the 2D graph of absolute error over the 5th term, with approximate and exact solutions to Examples 1–4. As for the figure, approximate and exact solutions are in very good agreement. Tables 1–4 show comparisons of the absolute error of the 5th approximate solution obtained by ATDM of Examples 1–4 at $\nu = 1$ with the absolute error of approximate solutions obtained by FRDTM [42], HPM [35], and HAM [43]. The results obtained from the suggested method are extremely similar to those obtained by FRDTM, HPM, and HAM. The convergence of the approximate solution to the exact solution for Examples 1–4 has been shown numerically as in Tables 5–12. The results show that the proposed method is a useful and efficient algorithm for solving certain classes of fractional-order differential equations with fewer calculations and iteration steps. The 3D graphs of these solutions are also sketched to show the behavior of the exact solutions in Figures 17–24.

The following 2D graphs show the real and imaginary parts of approximate and exact solutions to Example 1:

Figures 1 and 2 show the behavior of real imaginary in the interval $\tau \in [0, 1]$ between the 5th step iteration approximate and exact solutions of equation (39) at several values of ν when $\varpi = 0.05$, $a = 1$ and $b = 1$. The approximate result corresponds with the precise result at $\nu = 1$ and this proves the effectiveness and precision of the suggested method.

The graphs of absolute error for the real and imaginary parts of the 5th approximation and exact solutions to Example 1 are as follows:

Figures 9 and 10 demonstrate the 2D graph of real and imaginary parts of absolute error in the intervals $\tau \in [0, 1]$ when $\varpi = 0.05$, $a = 1$, and $b = 1$ are over the 5th terms, approximate and exact solutions of equation (39) at $\nu = 1$. As

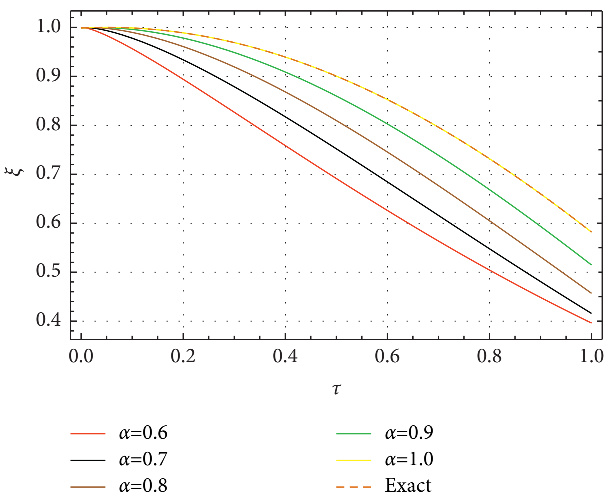

FIGURE 1: The approximate and exact solutions to the real part of Example 1.

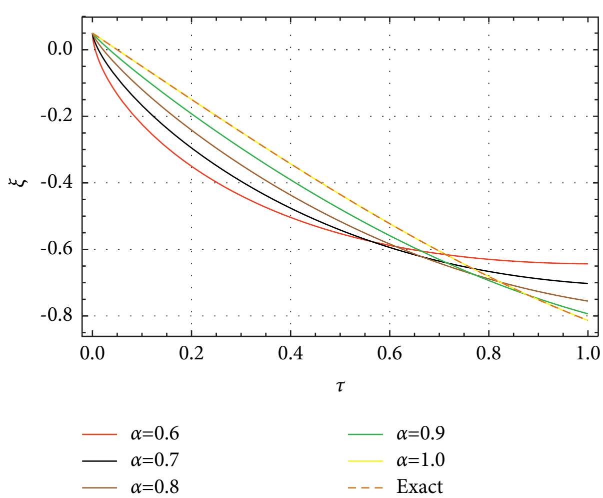

FIGURE 2: The approximate and exact solutions to the imaginary part of Example 1.

for the figures, approximate and exact solutions are in very good agreement.

The accuracy and capability of the numerical method can be determined using error functions. To demonstrate the accuracy and capability of the ATDM, we used recurrence and absolute error functions.

Table 1 shows comparisons of the real and imaginary parts of the absolute error of the 5th approximate solution obtained by ATDM in Example 1 at $\nu = 1$ with the absolute error of approximate solutions obtained by FRDTM [42]. The results obtained from the suggested method are extremely similar to those obtained by FRDTM.

The recurrence error $|\xi^5(\varpi,\tau) - \xi^4(\varpi,\tau)|$ between the 5th and 4th approximate solutions of the real part with different values of ν, when $\varpi = 0.05$, $a = 1$, and $b = 1$ in Example 1 are presented as follows:

The recurrence error $|\xi^5(\varpi,\tau) - \xi^4(\varpi,\tau)|$ between the 5th and 4th approximate solutions of the imaginary part with different values of ν, when $\varpi = 0.05$, $a = 1$, and $b = 1$ in Example 1 are presented as follows:

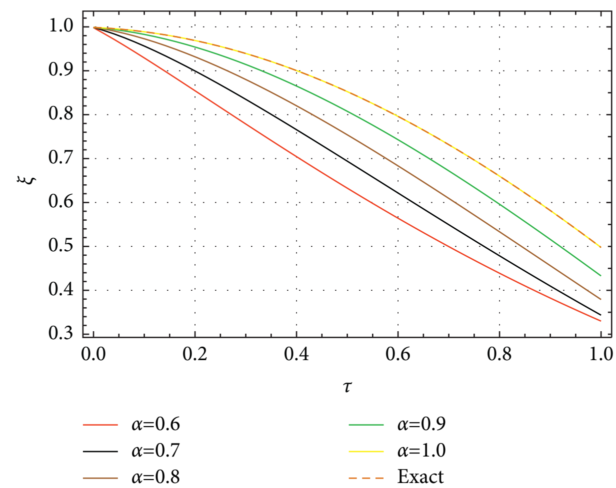

FIGURE 3: The approximate and exact solutions to the real part of Example 2.

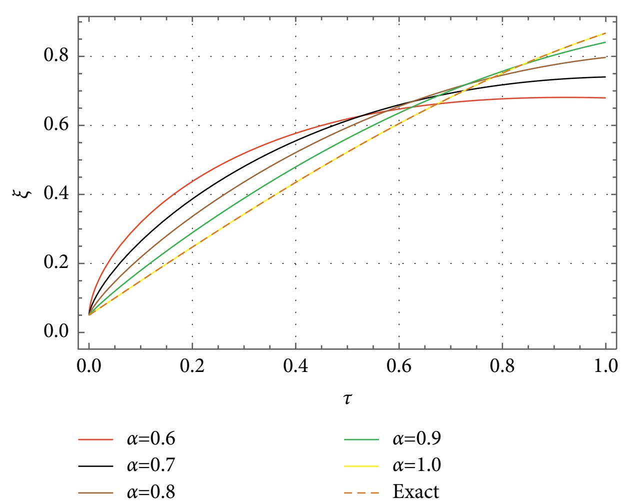

FIGURE 4: The approximate and exact solutions to the imaginary part of Example 2.

The convergence of the ATDM of real and imaginary of the approximate solution to the exact solution for equation (39) has been shown numerically as in Tables 5 and 6. The results show that the current technique is a useful and efficient algorithm for solving fractional-order differential equations with fewer calculations and iteration steps.

The following are 3D graphs for the real and imaginary parts of the exact solution to Example 1:

The real and imaginary parts of the exact solution equation (39) at $\nu = 1$ are shown in Figures 17 and 18 respectively in the intervals $\tau \in [0, 2]$, $\varpi \in [-2\pi, 2\pi]$ with $a = 1$ and $b = 1$.

The following 2D graphs show the real and imaginary parts of approximate and exact solutions to Example 2:

Figures 3 and 4 show the behavior of real and imaginary parts in the interval $\tau \in [0, 1]$ between the 5th step iteration

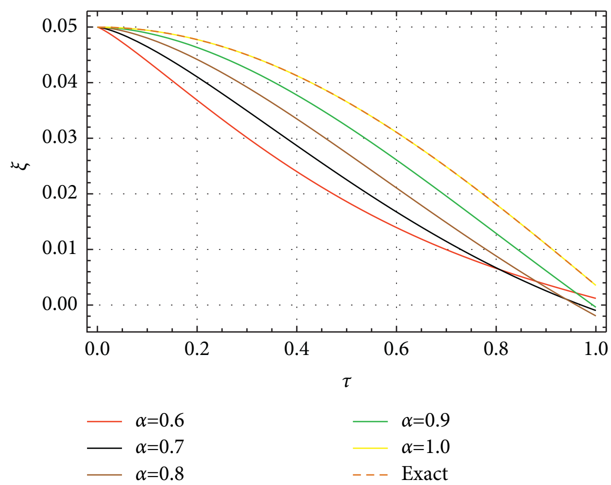

Figure 5: The approximate and exact solutions to the real part of Example 3.

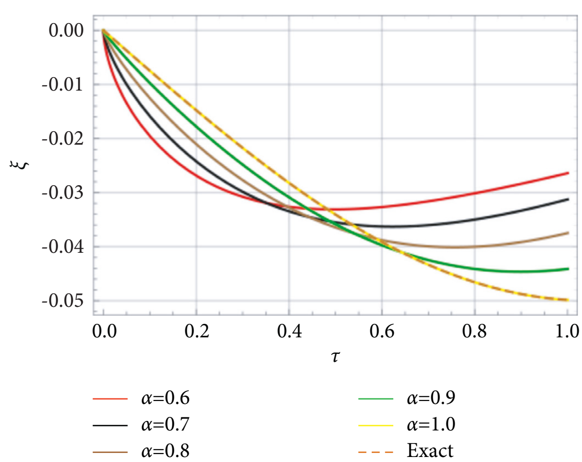

Figure 6: The approximate and exact solutions to the imaginary part of Example 3.

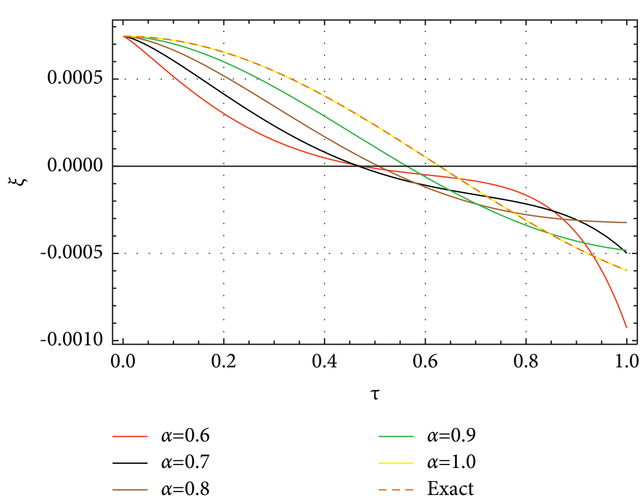

Figure 7: The approximate and exact solutions to the real part of Example 4.

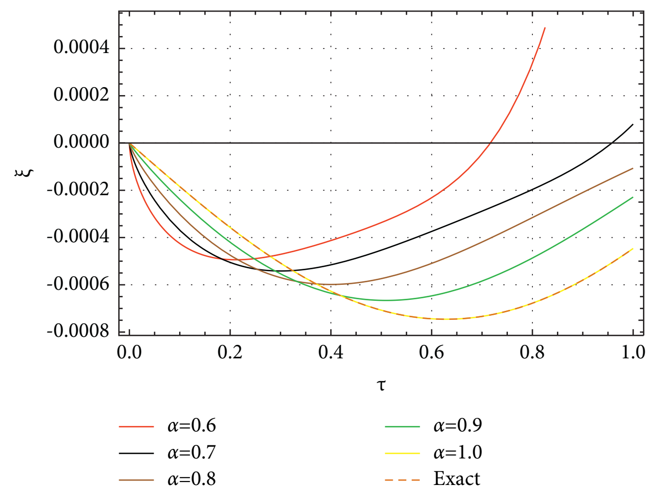

Figure 8: The approximate and exact solutions to the imaginary part of Example 4.

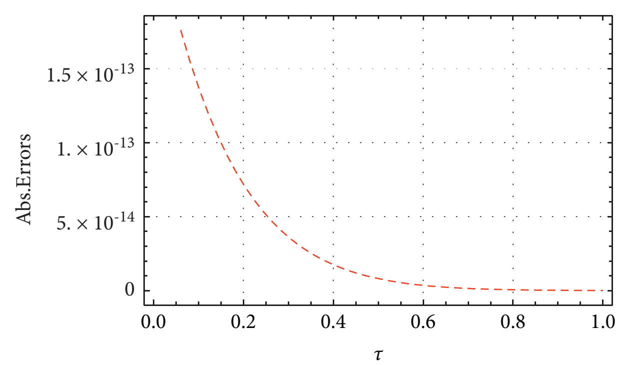

Figure 9: The absolute error for the real part of Example 1.

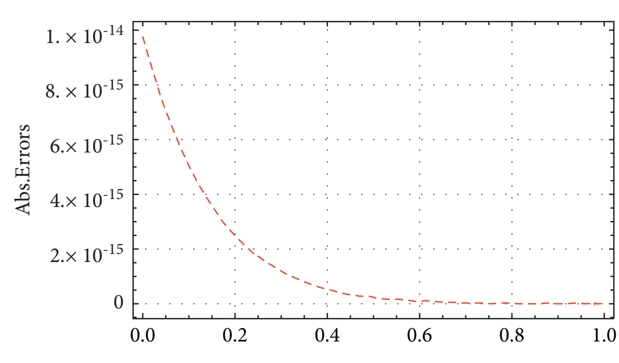

Figure 10: The absolute error for the imaginary part of Example 1.

approximate and exact solutions of equation (51) at several values of ν when $\varpi = 0.05$. The approximate result corresponds with the precise result at $\nu = 1$, and this proves the effectiveness and precision of the suggested method.

The graphs of absolute error for the real and imaginary parts of the 5th approximation and exact solutions to Example 2 are as follows:

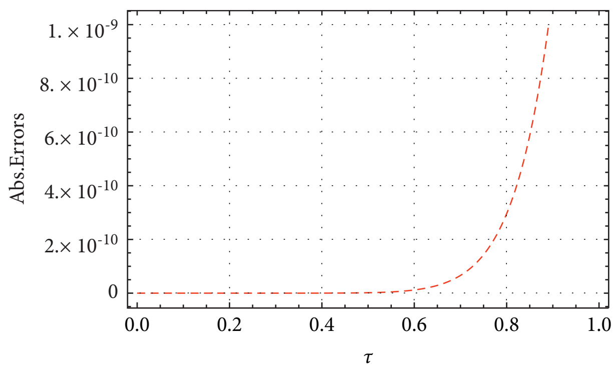

Figure 11: The absolute error for the real part of Example 2.

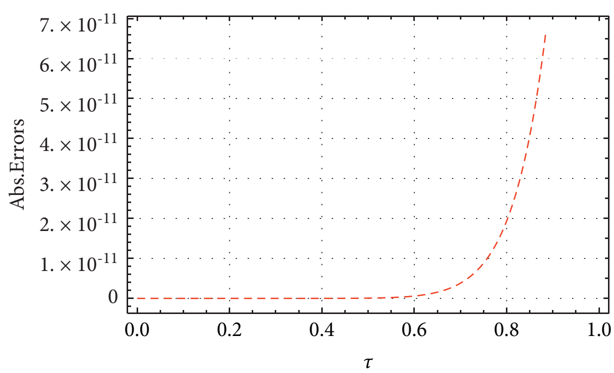

Figure 12: The absolute error for the imaginary part of Example 2.

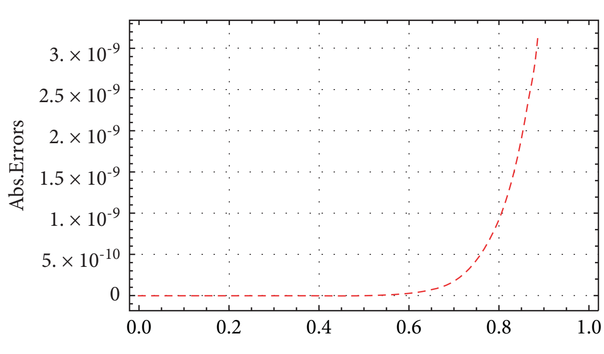

Figure 13: The absolute error for the real part of Example 3.

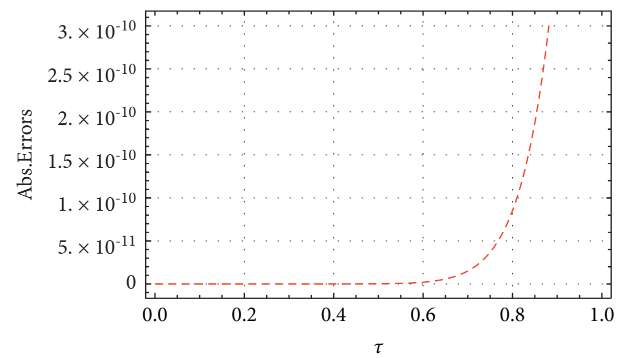

Figure 14: The absolute error for the imaginary part of Example 3.

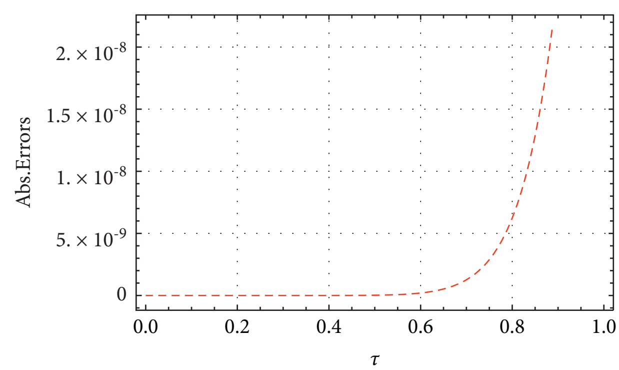

Figure 15: The absolute error for the real part of Example 4.

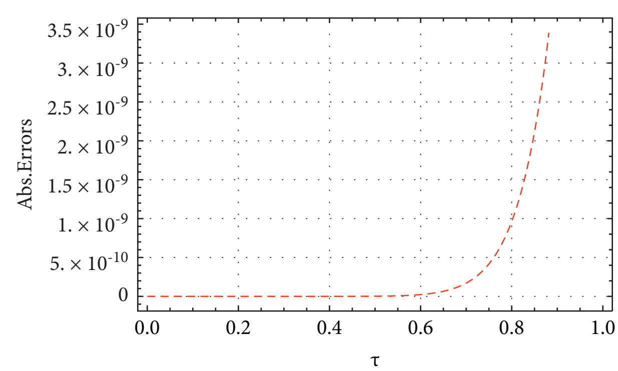

Figure 16: The absolute error for the imaginary part of Example 4.

Figures 11 and 12 demonstrate the 2D graph of real and imaginary parts of absolute error in the intervals $\tau \in [0, 1]$ when $\varpi = 0.05$ are over the 5th terms approximate and exact solutions of equation (51) at $\nu = 1$. As for the figures, approximate and precise solutions are in very good agreement.

Table 2 shows comparisons of the real and imaginary parts of absolute error of the 5th approximate solution obtained by ATDM of Example 2 at $\nu = 1$ with the absolute error of approximate solutions obtained by FRDTM [42]. The results obtained from the suggested method are extremely similar to those obtained by FRDTM.

The recurrence error $|\xi^5(\varpi, \tau) - \xi^4(\varpi, \tau)|$ between the 5th and 4th approximate solutions of the real part with different values of ν, when $\varpi = 0.05$ in Example 2 are presented as follows:

The recurrence error $|\xi^5(\varpi, \tau) - \xi^4(\varpi, \tau)|$ between the 5th and 4th approximate solutions of the imaginary part with different values of ν, when $\varpi = 0.05$ in Example 2 are presented as follows:

The convergence of the ATDM of real and imaginary of the approximate solution to the exact solution for equation (51) has been shown numerically as in Tables 7 and 8. The results show that the current technique is a useful and

Table 2: The absolute error in ATDM and FRDTM for Example 2 at $\nu = 2$.

τ	Real part [ATDM] Abs. error	Img. part [ATDM] Abs. error	Real part [FRDTM] Abs. error	Img. part [FRTDM] Abs. error
0.2	0	$2.775557561562891 \times 10^{-17}$	0	$2.775557561562891 \times 10^{-17}$
0.4	$3.508304757815494 \times 10^{-14}$	$2.886579864025407 \times 10^{-15}$	$3.508304757815494 \times 10^{-14}$	$2.886579864025407 \times 10^{-15}$
0.6	$4.519384866341625 \times 10^{-12}$	$4.35984581770299 \times 10^{-13}$	$4.519384866341625 \times 10^{-12}$	$4.35984581770299 \times 10^{-13}$
0.8	$1.423423601210061 \times 10^{-10}$	$1.593580822856211 \times 10^{-11}$	$1.423423601210061 \times 10^{-10}$	$1.593580822856211 \times 10^{-11}$
1.0	$2.065669746365017 \times 10^{-9}$	$2.633981921462691 \times 10^{-10}$	$2.065669746365017 \times 10^{-9}$	$2.633981921462691 \times 10^{-10}$

Table 3: The absolute error in ATDM and HPM for Example 3 at $\nu = 1$.

τ	Real part [ATDM] Abs. error	Img. part [ATDM] Abs. error	Real part [HPM] Abs. error	Img. part [HPM] Abs. error
0.2	$5.551115123125783 \times 10^{-17}$	0	$5.551115123125783 \times 10^{-17}$	0
0.4	$2.266797860528413 \times 10^{-13}$	$1.047079090099600 \times 10^{-14}$	$2.266797860528413 \times 10^{-13}$	$1.047079090099600 \times 10^{-14}$
0.6	$2.933806669824790 \times 10^{-11}$	$2.032304879939772 \times 10^{-12}$	$2.933806669824790 \times 10^{-11}$	$2.032304879939772 \times 10^{-12}$
0.8	$9.229918426778560 \times 10^{-10}$	$8.528888012504510 \times 10^{-11}$	$9.229918426778560 \times 10^{-10}$	$8.528888012504510 \times 10^{-11}$
1.0	$1.337196644298627 \times 10^{-8}$	$1.545451835949229 \times 10^{-9}$	$1.337196644298627 \times 10^{-8}$	$1.5454518359492290 \times 10^{-9}$

Table 4: The absolute error in ATDM and HAM for Example 4 at $\nu = 1$.

τ	Real part [ATDM] Abs. error	Img. part [ATDM] Abs. error	Real part [HAM] Abs. error	Img. part [HAM] Abs. error
0.2	$3.794707603699265 \times 10^{-16}$	$1.463672932855431 \times 10^{-17}$	$3.794707603699265 \times 10^{-16}$	$1.463672932855431 \times 10^{-17}$
0.4	$1.548127132131732 \times 10^{-12}$	$1.191737680761306 \times 10^{-13}$	$1.548127132131732 \times 10^{-12}$	$1.191737680761306 \times 10^{-13}$
0.6	$1.994952888051838 \times 10^{-10}$	$2.305647122877174 \times 10^{-11}$	$1.994952888051838 \times 10^{-10}$	$2.305647122877174 \times 10^{-11}$
0.8	$6.238188888683330 \times 10^{-9}$	$9.625127946185849 \times 10^{-10}$	$6.238188888683330 \times 10^{-9}$	$9.625127946185849 \times 10^{-10}$
1.0	$8.967831111224030 \times 10^{-8}$	$1.732387384885186 \times 10^{-8}$	$8.967831111224030 \times 10^{-8}$	$1.732387384885186 \times 10^{-8}$

Table 5: The recurrence error of the 5th approximate solution of the real part in Example 1.

τ	$\nu = 0.7$	$\nu = 0.8$	$\nu = 0.9$	$\nu = 1.0$
0.1	$1.9863230258832510 \times 10^{-11}$	$2.480476538225475 \times 10^{-13}$	$2.754480547804426 \times 10^{-15}$	$2.753540058639898 \times 10^{-17}$
0.2	$2.5462310564404910 \times 10^{-9}$	$6.356503419032404 \times 10^{-11}$	$1.41126628375623 \times 10^{-12}$	$2.820907153618413 \times 10^{-14}$
0.3	$4.3559264601363860 \times 10^{-8}$	$1.630598080005387 \times 10^{-9}$	$5.428928326273314 \times 10^{-11}$	$1.6274165548755540 \times 10^{-12}$
0.4	$3.2669475564040040 \times 10^{-7}$	$1.630154704745158 \times 10^{-8}$	$7.234972435809250 \times 10^{-10}$	$2.8912347348589850 \times 10^{-11}$
0.5	$1.5594317330665020 \times 10^{-6}$	$9.724388066839424 \times 10^{-8}$	$5.393791208135125 \times 10^{-9}$	$2.6938949149435820 \times 10^{-10}$
0.6	$5.5932228619978110 \times 10^{-6}$	$4.184575219876433 \times 10^{-7}$	$2.784754999984136 \times 10^{-8}$	$1.6687458133498650 \times 10^{-9}$
0.7	$1.6470066797307933 \times 10^{-5}$	$1.437319768581204 \times 10^{-6}$	$1.115745763781643 \times 10^{-7}$	$7.7992900939752010 \times 10^{-9}$
0.8	$4.1978532985731196 \times 10^{-5}$	$4.186076646645796 \times 10^{-6}$	$3.713180897405904 \times 10^{-7}$	$2.9660020264616400 \times 10^{-8}$
0.9	$9.5822726035593689 \times 10^{-5}$	$1.0748242434163506 \times 10^{-6}$	$1.072429735204339 \times 10^{-6}$	$9.6359264875560130 \times 10^{-8}$
1.0	$2.0050812724929500 \times 10^{-4}$	$2.4986212656296714 \times 10^{-5}$	$2.769704199336456 \times 10^{-6}$	$2.7648088107301450 \times 10^{-7}$

Table 6: The recurrence error of the 5th approximate solution of the imaginary part in Example 1.

τ	$\nu = 0.7$	$\nu = 0.8$	$\nu = 0.9$	$\nu = 1.0$
0.1	$5.729282854280857 \times 10^{-14}$	$5.566602532673186 \times 10^{-15}$	$9.391428658269753 \times 10^{-17}$	$1.127083924407682 \times 10^{-18}$
0.2	$6.735588070529998 \times 10^{-13}$	$1.29434773662193 \times 10^{-13}$	$2.86554558790132 \times 10^{-14}$	$8.979209489138208 \times 10^{-16}$
0.3	$2.240327760588405 \times 10^{-9}$	$2.657335380224294 \times 10^{-11}$	$3.928763432275554 \times 10^{-13}$	$3.7004114535955 \times 10^{-14}$
0.4	$2.415220588436187 \times 10^{-8}$	$5.443488739768476 \times 10^{-10}$	$3.891048192098205 \times 10^{-12}$	$3.947468488238387 \times 10^{-13}$
0.5	$1.477344106931362 \times 10^{-7}$	$4.825025026815447 \times 10^{-9}$	$9.526894455781187 \times 10^{-11}$	$1.232929037808270 \times 10^{-12}$
0.6	$6.392078149330569 \times 10^{-7}$	$2.727397229393246 \times 10^{-8}$	$8.267292729705227 \times 10^{-10}$	$7.495149197961302 \times 10^{-12}$
0.7	$2.187803743850105 \times 10^{-6}$	$1.152748324472957 \times 10^{-7}$	$4.630213360876863 \times 10^{-9}$	$1.0569208657930970 \times 10^{-10}$
0.8	$6.320873774992085 \times 10^{-6}$	$3.96750649205628 \times 10^{-7}$	$1.972744306783386 \times 10^{-8}$	$6.7041439426968450 \times 10^{-10}$
0.9	$1.606257206934282 \times 10^{-5}$	$1.171284786793358 \times 10^{-6}$	$6.92782295622906 \times 10^{-8}$	$3.0494721017930660 \times 10^{-9}$
1.0	$3.691229597776269 \times 10^{-5}$	$3.069260602197251 \times 10^{-6}$	$2.103049742344222 \times 10^{-7}$	$1.1247880551985750 \times 10^{-8}$

Table 7: The recurrence error of the the approximate solution of the real part in Example 2.

τ	$\nu = 0.7$	$\nu = 0.8$	$\nu = 0.9$	$\nu = 1.0$
0.1	$1.976971658223765 \times 10^{-11}$	$2.473641816908283 \times 10^{-13}$	$2.750095402344202 \times 10^{-15}$	$2.751035891508731 \times 10^{-17}$
0.2	$2.52678613921649 \times 10^{-9}$	$6.326039570110015 \times 10^{-11}$	$1.407076602719864 \times 10^{-12}$	$2.815778619333783 \times 10^{-14}$
0.3	$4.311799014005643 \times 10^{-8}$	$1.619798972797868 \times 10^{-9}$	$5.405728516404219 \times 10^{-11}$	$1.622980497927706 \times 10^{-12}$
0.4	$3.226514454036917 \times 10^{-7}$	$1.616576300475306 \times 10^{-8}$	$7.19494314294836 \times 10^{-10}$	$2.880731496644064 \times 10^{-11}$
0.5	$1.536892238892099 \times 10^{-6}$	$9.627636757901811 \times 10^{-8}$	$5.357333694498901 \times 10^{-9}$	$2.681667536373432 \times 10^{-10}$
0.6	$5.501465744903981 \times 10^{-6}$	$4.136441235299919 \times 10^{-7}$	$2.762589303466765 \times 10^{-8}$	$1.659660768720673 \times 10^{-9}$
0.7	$1.616936914302743 \times 10^{-5}$	$1.418630876198142 \times 10^{-6}$	$1.105549182157846 \times 10^{-7}$	$7.749774527601226 \times 10^{-9}$
0.8	$4.113778074791275 \times 10^{-5}$	$4.125554726718593 \times 10^{-6}$	$3.674935878917996 \times 10^{-7}$	$2.944491394597482 \times 10^{-8}$
0.9	$9.374043008389243 \times 10^{-5}$	$1.0577612629278684 \times 10^{-5}$	$1.060155771139881 \times 10^{-6}$	$9.557343069541972 \times 10^{-8}$
1.0	$1.9582134116140592 \times 10^{-4}$	$2.45549708950409 \times 10^{-5}$	$2.734871750812168 \times 10^{-6}$	$2.739767139418478 \times 10^{-7}$

Table 8: The recurrence error of the 5th approximate solution of the imaginary part in Example 2.

τ	$\nu = 0.7$	$\nu = 0.8$	$\nu = 0.9$	$\nu = 1.0$
0.1	$1.926007539341256 \times 10^{-12}$	$1.922465206587756 \times 10^{-14}$	$1.815440978456445 \times 10^{-16}$	$1.627499919875739 \times 10^{-18}$
0.2	$3.212183277944602 \times 10^{-10}$	$6.217126403566797 \times 10^{-12}$	$1.123792369482977 \times 10^{-13}$	$1.922772907632402 \times 10^{-15}$
0.3	$6.577805665150846 \times 10^{-9}$	$1.892287752233342 \times 10^{-10}$	$5.028971037475495 \times 10^{-12}$	$1.256513068851356 \times 10^{-13}$
0.4	$5.664659911177431 \times 10^{-8}$	$2.169068535347471 \times 10^{-9}$	$7.610081091968145 \times 10^{-11}$	$2.493643660279493 \times 10^{-12}$
0.5	$3.026797519340784 \times 10^{-7}$	$1.450910885437432 \times 10^{-8}$	$6.332736016444167 \times 10^{-10}$	$2.566730381652197 \times 10^{-11}$
0.6	$1.194404986717049 \times 10^{-6}$	$6.891376017773192 \times 10^{-8}$	$3.602715131890486 \times 10^{-9}$	$1.740543007331589 \times 10^{-10}$
0.7	$3.821136878718447 \times 10^{-6}$	$2.581914817482758 \times 10^{-7}$	$1.574595275095308 \times 10^{-8}$	$8.837938438846447 \times 10^{-10}$
0.8	$1.0480156108100884 \times 10^{-5}$	$8.126788825165077 \times 10^{-7}$	$5.66988415843565 \times 10^{-8}$	$3.628126275591497 \times 10^{-9}$
0.9	$2.5548636246620873 \times 10^{-5}$	$2.238467006737139 \times 10^{-6}$	$1.759964515566688 \times 10^{-7}$	$1.265411208128710 \times 10^{-8}$
1.0	$5.674529965660330 \times 10^{-5}$	$5.548386062052328 \times 10^{-6}$	$4.85763358662764 \times 10^{-7}$	$3.879371899481992 \times 10^{-8}$

Table 9: The recurrence error of the 5th approximate solution of the real part in Example 3.

τ	$\nu = 0.7$	$\nu = 0.8$	$\nu = 0.9$	$\nu = 1.0$
0.1	$5.718354659335265 \times 10^{-11}$	$7.147943324169061 \times 10^{-13}$	$7.942159249076738 \times 10^{-15}$	$7.942159249076745 \times 10^{-17}$
0.2	$7.319493963949132 \times 10^{-9}$	$1.829873490987278 \times 10^{-10}$	$4.066385535527289 \times 10^{-12}$	$8.132771071054586 \times 10^{-14}$
0.3	$1.250604163996619 \times 10^{-7}$	$4.689765614987320 \times 10^{-9}$	$1.563255204995775 \times 10^{-10}$	$4.689765614987315 \times 10^{-12}$
0.4	$9.368952273854868 \times 10^{-7}$	$4.684476136927436 \times 10^{-8}$	$2.081989394189970 \times 10^{-9}$	$8.327957576759896 \times 10^{-11}$
0.5	$4.467464577605666 \times 10^{-6}$	$2.792165361003536 \times 10^{-7}$	$1.551202978335300 \times 10^{-8}$	$7.756014891676498 \times 10^{-10}$
0.6	$1.6007733299156725 \times 10^{-5}$	$1.200579997436754 \times 10^{-6}$	$8.003866649578365 \times 10^{-8}$	$4.802319989747010 \times 10^{-9}$
0.7	$4.709310951212926 \times 10^{-5}$	$4.120647082311310 \times 10^{-6}$	$3.204947730686570 \times 10^{-7}$	$2.243463411480599 \times 10^{-8}$
0.8	$1.1992258910534259 \times 10^{-4}$	$1.1992258910534254 \times 10^{-5}$	$1.065978569825267 \times 10^{-6}$	$8.527828558602135 \times 10^{-8}$
0.9	$2.735071306660605 \times 10^{-4}$	$3.076955219993183 \times 10^{-5}$	$3.076955219993184 \times 10^{-6}$	$2.769259697993865 \times 10^{-7}$
1.0	$5.718354659335249 \times 10^{-4}$	$7.147943324169061 \times 10^{-5}$	$7.942159249076736 \times 10^{-6}$	$7.942159249076734 \times 10^{-7}$

Table 10: The recurrence error of the 5th approximate solution of the imaginary part in Example 3.

τ	$\nu = 0.7$	$\nu = 0.8$	$\nu = 0.9$	$\nu = 1.0$
0.1	$4.044352360290241 \times 10^{-12}$	$2.95593353802917 \times 10^{-14}$	$1.896521881939167 \times 10^{-16}$	$1.083021715783192 \times 10^{-18}$
0.2	$8.40968933466814 \times 10^{-10}$	$1.317524278577765 \times 10^{-11}$	$1.811985904661213 \times 10^{-13}$	$2.218028473923979 \times 10^{-15}$
0.3	$1.908458178643264 \times 10^{-8}$	$4.670482042212528 \times 10^{-10}$	$1.003363456757901 \times 10^{-11}$	$1.918540478858446 \times 10^{-13}$
0.4	$1.748682320562088 \times 10^{-7}$	$3.375983249079892 \times 10^{-8}$	$1.731218052350544 \times 10^{-10}$	$4.542522314596309 \times 10^{-12}$
0.5	$9.748056090119807 \times 10^{-7}$	$4.184376006926562 \times 10^{-8}$	$1.576742960965881 \times 10^{-9}$	$5.288191971597613 \times 10^{-11}$
0.6	$3.968383306108540 \times 10^{-7}$	$2.081736075628826 \times 10^{-7}$	$9.586393166413172 \times 10^{-9}$	$3.929170900702099 \times 10^{-10}$
0.7	$1.3004806485065536 \times 10^{-5}$	$4.646598110881215 \times 10^{-7}$	$4.409897082301801 \times 10^{-8}$	$2.141487801867844 \times 10^{-9}$
0.8	$3.636150797676397 \times 10^{-5}$	$2.617499157554769 \times 10^{-6}$	$1.654050363788450 \times 10^{-7}$	$9.303085700293241 \times 10^{-9}$
0.9	$9.005675804590360 \times 10^{-5}$	$7.379530772932580 \times 10^{-6}$	$5.308339629215292 \times 10^{-7}$	$3.398636902083380 \times 10^{-8}$
1.0	$2.0269777712677892 \times 10^{-4}$	$1.865067975614827 \times 10^{-5}$	$1.506460878596710 \times 10^{-6}$	$1.083021715783191 \times 10^{-7}$

Table 11: The recurrence error of the 5th approximate solution of the real part in Example 4.

τ	$\nu = 0.7$	$\nu = 0.8$	$\nu = 0.9$	$\nu = 1.0$
0.1	$1.410899077403071 \times 10^{-10}$	$1.763623846753835 \times 10^{-12}$	$1.959582051948707 \times 10^{-14}$	$1.959582051948706 \times 10^{-16}$
0.2	$1.80595081907593 \times 10^{-8}$	$4.514877047689823 \times 10^{-10}$	$1.003306010597737 \times 10^{-11}$	$2.006612021195475 \times 10^{-13}$
0.3	$3.085636282280515 \times 10^{-7}$	$1.15711360585519 \times 10^{-8}$	$3.857045352850636 \times 10^{-10}$	$1.157113605855191 \times 10^{-11}$
0.4	$2.311617048417188 \times 10^{-6}$	$1.155808524208595 \times 10^{-7}$	$5.136926774260415 \times 10^{-9}$	$2.054770709704167 \times 10^{-10}$
0.5	$1.1022649042211474 \times 10^{-5}$	$6.889155651382168 \times 10^{-7}$	$3.827308695212317 \times 10^{-8}$	$1.913654347606158 \times 10^{-9}$
0.6	$3.949614441319053 \times 10^{-5}$	$2.96221083098929 \times 10^{-6}$	$1.974807220659528 \times 10^{-7}$	$1.184884332395716 \times 10^{-8}$
0.7	$1.1619360589017545 \times 10^{-4}$	$1.0166940515390365 \times 10^{-5}$	$7.907620400859165 \times 10^{-7}$	$5.535334280601419 \times 10^{-8}$
0.8	$2.958869821974002 \times 10^{-4}$	$2.958869821974005 \times 10^{-5}$	0.000002630106508421338	$2.104085206737067 \times 10^{-7}$
0.9	$6.748286549347473 \times 10^{-4}$	$7.591822368015921 \times 10^{-5}$	$7.591822368015916 \times 10^{-6}$	$6.832640131214322 \times 10^{-7}$
1.0	$1.410899077403069 \times 10^{-3}$	$1.7636238467538362 \times 10^{-4}$	$1.959582051948707 \times 10^{-5}$	$1.959582051948706 \times 10^{-6}$

Table 12: The recurrence error of the 5th approximate solution of the imaginary part in Example 4.

τ	$\nu = 0.7$	$\nu = 0.8$	$\nu = 0.9$	$\nu = 1.0$
0.1	$1.663116214880405 \times 10^{-11}$	$1.215537262646501 \times 10^{-13}$	$7.79886620339425 \times 10^{-16}$	$4.453595572610698 \times 10^{-18}$
0.2	$3.458227535246130 \times 10^{-9}$	$5.417915641366231 \times 10^{-11}$	$7.451237851492589 \times 10^{-13}$	$9.120963732706710 \times 10^{-15}$
0.3	$7.847950572968780 \times 10^{-8}$	$1.920592896894366 \times 10^{-9}$	$4.126025345211919 \times 10^{-11}$	$7.889410949012672 \times 10^{-13}$
0.4	$7.190921222780890 \times 10^{-7}$	$2.414883590902916 \times 10^{-8}$	$7.119104761067955 \times 10^{-10}$	$1.867973372458334 \times 10^{-11}$
0.5	$4.008589930546624 \times 10^{-6}$	$1.720696657048121 \times 10^{-7}$	$6.483873192722287 \times 10^{-9}$	$2.174607213188817 \times 10^{-10}$
0.6	$1.6318762648010684 \times 10^{-5}$	$8.560502928660110 \times 10^{-7}$	$3.942110997503766 \times 10^{-8}$	$1.615751362357795 \times 10^{-9}$
0.7	$5.347828925356589 \times 10^{-5}$	$3.323770499911620 \times 10^{-6}$	$1.813435301914099 \times 10^{-7}$	$8.806213628229532 \times 10^{-9}$
0.8	$1.495255806774449 \times 10^{-4}$	$1.076366474421812 \times 10^{-5}$	$6.801776242977975 \times 10^{-7}$	$3.825609466794668 \times 10^{-8}$
0.9	$3.703308743231145 \times 10^{-4}$	$3.0346063333097793 \times 10^{-5}$	$2.182892321184059 \times 10^{-6}$	$6.832640131214322 \times 10^{-7}$
1.0	$8.335326149365687 \times 10^{-4}$	$7.669521633561604 \times 10^{-5}$	$6.194859624193012 \times 10^{-6}$	$4.453595572610698 \times 10^{-7}$

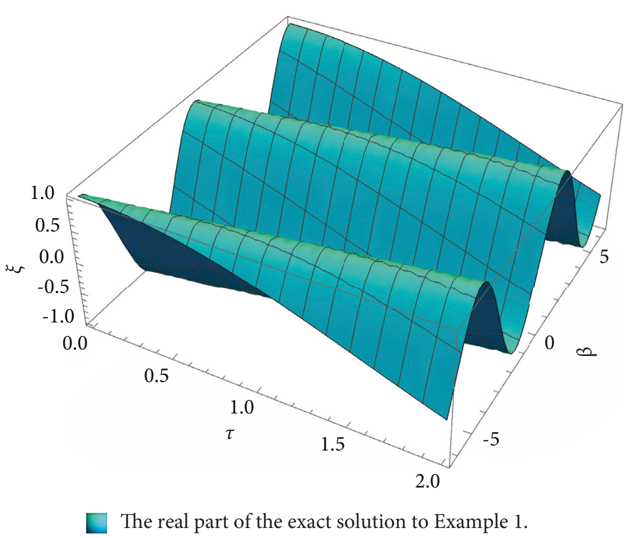

Figure 17: The real part of the exact solution to Example 1.

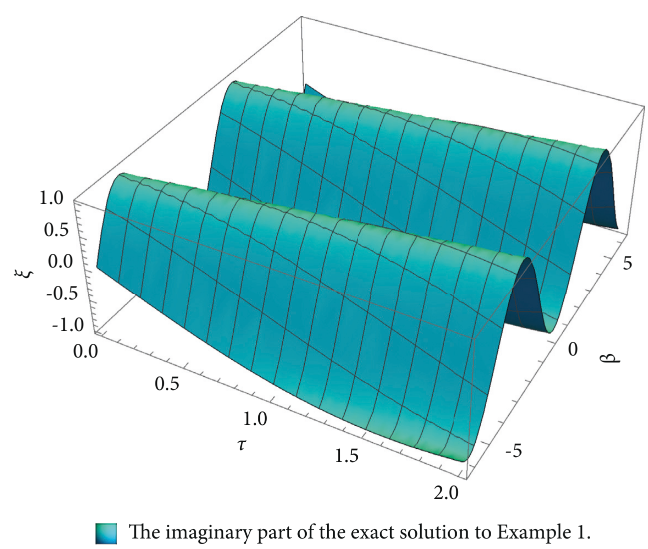

Figure 18: The imaginary part of the exact solution to Example 1.

efficient algorithm for solving fractional-order differential equations with fewer calculations and iteration steps.

The following are the 3D graphs for the real and imaginary parts of the exact solution to Example 2:

The real and imaginary parts of the exact solution equation (51) at $\nu = 1$ are shown in Figures 19 and 20 respectively in the intervals $\tau \in [0, 2]$, and $\varpi \in [-2\pi, 2\pi]$.

The following 2D graphs show the real and imaginary parts of approximate and exact solutions to Example 3:

Figures 5 and 6 show the behavior of the real and imaginary parts in the interval $\tau \in [0, 1]$ between the 5th step iteration approximate and exact solutions of equation (60) at several values of ν when $\varpi = 0.05$. The approximate result corresponds with the precise result at $\nu = 1$ and this proves the effectiveness and precision of the suggested method.

The 2D graphs of absolute error for the real and imaginary parts of the 5th approximation and exact solutions to Example 3 are as follows:

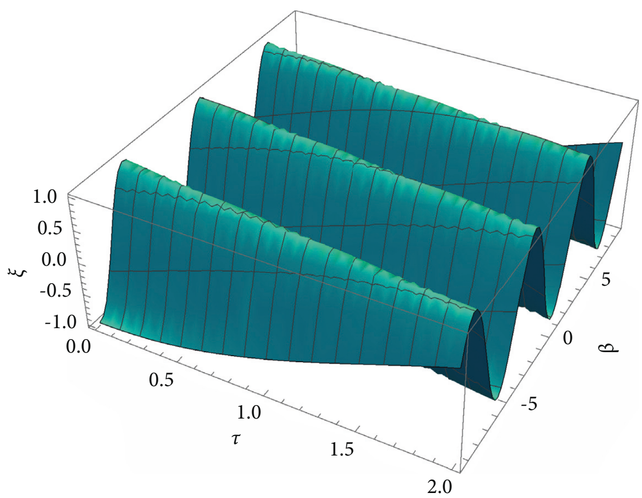

FIGURE 19: The real part of the exact solution to Example 2.

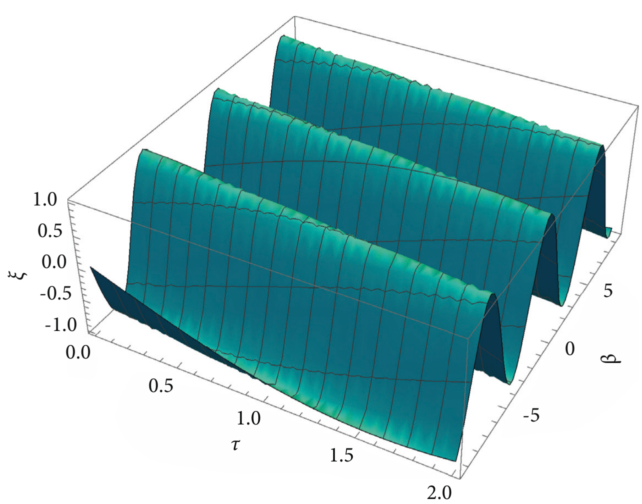

FIGURE 20: The imaginary part of the exact solution to Example 2.

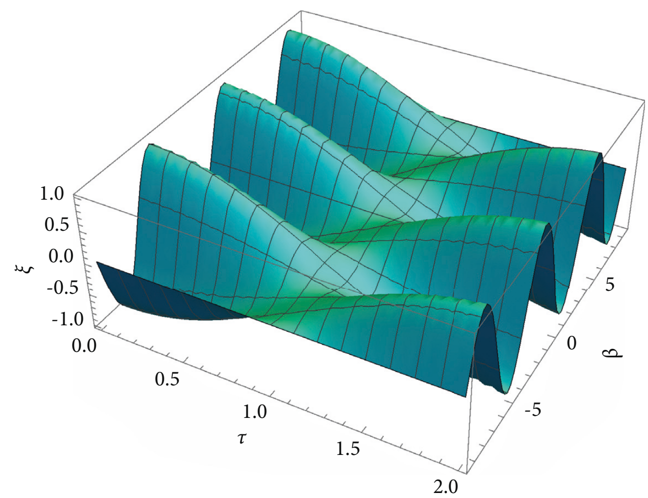

FIGURE 21: The real part of the exact solution to Example 3.

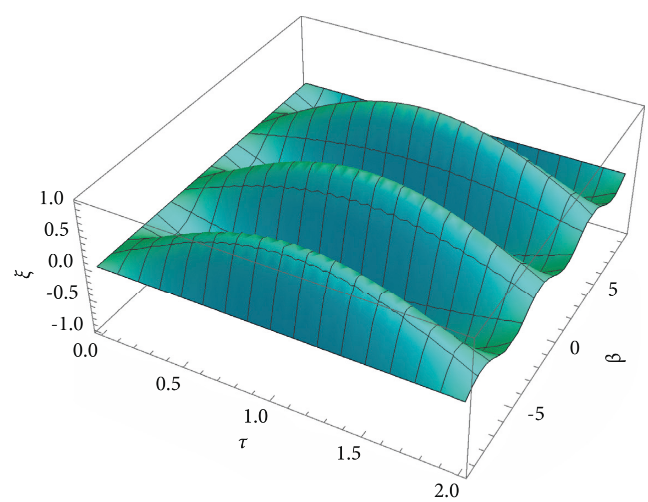

FIGURE 22: The imaginary part of the exact solution to Example 3.

Figures 11 and 12 demonstrate the 2D graph of real and imaginary parts of absolute error in the intervals $\tau \in [0, 1]$ when $\varpi = 0.05$ are over the 5th terms approximate and exact solutions of equation (60) at $\nu = 1$. As for the figures, approximate and precise solutions are in very good agreement.

Table 3 shows comparisons of the real and imaginary parts of the absolute error of the 5th approximate solution obtained by ATDM of Example 3 at $\nu = 1$ with the absolute error of approximate solutions obtained by HPM [35]. The results obtained from the suggested method are extremely similar to those obtained by HPM.

The recurrence error $|\xi^5(\varpi, \tau) - \xi^4(\varpi, \tau)|$ between the 5th and 4th approximate solution of the real part with different values of ν, when $\varpi = 0.05$ for Example 3 are presented as follows:

The recurrence error $|\xi^5(\varpi, \tau) - \xi^4(\varpi, \tau)|$ between the 5th and 4th approximate solution of the imaginary part with different values of ν, when $\varpi = 0.05$ for Example 3 are presented as follows:

The convergence of the ATDM of real and imaginary of the approximate solution to the exact solution for equation (60) has been shown numerically as in Tables 9 and 10. The results show that the proposed technique is a useful and efficient algorithm for solving fractional-order differential equations with fewer calculations and iteration steps.

The following are 3D graphs for the real and imaginary parts of the exact solution to Example 3:

The real and imaginary parts of the exact solution equation (60) at $\nu = 1$ are shown in Figures 21 and 22, respectively, in the intervals $\tau \in [0, 2], \varpi \in [-3\pi, 3\pi]$.

The following 2D graphs show the real and imaginary parts of approximate and exact solutions to Example 4:

Figures 7 and 8 show the behavior of the real and imaginary parts in the interval $\tau \in [0, 1]$ between the 5th step iteration approximate and exact solutions of equation

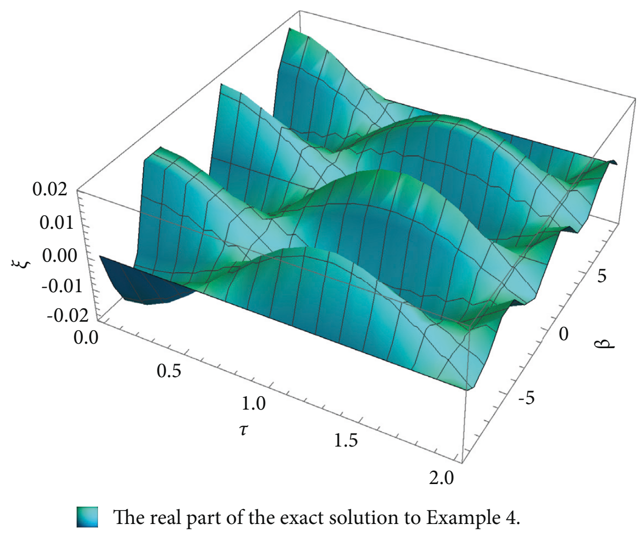

FIGURE 23: The real part of the exact solution to Example 4.

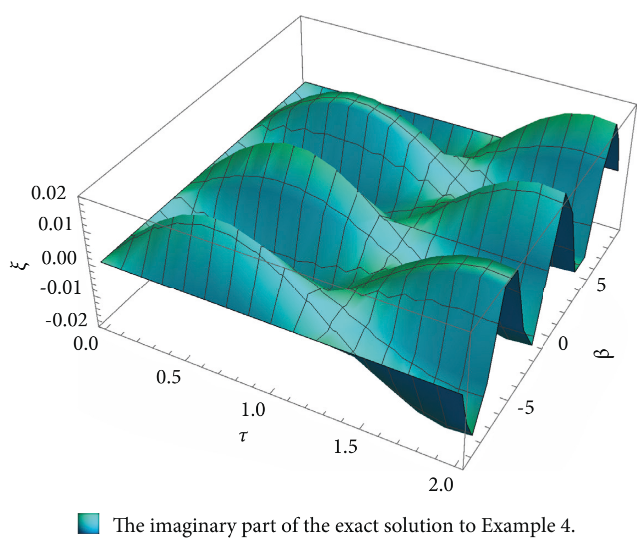

FIGURE 24: The imaginary part of the exact solution to Example 4.

(71) at several values of ν when $\varpi = 0.05, \beta = 0.10$, and $\mu = 0.15$. The approximate result corresponds with the precise result at $\nu = 1$ and this proves the effectiveness and precision of the recommended method.

The 2D graphs of absolute error for the real and imaginary parts of the 5th approximation and exact solutions to Example 4 are as follows:

Figures 15 and 16 demonstrate the 2D graph of real and imaginary parts of absolute error in the intervals $\tau \in [0, 1]$ when $\varpi = 0.05, \beta = 0.10$, and $\mu = 0.15$ are over the 5th terms approximate and exact solutions of equation (71) at $\nu = 1$. As for the figures, approximate and precise solutions are in very good agreement.

Table 4 shows comparisons of the real and imaginary parts of the absolute error of the 5th approximate solution obtained by ATDM of Example 4 at $\nu = 1$ with the absolute error of the approximate solution obtained by HAM [43]. The results obtained from the suggested method are extremely similar to those obtained by HAM.

The recurrence error $|\xi^5(\varpi, \beta, \mu, \tau) - \xi^4(\varpi, \beta, \mu, \tau)|$ between the 5th and 4th approximate solution of the real part with different values of ν, when $\varpi = 0.05, \beta = 0.10$, and $\mu = 0.15$ for Example 4 are presented.

The recurrence error $|\xi^5(\varpi, \beta, \mu, \tau) - \xi^4(\varpi, \beta, \mu, \tau)|$ between the 5th and 4th approximate solutions of the imaginary part with different values of ν, when $\varpi = 0.05, \beta = 0.10$, and $\mu = 0.15$ for Example 4 are presented.

The convergence of the ATDM of real and imaginary of the approximate solution to the exact solution for equation (71) has been shown numerically as in Tables 11 and 12. The results show that the proposed technique is a useful and efficient algorithm for solving fractional-order differential equations with fewer calculations and iteration steps.

The following are 3D graphs for the real and imaginary parts of the exact solution to Example 4:

The real and imaginary parts of the exact solution equation (71) at $\nu = 1$ are shown in Figures 23 and 24 respectively in the intervals $\tau \in [0, 2], \varpi \in [-3\pi, 3\pi]$ with $\beta = 0.1$ and $\mu = 0.2$.

6. Conclusion

The Aboodh transform decomposition method is effectively used in this study to obtain analytical approximate and exact solutions to time-fractional linear and nonlinear Schrodinger equations with zero and nonzero trapping potential that are regarded in the Caputo sense. The Aboodh transform is more closely related to the Laplace and Elzaki transforms. The Aboodh transform is a useful method for solving time-domain differential equations. The recurrence and absolute error of the four problems are analyzed to evaluate the efficiency and consistency of the presented method. In addition, numerical results are also compared with other methods such as the fractional reduced differential transform method (FRDTM), the homotopy analysis method (HAM), and the homotopy perturbation method (HPM). The results obtained by the proposed method show excellent agreement with these methods, which indicates its effectiveness and reliability. This method has the advantage of needing no assumptions regarding minor or important physical parameters in the problem. As a result, it can solve both weakly and strongly nonlinear problems, overcoming some of the drawbacks of traditional perturbation methods. Only a few computations are required to solve nonlinear fractional-order differential equations. As a result, it greatly improves homotopy analysis and homotopy perturbation techniques. The ATDM can construct expansion solutions for linear and nonlinear fractional-order differential equations without the requirement for perturbation, linearization, or discretization, unlike earlier analytic approximation methods.

Therefore, we concluded that our proposed technique is simple to apply, accurate, and efficient according to the results. It is significant to consider that implementing the ATDM to solve other kinds of ordinary and partial DEs of noninteger order is actively attainable. For example, fractional kdv equations, fractional phi-4 equations, fractional Schrodinger equations, and many more.

Data Availability

No data were generated or analyzed during the current study.

Conflicts of Interest

The authors declare that they have no competing interests.

Authors' Contributions

The authors declare that the study was realized in collaboration with equal responsibility. All authors read and approved the final manuscript.

References

[1] A. K. Mittal and L. K. Balyan, "Numerical solutions of two-dimensional fractional Schrodinger equation," *Mathematical Sciences*, vol. 14, no. 2, pp. 129–136, 2020.

[2] A. Liemert and A. Kienle, "Fractional Schrödinger equation in the presence of the linear potential," *Mathematics*, vol. 4, no. 2, p. 31, 2016.

[3] X. Guo and M. Xu, "Some physical applications of fractional Schrödinger equation," *Journal of Mathematical Physics*, vol. 47, no. 8, Article ID 082104, 2006.

[4] J. Wang, Y. Zhou, and W. Wei, "Fractional Schrödinger equations with potential and optimal controls," *Nonlinear Analysis: Real World Applications*, vol. 13, no. 6, pp. 2755–2766, 2012.

[5] S. Kumar, M. Niwas, and A. M. Wazwaz, "Lie symmetry analysis, exact analytical solutions and dynamics of solitons for (2+1)-dimensional NNV equations," *Physica Scripta*, vol. 95, no. 9, Article ID 095204, 2020.

[6] W. X. Ma, "Inverse scattering for nonlocal reverse-time nonlinear Schrödinger equations," *Applied Mathematics Letters*, vol. 102, Article ID 106161, 2020.

[7] M. A. Zaky, "An accurate spectral collocation method for nonlinear systems of fractional differential equations and related integral equations with nonsmooth solutions," *Applied Numerical Mathematics*, vol. 154, pp. 205–222, 2020.

[8] N. K. Vitanov and Z. I. Dimitrova, "Simple equations method (SEsM) and its particular cases: Hirota method," *AIP Conference Proceedings*, vol. 2321, no. 1, Article ID 030036, 2021.

[9] R. Hassan, M. El-Agamy, M. S. A. Latif, and H. Nour, "On Backlund transformation of Riccati equation method and its application to nonlinear partial differential equations and differential-difference equations," *Open Journal of Mathematical Sciences*, vol. 4, no. 1, pp. 56–62, 2020.

[10] D. Kumar, A. R. Seadawy, and A. K. Joardar, "Modified Kudryashov method via new exact solutions for some conformable fractional differential equations arising in mathematical biology," *Chinese Journal of Physics*, vol. 56, no. 1, pp. 75–85, 2018.

[11] D. Rani and V. Mishra, "Modification of Laplace Adomian decomposition method for solving nonlinear Volterra integral and integro-differential equations based on Newton Raphson formula," *European Journal of Pure and Applied Mathematics*, vol. 11, no. 1, pp. 202–214, 2018.

[12] A. Khan, M. I. Liaqat, M. Younis, and A. Alam, "Approximate and exact solutions to fractional order Cauchy reaction-diffusion equations by new combine techniques," *Journal of Mathematics*, vol. 2021, Article ID 5337255, 12 pages, 2021.

[13] M. I. Liaqat, A. Khan, and A. Akgül, "Adaptation on power series method with conformable operator for solving fractional order systems of nonlinear partial differential equations," *Chaos, Solitons & Fractals*, vol. 157, Article ID 111984, 2022.

[14] M. Ur Rehman and R. Ali Khan, "The Legendre wavelet method for solving fractional differential equations," *Communications in Nonlinear Science and Numerical Simulation*, vol. 16, no. 11, pp. 4163–4173, 2011.

[15] M. I. Liaqat, A. Khan, M. A. Alam, M. K. Pandit, S. Etemad, and S. Rezapour, "Approximate and closed-form solutions of Newell-Whitehead-Segel equations via modified conformable Shehu transform decomposition method," *Mathematical Problems in Engineering*, vol. 2022, Article ID 6752455, 14 pages, 2022.

[16] H. M. Ozaktas and M. A. Kutay, "The fractional Fourier transforms," in *Proceedings of the 2001 European Control Conference (ECC)*, pp. 1477–1483, IEEE, Porto, Portugal, September 2001.

[17] Y. Z. Povstenko, "Fractional heat conduction equation and associated thermal stress," *Journal of Thermal Stresses*, vol. 28, no. 1, pp. 83–102, 2004.

[18] L. Kexue and P. Jigen, "Laplace transform and fractional differential equations," *Applied Mathematics Letters*, vol. 24, no. 12, pp. 2019–2023, 2011.

[19] S. Kazem, "Exact solution of some linear fractional differential equations by Laplace transform," *International Journal of Nonlinear Science*, vol. 16, no. 1, pp. 3–11, 2013.

[20] S. Kumar, "A new analytical modelling for fractional telegraph equation via Laplace transform," *Applied Mathematical Modelling*, vol. 38, no. 13, pp. 3154–3163, 2014.

[21] Z. B. Li and J. H. He, "Fractional complex transform for fractional differential equations," *Mathematical and Computational Applications*, vol. 15, no. 5, pp. 970–973, 2010.

[22] H. Zhang, "A note on some sub-equation methods and new types of exact travelling wave solutions for two nonlinear partial differential equations," *Acta Applicandae Mathematica*, vol. 106, no. 2, pp. 241–249, 2009.

[23] T. M. Elzaki, "Application of new transform "Elzaki transform" to partial differential equations," *Global Journal of Pure and Applied Mathematics*, vol. 7, no. 1, pp. 65–70, 2011.

[24] A. Kiliçman, H. Eltayeb, and R. P. Agarwal, "On Sumudu transform and system of differential equations," *Abstract and Applied Analysis*, vol. 2010, Article ID 598702, 2010.

[25] L. Riabi, K. Belghaba, M. H. Cherif, and D. Ziane, "Homotopy perturbation method combined with ZZ transform to solve some nonlinear fractional differential equations," *International Journal of Analysis and Applications*, vol. 17, no. 3, pp. 406–419, 2019.

[26] K. S. Aboodh, "The new integral transform Aboodh transform," *Global Journal of Pure and Applied Mathematics*, vol. 9, no. 1, pp. 35–43, 2013.

[27] R. M. Jena and S. Chakraverty, "Q-homotopy analysis Aboodh transform method based solution of proportional delay time-fractional partial differential equations," *Journal of Interdisciplinary Mathematics*, vol. 22, no. 6, pp. 931–950, 2019.

[28] S. Rashid, K. T. Kubra, and J. L. G. Guirao, "Construction of an approximate analytical solution for multi-dimensional fractional Zakharov–Kuznetsov equation via Aboodh

Adomian decomposition method," *Symmetry*, vol. 13, no. 8, p. 1542, 2021.

[29] G. T. Tukaram and R. G. Anantha, "On Aboodh transform for fractional differential operator," *Malaya Journal of Matematik*, vol. 8, no. 1, pp. 225–229, 2020.

[30] G. O. Ojo and N. I. Mahmudov, "Aboodh transform iterative method for spatial diffusion of a biological population with fractional-order," *Mathematics*, vol. 9, no. 2, p. 155, 2021.

[31] M. A. Awuya and D. Subasi, "Aboodh transform iterative method for solving fractional partial differential equation with Mittag–Leffler Kernel," *Symmetry*, vol. 13, no. 11, p. 2055, 2021.

[32] Q. T. Ain, J. H. He, N. Anjum, and M. Ali, "The fractional complex transform: a novel approach to the time-fractional Schrödinger equation," *Fractals*, vol. 28, no. 7, Article ID 2050141, 2020.

[33] A. H. Bhrawy, J. F. Alzaidy, M. A. Abdelkawy, and A. Biswas, "Jacobi spectral collocation approximation for multi-dimensional time-fractional Schrödinger equations," *Nonlinear Dynamics*, vol. 84, no. 3, pp. 1553–1567, 2016.

[34] B. Hicdurmaz and A. Ashyralyev, "A stable numerical method for multidimensional time fractional Schrödinger equations," *Computers & Mathematics with Applications*, vol. 72, no. 6, pp. 1703–1713, 2016.

[35] A. Khalili Golmankhaneh, "Solving of the fractional non-linear and linear Schrodinger equations by homotopy perturbation method," 2008, https://arxiv.org/abs/0809.

[36] B. Ghanbari, "Abundant exact solutions to a generalized nonlinear Schrödinger equation with local fractional derivative," *Mathematical Methods in the Applied Sciences*, vol. 44, no. 11, pp. 8759–8774, 2021.

[37] Y. Zhang, A. Kumar, S. Kumar, D. Baleanu, and X. J. Yang, "Residual power series method for time-fractional Schrödinger equations," *Journal of Nonlinear Sciences and Applications*, vol. 9, no. 11, pp. 5821–5829, 2016.

[38] S. O. Edeki, G. O. Akinlabi, and S. A. Adeosun, "On a modified transformation method for exact and approximate solutions of linear Schrödinger equations," *AIP Conference proceedings*, vol. 1705, no. 1, Article ID 020048, 2016.

[39] A. Ravi Kanth and K. Aruna, "Two-dimensional differential transform method for solving linear and non-linear Schrödinger equations," *Chaos, Solitons & Fractals*, vol. 41, no. 5, pp. 2277–2281, 2009.

[40] D. Lu, A. Seadawy, and M. Arshad, "Applications of extended simple equation method on unstable nonlinear Schrödinger equations," *Optik*, vol. 140, pp. 136–144, 2017.

[41] A. R. Hadhoud, A. A. M. Rageh, and T. Radwan, "Computational solution of the time-fractional Schrödinger equation by using trigonometric B-spline collocation method," *Fractal and Fractional*, vol. 6, no. 3, p. 127, 2022.

[42] B. K. Singh and P. Kumar, "A new approximate solution of time-fractional, non-linear Schrodinger equations using fractional reduced differential transformation," 2016, https://arxiv.org/abs/1611.07171.

[43] A. K. Alomari, M. S. M. Noorani, and R. Nazar, "Explicit series solutions of some linear and nonlinear Schrodinger equations via the homotopy analysis method," *Communications in Nonlinear Science and Numerical Simulation*, vol. 14, no. 4, pp. 1196–1207, 2009.

[44] V. V. Kulish and J. L. Lage, "Application of fractional calculus to fluid mechanics," *Journal of Fluids Engineering*, vol. 124, pp. 803–806, 2002.

[45] Y. A. Rossikhin and M. V. Shitikova, "Application of fractional calculus for dynamic problems of solid mechanics: novel trends and recent results," *Applied Mechanics Reviews*, vol. 63, no. 1, 2010.

[46] K. Manimegalai, C. F. S. Zephania, P. K. Bera, P. Bera, S. K. Das, and T. Sil, "Study of strongly nonlinear oscillators using the Aboodh transform and the homotopy perturbation method," *The European Physical Journal Plus*, vol. 134, no. 9, pp. 462–510, 2019.

[47] H. M. Fahad and A. Fernandez, "Operational calculus for Caputo fractional calculus with respect to functions and the associated fractional differential equations," *Applied Mathematics and Computation*, vol. 409, Article ID 126400, 2021.

Hindawi
Journal of Mathematics
Volume 2022, Article ID 8781186, 14 pages
https://doi.org/10.1155/2022/8781186

Research Article

Numerical Analysis of Iterative Fractional Partial Integro-Differential Equations

Hayman Thabet,[1] **Subhash Kendre**,[2] **and Subhash Unhale**[3]

[1]*Department of Mathematics, University of Aden, Aden, Yemen*
[2]*Department of Mathematics, Savitribai Phule Pune University, Pune 411007, India*
[3]*C.K. Thakur Arts, Commerce and Science College, University of Mumbai, Mumbai, India*

Correspondence should be addressed to Hayman Thabet; haymanthabet@gmail.com

Received 23 February 2022; Revised 11 April 2022; Accepted 13 April 2022; Published 17 May 2022

Academic Editor: Mawardi Bahri

Many nonlinear phenomena are modeled in terms of differential and integral equations. However, modeling nonlinear phenomena with fractional derivatives provides a better understanding of processes having memory effects. In this paper, we introduce an effective model of iterative fractional partial integro-differential equations (FPIDEs) with memory terms subject to initial conditions in a Banach space. The convergence, existence, uniqueness, and error analysis are introduced as new theorems. Moreover, an extension of the successive approximations method (SAM) is established to solve FPIDEs in sense of Caputo fractional derivative. Furthermore, new results of stability analysis of solution are also shown.

1. Introduction

Most of the physical phenomena are modeled in ordinary differential equations (ODEs) and partial differential equations (PDEs). During the last decades, it has been noted that modeling complex phenomena, using fractional derivatives, provides a good fit due to their nonlocal nature. Fractional derivatives are effective tools to formulate processes having memory effects. Furthermore, fractional PDEs, which are considered the generalization of PDEs with fractional-order derivatives, have been widely used in many areas of sciences and engineering, and they have been the topics of many workshops and conferences due to their essential uses applied in numerous diverse and widespread fields in applied sciences [1–7]. Furthermore, FPIDEs are applicable in sciences and engineering, and many works in FPIDEs have been introduced (see, for example, [3, 8–11]), while studying iterative FPIDEs is very rare and currently an active area of research due to their particular applications in neural networks. However, iterative FPIDEs are useful tools for modeling the memory properties of various materials and processes, with a nonlinear relationship to time, such as anomalous diffusion, an elasticity theory, solids mechanic, and other applications [12–14]. The study of the theory of the iterative differential equations began with the work of Eder [15] where Eder worked on a solution of an iterative functional differential equation. Moreover, many studies on iterative differential equations have been conducted (see, for example, [16–18]).

In many physical systems described as models in terms of initial and boundary value problems, it is essential to develop techniques based on various types of successive approximations constructed explicitly in analytic forms. Several analytical and numerical methods for solving differential and integral equations are available in the literature. One of the powerful methods is the successive approximations method (SAM) which was introduced in 1891 by E. Picard, and it has been used to prove the existence and uniqueness of solutions of differential equations [19–22]. The SAM, which is also called the Picard iterative solutions method, has been increasingly applied to solve differential equations and integral equations [23, 24]. The SAM provides an approximate solution in a short series convergent with readily determinable terms [25].

The existence and uniqueness of solutions are proved with initial conditions for various types of iterative differential equations or iterative integro-differential in some works available in the literature, for example, the exact analytical solution for an iterative nonlinear differential equation was given in [26] where the authors studied a second-order nonlinear iterated differential equation, analytic solutions for an iterative differential equation were given in [27] where the authors studied an iterative functional differential equation, Yang and Zhang introduced solutions for iterative differential equations [28], and Zhang et al. [29] introduced the existence of wavefront solutions for an integral differential equation in a nonlinear nonlocal neuronal network. However, few works have been introduced for the stability analysis of solutions for iterative fractional integro-differential equations [30, 31].

This paper presents new analytical and numerical solutions of a new model called "iterative fractional partial integro-differential equation" of iterative Volterra-type equation. This model is solved by using the method of successive approximations. Moreover, the primary advances applied in this paper are very effective with applications of a Banach space and Gronwall–Bellman integral inequality in sense of Caputo derivative. The rest of the paper is organized as follows. Section 2 gives the preliminaries. Section 3 presents the description of the method of successive approximations, existence, uniqueness, convergence, and error analysis of the solution for the proposed model. Section 4 introduces solutions for two types of iterative FPIDEs. Numerical results and discussion are given in Section 5.

2. Preliminaries and Definitions

There are various definitions and theorems of fractional calculus available in the literature. This section presents some of these definitions and theorems that are needed in this paper and can be found in [32–36] and among other references cited therein.

Definition 1. Let $u(x,t)\colon \mathbb{R}\times(0,\infty)\longrightarrow\mathbb{R}$ and $n-1<\alpha<n\in\mathbb{N}$. The Riemann–Liouville integral of time fractional order α for a function u is defined by

$$\mathcal{I}_t^{\alpha}u(x,t)=\frac{1}{\Gamma(\alpha)}\int_0^t (t-\tau)^{\alpha-1}u(x,\tau)\mathrm{d}\tau, \tag{1}$$

where Γ is the well-known gamma function.

Definition 2. Let $u(x,t)\colon \mathbb{R}\times(0,\infty)\longrightarrow\mathbb{R}$ and $n-1<\alpha<n\in\mathbb{N}$. The Riemann–Liouville time fractional partial derivative of order α for a function u is defined by

$${}^{\mathrm{RL}}\mathcal{D}_t^{\alpha}u(x,t)=\frac{\partial^n}{\partial t^n}\int_0^t \frac{(t-\tau)^{n-\alpha-1}}{\Gamma(n-\alpha)}u(x,\tau)\mathrm{d}\tau. \tag{2}$$

Definition 3. Let $u(x,t)\colon \mathbb{R}\times(0,\infty)\longrightarrow\mathbb{R}$ and $n-1<\alpha<n\in\mathbb{N}$; then, the Caputo derivative of time fractional order α for a function u is

$$\begin{cases}\mathcal{D}_t^{\alpha}u(x,t) &= \displaystyle\int_0^t \frac{(t-\tau)^{n-\alpha-1}}{\Gamma(n-\alpha)}\frac{\partial^n u(x,\tau)}{\partial\tau^n}\mathrm{d}\tau,\\ \mathcal{D}_t^{\alpha}u(x,t) &= \dfrac{\partial^n u(x,t)}{\partial t^n}, \alpha=n\in\mathbb{N}.\end{cases} \tag{3}$$

Theorem 1 *Let $u(x,t)\colon \mathbb{R}\times(0,\infty)\longrightarrow\mathbb{R}$ and $n-1<\alpha<n\in\mathbb{N}$. Then,*

$$\begin{cases}\mathcal{I}_t^{\alpha}\mathcal{D}_t^{\alpha}u(x,t) &= u(x,t)-\displaystyle\sum_{k=0}^{n-1}\frac{t^k}{k!}\frac{\partial^k u(x,0^+)}{\partial t^k},\\ \mathcal{D}_t^{\alpha}\mathcal{I}_t^{\alpha}u(x,t) &= u(x,t).\end{cases} \tag{4}$$

Theorem 2 *Let $\alpha, t\in\mathbb{R}$, $t>0$, and $n-1<\alpha<n\in\mathbb{N}$. Then,*

$$\begin{cases}\mathcal{D}_t^{\alpha}t^q &= \dfrac{\Gamma(q+1)}{\Gamma(q-\alpha+1)}t^{q-\alpha}, \quad n\le q,\ q\in\mathbb{R},\\ \mathcal{D}_t^{\alpha}t^q &= 0, \quad q\le n-1.\end{cases} \tag{5}$$

Lemma 1 (Gronwall–Bellman inequality). *Let $u(x,t)$ be a nonnegative continuous function on $J\times J$, $J=[a,a+h]$, $0<a,h\in\mathbb{R}$. If $u(x,t)\le c+\int_a^t f(x,r)u(x,r)dr$ where f is an analytic function and c is a nonnegative constant, then $u(x,t)\le c\ \exp\left(\int_a^t f(x,r)dr\right)$.*

3. Description of the Numerical Scheme

In this section, we introduce an effective model of an iterative fractional partial integro-differential equation with memory term subject to initial value conditions of the following form:

$$\begin{cases}D_t^{\alpha}u(x,t) &= f(x,t)+\displaystyle\int_0^t K(x,r)u(x,u(x,r))\mathrm{d}r,\\ \dfrac{\partial^k u(x,0)}{\partial t^k} &= f_k(x), \quad k=0,1,2,\ldots,n-1,\ (x,t)\in J\times J,\ J=[0,T],\ n-1<\alpha<n,\end{cases} \tag{6}$$

where D_t^{α} is the α-th Caputo fractional partial derivative, $K(x,t)$ is a bivariate kernel, $f(x,t)$ and $f_k(x)$ are known analytic functions, and $u(x,t)$ is the unknown function to be determined.

To find the solution for the iterative fractional partial integro-differential equation (6), we introduce an extension of the SAM as follows. We assume that (6) has an approximate solution given by

$$u_{n+1}(x,t) = u_0 + \int_0^t \frac{(x-\tau)^{\alpha-1}}{\Gamma(\alpha)} \cdot \left(f(x,\tau) + \int_0^\tau K(x,r) u_n(x, u_n(x,r)) \mathrm{d}r \right) \mathrm{d}\tau, \tag{7}$$

for $n = 0, 1, 2, \ldots$ where $u_0(x,t)$ is of class C^1 from $[0,T]$ to $[0,T]$ for $|u_0'(x,t)| \le T$.

Our extension here is that all the components $u_n(x,t)$ are continuous where u_n can be given as a sum of successive differences in the following form:

$$u_n(x,t) = u_0(x,t) + \sum_{k=1}^{n} \left(u_k(x,t) - u_{k-1}(x,t)\right). \tag{8}$$

Next, if $(u_k(x,t) - u_{k-1}(x,t)$ converges, then $u_n(x,t)$ converges and the solution for (6) is given by

$$u(x,t) = \lim_{n \longrightarrow \infty} u_n(x,t). \tag{9}$$

Lemma 2. *Let a function $u \in C^1([0,T] \times [0,T])$ satisfy (6) on $[0,T] \times [0,T]$; then,*

$$u(x,t) = u_0 + \int_0^t \frac{(x-\tau)^{\alpha-1}}{\Gamma(\alpha)} \cdot \left(f(x,\tau) + \int_0^\tau K(x,r) u(x, u(x,r)) \mathrm{d}r \right) \mathrm{d}\tau. \tag{10}$$

3.1. Existence and Uniqueness. This section presents new results for existence and uniqueness of solution for the proposed model (6).

Theorem 3. *Suppose that $|u_0 + T^{\alpha}(N + T^3 k_T)/\Gamma(\alpha+1)| \le T$ and $0 < M < \Gamma(\alpha+1)/T^{\alpha+1} k_T - 1 < 1$. Then, there is a unique solution for equation (6).*

Proof. Let $B = C([0,T] \times [0,T])$ be a Banach space with a norm $\|u\| = \max_{(x,t)\in\Omega} |u(x,t)|, \Omega \subset J \times J, J = [0,T]$ and

$$S(\rho) = \left\{ u \in B\colon 0 \le u \le \rho, \left|u(x,t_1) - u(x,t_2)\right| \le M\left|t_1 - t_2\right|, \forall t_1, t_2 \in J \right\}, \tag{11}$$

where $\rho = u_0 + T^{\alpha}(N + T^2 k_T)/\Gamma(\alpha+1)$ and $k_T = \sup\{|K(x,t)|\colon 0 \le t \le T\}$.

Before we apply the Banach contraction principle, we need to define an operator $P\colon B \longrightarrow B$ as

$$P(u(x,t)) = u_0 + \int_0^t \frac{(t-\tau)^{\alpha-1}}{\Gamma(\alpha)} \cdot \left(f(x,\tau) + \int_0^\tau K(x,r) u(x, u(x,r)) \mathrm{d}r \right) \mathrm{d}\tau. \tag{12}$$

From (12), we have

$$\begin{aligned} 0 \le |P(u(x,t))| &= \left| u_0 + \int_0^t \frac{(t-\tau)^{\alpha-1}}{\Gamma(\alpha)} \left(f(x,\tau) + \int_0^\tau K(x,r) u(x, u(x,r)) \mathrm{d}r \right) \mathrm{d}\tau \right| \\ &\le u_0 + \int_0^t \frac{(t-\tau)^{\alpha-1}}{\Gamma(\alpha)} \left(\left| f(x,\tau) + \int_0^\tau K(x,r) u(x, u(x,r)) \mathrm{d}r \right| \right) \mathrm{d}\tau \\ &\le u_0 + \int_0^t \frac{(t-\tau)^{\alpha-1}}{\Gamma(\alpha)} \left(|f(x,\tau)| + \int_0^\tau |K(x,r)| |(x, u(x,r))| \mathrm{d}r \right) \mathrm{d}\tau \le u_0 + \frac{T^{\alpha}\left(N + T^3 k_T\right)}{\Gamma(\alpha+1)}. \end{aligned} \tag{13}$$

By similar argument, we obtain

$$
\begin{aligned}
\left|P(u(x,t_1)) - P(u(x,t_2))\right| &\leq \left|\int_0^{t_1} \frac{(t-\tau)^{\alpha-1}}{\Gamma(\alpha)}\left(f(x,\tau) + \int_0^{\tau} K(x,r)u(x,u(x,r))\mathrm{d}r\right)\mathrm{d}\tau - \int_0^{t_2} \frac{(t-\tau)^{\alpha-1}}{\Gamma(\alpha)}\right.\\
&\quad \cdot \left(f(x,\tau) + \int_0^{\tau} K(x,r)u(x,u(x,r))\mathrm{d}r\right)\mathrm{d}\tau| \\
&\leq \int_{t_2}^{t_1}\left|\frac{(t-\tau)^{\alpha-1}}{\Gamma(\alpha)}\right|\left(|f(x,\tau)| + \int_0^{\tau}|K(x,r)||u(x,u(x,r))|\mathrm{d}r\right)\mathrm{d}\tau \leq \frac{\left(N + k_T T^3\right)}{\Gamma(\alpha+1)}\left|t_1 - t_2\right|^{\alpha}.
\end{aligned}
\tag{14}
$$

This proves that P is a function from $S(\rho)$ to $S(\rho)$. Next, for $u, v \in S(\rho)$, we have

$$
\begin{aligned}
|P(u(x,t)) - P(v(x,t))| &\leq \int_0^t \frac{(x-\tau)^{\alpha-1}}{\Gamma(\alpha)}\left(\int_0^{\tau}(|K(x,r)||u(x,u(x,r)) - v(x,v(x,r))|)\mathrm{d}r\right)\mathrm{d}\tau\\
&\leq k_T \int_0^t \frac{(x-\tau)^{\alpha-1}}{\Gamma(\alpha)}\left(\int_0^{\tau}(|u(x,u(x,r)) - u(x,v(x,r))| + |u(x,v(x,r)) - v(x,v(x,r))|)\mathrm{d}r\right)\mathrm{d}\tau\\
&\leq k_T \int_0^t \frac{(x-\tau)^{\alpha-1}}{\Gamma(\alpha)}\left(\int_0^{\tau}(M(|u(x,r) - v(x,r)|) + |u(x,r) - v(x,r)|)\mathrm{d}r\right)\mathrm{d}\tau\\
&\leq k_T \int_0^t \frac{(x-\tau)^{\alpha-1}}{\Gamma(\alpha)}\left(\int_0^{\tau}(M+1)|u(x,r) - v(x,r)|\mathrm{d}r\right)\mathrm{d}\tau\\
&\leq T k_T (M+1)\|u - v\| \int_0^t \frac{(x-\tau)^{\alpha-1}}{\Gamma(\alpha)}\mathrm{d}\tau \leq \frac{T^{\alpha+1}k_T(M+1)}{\Gamma(\alpha+1)}\|u - v\|.
\end{aligned}
\tag{15}
$$

Therefore, we obtain

$$
\|(P(u(x,t)) - P(v(x,t))\| \leq \frac{T^{\alpha+1}k_T(M+1)}{\Gamma(\alpha+1)}\|u - v\|.
\tag{16}
$$

Since $M < \Gamma(\alpha+1)/T^{\alpha+1}k_T - 1$ which implies that $T^{\alpha+1}k_T(M+1)/\Gamma(\alpha+1) < 1$, then by Banach principle, the operator P has a unique fixed point. Therefore, equation (6) has a solution. ☐

Theorem 4 (convergence).. *If the assumptions of Theorem 3 are proposed, then (7) converges.*

Proof. Define the sequence $S_k = \max_{(x,t)\in J\times J}|u_k(x,t) - u_{k-1}(x,t)|$. Then,

$$
\begin{aligned}
S_0 &= \max_{(x,t)\in J\times J}\left|u_0(x,t)\right|,\\
S_1 &= \max_{(x,t)\in J\times J}\left|u_1(x,t)\right|\\
&= \max_{(x,t)\in J\times J}\left|u_0 + \int_0^t \frac{(t-\tau)^{\alpha-1}}{\Gamma(\alpha)}\left(f(x,\tau) + \int_0^{\tau}K(x,r)u_0(x,u_0(x,r))\mathrm{d}r\right)\mathrm{d}\tau\right| \leq \left|u_0 + \frac{T^{\alpha}}{\Gamma(\alpha+1)}\left(N + T^3 k_T\right)\right| < T.
\end{aligned}
\tag{17}
$$

Since u_0 is a function from $[0,T]$ to $[0,T]$, we get $U_1 \leq u_0 + T^{\alpha}/\Gamma(\alpha+1)(N + T^3 k_T) \leq T$:

$$
\begin{aligned}
S_2 &= \max_{(x,t)\in J\times J}\left|u_2(x,t)-u_1(x,t)\right| \\
&= \max_{(x,t)\in J\times J}\Bigg|u_0+\int_0^t \frac{(t-\tau)^{\alpha-1}}{\Gamma(\alpha)}\left(f(x,\tau)+\int_0^\tau K(x,r)u_1(x,u_1(x,r))\mathrm{d}r\right)\mathrm{d}\tau-u_0 \\
&\quad -\int_0^t \frac{(t-\tau)^{\alpha-1}}{\Gamma(\alpha)}\left(f(x,\tau)+\int_0^\tau K(x,r)u_0(x,u_0(x,r))\mathrm{d}r\right)\mathrm{d}\tau\Bigg| \\
&= \max_{(x,t)\in J\times J}\left|\int_0^t \frac{(t-\tau)^{\alpha-1}}{\Gamma(\alpha)}\left(\int_0^\tau K(x,r)\left(u_1(x,u_1(x,r))-u_0(x,u_0(x,r))\right)\mathrm{d}r\right)\mathrm{d}\tau\right| \\
&\leq \max_{(x,t)\in J\times J}\int_0^t \frac{(t-\tau)^{\alpha-1}}{\Gamma(\alpha)}\left(\int_0^\tau \left\|K(x,r)\left(u_1(x,u_1(x,r))-u_0(x,u_0(x,r))\right)\right\|\mathrm{d}r\right)\mathrm{d}\tau \leq TS_1 \leq T^2,
\end{aligned}
\tag{18}
$$

$$
\begin{aligned}
S_3 &= \max_{(x,t)\in J\times J}\left|u_3(x,t)-u_2(x,t)\right| \max_{(x,t)\in J\times J} \\
&\quad \cdot\Bigg|u_0+\int_0^t \frac{(t-\tau)^{\alpha-1}}{\Gamma(\alpha)}\left(f(x,\tau)+\int_0^\tau K(x,r)u_2(x,u_2(x,r))\mathrm{d}r\right)\mathrm{d}\tau-u_0 \\
&\quad -\int_0^t \frac{(x-\tau)^{\alpha-1}}{\Gamma(\alpha)}\left(f(x,\tau)+\int_0^\tau K(x,r)u_1(x,u_1(x,r))\mathrm{d}r\right)\mathrm{d}\tau\Bigg| \\
&= \max_{(x,t)\in J\times J}\left|\int_0^t \frac{(t-\tau)^{\alpha-1}}{\Gamma(\alpha)}\left(\int_0^\tau K(x,r)\left(u_2(x,u_2(x,r))-u_1(x,u_1(x,r))\right)\mathrm{d}r\right)\mathrm{d}\tau\right| \\
&\leq \max_{(x,t)\in J\times J}\int_0^t \frac{(t-\tau)^{\alpha-1}}{\Gamma(\alpha)}\left(\int_0^\tau \left|K(x,r)\left(u_2(x,u_2(x,r))-u_1(x,u_1(x,r))\right)\right|\mathrm{d}r\right)\mathrm{d}\tau \leq TS_2 \leq T^3.
\end{aligned}
\tag{19}
$$

By induction, we have $S_k \leq T^k$. Since $|u_0 + T^\alpha (N + T^3 k_T)/\Gamma(\alpha+1)| \leq T$, we get $T<1$ when $u_0 \geq 0$. Therefore, S_k goes to zero as k goes to infinity. For every subsequence $\{u_{kj}\}$ of $\{S_k\}$, there exists a subsequence $\{s_{kj}\}$ which uniformly converges and the limit must to be a solution of (6). Thus, $\{S_k\}$ uniformly goes to a unique solution of (6). □

3.2. Error Analysis. In this section, we evaluate the maximum absolute error of the proposed method for the solution series (7) for (6).

Theorem 5. *Suppose that the hypothesis of Theorem 3 holds. Let u_n and s_n be two solutions satisfying equation (6) for $0 \leq x, t \leq T$, $M>0$ with the initial approximations $u_n(x,t)$ and $s_n(x,t)$, respectively. Then, the maximum absolute error for a solution series (7) for (6) is estimated to be*

$$
\begin{aligned}
&\max_{(x,t)\in J\times J}\left|u_n(x,t)-s_n(x,t)\right| \\
&\quad \leq \exp\left(\frac{k_T(M+1)T^{\alpha+1}}{\Gamma(\alpha+1)}\right)\max_{(x,t)\in J\times J}\left|u_0(x,t)-s_0(x,t)\right|.
\end{aligned}
\tag{20}
$$

Proof. By using Theorem 3, we have

$$
\begin{aligned}
u_n(x,t) &= u_0(x,t)+\int_0^t \frac{(t-\tau)^{\alpha-1}}{\Gamma(\alpha)}\left(f(x,\tau)+\int_0^\tau K(x,r)u_{n-1}(x,u_{n-1}(x,r))\mathrm{d}r\right)\mathrm{d}\tau, \\
s_n(x,t) &= s_0(x,t)+\int_0^t \frac{(t-\tau)^{\alpha-1}}{\Gamma(\alpha)}\left(f(x,\tau)+\int_0^\tau K(x,r)s_{n-1}(x,s_{n-1}(x,r))\mathrm{d}r\right)\mathrm{d}\tau.
\end{aligned}
\tag{21}
$$

Next, by using Theorem 4, we have

$$
\begin{aligned}
\left|u_n - s_n\right| &= \left|u_0(x,t) - s_0(x,t) + \int_0^t \frac{(t-\tau)^{\alpha-1}}{\Gamma(\alpha)}\left(\int_0^t K(x,r)\left(u_n(x,u_n(x,r)) - s_n(x,s_n(x,r))\right)\mathrm{d}r\right)\mathrm{d}\tau\right| \\
&\le \left|u_0(x,t) - s_0(x,t)\right| + \left|\int_0^t \frac{(t-\tau)^{\alpha-1}}{\Gamma(\alpha)} k_T\left(\int_0^\tau \left(u_n(x,u_n(x,r)) - s_n(x,s_n(x,r))\right)\mathrm{d}r\right)\mathrm{d}\tau\right| \\
&= \left|u_0(x,t) - s_0(x,t)\right| + k_T\left|\int_0^t \frac{(t-\tau)^{\alpha-1}}{\Gamma(\alpha)}\left(\int_0^\tau \left(u_n(x,u_n(x,r)) - u_n(x,s_n(x,r)) + u_n(x,s_n(x,r)) - s_n(x,s_n(x,r)\right)\mathrm{d}r\right)\mathrm{d}\tau\right)\right| \\
&\le \left|u_0(x,t) - s_0(x,t)\right| + k_T\left|\int_0^t \frac{(t-\tau)^{\alpha-1}}{\Gamma(\alpha)}\left(\int_0^\tau (M+1)\left(u_n(x,r) - s_n(x,r)\right)\mathrm{d}r\right)\mathrm{d}\tau\right| \\
&= \left|u_0(x,t) - s_0(x,t)\right| + k_T(M+1)\left|\int_0^t\int_0^\tau \frac{(t-\tau)^{\alpha-1}}{\Gamma(\alpha)}\left(u_n(x,r) - s_n(x,r)\right)\mathrm{d}r\mathrm{d}\tau\right| \\
&= \left|u_0(x,t) - s_0(x,t)\right| + k_T(M+1)\left|\int_0^t\int_0^\tau \frac{(t-\tau)^{\alpha-1}}{\Gamma(\alpha)}\left(u_n(x,r) - s_n(x,r)\right)\mathrm{d}\tau\mathrm{d}r\right| \\
&\le \left|u_0(x,t) - s_0(x,t)\right| + \frac{k_T(M+1)T^\alpha}{\Gamma(\alpha+1)}\int_0^t \left|u_n(x,\tau) - s_n(x,\tau)\right|\mathrm{d}\tau.
\end{aligned}
\tag{22}
$$

By using Gronwall–Bellman inequality given by Lemma 1, we get

$$
\left|u_n(x,t) - s_n(x,t)\right| \le \left|u_0(x,t) - s_0(x,t)\right|\exp\left(\int_0^t \frac{k_T(M+1)T^\alpha}{\Gamma(\alpha+1)}\mathrm{d}r\right) \le \left|u_0(x,t) - s_0(x,t)\right|\exp\left(\frac{k_T(M+1)T^{\alpha+1}}{\Gamma(\alpha+1)}\right). \tag{23}
$$

Thus, we obtain

$$
\max_{(x,t)\in J\times J}\left|u_n(x,t) - s_n(x,t)\right| \le \exp\left(\frac{k_T(M+1)T^{\alpha+1}}{\Gamma(\alpha+1)}\right) \times \max_{(x,t)\in J\times J}\left|u_0(x,t) - s_0(x,t)\right|. \tag{24}
$$

This completes the proof of Theorem 5. □

3.3. Algorithms for Computer Implementations. In this section, we introduce algorithms for computing numerical results. Algorithm 1 computes the existence conditions given by Theorem 3.

Further, Algorithm 2 can be used to obtain particular approximate numerical solutions at particular values of the fractional order α.

4. Analytical Solutions for Iterative Volterra FPIDEs

This section introduces solutions for new examples of iterative FPIDEs. These examples are chosen since their solutions are not available in the literature or they have been solved previously some other well-known methods.for $0 \le x, t \le 0.75, 0 < \alpha < 1$.

Example 1. In this example, we solve the following iterative FPIDEs of Volterra type with initial value:

$$
\begin{cases}
D_t^\alpha u(x,t) &= \cos\left(\dfrac{x}{2}\right)\displaystyle\int_0^t u(x,u(x,r))\mathrm{d}r, \\
u(x,0) &= \dfrac{\sin(x)}{2},
\end{cases}
\tag{25}
$$

Input: $T<1,\ N=|f(x,t)|,\ k_T=K(x,t),\ u_0(x,0)=f(x),$
(1) **for** $0\le x\le 1,\ 0\le t\le 1,\ i-1<\alpha<i,$ **do**
(2) special treatment of the first element of line i;
(3) **for** $i=1,2,\ldots,n,$ **do**
(4) Compute $|u_0+T^\alpha(N+T^3k_T)/\Gamma(\alpha+1)|, \Gamma(\alpha+1)/T^{\alpha+1}k_T-1.$
Output: $|u_0+T^\alpha(N+T^3k_T)/\Gamma(\alpha+1)|<T,\ 0<\Gamma(\alpha+1)/T^{\alpha+1}k_T-1<1.$

Algorithm 1: The computation of the existence conditions.

Input: $T<1,\ N=|f(x,t)|,\ k_T=K(x,t),\ u_0(x,0)=f(x),$
(1) **for** $0\le x\le 1,\ 0\le t\le 1,\ i-1<\alpha<i,$ **do**
(2) special treatment of the first element of line i;
(3) **for** $i=1,2,\ldots,n,$ **do**
(4) Compute $|u_0+T^\alpha(N+T^3k_T)/\Gamma(\alpha+1)|, \Gamma(\alpha+1)/T^{\alpha+1}k_T-1.$;
(5) **if** $|u_0+T^\alpha(N+T^3k_T)/\Gamma(\alpha+1)|<T,\ \Gamma(\alpha+1)/T^{\alpha+1}k_T-1<1$ **then**
(6) Compute $u_{i+1}(x,t)=u_0+\int_0^t(x-\tau)^{\alpha-1}/\Gamma(\alpha)(f(x,\tau)+\int_0^\tau K(x,r)u_i(x,u_i(x,r))dr)d\tau.$
(7) **Output**: $u_{i+1}(x,t)=u_0+\int_0^t(x-\tau)^{\alpha-1}/\Gamma(\alpha)(f(x,\tau)+\int_0^\tau K(x,r)u_i(x,u_i(x,r))dr)d\tau.$

Algorithm 2: The computation of the numerical solutions.

Then, equation (25) is of form (6) with $T=0.75, N=0, k_T=1$ which satisfies

$$\left|u_0+\frac{T^\alpha\left(N+T^3k_T\right)}{\Gamma(\alpha+1)}\right|=\left|\frac{\sin(x)}{2}+\frac{0.75^\alpha\left(0+0.75^3\times\ \cos(x/2)\right)}{\Gamma(\alpha+1)}\right|<0.75=T, \tag{26}$$

where $0<M<\Gamma(\alpha+1)/T^{\alpha+1}k_T-1=\Gamma(\alpha+1)/0.75^{\alpha+1}|\cos(x/2)|-1<1$ for all $0\le x\le 0.75$ and $0<\alpha<1$.

As the hypotheses of Theorem 3 are satisfied, a unique solution for equation (25) exists.

Next, by using Theorem 4 and assuming that $u_0(x,t)=u(x,0)=\sin(x)/2$, the first few iterative solutions are

$$\begin{aligned} u_1(x,t)&=u_1(x,0)+\int_0^t\frac{(x-\tau)^{\alpha-1}}{\Gamma(\alpha)}\left(\cos\left(\frac{x}{2}\right)\int_0^t u_0(x,u_0(x,r))dr\right)d\tau,\ u_1(x,0)=0\\ &=\frac{1}{2\left(\alpha^2+\alpha\right)\Gamma(\alpha)}t^{\alpha+1}\sin(x)\cos\left(\frac{x}{2}\right), \end{aligned} \tag{27}$$

$$\begin{aligned} u_2(x,t)&=u_2(x,0)+\frac{1}{\Gamma(\alpha)}\int_0^t(x-\tau)^{\alpha-1}\left(\cos\left(\frac{x}{2}\right)\int_0^t u_1(x,u_1(x,r))dr\right)d\tau,\ u_2(x,0)=0\\ &=\frac{2^{-\alpha-2}\Gamma(\alpha+2)^{-\alpha-1}\Gamma(\alpha(\alpha+2)+3)t^{(\alpha+1)(\alpha+2)}\csc(x)(\sin(x)\cos(x/2))^{\alpha+3}}{\times(\alpha(\alpha+2)+2)\Gamma(\alpha(\alpha+3)+3)}, \end{aligned} \tag{28}$$

$$u_3(x,t) = u_2(x,0) + \int_0^t \frac{(x-\tau)^{\alpha-1}}{\Gamma(\alpha)}\left(\cos\left(\frac{x}{2}\right)\int_0^t u_2(x,u_2(x,r))\mathrm{d}r\right)\mathrm{d}\tau,\ u_3(x,0)=0,$$
$$= \frac{((\alpha(\alpha+2)+2)\Gamma(\alpha(\alpha+3)+3))^{-\alpha(\alpha+3)-3}}{\left(\alpha^2+\alpha+1\right)(\alpha(\alpha+5)+7)\Gamma(\alpha(\alpha(\alpha(\alpha+6)+13)+13)+8)}$$
$$\times\Gamma(\alpha(\alpha+3)(\alpha(\alpha+3)+4)+8)t^{\alpha(\alpha(\alpha(\alpha+6)+13)+13)+7}$$
$$\times\left(2^{-\alpha-2}\Gamma(\alpha+2)^{-\alpha-1}\Gamma(\alpha(\alpha+2)+3)\csc(x)\left(\sin(x)\cos\left(\frac{x}{2}\right)\right)^{\alpha+3}\right)^{\alpha(\alpha+3)+3}. \tag{29}$$

Therefore, the approximate solution of (25) is obtained by $u(x,t) \approx \sum_{i=0}^{3} u_i(x,t)$.

Example 2. In this example, we solve the following iterative FPIDEs of Volterra type with initial value:

$$\begin{cases} D_t^{\alpha}u(x,t) &= \dfrac{\sin(x)}{3} + \displaystyle\int_0^t u(x,u(x,r))\mathrm{d}r, \quad 0\le x,t\le 0.75, 0<\alpha<1, \\ u(x,0) &= 0. \end{cases} \tag{30}$$

Equation (30) is of form (8) with $T=0.75, N=|\sin(x)/3|, k_T=1$, which satisfies

$$\left|u_0 + \frac{T^{\alpha}\left(N+T^2k_T\right)}{\Gamma(\alpha+1)}\right| = \left|0 + \frac{0.75^{\alpha}\left(\sin(x)/3+0.75^3\right)}{\Gamma(\alpha+1)}\right| < 0.75 = T, \tag{31}$$

where $0<M<\Gamma(\alpha+1)/T^{\alpha+1}k_T - 1 < 1$ for all $x\in[0,0.75]$ and $0<\alpha<1$. As all the hypotheses of Theorem 3 are satisfied, a unique solution for (30) exists.

By using Theorem 4, we obtain a solution of (30) for different values of α. We assume that $u_0(x,t)=u(x,0)=0$ and by using Mathematica software, the first three iterative solutions are obtained as follows:

$$u_1(x,t) = \frac{1}{4\Gamma(\alpha)}\int_0^t (x-\tau)^{\alpha-1}\left(\sin(x)/3 + \int_0^t u_0(x,u_0(x,r))\mathrm{d}r\right)\mathrm{d}\tau = \frac{t^{\alpha}}{3\alpha\Gamma(\alpha)}\sin(x), \tag{32}$$

$$u_2(x,t) = \frac{1}{4\Gamma(\alpha)}\int_0^t (x-\tau)^{\alpha-1}\left(\frac{\sin(x)}{3} + \int_0^t u_1(x,u_1(x,r))\mathrm{d}r\right)\mathrm{d}\tau = \frac{3^{-\alpha-1}t^{\alpha}\sin(x)\left(2\times 3^{\alpha}\Gamma\left(\alpha^2+\alpha+2\right)+\Gamma\left(\alpha^2+2\right)t^{\alpha^2+1}(\sin(x)/\Gamma(\alpha+1))^{\alpha}\right)}{2\Gamma(\alpha+1)\Gamma\left(\alpha^2+\alpha+2\right)}, \tag{33}$$

Table 1: Numerical values of the iterative solution when $q_1 = q_2 = 0.5, 1$ and $\alpha = \beta = 0.5$ for Example 2.

x	t	$u_0(x,t)$	$\alpha = 0.5$ $u_1(x,t)$	$u_2(x,t)$	$u_3(x,t)$	$\alpha = 1$ $u_1(x,t)$	$u_2(x,t)$	$u_3(x,t)$	$\alpha = 0.5$ $\sum_{i=0}^{3} u_i$	$\alpha = 1$ $\sum_{i=0}^{3} u_i$
	0.25	0.123702	0.011541	2.901×10^{-6}	9.774×10^{-29}	0.003836	3.732×10^{-9}	1.035×10^{-61}	0.135246	0.127538
0.25	0.50	0.123702	0.032643	0.000039	1.892×10^{-23}	0.0153421	2.389×10^{-7}	1.138×10^{-49}	0.156384	0.139044
	0.75	0.123702	0.059970	0.000179	2.342×10^{-20}	0.034520	2.721×10^{-6}	1.258×10^{-42}	0.18385	158224
	0.25	0.239713	0.021840	0.000014	1.700×10^{-25}	0.007258	2.470×10^{-8}	5.750×10^{-56}	0.261567	0.246971
0.50	0.50	0.239713	0.061772	0.000188	3.291×10^{-20}	0.029033	1.581×10^{-6}	6.322×10^{-44}	0.301673	0.268747
	0.75	0.239713	0.113483	0.000859	4.073×10^{-17}	0.065323	0.000018	6.991×10^{-37}	0.354055	0.305054
	0.25	0.340819	0.029821	0.000030	5.667×10^{-24}	0.003836	6.038×10^{-8}	3.002×10^{-53}	0.370669	0.350730
0.75	0.50	0.340819	0.084346	0.000393	1.097×10^{-18}	0.039642	3.865×10^{-6}	3.301×10^{-41}	0.425558	0.380465
	0.75	0.340819	0.154953	0.001797	1.358×10^{-15}	0.089194	0.000044	3.649×10^{-34}	0.497569	0.430058

Table 2: Numerical values of the iterative solutions when $q_1 = q_2 = 0.5, 1$ and $\alpha = \beta = 0.5$ for Example 1.

x	t	$\alpha = 0.5$ $u_1(x,t)$	$u_2(x,t)$	$u_3(x,t)$	$\alpha = 1$ $u_1(x,t)$	$u_2(x,t)$	$u_3(x,t)$	$\alpha = 0.5$ $\sum_{i=1}^{3} u_i$	$\alpha = 1$ $\sum_{i=0}^{3} u_i$
	0.25	0.0465276	0.047411	0.047483	0.020617	0.020635	0.020644	0.141421	0.061895
0.25	0.50	0.065800	0.068773	0.068501	0.041234	0.041376	0.041340	0.20307	0.123950
	0.75	0.080588	0.086632	0.085550	0.061851	0.062329	0.062090	0.25277	0.186270
	0.25	0.090162	0.092546	0.092761	0.039952	0.040018	0.040052	0.275470	0.120023
0.50	0.50	0.127509	0.135527	0.134859	0.079904	0.080436	0.080304	0.397895	0.240645
	0.75	0.156166	0.172468	0.169670	0.119856	0.121652	0.120756	0.498304	0.362264
	0.25	0.128191	0.132233	0.132637	0.020617	0.056938	0.057005	0.393061	0.170746
0.75	0.50	0.181290	0.194884	0.193864	0.113606	0.114682	0.114415	0.570037	0.342704
	0.75	0.222034	0.249672	0.245134	0.170410	0.174040	0.172229	0.716839	0.516678

$$
\begin{aligned}
u_3(x,t) &= \frac{1}{4\Gamma(\alpha)} \int_0^t (x-\tau)^{\alpha-1}\left(\frac{\sin(x)}{3} + \int_0^t, u_2(x, u_2(x,r))\mathrm{d}r\right)\mathrm{d}\tau \\
&= \frac{\sin(x)}{12\Gamma(\alpha+1)\Gamma(\alpha+2)\Gamma\left(\alpha^2+\alpha+2\right)}\left(\left(3^{-\alpha}\Gamma\left(\alpha^2+2\right)t^{\alpha+1}\left(\frac{\sin(x)}{\Gamma(\alpha+1)}\right)^{\alpha}\right.\right. \\
&\quad \times \left(\frac{2^{-2\alpha-1}\left(2\times 3^{\alpha}\Gamma\left(\alpha^2+\alpha+2\right) + 4^{-\alpha^2-1}\Gamma\left(\alpha^2+2\right)\left(\sin(x)/\Gamma(\alpha+1)\right)^{\alpha}\right)}{\Gamma(\alpha+1)\Gamma\left(\alpha^2+\alpha+2\right)}\right)^{\alpha^2+\alpha+1} \\
&\quad \times \left(3^{-\alpha-1}\sin(x)\right)^{\alpha^2+\alpha+1} + \frac{4\Gamma(\alpha+2)\Gamma\left(\alpha^2+\alpha+2\right)t^{\alpha} + 2t\Gamma\left(\alpha^2+\alpha+2\right)}{\Gamma(\alpha+1)\Gamma\left(\alpha^2+\alpha+2\right)} \\
&\quad \times \left(2^{-2\alpha-1}3^{-\alpha-1}t\,\sin(x)\left(2\,3^{\alpha}\Gamma\left(\alpha^2+\alpha+2\right) + 2^{-2\left(\alpha^2+1\right)}\Gamma\left(\alpha^2+2\right)\right.\right. \\
&\quad \left.\left.\left.\left.\times\left(\frac{\sin(x)}{\Gamma(\alpha+1)}\right)^{\alpha}\right)\right)^{\alpha}\right)\right).
\end{aligned} \tag{34}
$$

Therefore, the third order term iterative solution (30) is $u(x,t) \approx \sum_{i=1}^{3} u_i(x,t)$.

5. Numerical Solutions and Discussion

Table 1 presents numerical solutions for equation (25) through various values of x, t when $\alpha = 0.5, 1$. Table 2 includes numerical values of the iterative solutions for equation (30) by different values of x, t at $\alpha = 0.5, 1$. In Figures 1(a) and 1(b), we plot the graphs of first-order iterative solution for (25) using various values of x, t at $\alpha = 0.5, 1$ respectively. We plot the graph of second-order iterative solution for (25) by various values of x, t at $\alpha = 0.5, 1$ in Figures 2(a) and 2(b), respectively. The iterative solution for Example 1 is graphically represented in Figures 3(a) and 3(b) through various points of x, t when $\alpha = 0.5, 1$, respectively. Figures 4(a) and 4(b) represent the graphs of solution through various values of t for a fixed value of $x = 0.75$ when $\alpha = 0.5, 1$, respectively, for Example 1. The first-order iterative solution for Example 2 is graphically represented in Figures 5(a) and 5(b) through various values of x, t when $\alpha = 0.5, 1$, respectively. The second order of iterative solution for Example 2 is graphically represented in Figures 6(a) and 6(b) by various values of x, t when $\alpha = 0.5, 1$, respectively. The third-order iterative solution for Example 2 is graphically represented in Figures 7(a) and 7(b) by various points of x, t at $\alpha = 0.5, 1$, respectively. The solution for Example 2 is graphically represented in

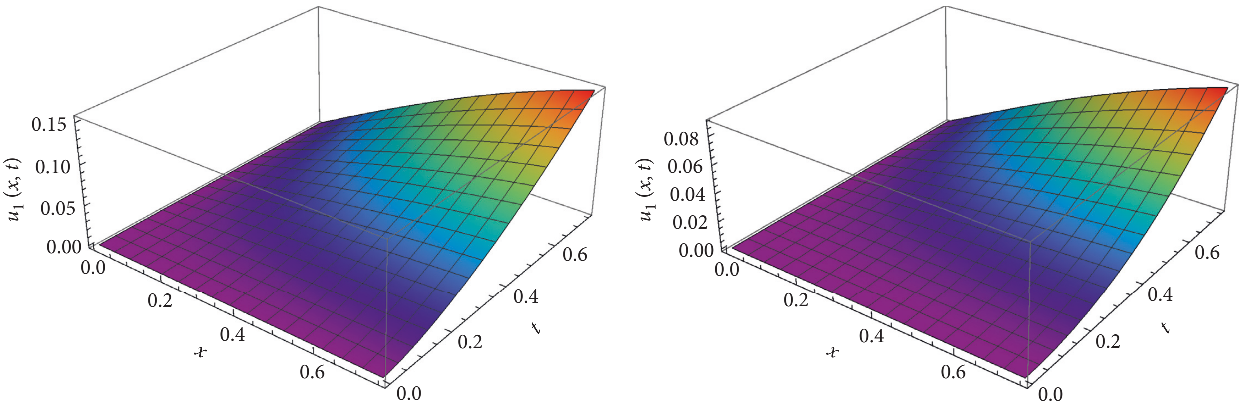

(a) (b)

FIGURE 1: The graphs of the first-order iterative solution $u_1(x, t)$ for (25) through various values of x, t at $\alpha = 0.5, 1$, respectively. (a) The graph of first-order iterative solution for (25) through various values of x, t at $\alpha = 0.5$. (b) The graph of the first-order iterative solution for (25) through various values of x, t at $\alpha = 1$.

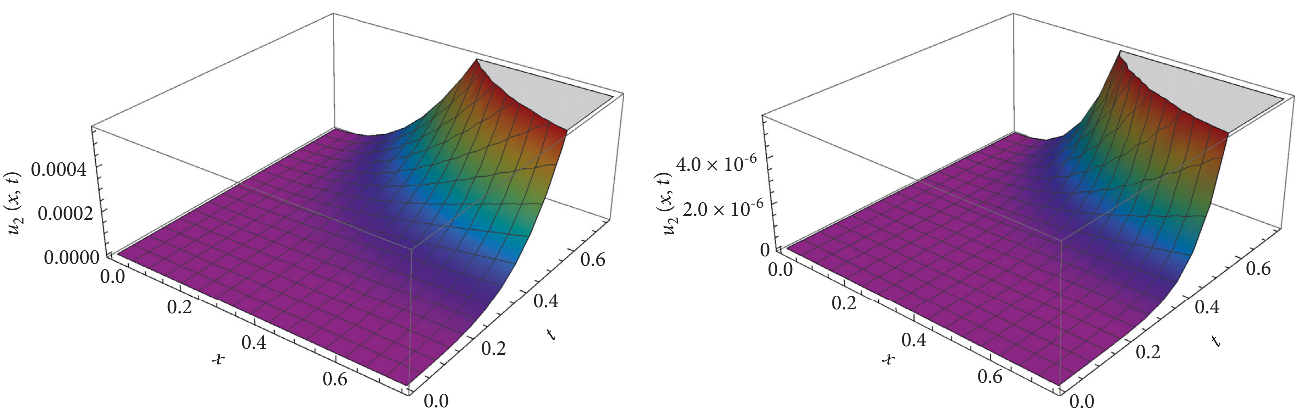

(a) (b)

FIGURE 2: The graphs of the second-order iterative solution $u_2(x, t)$ for (25) through various values of x, t at $\alpha = 0.5, 1$, respectively. (a) The graph of the second-order iterative solution for (25) through various values of x, t at $\alpha = 0.5$. (b) The graph of the second-order iterative solution for (25) through various values of x, t at $\alpha = 1$.

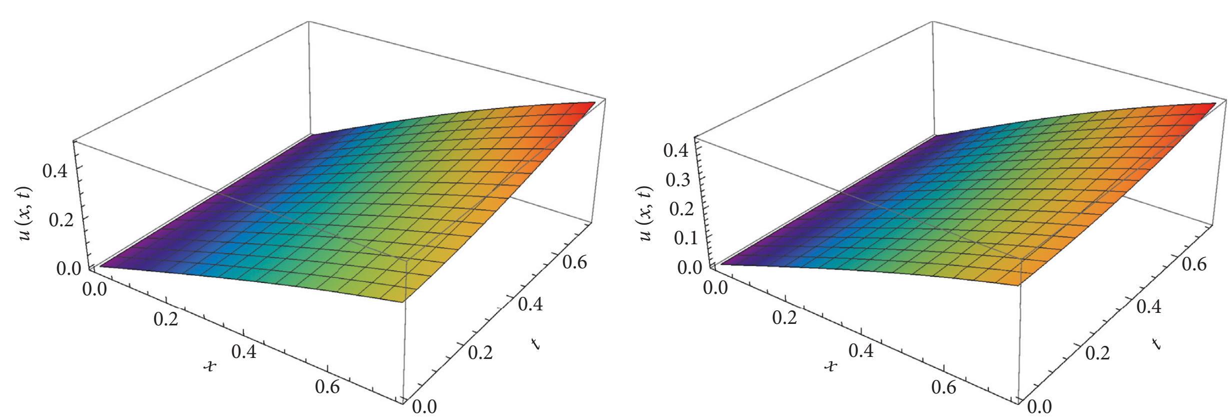

(a) (b)

FIGURE 3: The graphs of the approximate iterative solution $u(x, t)$ for (25) through various values of x, t at $\alpha = 0.5, 1$, respectively. (a) The graph of the approximate iterative solution $u(x, t)$ for (25) through various values of x, t at $\alpha = 0.5$. (b) The graph of the approximate iterative solution $u(x, t)$ for (25) through various values of x, t at $\alpha = 1$.

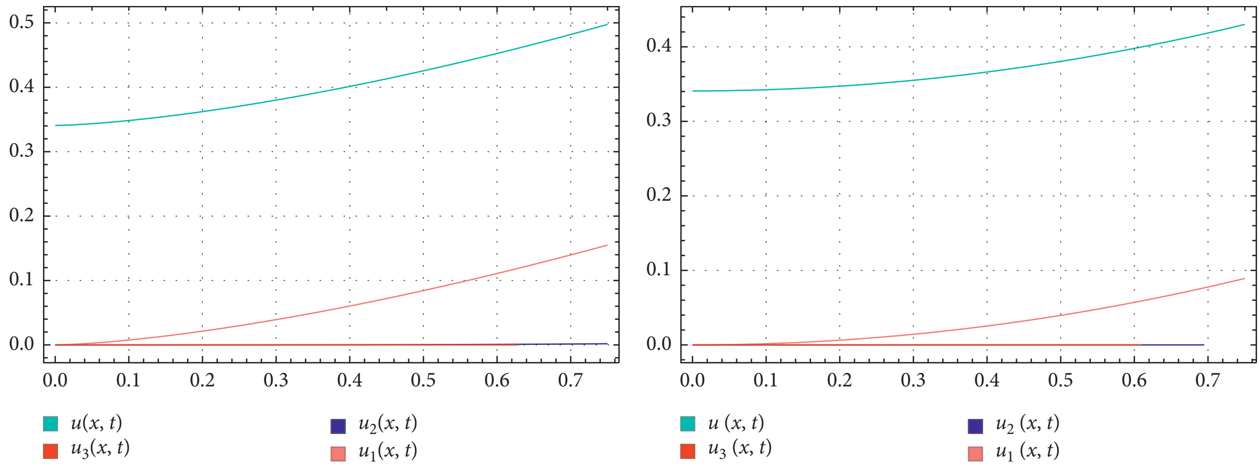

(a) (b)

Figure 4: The graphical comparison of the iterative solutions for (25) through various values of t at $x = 0.75$ and $\alpha = 0.5,\ 1$, respectively. (a) The graphical comparison of the iterative solutions for (25) through various values of t at $x = 0.75$ and $\alpha = 0.5$. (b) The graphical comparison of the iterative solutions for (25) through various values of t at $x = 0.75$ and $\alpha = 1$.

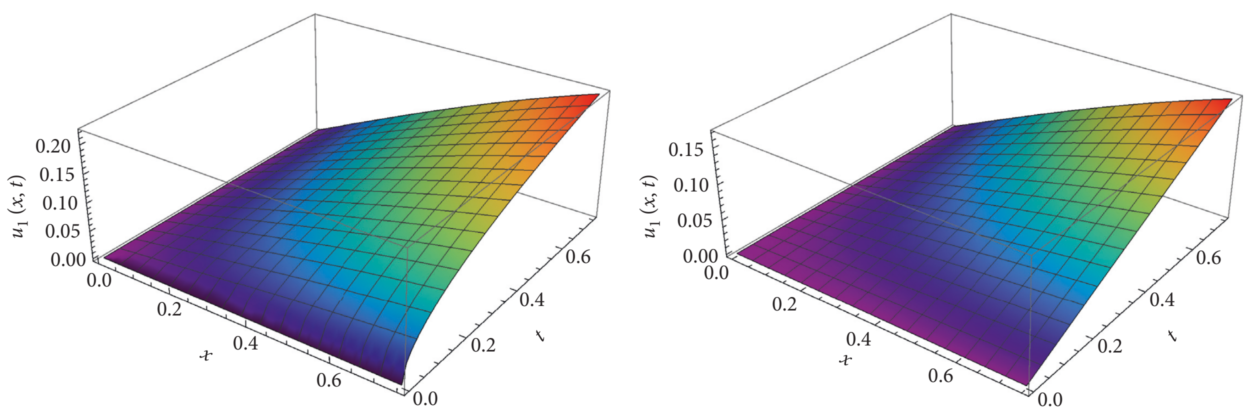

(a) (b)

Figure 5: The graphs of the first-order iterative solution $u_1(x,t)$ for (30) through various values of x, t at $\alpha = 0.5,\ 1$, respectively. (a) The graph of first-order iterative solution $u_1(x,t)$ for (30) through various values of x, t at $\alpha = 0.5$. (b) The graph of the first-order iterative solution $u_1(x,t)$ for (30) through various values of x, t at $\alpha = 1$.

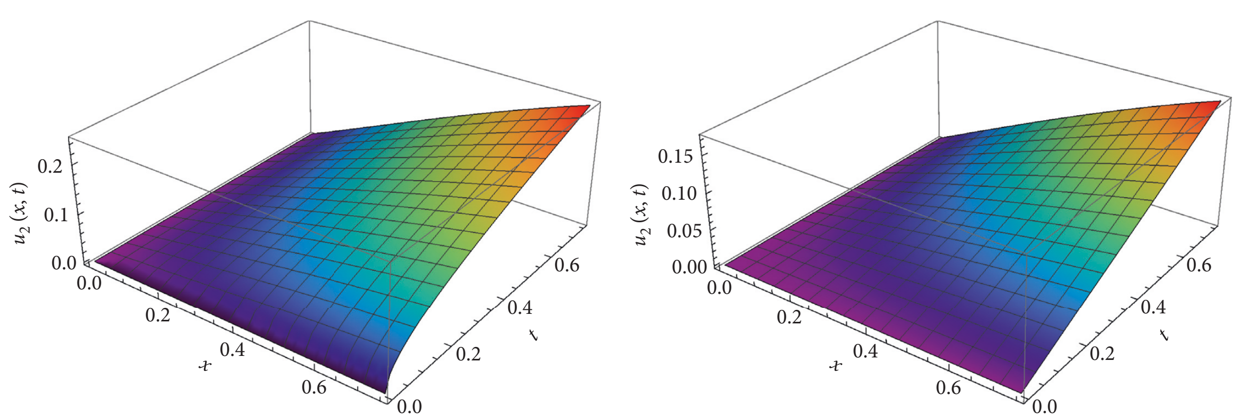

(a) (b)

Figure 6: The graphs of second-order iterative solution $u_2(x,t)$ for (30) through various points x, t at $\alpha = 0.5,\ 1$, respectively. (a) The graph of second-order iterative solution $u_2(x,t)$ for (30) through various values of x, t at $\alpha = 0.5$. (b) The graph of second-order iterative solution $u_2(x,t)$ for (30) through various values of x, t at $\alpha = 1$.

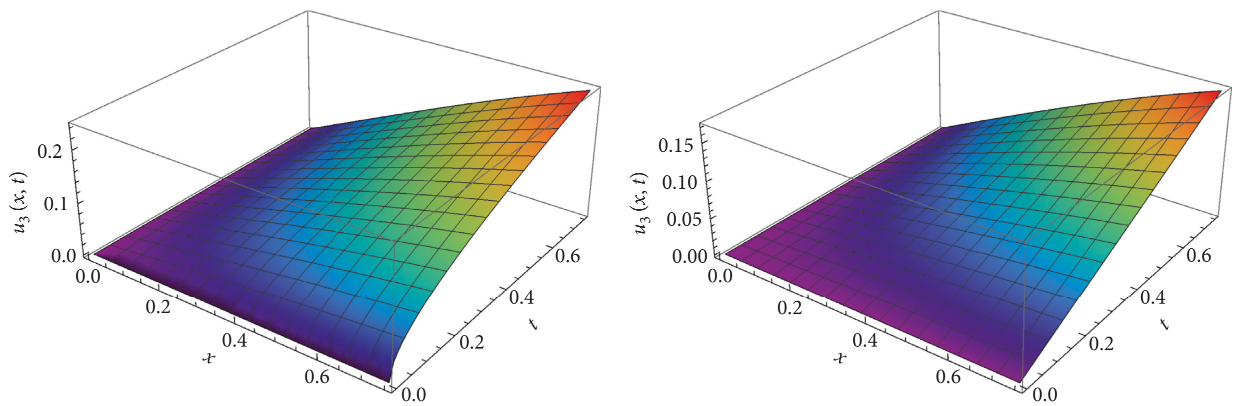

(a) (b)

Figure 7: The graphs of the third-order iterative solution $u_3(x,t)$ for (30) through various values of x, t at $\alpha = 0.5$, 1, respectively. (a) The graph of third-order iterative solution $u_3(x,t)$ for (30) through various values of x, t at $\alpha = 0.5$. (b) The graph of the third-order iterative solution $u_3(x,t)$ for (30) through various values of x, t at $\alpha = 1$.

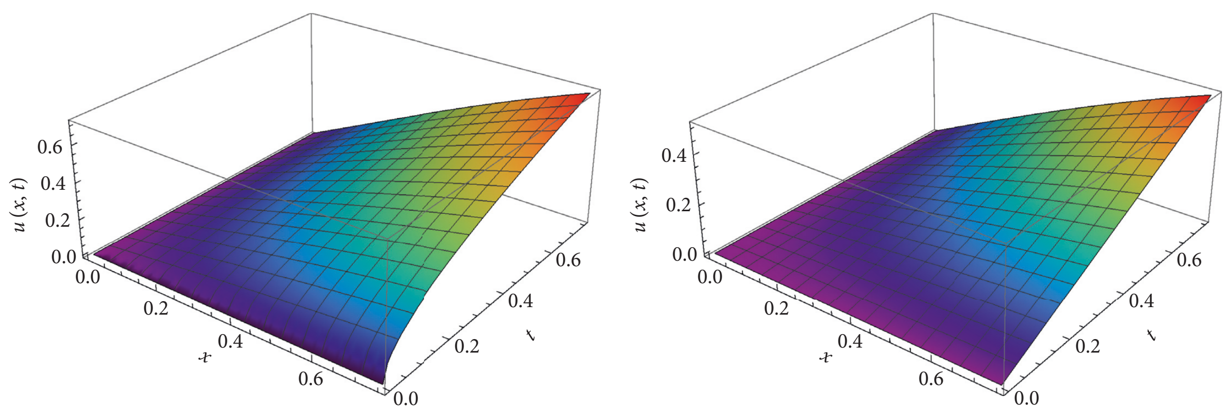

(a) (b)

Figure 8: The graphs of the third-order approximate iterative solution $u(x,t)$ for (30) through various values of x, t at $\alpha = 0.5$, 1, respectively. (a) The graph of the approximate iterative solution $u(x,t)$ for (30) through various values of x, t at $\alpha = 0.5$. (b) The graph of the approximate iterative solution $u(x,t)$ for (30) through various values of x, t at $\alpha = 1$.

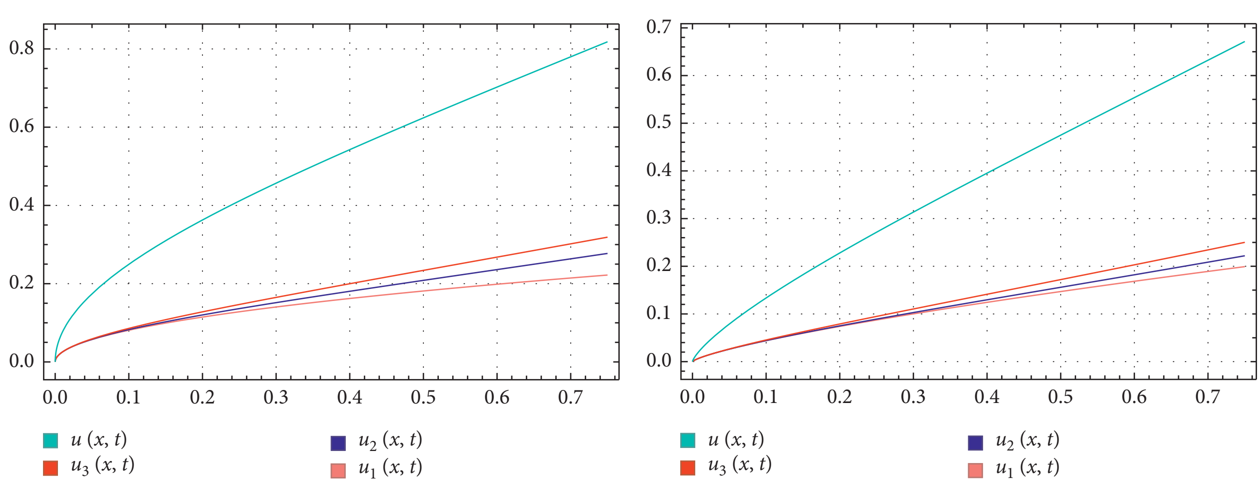

(a) (b)

Figure 9: The graphical comparison of solutions for (30) through various values of t at $x = 0.75$, $\alpha = 0.5$, 1, respectively. (a) The graphical comparison of solutions for (30) through various values of t at $x = 0.75$; $\alpha = 0.5$. (b) The graphical comparison of solutions for (30) through various values of t at $x = 0.75$; $\alpha = 1$.

Figures 8(a) and 8(b) using various points of x, t when $\alpha = 0.5, 1$, respectively. In Figures 9(a) and 9(b), we plot the graphs of the solution through different values of t for a fixed value of $x = 0.75$ when $\alpha = 0.5, 1$, respectively, for Example 2.

6. Conclusion

In this paper, we introduced a model of FPIDEs. The proposed model is iterative with fractional derivative, which can be used in neural networks and help us to describe how the input data can be accessed. For instance, for subdiffusion in the porous media, fractional-order derivatives determine the decaying rate of the breakthrough curve for long-term observations. Moreover, new results on the local existence, uniqueness, and stability analysis of the solution for the proposed model were introduced. Furthermore, we extended the method of successive approximations to solve FPIDEs with memory terms subject to initial conditions in a Banach space. This extension derives good approximations and reliable techniques to handle iterative FPIDEs. New solutions for Volterra types of iterative FPIDEs were introduced. The numerical solutions were successfully obtained which confirm the presented results.

Data Availability

The datasets used or analyzed during the current study are available from the corresponding author on reasonable request.

Conflicts of Interest

The authors declare that they have no conflicts of interest.

References

[1] M. Dehghan and M. Abbaszadeh, "Analysis of the element free Galerkin (EFG) method for solving fractional cable equation with Dirichlet boundary condition," *Applied Numerical Mathematics*, vol. 109, pp. 208–234, 2016.

[2] H. Thabet, S. Kendre, and J. Peters, "Analytical solutions for nonlinear systems of conformable space-time fractional partial differential equations via generalized fractional differential transform," *Vietnam Journal of Mathematics*, vol. 47, no. 2, pp. 487–507, 2019.

[3] H. Zhang, R. Ye, J. Cao, A. Ahmed, X. Li, and Y. Wan, "Lyapunov functional approach to stability analysis of riemann-liouville fractional neural networks with time-varying delays," *Asian Journal of Control*, vol. 20, no. 5, pp. 1938–1951, 2018.

[4] H. Thabet and S. Kendre, "Modified least squares homotopy perturbation method for solving fractional partial differential equations," *Malaya Journal of Matematik*, vol. 06, no. 02, pp. 420–427, 2018.

[5] M. Kaplan, A. R. Butt, H. Thabet, A. Akbulut, N. Raza, and D. Kumar, "An effective computational approach and sensitivity analysis to pseudo-parabolic-type equations," *Waves in Random and Complex Media*, pp. 1–15, 2021.

[6] H. Thabet, S. Kendre, and J. Peters, "Advances in solving conformable nonlinear partial differential equations and new exact wave solutions for Oskolkov-type equations," *Mathematical Methods in the Applied Sciences*, vol. 45, no. 5, pp. 2658–2673, 2022.

[7] H. Thabet, S. Kendre, D. Baleanu, and J. Peters, "Exact analytical solutions for nonlinear systems of conformable partial differential equations via an analytical approach," *UPB Scientific Bulletin, Series A: Applied Mathematics and Physics*, vol. 84, no. 1, pp. 109–120, 2022.

[8] J. R. Loh, C. Phang, and A. Isah, "New operational matrix via genocchi polynomials for solving fredholm-volterra fractional integro-differential equations," *Advances in Mathematical Physics*, vol. 2017, pp. 1–12, 2017.

[9] J. R. Loh and C. Phang, "A new numerical scheme for solving system of Volterra integro-differential equation," *Alexandria Engineering Journal*, vol. 57, no. 2, pp. 1117–1124, 2018.

[10] J. R. Loh and C. Phang, "Numerical solution of fredholm fractional integro-differential equation with right-sided caputo's derivative using Bernoulli polynomials operational matrix of fractional derivative," *Mediterranean Journal of Mathematics*, vol. 16, no. 2, pp. 28–25, 2019.

[11] J. R. Loh, C. Phang, and K. G. Tay, "New method for solving fractional partial integro-differential equations by combination of Laplace transform and resolvent kernel method," *Chinese Journal of Physics*, vol. 67, pp. 666–680, 2020.

[12] F. Abdolrazaghi and A. Razani, "On the weak solutions of an overdetermined system of nonlinear fractional partial integro-differential equations," *Miskolc Mathematical Notes*, vol. 20, no. 1, pp. 3–6, 2019.

[13] K. Al-Khaled, A. Darweesh, and M. H. Yousef, "Convergence of numerical schemes for the solution of partial integro-differential equations used in heat transfer," *Journal of Applied Mathematics and Computing*, vol. 61, no. 1-2, pp. 657–675, 2019.

[14] H. Dehestani, Y. Ordokhani, and M. Razzaghi, "Pseudo-operational matrix method for the solution of variable-order fractional partial integro-differential equations," *Engineering with Computers*, vol. 37, no. 3, pp. 1791–1806, 2020.

[15] E. Eder, "The functional differential equation $x'(t) = x(x(t))$," *Journal of Differential Equations*, vol. 54, no. 3, pp. 390–400, 1984.

[16] M. I. Berenguer and D. Gámez, "Projected iterations of fixed-point type to solve nonlinear partial volterra integro-differential equations," *Bulletin of the Malaysian Mathematical Sciences Society*, vol. 43, no. 6, pp. 4431–4442, 2020.

[17] C. Bao, Y. Pu, and Y. Zhang, "Fractional-order deep backpropagation neural network," *Computational Intelligence and Neuroscience*, vol. 201810 pages, 2018.

[18] G. Pang, L. Lu, and G. E. Karniadakis, "fPINNs: fractional physics-informed neural networks," *SIAM Journal on Scientific Computing*, vol. 41, no. 4, pp. A2603–A2626, 2019.

[19] D. J. White, "Dynamic programming, Markov chains, and the method of successive approximations," *Journal of Mathematical Analysis and Applications*, vol. 6, no. 3, pp. 373–376, 1963.

[20] R. E. Larson and A. J. Korsak, "A dynamic programming successive approximations technique with convergence proofs," *Automatica*, vol. 6, no. 2, pp. 245–252, 1970.

[21] R. F. Curtain and A. J. Pritchard, *Functional Analysis in Modern Applied Mathematics*, Academic Press, Cambridge, MA, USA, 1977.

[22] Z. Aganovic and Z. Gajic, "Successive approximation procedure for the optimal control of bilinear systems," *[Proceedings 1992] IEEE International Conference on Systems Engineering*, vol. 39, no. 9, pp. 440–443, 1992.

[23] A. M. A. El-Sayed, H. H. G. Hashem, and E. A. A. Ziada, "Picard and Adomian decomposition methods for a quadratic integral equation of fractional order," *Computational and Applied Mathematics*, vol. 33, no. 1, pp. 95–109, 2014.

[24] A. M. A. El-Sayed, H. H. G. Hashem, and E. A. A. Ziada, "Picard and adomian methods for quadratic integral equation," *Computational and Applied Mathematics*, vol. 29, no. 3, pp. 447–463, 2010.

[25] H. Jafari, "A comparison between the variational iteration method and the successive approximations method," *Applied Mathematics Letters*, vol. 32, no. 1, pp. 1–5, 2014.

[26] H. Liu and W. Li, "The exact analytic solutions of a nonlinear differential iterative equation," *Nonlinear Analysis: Theory, Methods & Applications*, vol. 69, no. 8, pp. 2466–2478, 2008.

[27] X.-P. Wang and J.-G. Si, "Analytic solutions of an iterative functional differential equation," *Journal of Mathematical Analysis and Applications*, vol. 262, no. 2, pp. 490–498, 2001.

[28] D. Yang and W. Zhang, "Solutions of equivariance for iterative differential equations," *Applied Mathematics Letters*, vol. 17, no. 7, pp. 759–765, 2004.

[29] L. Zhang, L. Zhang, J. Yuan, and C. M. Khalique, "Existence of wave front solutions of an integral differential equation in nonlinear nonlocal neuronal network," *Abstract and Applied Analysis*, vol. 2014, no. 2, 2014.

[30] R. W. Ibrahim, "Existence of iterative cauchy fractional differential equation," *Journal of Mathematics*, vol. 2013, no. 3, 7 pages, 2013.

[31] M. Podisuk, "More on simple iterative ordinary differential equation," *Procedia - Social and Behavioral Sciences*, vol. 88, no. 3, pp. 187–195, 2013.

[32] H. Thabet, S. Kendre, and D. Chalishajar, "New analytical technique for solving a system of nonlinear fractional partial differential equations," *Mathematics*, vol. 5, no. 4, p. 47, 2017.

[33] H. Thabet and S. Kendre, *Elementary Course in Fractional Calculus*, LAP LAMBERT Academic Publishing, 2018.

[34] H. Thabet and S. Kendre, "New modification of Adomian decomposition method for solving a system of nonlinear fractional partial differential equations," *International Journal of Advances in Applied Mathematics and Mechanics*, vol. 6, no. 3, pp. 1–13, 2019.

[35] H. Thabet, S. Kendre, and J. Peters, "Travelling wave solutions for fractional Korteweg-de Vries equations via an approximate-analytical method," *AIMS Mathematics*, vol. 4, no. 4, pp. 1203–1222, 2019.

[36] H. Thabet, S. Kendre, J. Peters, and M. Kaplan, "Solitary wave solutions and traveling wave solutions for systems of time-fractional nonlinear wave equations via an analytical approach," *Computational and Applied Mathematics*, vol. 39, no. 3, p. 144, 2020.

Hindawi
Journal of Mathematics
Volume 2022, Article ID 8173785, 17 pages
https://doi.org/10.1155/2022/8173785

Research Article

New Generalized Riemann–Liouville Fractional Integral Versions of Hadamard and Fejér–Hadamard Inequalities

Kamsing Nonlaopon,[1] **Ghulam Farid**,[2] **Ammara Nosheen**,[3] **Muhammad Yussouf**,[3] **and Ebenezer Bonyah**[4]

[1]*Department of Mathematics, Faculty of Science, Khon Kaen University, Khon Kaen 40002, Thailand*
[2]*Department of Mathematics, COMSATS University Islamabad, Attock Campus, Attock, Pakistan*
[3]*Department of Mathematics,, University of Sargodha, Sargodha, Pakistan*
[4]*Department of Mathematics Education, Akenten Appiah Menka University of Skills Training and Entrepreneurial Development, Kumasi, Ghana*

Correspondence should be addressed to Ebenezer Bonyah; ebonyah@aamusted.edu.gh

Received 20 January 2022; Revised 5 March 2022; Accepted 14 March 2022; Published 26 April 2022

Academic Editor: Mawardi Bahri

In this paper, a new class of functions, namely, exponentially $(\alpha, h-m)-p$-convex functions is introduced to unify various classes of functions already defined in the subject of convex analysis. By using this class of functions, generalized versions of well known fractional integral inequalities of Hadamard and Fejér–Hadamard type are obtained. The results of this paper generate fractional integral inequalities of Hadamard and Fejér–Hadamard type for various types of convex and exponentially convex functions simultaneously.

1. Introduction and Preliminary Results

Inequalities are important tools for mathematical modeling of problems that occur in the diverse fields of science and engineering. Convex functions are very useful in establishing new and generalized inequalities. For example, Jensen's inequality for convex functions is one of the most celebrating inequalities in the literature. Many classical inequalities are direct consequences of Jensen's inequality. Motivated from the properties and representations of convex functions, researchers have published a lot of new definitions of functions which are usually utilized for extensions, refinements, and generalizations of well known inequalities. In recent decades, it becomes a fashion for authors to generalize the classical concepts related to ordinary derivatives and integrals via fractional integral/derivative operators. These techniques are used frequently in generalizing the classical mathematical inequalities. For a detailed study, we refer the readers to [1–13].

The goal of this paper is to establish general Riemann–Liouville fractional integral inequalities of Hadamard and Fejér–Hadamard type by defining a new class of functions which will concurrently hold for many kinds of convex and exponentially convex functions. Next, we give definitions of Riemann–Liouville fractional integrals which we will utilize to establish main results. After that we will give definition of convex function with a detailed discussion on related definitions.

Definition 1 (see [14]). Let $f \in L_1[a,b]$. Then, the left- and right-sided Riemann–Liouville fractional integrals of f of order $\tau \in \mathbb{R}$ $(\tau > 0)$ are given as follows:

$$I_{a^+}^{\tau} f(x) = \frac{1}{\Gamma(\tau)} \int_a^x (x-t)^{\tau-1} f(t)\mathrm{d}t, \quad x > a, \tag{1}$$

$$I_{b^-}^{\tau} f(x) = \frac{1}{\Gamma(\tau)} \int_x^b (t-x)^{\tau-1} f(t)\mathrm{d}t, \quad x < b, \tag{2}$$

where $\Gamma(\cdot)$ is the gamma function.

Definition 2 (see [15]). A real-valued function $f\colon [a,b] \longrightarrow \mathbb{R}$ is called convex if the following inequality holds:

$$f(tx+(1-t)y) \le tf(x)+(1-t)f(y),\quad \forall x,y\in[a,b], t\in[0,1]. \tag{3}$$

There are many kinds of functions which have been defined inspiring by inequality (3). For example, functions, namely, p-convex [16], h-convex [17], m-convex [15], s-convex [18], harmonically convex [6], and many others are defined just by convenient possible modifications in the inequality (3). Moreover, (s,m)-convex [19], (α,m)-convex [20], $(h-m)$-convex [21], $(\alpha,h-m)$-convex [22], and (p,h)-convex [3] functions have been defined elegantly after the definition of convex function. Further, in [23], the notion of $(\alpha,h-m)-p$-convex function is defined which unifies all the aforementioned convexities.

There also exists a class of exponentially convex functions stated as follows.

Definition 3 (see [24]). A real-valued function $f\colon J\subset \mathbb{R}\longrightarrow \mathbb{R}_+$ is called exponentially convex on J if the following inequality holds:

$$f(tx+(1-t)y) \le \frac{tf(x)}{e^{\eta x}}+\frac{(1-t)f(y)}{e^{\eta y}},\quad t\in[0,1], \forall x,y\in J, \eta\in\mathbb{R}. \tag{4}$$

The term exponentially convex function is used likewise to convex function, and notions of exponentially p-convex [25], exponentially h-convex [26], exponentially s-convex [25] have been introduced. Also, definitions of exponentially (s,m)-convex [27], exponentially (α,m)-convex [26], exponentially $(h-m)$-convex [26], exponentially $(\alpha,h-m)$-convex [28], and exponentially (p,h)-convex [29] functions have been published.

The exponentially $(\alpha,h-m)$-convex function is defined as follows.

Definition 4 (see [28]). Let $J\subseteq\mathbb{R}$ be an interval containing $(0,1)$, and let $h\colon J\longrightarrow\mathbb{R}$ be a nonnegative function. Then, a function $f\colon I\longrightarrow\mathbb{R}$ on an interval of real line is said to be exponentially $(\alpha,h-m)$-convex, if for all $x,y\in I$, $t\in(0,1)$, $\alpha,m\in[0,1]$, and $\eta\in\mathbb{R}$, the following inequality holds:

$$f(tx+m(1-t)y) \le \frac{h(t^\alpha)f(x)}{e^{\eta u_1}}+\frac{mh(1-t^\alpha)f(y)}{e^{\eta y}}. \tag{5}$$

The following example is important to distinguish an exponentially convex function from convex function.

Example 1 (see [30]). The function $f(x)=x\exp(-x)$ is exponentially $(1,I_d-1)$-convex function but not $(1,I_d-1)$-convex function. More precisely the function f is exponentially convex function on $[0,\infty)$ but not a convex function on this domain.

All the aforementioned definitions have been used to derive Hadamard and Fejér–Hadamard type inequalities. We are motivated to combine all types of convexities and exponential convexities in a single definition. We will define exponentially $(\alpha,h-m)-p$-convex function and prove Hadamard and Fejér–Hadamard type inequalities which will unify a plenty of classical inequalities.

The paper is organized as follows: In Section 2, a new class of functions will be called exponentially $(\alpha,h-m)-p$-convex function. Some new definitions will be deduced in connection with existing definitions in the literature of mathematical inequalities. In Section 3, we will present the Hadamard and Fejér–Hadamard inequalities for newly defined functions via Riemann–Liouville fractional integrals. We will identify a number of implications of the results established in this section.

2. Exponentially $(\alpha,h-m)-p$-Convex Function and Deduced Definitions

We define exponentially $(\alpha,h-m)-p$-convex function as follows.

Definition 5. Let $J\subseteq\mathbb{R}$ be an interval containing $(0,1)$, and let $h\colon J\longrightarrow\mathbb{R}$ be a nonnegative function. Let $I\subset(0,\infty)$ be a real interval and $p\in\mathbb{R}\setminus\{0\}$. A function $f\colon I\longrightarrow\mathbb{R}$ is called exponentially $(\alpha,h-m)-p$-convex if for $t\in(0,1)$, $\eta\in\mathbb{R}$ and $(\alpha,m)\in[0,1]^2$, the following inequality holds:

$$f\left(\left(ta^p+m(1-t)b^p\right)^{1/p}\right) \le \frac{h(t^\alpha)f(a)}{e^{\eta a}}+\frac{mh(1-t^\alpha)f(b)}{e^{\eta b}}, \tag{6}$$

where $a,b\in I$ provided $(ta^p+m(1-t)b^p)^{1/p}\in I$.

Remark 1. The following convex functions are reproduced from above definition:

(i) In Definition 5, if we put $p=-1$, $m=\alpha=1$, and $\eta=0$, we have harmonically h-convex function reproduced (see Definition 2.10 in [31]).

(ii) In Definition 5, for $p=1$ and $\eta=0$, we have $(\alpha,h-m)$-convex function reproduced (see Definition 4.5 in [20]).

(iii) In Definition 5, for $\alpha=m=1$ and $\eta=0$, we have (p,h)-convex function reproduced (see [3]).

(iv) In Definition 5, for $p=1$, exponentially $(\alpha,h-m)$-convex function is reproduced (see Definition 1 in [26]). For further deduced functions, see Remark 1 in [26].

(v) In Definition 5, for $\alpha=p=1$, exponentially $(h-m)$-convex function is reproduced (see Definition 2 in [26]).

(vi) In Definition 5, for $p = 1$ and $h(t) = t$, exponentially (α, m)-convex function is reproduced (see Definition 3 in [26]).

(vii) In Definition 5, for $p = -1$, $\alpha = m = 1$, $h(t) = t^s$, and $\eta = 0$, we have harmonic s-convex function in second sense reproduced (see Remark 1 in [32]).

(viii) In Definition 5, for $p = -1$, $\alpha = m = 1$, $h(t) = t$, and $\eta = 0$, we have harmonic convex function reproduced (see [33]).

(ix) In Definition 5, for $p = 1$, $\alpha = 1$, $h(t) = t^s$, and $\eta = 0$, we have (s, m)-convex function in second sense reproduced (see Definition 1.2 in [19]).

(x) In Definition 5, for $p = -1$, $\alpha = 1$, $h(t) = t$, and $\eta = 0$, we have m-HA-convex function reproduced (see Definition 2 in [34]).

(xi) In Definition 5, for $p = -1$, $h(t) = t$, and $\eta = 0$, (α, m)-HA-convex function is reproduced (see Definition 2.1 in [35]).

For $\alpha = 1$ in (6), we get exponentially $(h - m) - p$-convex function as follows:

$$f\left(\left(ta^p + m(1-t)b^p\right)^{1/p}\right) \le \frac{h(t) f(a)}{e^{\eta a}} + \frac{mh(1-t) f(b)}{e^{\eta b}}. \tag{7}$$

For $h(t) = t$ in (6), we get exponentially $(\alpha, m) - p$-convex function as follows:

$$f\left(\left(ta^p + m(1-t)b^p\right)^{1/p}\right) \le \frac{t^\alpha f(a)}{e^{\eta a}} + \frac{m\left(1-t^\alpha\right) f(b)}{e^{\eta b}}. \tag{8}$$

For $m = 1$ in (6), we get exponentially $(\alpha, h) - p$-convex function as follows:

$$f\left(\left(ta^p + (1-t)b^p\right)^{1/p}\right) \le \frac{h\left(t^\alpha\right) f(a)}{e^{\eta a}} + \frac{h\left(1-t^\alpha\right) f(b)}{e^{\eta b}}. \tag{9}$$

For $\alpha = 1$ and $h(t) = t^s$ in (6), we get exponentially $(s, m) - p$-convex function as follows:

$$f\left(\left(ta^p + m(1-t)b^p\right)^{1/p}\right) \le \frac{t^s f(a)}{e^{\eta a}} + \frac{m(1-t)^s f(b)}{e^{\eta b}}. \tag{10}$$

For $h(t) = t^s$ in (6), we get exponentially $(s, m) - p$-Godunova–Levin function of second kind as follows:

$$f\left(\left(ta^p + m(1-t)b^p\right)^{1/p}\right) \le \frac{1}{t^s} \frac{f(a)}{e^{\eta a}} + \frac{m}{(1-t)^s} \frac{f(b)}{e^{\eta b}}. \tag{11}$$

For $m = \alpha = 1$ and $h(t) = 1$ in (6), we get exponentially (p, P)-convex function as follows:

$$f\left(\left(ta^p + (1-t)b^p\right)^{1/p}\right) \le \frac{f(a)}{e^{\eta a}} + \frac{f(b)}{e^{\eta b}}. \tag{12}$$

For $\alpha = m = 1$, $p = -1$, and $h(t) = (1/t)$ in (6), we get exponentially Godunova–Levin type exponentially harmonic convex function as follows:

$$f\left(\frac{ab}{tb + (1-t)a}\right) \le \frac{1}{t} \frac{f(a)}{e^{\eta a}} + \frac{1}{1-t} \frac{f(b)}{e^{\eta b}}. \tag{13}$$

For $\alpha = m = 1$, $p = -1$, and $h(t) = (1/t^s)$ in (6), we get exponentially harmonic convex function as follows:

$$f\left(\frac{ab}{tb + (1-t)a}\right) \le \frac{1}{t^s} \frac{f(a)}{e^{\eta a}} + \frac{1}{(1-t)^s} \frac{f(b)}{e^{\eta b}}. \tag{14}$$

For $p = -1$ in (6), we get exponentially $(\alpha, h - m)$-HA-convex function as follows:

$$f\left(\frac{ab}{tb + m(1-t)a}\right) \le \frac{h\left(t^\alpha\right) f(a)}{e^{\eta a}} + \frac{mh\left(1-t^\alpha\right) f(b)}{e^{\eta b}}. \tag{15}$$

For $p = -1$ and $m = 1$ in (6), we get exponentially (α, h)-HA-convex function as follows:

$$f\left(\frac{ab}{tb + (1-t)a}\right) \le \frac{h\left(t^\alpha\right) f(a)}{e^{\eta a}} + \frac{h\left(1-t^\alpha\right) f(b)}{e^{\eta b}}. \tag{16}$$

For $p = -1$, $m = \alpha = 1$, and $h(t) = t$ in (6), we get exponentially HA-convex function as follows:

$$f\left(\frac{ab}{tb + (1-t)a}\right) \le \frac{t f(a)}{e^{\eta a}} + \frac{(1-t) f(b)}{e^{\eta b}}. \tag{17}$$

For $p = -1$ and $h(t) = t$ in (6), we get exponentially (α, m)-HA-convex function as follows:

$$f\left(\frac{ab}{tb + m(1-t)a}\right) \le \frac{t^\alpha f(a)}{e^{\eta a}} + \frac{m\left(1-t^\alpha\right) f(b)}{e^{\eta b}}. \tag{18}$$

From now to onward, we will use the notation $E_p(\alpha, h - m)$ for exponentially $(\alpha, h - m) - p$-convex function.

3. Inequalities of Hadamard Type for $E_p(\alpha, h - m)$ Function

Theorem 1. *Let $f: I \subset (0, \infty) \longrightarrow \mathbb{R}$ be an $E_p(\alpha, h - m)$ positive function as defined in Definition 5 and $f \in L_1[a, b]$, $a, b \in I, a < b$. Then, for $(\alpha, m) \in (0, 1]^2$, one can have fractional integral inequalities for operators (1) and (2) as follows.*

(i) For $p > 0$, we have

$$f\left(\left(\frac{a^p+mb^p}{2}\right)^{1/p}\right)\leq\frac{\Gamma(\tau+1)}{(mb^p-a^p)^{\tau}}\left(\mathfrak{D}_1(\eta)h\left(\frac{1}{2^{\alpha}}\right)(I^{\tau}_{a^p+}f^{\circ}\xi)(mb^p)+\mathfrak{D}_2(\eta)m^{\tau+1}h\left(\frac{2^{\alpha}-1}{2^{\alpha}}\right)(I^{\tau}_{b^p-}f^{\circ}\xi)\left(\frac{a^p}{m}\right)\right)$$
$$\leq\tau\left\{\left(\mathfrak{D}_1(\eta)h\left(\frac{1}{2^{\alpha}}\right)\frac{f(a)}{e^{\eta a}}+\mathfrak{D}_2(\eta)mh\left(\frac{2^{\alpha}-1}{2^{\alpha}}\right)\frac{f(b)}{e^{\eta b}}\right)\int_0^1 t^{\tau-1}h(t^{\alpha})\mathrm{d}t\right.$$
$$\left.+m\left(\mathfrak{D}_1(\eta)h\left(\frac{1}{2^{\alpha}}\right)\frac{f(b)}{e^{\eta b}}+\mathfrak{D}_2(\eta)mh\left(\frac{2^{\alpha}-1}{2^{\alpha}}\right)\frac{f(a/m^2)}{e^{(\eta a/m^2)}}\right)\int_0^1 t^{\tau-1}h(1-t^{\alpha})\mathrm{d}t\right\}, \tag{19}$$

where $\xi(z)=z^{1/p}$, $z\in[a^p,mb^p]$, $\mathfrak{D}_1(\eta)=e^{-\eta bm^{1/p}}$ for $\eta<0$, $\mathfrak{D}_1(\eta)=e^{-\eta a}$ for $\eta\geq 0$, $\mathfrak{D}_2(\eta)=e^{-\eta(a/(m^{(1/p)}))}$ for $\eta>0$, and $\mathfrak{D}_2(\eta)=e^{-\eta b}$ for $\eta\leq 0$.

(ii) For $p<0$, we have

$$f\left(\left(\frac{a^p+mb^p}{2}\right)^{1/p}\right)\leq\frac{\Gamma(\tau+1)}{(a^p-mb^p)^{\tau}}\left(\mathfrak{D}_3(\eta)h\left(\frac{1}{2^{\alpha}}\right)(I^{\tau}_{a^p-}f^{\circ}\xi)(mb^p)+\mathfrak{D}_4(\eta)m^{\tau+1}h\left(\frac{2^{\alpha}-1}{2^{\alpha}}\right)(I^{\tau}_{b^p+}f^{\circ}\xi)\left(\frac{a^p}{m}\right)\right)$$
$$\leq\tau\left\{\left(\mathfrak{D}_3(\eta)h\left(\frac{1}{2^{\alpha}}\right)\frac{f(a)}{e^{\eta a}}+\mathfrak{D}_4(\eta)mh\left(\frac{2^{\alpha}-1}{2^{\alpha}}\right)\frac{f(b)}{e^{\eta b}}\right)\int_0^1 t^{\tau-1}h(t^{\alpha})\mathrm{d}t\right.$$
$$\left.+m\left(\mathfrak{D}_3(\eta)h\left(\frac{1}{2^{\alpha}}\right)\frac{f(b)}{e^{\eta b}}+\mathfrak{D}_4(\eta)mh\left(\frac{2^{\alpha}-1}{2^{\alpha}}\right)\frac{f(a/m^2)}{e^{(\eta a/m^2)}}\right)\int_0^1 t^{\tau-1}h(1-t^{\alpha})\mathrm{d}t\right\}, \tag{20}$$

where $\xi(z)=z^{1/p}$, $z\in[mb^p,a^p]$, $\mathfrak{D}_3(\eta)=e^{-\eta bm^{1/p}}$ for $\eta<0$, $\mathfrak{D}_3(\eta)=e^{-\eta a}$ for $\eta\geq 0$, $\mathfrak{D}_4(\eta)=e^{-\eta(a/m^{1/p})}$ for $\eta<0$, and $\mathfrak{D}_4(\eta)=e^{-\eta b}$ for $\eta\geq 0$.

Proof. (i) By using (6), one can have the following inequality:

$$f\left(\left(\frac{x^p+my^p}{2}\right)^{1/p}\right)\leq h\left(\frac{1}{2^{\alpha}}\right)\frac{f(x)}{e^{\eta x}}+mh\left(\frac{2^{\alpha}-1}{2^{\alpha}}\right)\frac{f(y)}{e^{\eta y}}. \tag{21}$$

For $x=(ta^p+m(1-t)b^p)^{1/p}$ and $y=(tb^p+(1-t)(a^p/m))^{1/p}$ in (21), we get

$$f\left(\left(\frac{a^p+mb^p}{2}\right)^{1/p}\right)\leq h\left(\frac{1}{2^{\alpha}}\right)\frac{f\left((ta^p+m(1-t)b^p)^{1/p}\right)}{e^{\eta\left((ta^p+m(1-t)b^p)^{1/p}\right)}}+mh\left(\frac{2^{\alpha}-1}{2^{\alpha}}\right)\frac{f\left((tb^p+(1-t)(a^p/m))^{1/p}\right)}{e^{\eta\left((tb^p+(1-t)(a^p/m))^{1/p}\right)}}. \tag{22}$$

Multiplying the above inequality with $t^{\tau-1}$ on both sides and integrating over $[0,1]$, we have

$$f\left(\left(\frac{a^p+mb^p}{2}\right)^{1/p}\right)\int_0^1 t^{\tau-1}\mathrm{d}t\leq h\left(\frac{1}{2^{\alpha}}\right)\int_0^1\frac{t^{\tau-1}f\left((ta^p+m(1-t)b^p)^{1/p}\right)}{e^{\eta\left((ta^p+m(1-t)b^p)^{1/p}\right)}}\mathrm{d}t$$
$$+mh\left(\frac{2^{\alpha}-1}{2^{\alpha}}\right)\int_0^1\frac{t^{\tau-1}f\left((tb^p+(1-t)(a^p/m))^{1/p}\right)}{e^{\eta\left((tb^p+(1-t)(a^p/m))^{1/p}\right)}}\mathrm{d}t. \tag{23}$$

Set $ta^p+m(1-t)b^p=x$, that is, $t=(mb^p-x)/(mb^p-a^p)$ and $tb^p+(1-t)(a^p/m)=y$, that is, $t=(y-(a^p/m))/(b^p-(a^p/m))$ in right hand side of the above inequality. Then, after some calculations, one can obtain the first inequality of (19).

On the other hand, by using (6) on the right hand side of (22), one can obtain the inequality as follows:

$$\begin{aligned}
&h\left(\frac{1}{2^{\alpha}}\right)\frac{f\left(\left(ta^{p}+m(1-t)b^{p}\right)^{1/p}\right)}{e^{\eta\left(\left(ta^{p}+m(1-t)b^{p}\right)^{1/p}\right)}}+mh\left(\frac{2^{\alpha}-1}{2^{\alpha}}\right)\frac{f\left(\left(tb^{p}+(1-t)\left(a^{p}/m\right)\right)^{1/p}\right)}{e^{\eta\left(\left(tb^{p}+(1-t)\left(a^{p}/m\right)\right)^{1/p}\right)}}\\
&\leq\frac{h\left(1/2^{\alpha}\right)}{e^{\eta\left(\left(ta^{p}+m(1-t)b^{p}\right)^{1/p}\right)}}\left(h\left(t^{\alpha}\right)\frac{f(a)}{e^{\eta a}}+\frac{mh\left(1-t^{\alpha}\right)f(b)}{e^{\eta b}}\right)\\
&+\frac{mh\left(\left(2^{\alpha}-1\right)/2^{\alpha}\right)}{e^{\eta\left(\left(tb^{p}+(1-t)\left(a^{p}/m\right)\right)^{1/p}\right)}}\left(\frac{h\left(t^{\alpha}\right)f(b)}{e^{\eta b}}+\frac{mh\left(1-t^{\alpha}\right)f\left(a/m^{2}\right)}{e^{\left(\eta a/m^{2}\right)}}\right).
\end{aligned}\tag{24}$$

Multiplying the above inequality with $t^{\tau-1}$, by integrating over $[0,1]$, one can get

$$\begin{aligned}
&\mathfrak{D}_1(\eta)h\left(\frac{1}{2^{\alpha}}\right)\int_0^1 t^{\tau-1}f\left(\left(ta^{p}+m(1-t)b^{p}\right)^{1/p}\right)dt\\
&+\mathfrak{D}_2(\eta)mh\left(\frac{2^{\alpha}-1}{2^{\alpha}}\right)\int_0^1 t^{\tau-1}f\left(\left(tb^{p}+(1-t)\frac{a^{p}}{m}\right)^{1/p}\right)dt\\
&\leq\left(\mathfrak{D}_1(\eta)h\left(\frac{1}{2^{\alpha}}\right)\frac{f(a)}{e^{\eta a}}+\mathfrak{D}_2(\eta)mh\left(\frac{2^{\alpha}-1}{2^{\alpha}}\right)\frac{f(b)}{e^{\eta b}}\right)\int_0^1 t^{\tau-1}h\left(t^{\alpha}\right)dt\\
&+m\left(\mathfrak{D}_1(\eta)h\left(\frac{1}{2^{\alpha}}\right)\frac{f(b)}{e^{\eta b}}+\mathfrak{D}_2(\eta)mh\left(\frac{2^{\alpha}-1}{2^{\alpha}}\right)\frac{f\left(a/m^{2}\right)}{e^{\left(\eta a/m^{2}\right)}}\right)\int_0^1 t^{\tau-1}h\left(1-t^{\alpha}\right)dt.
\end{aligned}\tag{25}$$

Set $ta^{p}+m(1-t)b^{p}=x$, that is. $t=(mb^{p}-x)/(mb^{p}-a^{p})$ and $tb^{p}+(1-t)(a^{p}/m)=y$, that is, $t=(y-(a^{p}/m))/(b^{p}-(a^{p}/m))$ in (25). Then, after some calculations, the second inequality of (19) is obtained.

(ii) Proof is similar as (i). □

Remark 2.

(i) In Theorem 1 (i), if we put $\alpha=m=1$, $h(t)=t$, $\eta=0$, and $p=1$, then Theorem 2 in [12] is reproduced.

(ii) In Theorem 1 (i), if we put $\alpha=m=1$, $p=1$, $h(t)=t$, $\eta=0$, and $\tau=1$, then classical Hadamard inequality is reproduced.

(iii) In Theorem 1 (ii), if we put $\alpha=m=1$, $h(t)=t$, $\eta=0$, and $p=-1$, then Theorem 4 in [8] is reproduced.

The other variant of the Hadamard inequality is stated and proved as follows.

Theorem 2. *Let the assumptions of Theorem 1 hold. Then, we have the following inequalities.*

(i) For $p>0$, we have

$$\begin{aligned}
&f\left(\left(\frac{a^{p}+mb^{p}}{2}\right)^{1/p}\right)\leq\Gamma(\tau+1)\left(\frac{2}{mb^{p}-a^{p}}\right)^{\tau}\\
&\times\left(\mathfrak{D}_1(\eta)h\left(\frac{1}{2^{\alpha}}\right)\left(I^{\tau}_{\left(\left(a^{p}+mb^{p}\right)/2\right)^{+}}f\circ\xi\right)\left(mb^{p}\right)+\mathfrak{D}_2(\eta)m^{\tau+1}h\left(\frac{2^{\alpha}-1}{2^{\alpha}}\right)\left(I^{\tau}_{\left(\left(a^{p}+mb^{p}\right)/2m\right)^{-}}f^{\circ}\xi\right)\left(\frac{a^{p}}{m}\right)\right)\\
&\leq\tau\left\{\left(\mathfrak{D}_1(\eta)h\left(\frac{1}{2^{\alpha}}\right)\frac{f(a)}{e^{\eta a}}+\mathfrak{D}_2(\eta)mh\left(\frac{2^{\alpha}-1}{2^{\alpha}}\right)\frac{f(b)}{e^{\eta b}}\right)\int_0^1 t^{\tau-1}h\left(\left(\frac{t}{2}\right)^{\alpha}\right)dt\right.\\
&\left.+m\left(\mathfrak{D}_1(\eta)h\left(\frac{1}{2^{\alpha}}\right)\frac{f(b)}{e^{\eta b}}+\mathfrak{D}_2(\eta)mh\left(\frac{2^{\alpha}-1}{2^{\alpha}}\right)\frac{f\left(a/m^{2}\right)}{e^{\left(\eta a/m^{2}\right)}}\right)\int_0^1 t^{\tau-1}h\left(1-\left(\frac{t}{2}\right)^{\alpha}\right)dt\right\},
\end{aligned}\tag{26}$$

where $\xi(z) = z^{1/p}$, $z \in [a^p, mb^p]$, $\mathfrak{D}_1(\eta)$, and $\mathfrak{D}_2(\eta)$ are same as given in Theorem 1 (i).

(ii) For $p < 0$, we have

$$f\left(\left(\frac{a^p + mb^p}{2}\right)^{1/p}\right) \leq \Gamma(\tau+1)\left(\frac{2}{a^p - mb^p}\right)^{\tau} \times\left(\mathfrak{D}_3(\eta) h\left(\frac{1}{2^\alpha}\right)\left(I^{\tau}_{((a^p+mb^p)/2)^-} f \circ \xi\right)(mb^p) + \mathfrak{D}_4(\eta) m^{\tau+1} h\left(\frac{2^\alpha - 1}{2^\alpha}\right)\left(I^{\tau}_{((a^p+mb^p)/2m)^+} f^{\circ}\xi\right)\left(\frac{a^p}{m}\right)\right)$$
$$\leq \tau\left\{\left(\mathfrak{D}_3(\eta) h\left(\frac{1}{2^\alpha}\right)\frac{f(a)}{e^{\eta a}} + \mathfrak{D}_4(\eta) m h\left(\frac{2^\alpha - 1}{2^\alpha}\right)\frac{f(b)}{e^{\eta b}}\right)\int_0^1 t^{\tau-1} h\left(\left(\frac{t}{2}\right)^{\alpha}\right) dt + m\left(\mathfrak{D}_3(\eta) h\left(\frac{1}{2^\alpha}\right)\frac{f(b)}{e^{\eta b}} + \mathfrak{D}_4(\eta) m h\left(\frac{2^\alpha - 1}{2^\alpha}\right)\frac{f(a/m^2)}{e^{(\eta a/m^2)}}\right)\int_0^1 t^{\tau-1} h\left(1 - \left(\frac{t}{2}\right)^{\alpha}\right) dt\right\}, \tag{27}$$

where $\xi(z) = z^{(1/p)}$, $z \in [mb^p, a^p]$, $\mathfrak{D}_3(\eta)$, and $\mathfrak{D}_4(\eta)$ are same as given in Theorem 1 (ii).

Proof. (i) For $x = ((t/2)a^p + m(1 - (t/2))b^p)^{1/p}$ and $y = ((t/2)b^p + (1 - (t/2))(a^p/m))^{1/p}$ in (21), we get

$$f\left(\left(\frac{a^p + mb^p}{2}\right)^{1/p}\right) \leq h\left(\frac{1}{2^\alpha}\right)\frac{f\left(((t/2)a^p + m(1-(t/2))b^p)^{1/p}\right)}{e^{\eta\left(((t/2)a^p + m(1-(t/2))b^p)^{1/p}\right)}} + mh\left(\frac{2^\alpha - 1}{2^\alpha}\right)\frac{f\left(((t/2)b^p + (1-(t/2))(a^p/m))^{1/p}\right)}{e^{\eta\left(((t/2)b^p + (1-(t/2))(a^p/m))^{1/p}\right)}}. \tag{28}$$

Multiplying the above inequality with $t^{\tau-1}$ on both sides and integrating over $[0,1]$, we have

$$f\left(\left(\frac{a^p + mb^p}{2}\right)^{1/p}\right)\int_0^1 t^{\tau-1} dt \leq h\left(\frac{1}{2^\alpha}\right)\int_0^1 \frac{t^{\tau-1} f\left(((t/2)a^p + m(1-(t/2))b^p)^{1/p}\right)}{e^{\eta\left(((t/2)a^p + m(1-(t/2))b^p)^{1/p}\right)}} dt + mh\left(\frac{2^\alpha - 1}{2^\alpha}\right)\int_0^1 \frac{t^{\tau-1} f\left(((t/2)b^p + (1-(t/2))(a^p/m))^{1/p}\right)}{e^{\eta\left(((t/2)b^p + (1-(t/2))(a^p/m))^{1/p}\right)}} dt. \tag{29}$$

Set $(t/2)a^p + m(1 - (t/2))b^p = x$, that is, $(t/2) = (mb^p - x)/(mb^p - a^p)$ and $(1 - (t/2))(a^p/m) + (t/2)b^p = y$, that is, $(t/2) = (y - (a^p/m))/(b^p - (a^p/m))$ in right hand side of the above inequality. Then, after some calculations, one can obtain the first inequality of (26).

On the other hand, by applying the $E_p(\alpha, h - m)$ of f, from right hand side of (28), one can obtain the following inequality:

$$h\left(\frac{1}{2^\alpha}\right)\frac{f\left(((t/2)a^p + m(1-(t/2))b^p)^{1/p}\right)}{e^{\eta\left(((t/2)a^p + m(1-(t/2))b^p)^{1/p}\right)}} + mh\left(\frac{2^\alpha - 1}{2^\alpha}\right)\frac{f\left(((t/2)b^p + (1-(t/2))(a^p/m))^{1/p}\right)}{e^{\eta\left(((t/2)b^p + (1-(t/2))(a^p/m))^{1/p}\right)}}$$
$$\leq \frac{h(1/2^\alpha)}{e^{\eta\left(((t/2)a^p + m(1-(t/2))b^p)^{1/p}\right)}}\left(h\left(\left(\frac{t}{2}\right)^{\alpha}\right)\frac{f(a)}{e^{\eta a}} + mh\left(1 - \left(\frac{t}{2}\right)^{\alpha}\right)\frac{f(b)}{e^{\eta b}}\right) + \frac{mh((2^\alpha - 1)/2^\alpha)}{e^{\eta\left(((t/2)b^p + (1-(t/2))(a^p/m))^{1/p}\right)}}\left(h\left(\left(\frac{t}{2}\right)^{\alpha}\right)\frac{f(b)}{e^{\eta b}} + mh\left(1 - \left(\frac{t}{2}\right)^{\alpha}\right)\frac{f(a/m^2)}{e^{(\eta a/m^2)}}\right). \tag{30}$$

Multiplying $t^{\tau-1}$ on both sides of (30), then by integrating on $[0,1]$, one can get

$$\begin{aligned}
&\mathfrak{D}_1(\eta)h\left(\frac{1}{2^\alpha}\right)\int_0^1 t^{\tau-1}f\left(\left(\frac{t}{2}a^p+m\left(1-\frac{t}{2}\right)b^p\right)^{1/p}\right)\mathrm{d}t\\
&+\mathfrak{D}_2(\eta)mh\left(\frac{2^\alpha-1}{2^\alpha}\right)\int_0^1 t^{\tau-1}f\left(\left(\frac{t}{2}b^p+\left(1-\frac{t}{2}\right)\frac{a^p}{m}\right)^{1/p}\right)\mathrm{d}t\\
&\leq\left(\mathfrak{D}_1(\eta)h\left(\frac{1}{2^\alpha}\right)\frac{f(a)}{e^{\eta a}}+\mathfrak{D}_2(\eta)mh\left(\frac{2^\alpha-1}{2^\alpha}\right)\frac{f(b)}{e^{\eta b}}\right)\int_0^1 t^{\tau-1}h\left(\left(\frac{t}{2}\right)^\alpha\right)\mathrm{d}t\\
&+m\left(\mathfrak{D}_1(\eta)h\left(\frac{1}{2^\alpha}\right)\frac{f(b)}{e^{\eta b}}+\mathfrak{D}_2(\eta)mh\left(\frac{2^\alpha-1}{2^\alpha}\right)\frac{f\left(a/m^2\right)}{e^{\left(\eta a/m^2\right)}}\right)\int_0^1 t^{\tau-1}h\left(1-\left(\frac{t}{2}\right)^\alpha\right)\mathrm{d}t.
\end{aligned}\tag{31}$$

Set $(t/2)a^p+m(1-(t/2))b^p=x$, that is, $(t/2)=(mb^p-x)/(mb^p-a^p)$ and $(1-(t/2))(a^p/m)+(t/2)b^p=y$, that is, $(t/2)=(y-(a^p/m))/(b^p-(a^p/m))$ in (31). Then, after some calculations, the second inequality of (26) is obtained.

(ii) Proof is similar as (i). □

Remark 3.

(i) In Theorem 2 (i), if we put $\alpha=1=m$, $\eta=0$, $p>0$, and $h(t)=t$, then Theorem 2.1(i) in [36] is reproduced.

(ii) In Theorem 2 (ii), if we put $\alpha=1=m$, $\eta=0$, $p<0$, and $h(t)=t$, then Theorem 2.1(ii) in [36] is reproduced.

(iii) In Theorem 2 (i), if we put $\alpha=1=m$, $p=1$, $\eta=0$, and $h(t)=t$, then Corollary 2.1 in [36] is reproduced.

Remark 4. From Theorems 1 and 2, one can deduce results for convex, exponentially convex, $E_p(1,I_d-1)$, $E_p(1,I_d-m)$, $E_p(1,h-1)$, $E_p(\alpha,I_d-m)$, $E_p(1,h-m)$, and $E_p(1,h-1)$ functions.

4. Fejér–Hadamard Type Inequalities for $E_p(\alpha,h-m)$ Function

Theorem 3. *Let $f\colon I\longrightarrow\mathbb{R}$ be an $E_p(\alpha,h-m)$ positive function as given in Definition 5 and $f((a^p+mb^p-x)/m)=f(x)$, $a,b\in I, a<b$, $m\neq 0$. If $g\colon I\longrightarrow\mathbb{R}$ is a positive function and $f,g\in L_1[a,b]$, then one can have fractional integral inequalities for operators (1) and (2) as follows.*

(i) For $p>0$, we have

$$\begin{aligned}
&f\left(\left(\frac{a^p+mb^p}{2}\right)^{1/p}\right)\left(I^\tau_{a^{p+}}g\circ\xi\right)(mb^p)\\
&\leq\mathfrak{D}_1(\eta)h\left(\frac{1}{2^\alpha}\right)\left(I^\tau_{a^{p+}}fg\circ\xi\right)(mb^p)+\mathfrak{D}_2(\eta)m^{\tau+1}h\left(\frac{2^\alpha-1}{2^\alpha}\right)\left(I^\tau_{b^{p-}}fg^\circ\xi\right)\left(\frac{a^p}{m}\right)\\
&\leq\frac{(mb^p-a^p)^\tau}{\Gamma(\tau)}\left\{\left(\mathfrak{D}_1(\eta)h\left(\frac{1}{2^\alpha}\right)\frac{f(a)}{e^{\eta a}}+\mathfrak{D}_2(\eta)mh\left(\frac{2^\alpha-1}{2^\alpha}\right)\frac{f(b)}{e^{\eta b}}\right)\right.\\
&\times\int_0^1 t^{\tau-1}g\left(\left(ta^p+m(1-t)b^p\right)^{1/p}\right)h(t^\alpha)\mathrm{d}t\\
&+m\left(\mathfrak{D}_1(\eta)h\left(\frac{1}{2^\alpha}\right)\frac{f(b)}{e^{\eta b}}+\mathfrak{D}_2(\eta)mh\left(\frac{2^\alpha-1}{2^\alpha}\right)\frac{f\left(a/m^2\right)}{e^{\left(\eta a/m^2\right)}}\right)\\
&\left.\times\int_0^1 t^{\tau-1}g\left(\left(ta^p+m(1-t)b^p\right)^{1/p}\right)h(1-t^\alpha)\mathrm{d}t\right\},
\end{aligned}\tag{32}$$

where $\xi(z) = z^{1/p}$, $z \in [a^p, mb^p]$, $fg\circ\xi = (f\circ\xi)(g\circ\xi)$, $\mathfrak{D}_1(\eta)$, and $\mathfrak{D}_2(\eta)$ are same as given in Theorem 1 (i).

(ii) For $p<0$, we have

$$\begin{aligned}
&f\left(\left(\frac{a^p+mb^p}{2}\right)^{1/p}\right)\left(I^{\tau}_{a^p-}g\circ\xi\right)(mb^p)\\
&\leq \mathfrak{D}_3(\eta)h\left(\frac{1}{2^\alpha}\right)\left(I^{\tau}_{a^p-}fg\circ\xi\right)(mb^p)+\mathfrak{D}_4(\eta)m^{\tau+1}h\left(\frac{2^\alpha-1}{2^\alpha}\right)\left(I^{\tau}_{b^p+}fg\circ\xi\right)\left(\frac{a^p}{m}\right)\\
&\leq \frac{(a^p-mb^p)^\tau}{\Gamma(\tau)}\left\{\left(\mathfrak{D}_3(\eta)h\left(\frac{1}{2^\alpha}\right)\frac{f(a)}{e^{\eta a}}+\mathfrak{D}_4(\eta)mh\left(\frac{2^\alpha-1}{2^\alpha}\right)\frac{f(b)}{e^{\eta b}}\right)\right.\\
&\quad\times\int_0^1 t^{\tau-1}g\left(\left(ta^p+m(1-t)b^p\right)^{1/p}\right)h(t^\alpha)\mathrm{d}t\\
&\quad+m\left(\mathfrak{D}_3(\eta)h\left(\frac{1}{2^\alpha}\right)\frac{f(b)}{e^{\eta b}}+\mathfrak{D}_4(\eta)mh\left(\frac{2^\alpha-1}{2^\alpha}\right)\frac{f(a/m^2)}{e^{(\eta a/m^2)}}\right)\\
&\quad\left.\times\int_0^1 t^{\tau-1}g\left(\left(ta^p+m(1-t)b^p\right)^{1/p}\right)h(1-t^\alpha)\mathrm{d}t\right\},
\end{aligned}\tag{33}$$

where $\xi(z) = z^{1/p}$, $z \in [mb^p, a^p]$, $fg\circ\xi = (f\circ\xi)(g\circ\xi)$, $\mathfrak{D}_3(\eta)$, and $\mathfrak{D}_4(\eta)$ are same as given in Theorem 1 (ii).

Proof. (i) Multiplying (22) by $t^{\tau-1}g((ta^p+m(1-t)b^p)^{1/p})$, then making integration on $[0,1]$, the following inequality is yielded:

$$\begin{aligned}
&f\left(\left(\frac{a^p+mb^p}{2}\right)^{1/p}\right)\int_0^1 t^{\tau-1}g\left(\left(ta^p+m(1-t)b^p\right)^{1/p}\right)\mathrm{d}t\\
&\leq \mathfrak{D}_1(\eta)h\left(\frac{1}{2^\alpha}\right)\int_0^1 t^{\tau-1}f\left(\left(ta^p+m(1-t)b^p\right)^{1/p}\right)g\left(\left(ta^p+m(1-t)b^p\right)^{1/p}\right)\mathrm{d}t\\
&\quad+\mathfrak{D}_2(\eta)mh\left(\frac{2^\alpha-1}{2^\alpha}\right)\int_0^1 t^{\tau-1}f\left(\left(tb^p+(1-t)\frac{a^p}{m}\right)^{1/p}\right)g\left(\left(ta^p+m(1-t)b^p\right)^{1/p}\right)\mathrm{d}t.
\end{aligned}\tag{34}$$

For $ta^p+m(1-t)b^p = x$, that is, $(1-t)(a^p/m)+tb^p = ((a^p+mb^p-x)/m)$ in (34) and then utilizing condition $f(x) = f((a^p+mb^p-x)/m)$ and equations (1) and (2), the first inequality of (32) can be achieved.

Now, multiplying $t^{\tau-1}g((ta^p+m(1-t)b^p)^{1/p})$ with (24) and integrating over $[0,1]$, we have

$$\begin{aligned}
&\mathfrak{D}_1(\eta)h\left(\frac{1}{2^\alpha}\right)\int_0^1 t^{\tau-1}f\left(\left(ta^p+m(1-t)b^p\right)^{1/p}\right)g\left(\left(ta^p+m(1-t)b^p\right)^{1/p}\right)\mathrm{d}t\\
&\quad+\mathfrak{D}_2(\eta)mh\left(\frac{2^\alpha-1}{2^\alpha}\right)\int_0^1 t^{\tau-1}f\left(\left(tb^p+(1-t)\frac{a^p}{m}\right)^{1/p}\right)g\left(\left(ta^p+m(1-t)b^p\right)^{1/p}\right)\mathrm{d}t
\end{aligned}$$

$$\leq\left(\mathfrak{D}_1(\eta)h\left(\frac{1}{2^{\alpha}}\right)\frac{f(a)}{e^{\eta a}}+\mathfrak{D}_2(\eta)mh\left(\frac{2^{\alpha}-1}{2^{\alpha}}\right)\frac{f(b)}{e^{\eta b}}\right)\int_0^1 t^{\tau-1}g\left(\left(ta^p+m(1-t)b^p\right)^{1/p}\right)h\left(t^{\alpha}\right)dt$$
$$+m\left(\mathfrak{D}_1(\eta)h\left(\frac{1}{2^{\alpha}}\right)\frac{f(b)}{e^{\eta b}}+\mathfrak{D}_2(\eta)mh\left(\frac{2^{\alpha}-1}{2^{\alpha}}\right)\frac{f\left(a/m^2\right)}{e^{\left(\eta a/m^2\right)}}\right)\int_0^1 t^{\tau-1}g\left(\left(ta^p+m(1-t)b^p\right)^{1/p}\right)h\left(1-t^{\alpha}\right)dt. \tag{35}$$

Again, setting $ta^p+m(1-t)b^p=x$, that is, $(1-t)(a^p/m)+tb^p=((a^p+mb^p-x)/m)$ in (35) and utilizing condition $f(x)=f((a^p+mb^p-x)/m)$, then by using definitions (1) and (2), one can get second inequality of (32).

(ii) Proof is similar as (i). □

Remark 5.

(i) In Theorem 3 (i), if we put $\alpha=m=1$, $h(t)=t$, $g(x)=1$, $\eta=0$, and $p=1$ then Theorem 2 in [12] is reproduced.

(ii) In Theorem 3 (i), if we put $\alpha=m=1$, $p=1$, $h(t)=t$, $g(x)=1$, $\eta=0$, and $\tau=1$, then the Hadamard inequality is reproduced.

(iii) In Theorem 3 (i), if we put $\alpha=m=1$, $p=1$, $h(t)=t$, $\eta=0$, and $\tau=1$ then classical Fejér–Hadamard inequality is reproduced.

(iv) In Theorem 3 (ii), if we put $\alpha=m=1$, $h(t)=t$, $g(x)=1$, $\eta=0$, and $p=-1$, then Theorem 4 in [8] is reproduced.

(v) In Theorem 3 (ii), if we put $\alpha=m=1$, $h(t)=t$, $\eta=0$, and $p=-1$ then Theorem 5 in [8] is reproduced.

The second variant of the Fejér–Hadamard inequality is stated and proved as follows.

Theorem 4. *Let the assumptions of Theorem 3 hold. Then, we have the following inequalities.*

(i) For $p>0$, we have

$$f\left(\left(\frac{a^p+mb^p}{2}\right)^{1/p}\right)\left(I^{\tau}_{((a^p+mb^p)/2)^+}g\circ\xi\right)\left(mb^p\right)$$
$$\leq\mathfrak{D}_1(\eta)h\left(\frac{1}{2^{\alpha}}\right)\left(I^{\tau}_{((a^p+mb^p)/2)^+}fg\circ\xi\right)\left(mb^p\right)+\mathfrak{D}_2(\eta)m^{\tau+1}h\left(\frac{2^{\alpha}-1}{2^{\alpha}}\right)\left(I^{\tau}_{((a^p+mb^p)/2m)^-}fg\circ\xi\right)\left(\frac{a^p}{m}\right)$$
$$\leq\frac{1}{\Gamma(\tau)}\left(\frac{mb^p-a^p}{2}\right)^{\tau}\left\{\left(\mathfrak{D}_1(\eta)h\left(\frac{1}{2^{\alpha}}\right)\frac{f(a)}{e^{\eta a}}+\mathfrak{D}_2(\eta)mh\left(\frac{2^{\alpha}-1}{2^{\alpha}}\right)\frac{f(b)}{e^{\eta b}}\right)\right.$$
$$\times\int_0^1 t^{\tau-1}g\left(\left(\frac{t}{2}a^p+m\left(1-\frac{t}{2}\right)b^p\right)^{1/p}\right)h\left(\left(\frac{t}{2}\right)^{\alpha}\right)dt+m\left(\mathfrak{D}_1(\eta)h\left(\frac{1}{2^{\alpha}}\right)\frac{f(b)}{e^{\eta b}}\right.$$
$$\left.\left.+\mathfrak{D}_2(\eta)mh\left(\frac{2^{\alpha}-1}{2^{\alpha}}\right)\frac{f\left(a/m^2\right)}{e^{\left(\eta a/m^2\right)}}\right)\int_0^1 t^{\tau-1}g\left(\left(\frac{t}{2}a^p+m\left(1-\frac{t}{2}\right)b^p\right)^{1/p}\right)h\left(1-\left(\frac{t}{2}\right)^{\alpha}\right)dt\right\}, \tag{36}$$

where $\xi(z)=z^{1/p}$, $z\in[a^p,mb^p]$, $fg\circ\xi=(f\circ\xi)(g\circ\xi)$, $\mathfrak{D}_1(\eta)$, and $\mathfrak{D}_2(\eta)$ are same as given in Theorem 1 (i).

(ii) For $p<0$, we have

$$f\left(\left(\frac{a^p+mb^p}{2}\right)^{1/p}\right)\left(I^{\tau}_{((a^p+mb^p)/2)^-}g\circ\xi\right)\left(mb^p\right)$$
$$\leq\mathfrak{D}_3(\eta)h\left(\frac{1}{2^{\alpha}}\right)\left(I^{\tau}_{((a^p+mb^p)/2)^-}fg\circ\xi\right)\left(mb^p\right)+\mathfrak{D}_4(\eta)m^{\tau+1}h\left(\frac{2^{\alpha}-1}{2^{\alpha}}\right)\left(I^{\tau}_{((a^p+mb^p)/2m)^+}fg\circ\xi\right)\left(\frac{a^p}{m}\right)$$

$$\leq \frac{1}{\Gamma(\tau)}\left(\frac{a^p - mb^p}{2}\right)^{\tau}\Bigg\{\left(\mathfrak{D}_3(\eta)h\left(\frac{1}{2^\alpha}\right)\frac{f(a)}{e^{\eta a}} + \mathfrak{D}_4(\eta)mh\left(\frac{2^\alpha - 1}{2^\alpha}\right)\frac{f(b)}{e^{\eta b}}\right)$$
$$\times \int_0^1 t^{\tau-1} g\left(\left(\frac{t}{2}a^p + m\left(1-\frac{t}{2}\right)b^p\right)^{1/p}\right)h\left(\left(\frac{t}{2}\right)^{\alpha}\right)dt + m\left(\mathfrak{D}_3(\eta)h\left(\frac{1}{2^\alpha}\right)\frac{f(b)}{e^{\eta b}}\right.$$
$$\left. + \mathfrak{D}_4(\eta)mh\left(\frac{2^\alpha - 1}{2^\alpha}\right)\frac{f\left(a/m^2\right)}{e^{\left(\eta a/m^2\right)}}\right)\int_0^1 t^{\tau-1} g\left(\left(\frac{t}{2}a^p + m\left(1-\frac{t}{2}\right)b^p\right)^{1/p}\right)h\left(1-\left(\frac{t}{2}\right)^{\alpha}\right)dt\Bigg\}, \tag{37}$$

where $\xi(z) = z^{1/p}$, $z \in [mb^p, a^p]$, $fg \circ \xi = (f\circ\xi)(g\circ\xi)$, $\mathfrak{D}_3(\eta)$, and $\mathfrak{D}_4(\eta)$ are same as given in Theorem 1 (ii).

Proof. (i) Multiplying (28) by $t^{\tau-1}g(((t/2)a^p + m(1-(t/2))b^p)^{1/p})$ and integrating over $[0,1]$, the following inequality is yielded:

$$f\left(\left(\frac{a^p + mb^p}{2}\right)^{1/p}\right)\int_0^1 t^{\tau-1} g\left(\left(\frac{t}{2}a^p + m\left(1-\frac{t}{2}\right)b^p\right)^{1/p}\right)dt$$
$$\leq \mathfrak{D}_1(\eta)h\left(\frac{1}{2^\alpha}\right)\int_0^1 t^{\tau-1} f\left(\left(\frac{t}{2}a^p + m\left(1-\frac{t}{2}\right)b^p\right)^{1/p}\right)g\left(\left(\frac{t}{2}a^p + m\left(1-\frac{t}{2}\right)b^p\right)^{1/p}\right)dt$$
$$+ \mathfrak{D}_2(\eta)mh\left(\frac{2^\alpha - 1}{2^\alpha}\right)\int_0^1 t^{\tau-1} f\left(\left(\frac{t}{2}b^p + \left(1-\frac{t}{2}\right)\frac{a^p}{m}\right)^{1/p}\right)g\left(\left(\frac{t}{2}a^p + m\left(1-\frac{t}{2}\right)b^p\right)^{1/p}\right)dt. \tag{38}$$

Setting $(t/2)a^p + m(1-(t/2))b^p = x$, that is $(1-(t/2))(a^p/m) + (t/2)b^p = (a^p + mb^p - x)/m$ in (38) and using condition $f(x) = f((a^p + mb^p - x)/m)$ and the definitions (1), (2), one can get first inequality of (36).

Now, multiplying $t^{\tau-1}g(((t/2)a^p + m(1-(t/2))b^p)^{1/p})$ with (30) and integrating over $[0,1]$, we have

$$\mathfrak{D}_1(\eta)h\left(\frac{1}{2^\alpha}\right)\int_0^1 t^{\tau-1} f\left(\left(\frac{t}{2}a^p + m\left(1-\frac{t}{2}\right)b^p\right)^{1/p}\right)g\left(\left(\frac{t}{2}a^p + m\left(1-\frac{t}{2}\right)b^p\right)^{1/p}\right)dt$$
$$+ \mathfrak{D}_2(\eta)mh\left(\frac{2^\alpha - 1}{2^\alpha}\right)\int_0^1 t^{\tau-1} f\left(\left(\frac{t}{2}b^p + \left(1-\frac{t}{2}\right)\frac{a^p}{m}\right)^{1/p}\right)g\left(\left(\frac{t}{2}a^p + m\left(1-\frac{t}{2}\right)b^p\right)^{1/p}\right)dt$$
$$\leq \left(\mathfrak{D}_1(\eta)h\left(\frac{1}{2^\alpha}\right)\frac{f(a)}{e^{\eta a}} + \mathfrak{D}_2(\eta)mh\left(\frac{2^\alpha - 1}{2^\alpha}\right)\frac{f(b)}{e^{\eta b}}\right)\int_0^1 t^{\tau-1} g\left(\left(\frac{t}{2}a^p + m\left(1-\frac{t}{2}\right)b^p\right)^{1/p}\right)h\left(\left(\frac{t}{2}\right)^{\alpha}\right)dt$$
$$+ m\left(\mathfrak{D}_1(\eta)h\left(\frac{1}{2^\alpha}\right)\frac{f(b)}{e^{\eta b}} + \mathfrak{D}_2(\eta)mh\left(\frac{2^\alpha - 1}{2^\alpha}\right)\frac{f\left(a/m^2\right)}{e^{\left(\eta a/m^2\right)}}\right)\int_0^1 t^{\tau-1} g\left(\left(\frac{t}{2}a^p + m\left(1-\frac{t}{2}\right)b^p\right)^{1/p}\right)h\left(1-\left(\frac{t}{2}\right)^{\alpha}\right)dt. \tag{39}$$

Again for $(t/2)a^p + m(1-(t/2))b^p = x$, that is, $(1-(t/2))(a^p/m) + (t/2)b^p = (a^p + mb^p - x)/m$ in (39) and the utilizing condition $f(x) = f((a^p + mb^p - x)/m)$ and equations (1) and (2), the second inequality of (36) can be achieved.

(ii) Proof is similar as (i). □

Remark 6.

(i) In Theorem 4 (i), if we put $\alpha = 1 = m$, $p > 0$, $g(x) = 1$, $\eta = 0$, and $h(t) = t$, then Theorem 2.1 (i) in [36] is reproduced.

(ii) In Theorem 4 (ii), if we put $\alpha = 1 = m$, $p < 0$, $g(x) = 1$, $\eta = 0$, and $h(t) = t$, then Theorem 2.1(ii) in [36] is reproduced.

(iii) In Theorem 4 (i), if we put $\alpha = 1 = m$, $p = 1$, $g(x) = 1$, $\eta = 0$, and $h(t) = t$, then Corollary 2.1 in [36] is reproduced.

Remark 7. From Theorems 3 and 4, one can deduce results for convex, exponentially convex, $E_p(1, I_d - 1)$, $E_p(1, I_d - m)$, $E_p(1, h - 1)$, $E_p(\alpha, I_d - m)$, $E_p(1, h - m)$, and $E_p(1, h - 1)$ functions.

4.1. Results for $E_p(h-m)$ Function. For $\alpha = 1$ in Theorems 1–4, one can obtain the results for $E_p(h-m)$ function:

Theorem 5. *With the same conditions of Theorem 1, for $E_p(h-m)$ functions, the following inequalities hold:*

(i) For $p>0$, we have

$$\begin{aligned}\frac{1}{h(1/2)}f\left(\left(\frac{a^p+mb^p}{2}\right)^{1/p}\right) &\leq \frac{\Gamma(\tau+1)}{(mb^p-a^p)^\tau}\left(\mathfrak{D}_1(\eta)\left(I^\tau_{a^{p+}}f\circ\xi\right)(mb^p)+\mathfrak{D}_2(\eta)m^{\tau+1}\left(I^\tau_{b^{p-}}f\circ\xi\right)\left(\frac{a^p}{m}\right)\right)\\ &\leq \tau\left\{\left(\mathfrak{D}_1(\eta)\frac{f(a)}{e^{\eta a}}+\mathfrak{D}_2(\eta)\frac{mf(b)}{e^{\eta b}}\right)\int_0^1 t^{\tau-1}h(t)\mathrm{d}t\right.\\ &\left.+m\left(\mathfrak{D}_1(\eta)\frac{f(b)}{e^{\eta b}}+\mathfrak{D}_2(\eta)m\frac{f(a/m^2)}{e^{(\eta a/m^2)}}\right)\int_0^1 t^{\tau-1}h(1-t)\mathrm{d}t\right\}.\end{aligned} \tag{40}$$

(ii) For $p<0$, we have

$$\begin{aligned}\frac{1}{h(1/2)}f\left(\left(\frac{a^p+mb^p}{2}\right)^{1/p}\right) &\leq \frac{\Gamma(\tau+1)}{(a^p-mb^p)^\tau}\left(\mathfrak{D}_3(\eta)\left(I^\tau_{a^{p-}}f\circ\xi\right)(mb^p)+\mathfrak{D}_4(\eta)m^{\tau+1}\left(I^\tau_{b^{p+}}f\circ\xi\right)\left(\frac{a^p}{m}\right)\right)\\ &\leq \tau\left\{\left(\mathfrak{D}_3(\eta)\frac{f(a)}{e^{\eta a}}+\mathfrak{D}_4(\eta)m\frac{f(b)}{e^{\eta b}}\right)\int_0^1 t^{\tau-1}h(t)\mathrm{d}t\right.\\ &\left.+m\left(\mathfrak{D}_3(\eta)\frac{f(b)}{e^{\eta b}}+\mathfrak{D}_4(\eta)m\frac{f(a/m^2)}{e^{(\eta a/m^2)}}\right)\int_0^1 t^{\tau-1}h(1-t)\mathrm{d}t\right\}.\end{aligned} \tag{41}$$

Theorem 6. *With the same conditions of Theorem 2, for $E_p(h-m)$ function, the following inequalities hold:*

(i) For $p>0$, we have

$$\begin{aligned}\frac{1}{h(1/2)}f\left(\left(\frac{a^p+mb^p}{2}\right)^{1/p}\right) &\leq \Gamma(\tau+1)\left(\frac{2}{mb^p-a^p}\right)^\tau\left(\mathfrak{D}_1(\eta)\left(I^\tau_{((a^p+mb^p)/2)^+}f\circ\xi\right)(mb^p)+\mathfrak{D}_2(\eta)m^{\tau+1}\left(I^\tau_{((a^p+mb^p)/2m)^-}f\circ\xi\right)\left(\frac{a^p}{m}\right)\right)\\ &\leq \tau\left\{\left(\mathfrak{D}_1(\eta)\frac{f(a)}{e^{\eta a}}+\mathfrak{D}_2(\eta)m\frac{f(b)}{e^{\eta b}}\right)\int_0^1 t^{\tau-1}h\left(\frac{t}{2}\right)\mathrm{d}t\right.\\ &\left.+m\left(\mathfrak{D}_1(\eta)\frac{f(b)}{e^{\eta b}}+\mathfrak{D}_2(\eta)m\frac{f(a/m^2)}{e^{(\eta a/m^2)}}\right)\int_0^1 t^{\tau-1}h\left(1-\frac{t}{2}\right)\mathrm{d}t\right\}.\end{aligned} \tag{42}$$

(ii) For $p<0$, we have

$$\begin{aligned}\frac{1}{h(1/2)}f\left(\left(\frac{a^p+mb^p}{2}\right)^{1/p}\right) &\leq \Gamma(\tau+1)\left(\frac{2}{a^p-mb^p}\right)^\tau\left(\mathfrak{D}_3(\eta)\left(I^\tau_{((a^p+mb^p)/2)^-}f\circ\xi\right)(mb^p)+\mathfrak{D}_4(\eta)m^{\tau+1}\left(I^\tau_{((a^p+mb^p)/2m)^+}f\circ\xi\right)\left(\frac{a^p}{m}\right)\right)\\ &\leq \tau\left\{\left(\mathfrak{D}_3(\eta)\frac{f(a)}{e^{\eta a}}+\mathfrak{D}_4(\eta)m\frac{f(b)}{e^{\eta b}}\right)\int_0^1 t^{\tau-1}h\left(\frac{t}{2}\right)\mathrm{d}t\right.\\ &\left.+m\left(\mathfrak{D}_3(\eta)\frac{f(b)}{e^{\eta b}}+\mathfrak{D}_4(\eta)m\frac{f(a/m^2)}{e^{(\eta a/m^2)}}\right)\int_0^1 t^{\tau-1}h\left(1-\frac{t}{2}\right)\mathrm{d}t\right\}.\end{aligned} \tag{43}$$

Theorem 7. *With the same conditions of Theorem 3, for $E_p(h-m)$ functions, the following inequalities hold:*

(i) For $p>0$, we have

$$\frac{1}{h(1/2)}f\left(\left(\frac{a^p+mb^p}{2}\right)^{1/p}\right)\left(I^{\tau}_{a^{p+}}g\circ\xi\right)(mb^p)\leq \mathfrak{D}_1(\eta)\left(I^{\tau}_{a^{p+}}fg\circ\xi\right)(mb^p)+\mathfrak{D}_2(\eta)m\left(I^{\tau}_{b^{p-}}fg\circ\xi\right)\left(\frac{a^p}{m}\right)$$
$$\leq\frac{(mb^p-a^p)^{\tau}}{\Gamma(\tau)}\left\{\left(\mathfrak{D}_1(\eta)\frac{f(a)}{e^{\eta a}}+\mathfrak{D}_2(\eta)m\frac{f(b)}{e^{\eta b}}\right)\int_0^1 t^{\tau-1}g\left(\left(ta^p+m(1-t)b^p\right)^{1/p}\right)h(t)\mathrm{d}t\right.$$
$$\left.+m\left(\mathfrak{D}_1(\eta)\frac{f(b)}{e^{\eta b}}+\mathfrak{D}_2(\eta)m\frac{f\left(a/m^2\right)}{e^{\left(\eta a/m^2\right)}}\right)\int_0^1 t^{\tau-1}g\left(\left(ta^p+m(1-t)b^p\right)^{1/p}\right)h(1-t)\mathrm{d}t\right\}. \tag{44}$$

(ii) For $p<0$, we have

$$\frac{1}{h(1/2)}f\left(\left(\frac{a^p+mb^p}{2}\right)^{1/p}\right)\left(I^{\tau}_{a^{p-}}g\circ\xi\right)(mb^p)\leq \mathfrak{D}_3(\eta)\left(I^{\tau}_{a^{p-}}fg\circ\xi\right)(mb^p)+\mathfrak{D}_4(\eta)m\left(I^{\tau}_{b^{p+}}fg\circ\xi\right)\left(\frac{a^p}{m}\right)$$
$$\leq\frac{(a^p-mb^p)^{\tau}}{\Gamma(\tau)}\left\{\left(\mathfrak{D}_3(\eta)\frac{f(a)}{e^{\eta a}}+\mathfrak{D}_4(\eta)m\frac{f(b)}{e^{\eta b}}\right)\int_0^1 t^{\tau-1}g\left(\left(ta^p+m(1-t)b^p\right)^{1/p}\right)h(t)\mathrm{d}t\right.$$
$$\left.+m\left(\mathfrak{D}_3(\eta)\frac{f(b)}{e^{\eta b}}+\mathfrak{D}_4(\eta)m\frac{f\left(a/m^2\right)}{e^{\left(\eta a/m^2\right)}}\right)\int_0^1 t^{\tau-1}g\left(\left(ta^p+m(1-t)b^p\right)^{1/p}\right)h(1-t)\mathrm{d}t\right\}. \tag{45}$$

Theorem 8. *With the same conditions of Theorem 4, for $E_p(h-m)$ functions, the following inequalities hold:*

(i) For $p>0$, we have

$$\frac{1}{h(1/2)}f\left(\left(\frac{a^p+mb^p}{2}\right)^{1/p}\right)\left(I^{\tau}_{((a^p+mb^p)/2)^+}g\circ\xi\right)(mb^p)$$
$$\leq\mathfrak{D}_1(\eta)\left(I^{\tau}_{((a^p+mb^p)/2)^+}fg\circ\xi\right)(mb^p)+\mathfrak{D}_2(\eta)m^{\tau+1}\left(I^{\tau}_{((a^p+mb^p)/2m)^-}fg\circ\xi\right)\left(\frac{a^p}{m}\right)$$
$$\leq\frac{1}{\Gamma(\tau)}\left(\frac{mb^p-a^p}{2}\right)^{\tau}\left\{\left(\mathfrak{D}_1(\eta)\frac{f(a)}{e^{\eta a}}+\mathfrak{D}_2(\eta)m\frac{f(b)}{e^{\eta b}}\right)\int_0^1 t^{\tau-1}g\left(\left(\frac{t}{2}a^p+m\left(1-\frac{t}{2}\right)b^p\right)^{1/p}\right)h\left(\frac{t}{2}\right)\mathrm{d}t\right.$$
$$\left.+m\left(\mathfrak{D}_1(\eta)\frac{f(b)}{e^{\eta b}}+\mathfrak{D}_2(\eta)m\frac{f\left(a/m^2\right)}{e^{\left(\eta a/m^2\right)}}\right)\int_0^1 t^{\tau-1}g\left(\left(\frac{t}{2}a^p+m\left(1-\frac{t}{2}\right)b^p\right)^{1/p}\right)h\left(1-\frac{t}{2}\right)\mathrm{d}t\right\}. \tag{46}$$

(ii) For $p<0$, we have

$$
\begin{aligned}
&\frac{1}{h(1/2)} f\left(\left(\frac{a^p+mb^p}{2}\right)^{1/p}\right)\left(I^{\tau}_{((a^p+mb^p)/2)^-} g\circ\xi\right)(mb^p)\\
&\leq \mathfrak{D}_3(\eta)\left(I^{\tau}_{((a^p+mb^p)/2)^-} fg\circ\xi\right)(mb^p)+\mathfrak{D}_4(\eta)m^{\tau+1}\left(I^{\tau}_{((a^p+mb^p)/2m)^+} fg\circ\xi\right)\left(\frac{a^p}{m}\right)\\
&\leq \frac{1}{\Gamma(\tau)}\left(\frac{a^p-mb^p}{2}\right)^{\tau}\left\{\left(\mathfrak{D}_3(\eta)\frac{f(a)}{e^{\eta a}}+\mathfrak{D}_4(\eta)m\frac{f(b)}{e^{\eta b}}\right)\int_0^1 t^{\tau-1} g\left(\left(\frac{t}{2}a^p+m\left(1-\frac{t}{2}\right)b^p\right)^{1/p}\right)h\left(\frac{t}{2}\right)\mathrm{d}t\right.\\
&\left.+m\left(\mathfrak{D}_3(\eta)\frac{f(b)}{e^{\eta b}}+\mathfrak{D}_4(\eta)m\frac{f\left(a/m^2\right)}{e^{(\eta a/m^2)}}\right)\int_0^1 t^{\tau-1} g\left(\left(\frac{t}{2}a^p+m\left(1-\frac{t}{2}\right)b^p\right)^{1/p}\right)h\left(1-\frac{t}{2}\right)\mathrm{d}t\right\}.
\end{aligned}
\tag{47}
$$

4.2. Results for $E_p(\alpha-m)$ Functions. For $h(t)=t$ in Theorems 1–4, one can obtain the results for $E_p(\alpha-m)$ function as follows.

Theorem 9. *With the same conditions of Theorem 1, for $E_p(\alpha-m)$ functions, the following inequalities hold:*

(1) For $p>0$, we have

$$
\begin{aligned}
2^{\alpha} f\left(\left(\frac{a^p+mb^p}{2}\right)^{1/p}\right) &\leq \frac{\Gamma(\tau+1)}{(mb^p-a^p)^{\tau}}\left(\mathfrak{D}_1(\eta)\left(I^{\tau}_{a^{p+}} f\circ\xi\right)(mb^p)+\mathfrak{D}_2(\eta)m^{\tau+1}\left(2^{\alpha}-1\right)\left(I^{\tau}_{b^{p-}} f\circ\xi\right)\left(\frac{a^p}{m}\right)\right)\\
&\leq \frac{\tau}{\tau+\alpha}\left\{\left(\mathfrak{D}_1(\eta)\frac{f(a)}{e^{\eta a}}+\mathfrak{D}_2(\eta)m\left(2^{\alpha}-1\right)\frac{f(b)}{e^{\eta b}}\right)\right.\\
&\left.+\frac{m\alpha}{\tau+\alpha}\left(\mathfrak{D}_1(\eta)\frac{f(b)}{e^{\eta b}}+m\left(2^{\alpha}-1\right)\mathfrak{D}_2(\eta)\frac{f\left(a/m^2\right)}{e^{(\eta a/m^2)}}\right)\right\}.
\end{aligned}
\tag{48}
$$

(ii) For $p<0$, we have

$$
\begin{aligned}
2^{\alpha} f\left(\left(\frac{a^p+mb^p}{2}\right)^{1/p}\right) &\leq \frac{\Gamma(\tau+1)}{(a^p-mb^p)^{\tau}}\left(\mathfrak{D}_3(\eta)\left(I^{\tau}_{a^{p-}} f\circ\xi\right)(mb^p)+\mathfrak{D}_4(\eta)m^{\tau+1}\left(2^{\alpha}-1\right)\left(I^{\tau}_{b^{p+}} f\circ\xi\right)\left(\frac{a^p}{m}\right)\right)\\
&\leq \frac{\tau}{\tau+\alpha}\left\{\left(\mathfrak{D}_3(\eta)\frac{f(a)}{e^{\eta a}}+\mathfrak{D}_4(\eta)m\left(2^{\alpha}-1\right)\frac{f(b)}{e^{\eta b}}\right)\right.\\
&\left.+\frac{m\alpha}{\tau+\alpha}\left(\mathfrak{D}_3(\eta)\frac{f(b)}{e^{\eta b}}+m\left(2^{\alpha}-1\right)\mathfrak{D}_4(\eta)\frac{f\left(a/m^2\right)}{e^{(\eta a/m^2)}}\right)\right\}.
\end{aligned}
\tag{49}
$$

Theorem 10. *With the same conditions of Theorem 2, for $E_p(\alpha - m)$ functions, the following inequalities hold:*

(i) For $p > 0$, we have

$$\begin{aligned}2^{\alpha} f\left(\left(\frac{a^p + mb^p}{2}\right)^{1/p}\right) &\leq \Gamma(\tau+1)\left(\frac{2}{mb^p - a^p}\right)^{\tau} \\ &\times\left(\mathfrak{D}_1(\eta)\left(I^{\tau}_{((a^p+mb^p)/2)^+} f\circ\xi\right)(mb^p) + \mathfrak{D}_2(\eta)m^{\tau+1}(2^{\alpha}-1)\left(I^{\tau}_{((a^p+mb^p)/2m)^-} f\circ\xi\right)\left(\frac{a^p}{m}\right)\right) \\ &\leq \frac{\tau}{2^{\alpha}(\tau+\alpha)}\left(\mathfrak{D}_1(\eta)\frac{f(a)}{e^{\eta a}} + \mathfrak{D}_2(\eta)m(2^{\alpha}-1)\frac{f(b)}{e^{\eta b}}\right) \\ &+ m\left(1 - \frac{\tau}{2^{\tau}(\tau+\alpha)}\right)\left(\mathfrak{D}_1(\eta)\frac{f(b)}{e^{\eta b}} + \mathfrak{D}_2(\eta)m(2^{\alpha}-1)\frac{f(a/m^2)}{e^{(\eta a/m^2)}}\right).\end{aligned} \tag{50}$$

(ii) For $p < 0$, we have

$$\begin{aligned}2^{\alpha} f\left(\left(\frac{a^p + mb^p}{2}\right)^{1/p}\right) &\leq \Gamma(\tau+1)\left(\frac{2}{a^p - mb^p}\right)^{\tau} \\ &\times\left(\mathfrak{D}_3(\eta)\left(I^{\tau}_{((a^p+mb^p)/2)^-} f\circ\xi\right)(mb^p) + \mathfrak{D}_4(\eta)m^{\tau+1}(2^{\alpha}-1)\left(I^{\tau}_{((a^p+mb^p)/2m)^+} f\circ\xi\right)\left(\frac{a^p}{m}\right)\right) \\ &\leq \frac{\tau}{2^{\alpha}(\tau+\alpha)}\left(\mathfrak{D}_3(\eta)\frac{f(a)}{e^{\eta a}} + \mathfrak{D}_4(\eta)m(2^{\alpha}-1)\frac{f(b)}{e^{\eta b}}\right) \\ &+ m\left(1 - \frac{\tau}{2^{\tau}(\tau+\alpha)}\right)\left(\mathfrak{D}_3(\eta)\frac{f(b)}{e^{\eta b}} + \mathfrak{D}_4(\eta)m(2^{\alpha}-1)\frac{f(a/m^2)}{e^{(\eta a/m^2)}}\right).\end{aligned} \tag{51}$$

Theorem 11. *Under the assumptions of Theorem 3, for $E_p(\alpha - m)$ functions, the following inequalities hold:*

(i) For $p > 0$, we have

$$\begin{aligned}&2^{\alpha} f\left(\left(\frac{a^p + mb^p}{2}\right)^{1/p}\right)\left(I^{\tau}_{a^{p+}} g\circ\xi\right)(mb^p) \\ &\leq \mathfrak{D}_1(\eta)\left(I^{\tau}_{a^{p+}} fg\circ\xi\right)(mb^p) + \mathfrak{D}_2(\eta)m^{\tau+1}(2^{\alpha}-1)\left(I^{\tau}_{b^{p-}} fg\circ\xi\right)\left(\frac{a^p}{m}\right) \\ &\leq \left(\mathfrak{D}_1(\eta)\frac{f(a)}{e^{\eta a}} + \mathfrak{D}_2(\eta)m(2^{\alpha}-1)\frac{f(b)}{e^{\eta b}}\right)\left(I^{\tau+\alpha}_{a^{p+}} g\circ\xi\right)(mb^p) \\ &+ m\left(\mathfrak{D}_1(\eta)\frac{f(b)}{e^{\eta b}} + \mathfrak{D}_2(\eta)m(2^{\alpha}-1)\frac{f(a/m^2)}{e^{(\eta a/m^2)}}\right)\left(\left(I^{\tau}_{a^{p+}} g\circ\xi\right)(mb^p) - \left(I^{\tau+\alpha}_{a^{p+}} g\circ\xi\right)(mb^p)\right).\end{aligned} \tag{52}$$

(ii) For $p < 0$, we have

$$2^{\alpha} f\left(\left(\frac{a^{p}+mb^{p}}{2}\right)^{1/p}\right)\left(I_{a^{p}-}^{\tau} g\circ\xi\right)(mb^{p}) \leq \mathfrak{D}_3(\eta)\left(I_{a^{p}-}^{\tau} fg\circ\xi\right)(mb^{p}) + \mathfrak{D}_4(\eta)m^{\tau+1}\left(2^{\alpha}-1\right)\left(I_{b^{p}+}^{\tau} fg\circ\xi\right)\left(\frac{a^{p}}{m}\right)$$
$$\leq \left(\mathfrak{D}_3(\eta)\frac{f(a)}{e^{\eta a}} + \mathfrak{D}_4(\eta)m\left(2^{\alpha}-1\right)\frac{f(b)}{e^{\eta b}}\right)\left(I_{a^{p}-}^{\tau+\alpha} g\circ\xi\right)(mb^{p})$$
$$+ m\left(\mathfrak{D}_3(\eta)\frac{f(b)}{e^{\eta b}} + \mathfrak{D}_4(\eta)m\left(2^{\alpha}-1\right)\frac{f\left(a/m^{2}\right)}{e^{\left(\eta a/m^{2}\right)}}\right)\left(\left(I_{a^{p}-}^{\tau} g\circ\xi\right)(mb^{p}) - \left(I_{a^{p}-}^{\tau+\alpha} g\circ\xi\right)(mb^{p})\right). \tag{53}$$

Theorem 12. *With the same conditions of Theorem 4, for $E_p(\alpha - m)$ functions,*

(i) For $p > 0$, we have

$$2^{\alpha} f\left(\left(\frac{a^{p}+mb^{p}}{2}\right)^{1/p}\right)\left(I_{((a^{p}+mb^{p})/2)^{+}}^{\tau} g\circ\xi\right)(mb^{p}) \leq \mathfrak{D}_1(\eta)\left(I_{((a^{p}+mb^{p})/2)^{+}}^{\tau} fg\circ\xi\right)(mb^{p}) + \mathfrak{D}_2(\eta)m^{\tau+1}\left(2^{\alpha}-1\right)\left(I_{((a^{p}+mb^{p})/2m)^{-}}^{\tau} fg\circ\xi\right)\left(\frac{a^{p}}{m}\right)$$
$$\leq \frac{1}{2^{\alpha}}\left(\mathfrak{D}_1(\eta)\frac{f(a)}{e^{\eta a}} + \mathfrak{D}_2(\eta)m\left(2^{\alpha}-1\right)\frac{f(b)}{e^{\eta b}}\right)\left(I_{((a^{p}+mb^{p})/2)^{+}}^{\tau+\alpha} g\circ\xi\right)(mb^{p}) + m\left(\mathfrak{D}_1(\eta)\frac{f(b)}{e^{\eta b}}\right.$$
$$\left. + \mathfrak{D}_2(\eta)m\left(2^{\alpha}-1\right)\frac{f\left(a/m^{2}\right)}{e^{\left(\eta a/m^{2}\right)}}\right)\left(\left(I_{((a^{p}+mb^{p})/2)^{+}}^{\tau} g\circ\xi\right)(mb^{p}) - \frac{1}{2^{\alpha}}\left(I_{((a^{p}+mb^{p})/2)^{+}}^{\tau+\alpha} g\circ\xi\right)(mb^{p})\right). \tag{54}$$

(ii) For $p < 0$, we have

$$2^{\alpha} f\left(\left(\frac{a^{p}+mb^{p}}{2}\right)^{1/p}\right)\left(I_{((a^{p}+mb^{p})/2)^{-}}^{\tau} g\circ\xi\right)(mb^{p})$$
$$\leq \mathfrak{D}_3(\eta)\left(I_{((a^{p}+mb^{p})/2)^{-}}^{\tau} fg\circ\xi\right)(mb^{p}) + \mathfrak{D}_4(\eta)m^{\tau+1}\left(2^{\alpha}-1\right)\left(I_{((a^{p}+mb^{p})/2m)^{+}}^{\tau} fg\circ\xi\right)\left(\frac{a^{p}}{m}\right)$$
$$\leq \frac{1}{2^{\alpha}}\left(\mathfrak{D}_3(\eta)\frac{f(a)}{e^{\eta a}} + \mathfrak{D}_4(\eta)m\left(2^{\alpha}-1\right)\frac{f(b)}{e^{\eta b}}\right)\left(I_{((a^{p}+mb^{p})/2)^{-}}^{\tau+\alpha} g\circ\xi\right)(mb^{p}) + m\left(\mathfrak{D}_3(\eta)\frac{f(b)}{e^{\eta b}}\right.$$
$$\left. + \mathfrak{D}_4(\eta)m\left(2^{\alpha}-1\right)\frac{f\left(a/m^{2}\right)}{e^{\left(\eta a/m^{2}\right)}}\right)\left(\left(I_{((a^{p}+mb^{p})/2)^{-}}^{\tau} g\circ\xi\right)(mb^{p}) - \frac{1}{2^{\alpha}}\left(I_{((a^{p}+mb^{p})/2)^{-}}^{\tau+\alpha} g\circ\xi\right)(mb^{p})\right). \tag{55}$$

Remark 8. From Theorems 1–4, one can deduce results for exponentially $(\alpha, h) - p$-convex function, exponentially $(s, m) - p$-convex function of second kind, exponentially $(s, m) - p$-Godunova–Levin-convex function of second kind, exponentially (p, P)-convex function, Godunova–Levin type exponentially harmonic convex function, s-Godunova–Levin type exponentially harmonic convex function, exponentially $(\alpha, h - m)$-HA-convex function, exponentially (α, h)-HA-convex function, exponentially HA-convex function, and exponentially (α, m)-HA-convex function.

5. Conclusion

The Hadamard and the Fejér–Hadamard inequalities for Riemann–Liouville fractional integrals are proved by applying a generalized class of functions. Two fractional versions of the Hadamard inequality lead to almost all variants of such inequalities already published by different authors using various kinds of convex functions. Hadamard type inequalities for some new classes of functions are also given. Two fractional versions of the Fejér–Hadamard inequality are also proved which appear as generalizations of the Hadamard inequalities. By using the generalized convexity defined in this paper, one can obtain extensions of other classical integral inequalities hold for convex and related functions. It is also possible to establish these inequalities for many kinds of integral operators already existing in the literature.

Data Availability

No data were used to support this study.

Conflicts of Interest

The authors declare that they have no conflicts of interest.

References

[1] B. Ahmad, A. Alsaedi, M. Kirane, and B. T. Torebek, “Hermite-Hadamard, Hermite-Hadamard-Fejér, Dragomir-Agarwal and Pachpatte type inequalities for convex functions via new fractional integrals,” *Journal of Computational and Applied Mathematics*, vol. 353, pp. 120–129, 2019.

[2] F. Chen and S. Wu, “Hermite-Hadamard type inequalities for harmonically convex functions,” *Journal of Applied Mathematics*, vol. 2014, Article ID 386206, 1614 pages, 2014.

[3] Z. B. Fang and R. Shi, “On the (p, h)-convex function and some integral inequalities,” *Journal of Inequalities and Applications*, vol. 2014, 16 pages, 2014.

[4] X. Feng, B. Feng, G. Farid, S. Bibi, Q. Xiaoyan, and Z. Wu, “Caputo fractional derivative Hadamard inequalities for strongly m-convex functions,” *Journal of Function Spaces*, vol. 2021, Article ID 6642655, 11 pages, 2021.

[5] İ. İscan, “Hermite-Hadamard-Fejér type inequalities for convex functions via fractional integrals,” *Studia Universitatis Babeş-Bolyai Mathematica*, vol. 60, no. 3, pp. 355–366, 2015.

[6] İ. İscan and S. Wu, “Hermite-Hadamard type inequalities for harmonically convex functions via fractional integrals,” *Applied Mathematics and Computation*, vol. 238, pp. 237–244, 2014.

[7] C. Y. Jung, M. Yussouf, Y. M. Chu, G. Farid, and S. M. Kang, “Generalized fractional Hadamard and Fejér-Hadamard inequalities for generalized harmonically convex functions,” *Jurnal Matematika*, vol. 2020, Article ID 8245324, 13 pages, 2020.

[8] M. Kunt, İ. İscan, N. Yazi, and U. Gozutok, “On new inequalities of Hermite-Hadamard-Fejér type inequalities for harmonically convex functions via fractional integrals,” *Springer Plus*, vol. 5, no. 1, pp. 1–19, 2016.

[9] R. N. Liu and R. Xu, “Some fractional Hermite-Hadamard-type integral inequalities with $s-(\alpha, m)$-convex functions and their applications,” *Advances in Difference Equations*, vol. 2021, no. 1, pp. 1–16, 2021.

[10] X. Qiang, G. Farid, M. Yussouf, K. A. Khan, and A. U. Rehman, “New generalized fractional versions of Hadamard and Fejér inequalities for harmonically convex functions,” *Journal of Inequalities and Applications*, vol. 2020, p. 191, 2020.

[11] Y. Rao, M. Yussouf, G. Farid, J. Pečarić, and I. Tlili, “Further generalizations of Hadamard and Fejér-Hadamard inequalities and error estimations,” *Advances in Difference Equations*, vol. 2020, p. 421, 2020.

[12] M. Z. Sarikaya, E. Set, H. Yaldiz, and N. Basak, “Hermite-Hadamard inequalities for fractional integrals and related fractional inequalities,” *Journal of Mathematical and Computer Modelling*, vol. 57, pp. 2403–2407, 2013.

[13] X. Yang, G. Farid, W. Nazeer, M. Yussouf, Y. M. Chu, and C. Dong, “Fractional generalized Hadamard and the Fejér-Hadamard type inequalities for m-convex functions,” *AIMS Mathematics*, vol. 5, no. 6, pp. 6325–6340, 2020.

[14] R. Gorenflo and F. Mainardi, “Fractional calculus: integral and differential equations of fractional order,” *CISM Lectures Notes*, pp. 223–276, International Centre for Mechanical Sciences Palazzo del Torso, Piazza Garibaldi, Udine, Italy, 1997.

[15] G. H. Toader, “Some generalizations of the convexity,” in *Proceedings of the Colloquium on Approximation and Optimization*, pp. 329–338, Universitatea Cluj-Napoca, Clujnapoca, Romania, 1985.

[16] İ. İscan, “Ostrowski type inequalities for p-convex functions,” *New Trends in Mathematical Sciences*, vol. 4, no. 3, pp. 140–150, 2016.

[17] S. Varošanec, “On h-convexity,” *Journal of Mathematical Analysis and Applications*, vol. 326, pp. 303–311, 2007.

[18] H. Hudzik and L. Maligranda, “Some remarks on s-convex functions,” *Aequationes Mathematicae*, vol. 48, pp. 100–111, 1994.

[19] J. Park, “Generalization of Ostrowski-type inequalities for differentiable real (s, m)-convex mappings,” *Far East Journal of Mathematical Sciences*, vol. 49, pp. 157–171, 2011.

[20] V. G. Mihesan, *A Generalization of the Convexity, Seminar on Funcional Equations*, Approximation and Convexity, Cluj-napoca, Romania, 1993.

[21] M. E. Özdemir, A. O. Akdemri, and E. Set, “On $(h-m)$–convexity and Hadamard-type inequalities,” *Transylvanian Journal of Mathematics and Mechanics*, vol. 8, no. 1, pp. 51–58, 2016.

[22] G. Farid, A. U. Rehman, and Q. U. Ain, “k-Fractional integral inequalities of Hadamard type for $(h-m)$-convex functions,” *Computational Methods for Differential Equations*, vol. 8, pp. 119–140, 2020.

[23] W. Jia, M. Yussouf, G. Farid, and K. A. Khan, “Hadamard and Fejér-Hadamard inequalities for $(\alpha, h-m)-p$-convex functions via Riemann-Liouville fractional integrals,” *Mathematical Problems in Engineering*, vol. 2021, Article ID 9945114, 12 pages, 2021.

[24] M. U. Awan, M. A. Noor, and K. I. Noor, “Hermite-Hadamard inequalities for exponentially convex functions,” *Applied Mathematics and Information Sciences*, vol. 12, no. 2, pp. 404–409, 2018.

[25] N. Mehreen and M. Anwar, “Hermite–Hadamard type inequalities for exponentially p-convex functions and exponentially s-convex functions in the second sense with applications,” *Journal of Inequalities and Applications*, vol. 2019, p. 92, 2019.

[26] H. Qi, M. Yussouf, S. Mehmood, Y. M. Chu, and G. Farid, “Fractional integral versions of Hermite-Hadamard type inequality for generalized exponentially convexity,” *AIMS Mathematics*, vol. 5, no. 6, pp. 6030–6042, 2020.

[27] X. Qiang, G. Farid, J. Pečarić, and S. B. Akbar, “Generalized fractional integral inequalities for exponentially (s, m)-convex functions,” *Journal of Inequalities and Applications*, vol. 2020, p. 70, 2020.

[28] W. He, G. Farid, K. Mahreen, M. Zahra, and N. Chen, “On an integral and consequent fractional integral operators via generalized convexity,” *AIMS Mathematics*, vol. 5, no. 6, pp. 7631–7647, 2020.

[29] N. Mehreen and M. Anwar, “Hermite-Hadamard type inequalities via exponentially (p, h)-convex functions,” *IEEE Access*, vol. 8, pp. 37589–37595, 2020.

[30] G. Farid, L. Guran, X. Qiang, and Y.-M. Chu, “Study on fractional Hadamard type inequalities associated with generalized exponentially convexity,” *UPB Scientific Bulletin, Series A*, vol. 84, no. 4, pp. 159–170, 2021.

[31] M. A. Noor, K. I. Noor, M. U. Awan, and S. Costaache, “Some integral inequalities for harmonically h-convex functions,” *UPB Scientific Bulletin, Series A*, vol. 77, no. 1, pp. 5–16, 2015.

[32] I. B. Baloch, İ. İscan, and S. S. Dragomir, “Fejér type inequalities for harmonically (s, m)-convex functions,”

International Journal of Analysis and Applications, vol. 12, no. 2, pp. 188–197, 2016.

[33] İ. İscan, "Hermite Hadamard type inequalities for harmonically convex functions," *Hacettepe Journal of Mathematics and Statistics*, vol. 43, no. 6, pp. 935–942, 2014.

[34] B.-Y. Xi, F. Qi, and T.-Y. Zhanga, "Some inequalities of Hermite-Hadamard type for m-harmonic-arithmetically convex functions," *ScienceAsia*, vol. 41, pp. 357–361, 2015.

[35] C.-Y. He, Y. Wang, B.-Y. Xi, and F. Qi, "Hermite-Hadamard type inequalities for (α, m)-HA and strongly (α, m)-HA convex functions," *The Journal of Nonlinear Science and Applications*, vol. 10, pp. 205–214, 2017.

[36] M. Kunt and İ. İscan, "Hermite-Hadamard type inequalities for p-convex functions via fractional integrals," *Moroccan Journal of Pure and Applied Analysis*, vol. 3, no. 1, pp. 22–35, 2017.